Akhilendra Pratap Singh
Nikhil Sharma
Ramesh Agarwal
Avinash Kumar Agarwal   *Editors*

Advanced Combustion Techniques and Engine Technologies for the Automotive Sector

Springer

Energy, Environment, and Sustainability

Series Editor

Avinash Kumar Agarwal, Department of Mechanical Engineering, Indian Institute of Technology Kanpur, Kanpur, Uttar Pradesh, India

This books series publishes cutting edge monographs and professional books focused on all aspects of energy and environmental sustainability, especially as it relates to energy concerns. The Series is published in partnership with the International Society for Energy, Environment, and Sustainability. The books in these series are edited or authored by top researchers and professional across the globe. The series aims at publishing state-of-the-art research and development in areas including, but not limited to:

- Renewable Energy
- Alternative Fuels
- Engines and Locomotives
- Combustion and Propulsion
- Fossil Fuels
- Carbon Capture
- Control and Automation for Energy
- Environmental Pollution
- Waste Management
- Transportation Sustainability

More information about this series at http://www.springer.com/series/15901

Akhilendra Pratap Singh · Nikhil Sharma ·
Ramesh Agarwal · Avinash Kumar Agarwal
Editors

Advanced Combustion Techniques and Engine Technologies
for the Automotive Sector

Editors
Akhilendra Pratap Singh
Department of Mechanical Engineering
Indian Institute of Technology Kanpur
Kanpur, India

Nikhil Sharma
Combustion and Propulsion Systems
Chalmers University of Technology
Gothenburg, Sweden

Ramesh Agarwal
Department of Mechanical Engineering
and Materials Science
Washington University in St. Louis
St. Louis, MO, USA

Avinash Kumar Agarwal
Department of Mechanical Engineering
Indian Institute of Technology Kanpur
Kanpur, India

Preface

Energy demand has been rising remarkably due to increasing population and urbanization. Global economy and society are significantly dependent on energy availability because it touches every facet of human life and activities. Transportation and power generation are two major examples. Without transportation by millions of personalized and mass transport vehicles and availability of 24×7 power, human civilization would not have reached contemporary living standards.

The International Society for Energy, Environment, and Sustainability (ISEES) was founded at Indian Institute of Technology Kanpur (IIT Kanpur), India, in January 2014 with an aim to spread knowledge/awareness and catalyze research activities in the fields of energy, environment, sustainability, and combustion. The society's goal is to contribute to the development of clean, affordable, and secure energy resources and a sustainable environment for the society and to spread knowledge in the above-mentioned areas and create awareness about the environmental challenges, which the world is facing today. The unique way adopted by the society was to break the conventional silos of specializations (engineering, science, environment, agriculture, biotechnology, materials, fuels, etc.) to tackle the problems related to energy, environment, and sustainability in a holistic manner. This is quite evident by the participation of experts from all fields to resolve these issues. The ISEES is involved in various activities such as conducting workshops, seminars, and conferences,. in the domains of its interests. The society also recognizes the outstanding works done by the young scientists and engineers for their contributions in these fields by conferring them awards under various categories.

Third International Conference on "Sustainable Energy and Environmental Challenges" (III-SEEC) was organized under the auspices of ISEES from December 18–21, 2018, at Indian Institute of Technology Roorkee. This conference provided a platform for discussions between eminent scientists and engineers from various countries including India, USA, Norway, Finland, Sweden, Malaysia, Austria, HongKong, Bangladesh, and Australia. In this conference, eminent speakers from all over the world presented their views related to different aspects of energy, combustion, emissions, and alternative energy resource for sustainable development and cleaner environment. The conference presented five high-voltage plenary talks

from globally renowned experts on topical themes, namely "The Evolution of Laser Ignition Over more than Four Decades" by Prof. Ernst Wintner, Technical University of Vienna, Austria; "Transition to Low Carbon Energy Mix for India", Dr. Bharat Bhargava, ONGC Energy Center; "Energy Future of India", By Dr. Vijay Kumar Saraswat, Honorable Member (S&T) NITI Aayog, Government of India; "Air Quality Monitoring and Assessment in India" by Dr. Gurfan Beig, Safar and "Managing Large Technical Institutions and Assessment Criterion for Talent Recruitment and Retention" by Prof. Ajit Chaturvedi, Director, IIT Roorkee.

The conference included 24 technical sessions on topics related to energy and environmental sustainability including five plenary talks, 27 keynote talks, and 15 invited talks from prominent scientists, in addition to 84 contributed talks and 50 poster presentations by students and researchers. The technical sessions in the conference included advances in IC engines, solar energy, environmental biotechnology, combustion, environmental sustainability, coal and biomass combustion/gasification, air and water pollution, biomass to fuels/chemicals, combustion/Gas Turbines/Fluid Flow/Sprays, Energy and Environmental Sustainability, Atomization and Sprays, Sustainable Transportation and Environmental Issues, New Concepts in Energy Conservation, Waste to wealth. One of the highlights of the conference was the Rapid Fire Poster Sessions in (i) engine/fuels/emissions, (ii) renewable and sustainable energy, and (iii) biotechnology, where 50 students participated with great enthusiasm and won many prizes in a fiercely competitive environment. Two hundred plus participants and speakers attended this four days conference, which also hosted Dr. Vijay Kumar Saraswat, Hon. Member (S&T) NITI Aayog, Government of India, as the chief guest for the book release ceremony, where 14 ISEES books published by Springer, Singapore under a special dedicated series "Energy, environment and sustainability" were released. This was the second time in a row that such significant and high-quality outcome has been achieved by any society in India. The conference concluded with a panel discussion on "Challenges, Opportunities and Directions for National Energy Security," where the panelists were Prof. Ernst Wintner, Technical University of Vienna; Prof. Vinod Garg, Central University of Punjab, Bhatinda; Prof. Avinash Kumar Agarwal, IIT Kanpur; and Dr. Michael Sauer, Boku University for Natural Resources, Austria. The panel discussion was moderated by Prof. Ashok Pandey, Chairman, ISEES. This conference laid out the roadmap for technology development, opportunities and challenges in energy, environment, and sustainability domain. All these topics are very relevant for the country and the world in present context. We acknowledge the support received from various funding agencies and organizations for the successful conduct of the Third ISEES Conference III-SEEC, where these books germinated. We would, therefore, like to acknowledge NIT Srinagar, Uttarakhand (TEQIP) (Special thanks to Prof. S. Soni, Director, NIT, UK), SERB, Government of India (Special thanks to Dr. Rajeev Sharma, Secretary); UP Bioenergy Development Board, Lucknow (Special thanks to Sh. P. S. Ojha), CSIR, and our publishing partner Springer (Special thanks to Swati Meherishi).

The editors would like to express their sincere gratitude to large number of authors from all over the world for submitting their high-quality work in a timely manner and revising it appropriately at a short notice. We would like to express our

special thanks to Dr. Atul Dhar, Dr. Pravesh Chandra Shukla, Dr. Nirendra Nath Mustafi, Prof. V. S. Moholkar, Prof. V. Ganeshan, Dr. Joonsik Hwang, Dr. Biplab Das and Dr. Veena Chaudhary, Dr. Jai Gopal Gupta, and Dr. Chetan Patel, who reviewed various chapters of this monograph and provided their valuable suggestions to improve the manuscripts.

This book is based on advanced combustion strategies and engine technologies for automotive sector. This book includes chapters on advanced combustion technologies such as gasoline direct ignition (GDI), spark assisted compression ignition (SACI), and gasoline compression ignition (GCI). In this book, more emphasis is given on technologies, which have the potential for utilization of alternative fuels as well as emission reduction. One of the most viable solutions in the present scenario for India is the adaptation of methanol as a fuel for automobile sector. Therefore, one section of this book is specially focussed on the techniques for methanol utilization techniques. All authors of this book are among top researchers in their field, and therefore, the piece of information catered herein by their meticulous efforts shall be worth full enough to look into it. We hope that the book would be of great interest to the professionals, postgraduate students involved in fuels, IC engines, engine instrumentation, and environmental research.

Kanpur, India   Akhilendra Pratap Singh
Gothenburg, Sweden   Nikhil Sharma
St. Louis, USA   Ramesh Agarwal
Kanpur, India   Avinash Kumar Agarwal

Contents

Editors and Contributors

About the Editors

Dr. Akhilendra Pratap Singh is working at IIT Kanpur. He received his Masters and PhD in Mechanical Engineering from Indian Institute of Technology Kanpur, India in 2010 and 2016, respectively. His areas of research include advanced low-temperature combustion; optical diagnostics with special reference to engine endoscopy and PIV; combustion diagnostics; engine emissions measurement; particulate characterization and their control; and alternative fuels. He has edited 7 books and authored 21 chapters, 40 research articles in international journals and conferences. He has been awarded with "ISEES Best Ph.D. Thesis Award (2017)," "SERB Indo-US Postdoctoral Fellowship," (2017) and "IEI Young Engineer Award" (2017). He is a member of numerous professional societies, including SAE, ASME, and ISEES.

Dr. Nikhil Sharma joined as a PostDoctoral Researcher at the division of Combustion and Propulsion Systems, Chalmers University of Technology, Sweden, since 2018. Prior to that, he worked as a CSIR Pool Scientist at the Engine Research Laboratory, IIT Kanpur, India. During his doctoral at Indian Institute of Technology Kanpur, he was mainly involved in gasoline spray and particulate investigations from direct injection engines. His areas of research include spray characteristics, exhaust gas after treatment system, particulate filters, and renewable fuels. Till now, he has published more than 15 technical articles in international journals and conference proceedings.

Prof. Ramesh Agarwal is a Professor in School of Engineering & Applied Science, Washington University, St. Louis, the USA. He has received numerous prestigious awards including SAE International Medal of Honor (2015), AIAA Reed Aeronautics Award (2015), SAE Aerospace Engineering Leadership Award (2013), SAE Clarence Kelly Johnson Award (2009), AIAA Aerodynamics Award (2008), Royal Aeronautical Society Gold Award (2007), and ASME Fluids Engineering Award (2001) to name a few. He has published more than 500 peer-reviewed journal/ conference papers and edited several books/ chapters.

Prof. Avinash Kumar Agarwal joined IIT Kanpur in 2001. He worked at the Engine Research Center, UW@Madison, the USA, as a PostDoctoral Fellow (1999–2001). His interests are IC engines, combustion, alternate and conventional fuels, lubricating oil tribology, optical diagnostics, laser ignition, HCCI, emissions and particulate control, and large bore engines. He has published 270+ peer-reviewed international journal and conference papers, 35 edited books, 63 chapters and has 7850+ Scopus and 11900+ Google Scholar Citations. He is an associate editor of ASME Journal of Energy Resources Technology. He has edited "Handbook of Combustion" (five Volumes; 3168 pages), published by Wiley VCH, Germany. He is a Fellow of SAE (2012), Fellow of ASME (2013), Fellow of NASI (2018), Fellow of Royal Society of Chemistry (2018), Fellow of ISEES (2015), and a Fellow of INAE (2015). He is a recipient of several

prestigious awards such as Clarivate Analytics India Citation Award-2017 in Engineering and Technology; NASI-Reliance Industries Platinum Jubilee Award-2012; INAE Silver Jubilee Young Engineer Award-2012; Dr. C. V. Raman Young Teachers Award: 2011; SAE Ralph R. Teetor Educational Award -2008; INSA Young Scientist Award-2007; UICT Young Scientist Award-2007; INAE Young Engineer Award-2005. He received Prestigious Shanti Swarup Bhatnagar Award-2016 in Engineering Sciences.

Contributors

Avinash Kumar Agarwal Engine Research Laboratory, Department of Mechanical Engineering, Indian Institute of Technology Kanpur, Kanpur, Uttar Pradesh, India

Ramesh Agarwal Department of Mechanical Engineering and Materials Science, Washington University in St. Louis, St. Louis, USA

Tushar Agarwal Engine Research Laboratory, Department of Mechanical Engineering, Indian Institute of Technology Kanpur, Kanpur, Uttar Pradesh, India

Rabinder Singh Bharj Department of Mechanical Engineering, Dr. B. R. Ambedkar National Institute of Technology, Jalandhar, India

Sayan Biswas Sandia National Laboratories, Livermore, CA, USA

Aneissha Chebolu Department of Mechanical Engineering, IIT Madras, Chennai, India

Isaac Ekoto Sandia National Laboratories, Livermore, CA, USA

Sreelekha Etikyala Chalmers University of Technology, Gothenburg, Sweden; Volvo Cars Corporation, Gothenburg, Sweden

Vamshi Krishna Gunda Chalmers University of Technology, Gothenburg, Sweden;
Volvo Cars Corporation, Gothenburg, Sweden

Gazala Habib Department of Civil Engineering, Indian Institute of Technology Delhi, New Delhi, India

Jai Prakash Aerosol and Air Quality Research Laboratory, Washington University, St. Louis, MO, USA

Ankur Kalwar Engine Research Laboratory, Department of Mechanical Engineering, Indian Institute of Technology Kanpur, Kanpur, Uttar Pradesh, India

Vikram Kumar Engine Research Laboratory, Department of Mechanical Engineering, Indian Institute of Technology Kanpur, Kanpur, Uttar Pradesh, India

Nirendra Nath Mustafi Department of Mechanical Engineering, Indian Institute of Technology Kanpur, Kanpur, Uttar Pradesh, India;
Department of Mechanical Engineering, Rajshahi University of Engineering and Technology, Rajshahi, Bangladesh

Nikhil Sharma Combustion and Propulsion Systems, Chalmers University of Technology, Gothenburg, Sweden

Akhilendra Pratap Singh Engine Research Laboratory, Department of Mechanical Engineering, Indian Institute of Technology Kanpur, Kanpur, Uttar Pradesh, India

Gurkamal Nain Singh Department of Mechanical Engineering, Dr. B. R. Ambedkar National Institute of Technology, Jalandhar, India

Vishnu Singh Solanki Department of Mechanical Engineering, Indian Institute of Technology Kanpur, Kanpur, Uttar Pradesh, India

Utkarsha Sonawane Department of Mechanical Engineering, Indian Institute of Technology Kanpur, Kanpur, Uttar Pradesh, India

Hardikk Valera Department of Mechanical Engineering, Dr. B. R. Ambedkar National Institute of Technology, Jalandhar, India;
Engine Research Laboratory, Department of Mechanical Engineering, Indian Institute of Technology Kanpur, Kanpur, Uttar Pradesh, India

Part I
General

Chapter 1
Introduction to Advanced Combustion Techniques and Engine Technologies for Automotive Sector

Akhilendra Pratap Singh, Nikhil Sharma, Ramesh Agarwal and Avinash Kumar Agarwal

Abstract To resolve the transportation sector issues such as rapidly increasing petroleum consumption and stringent emission norms for vehicles, researchers have proposed three solution strategies namely advanced combustion techniques, after-treatment systems and alternative fuels. This book covers all three aspects for automotive sector. A dedicated section of this book is based on methanol, which discusses about the methanol utilization strategies in vehicles, especially in two wheelers. Second section of this book is based on advanced combustion techniques, which includes gasoline compression ignition (GCI), gasoline direct injection (GDI), and spark assisted compression ignition (SACI). Fourth section is based on emissions and after treatments systems. Last section of this book includes two different aspects. First is the vehicle lightweighting and second is the development of UAVs for defence applications. Overall this book emphasizes on different techniques, which can improve engine efficiency and reduce harmful emissions for a sustainable transport system.

Keywords Advanced engine techniques · Alternative fuels · Methanol · Emission control

Currently, energy and environment are the two major issues for transportation sector. Rapidly dwindling petroleum reserves are already alarming, which shows the immediate requirement of alternative fuels. Emissions from vehicles also pushing researchers to develop energy efficient and clean combustion techniques (World Health Organization 2018). This book is based on all these aspects related to internal combustion (IC) engines. First section of this book includes one chapter based on introduction of different sections and presents the important aspects of each section.

A. P. Singh · A. K. Agarwal (✉)
Engine Research Laboratory, Department of Mechanical Engineering, Indian Institute of Technology Kanpur, Kanpur, Uttar Pradesh 208016, India
e-mail: akag@iitk.ac.in

N. Sharma
Combustion and Propulsion Systems, Chalmers University of Technology, Gothenburg, Sweden

R. Agarwal
Department of Mechanical Engineering and Materials Science, Washington University in St. Louis, St. Louis, USA

Second section of this book is based on methanol utilization techniques. In India, methanol can be produced from different stray carbon resources such as high ash coal, municipal solid waste (MSW) and low-value agricultural biomass. Indian transport sector, two-wheelers play a dominant role compared to four wheelers (Society of Indian Automobile Manufacturers 2018). Therefore, it is important to develop the technologies for alternative fuel utilization in two wheelers. First chapter of this section discusses about the engine control unit (ECU) calibration process for adaptation of methanol in modern two-wheelers. This chapter covers all the challenges in developing the retrofitment kit for existing electronic fuel injection (EFI) two-wheelers with minimal structural changes for successful M85 adaptation. This chapter primarily deals with the methodology for theoretical and experimental investigations for ECU calibration, which can ensure flawless performance and on-road drivability of M85 fuelled motorcycle. Second chapter of this section discusses the material compatibility of methanol with different engine components because methanol has compatibility issues with soft components of fuel injection systems. In this chapter, various research data were studied and cited to understand material compatibility aspects and engineering challenges for engine parts made of metals, elastomers, and plastics. The corrosion, wear of engine components are studied and suggested the suitable material for the engine parts which are coming in contact with methanol. Last chapter of this section is based on development of M15-fuelled two wheelers. In this chapter, conventional carburetor assisted two-wheelers is described. Carburetor is an essential component of these engines, which delivers the fuel to the combustion chamber however, conventional carburetors are designed to operate with gasoline. Therefore, it become necessary to modify design parameters of carburetor to operate with M15. This chapter deals with these challenges and presents possible solutions for using M15 in carburetor assisted two-wheelers.

Third section of the book is based on advanced combustion techniques. First chapter of this section is based on gasoline compression ignition (GCI) technique, which is a futuristic engine technology that takes advantage of good volatility, high auto-ignition temperature of the gasoline and high compression ratio (CR) of the diesel engine for higher thermal efficiency and lower particulate matter (PM) and NOx emissions (Hao et al. 2016). This chapter discusses about the development aspects and challenges involved in practical implementation of GCI technology in commercial engines. There are several issues such as cold start, high CO and HC emissions, combustion stability at part load, and high combustion noise at medium and full load, which need to be resolved. Detailed discussion about the effect of various control strategies on the GCI engine combustion, performance and emissions, optimum fuel requirement of the GCI engine, and adaption of GCI technique in the modern CI engines are few key aspects of this chapter. Next two chapters of this section describe about the gasoline direct injection (GDI) technique. In last few years, this technology became very popular due to its high power output, thermal efficiency and fuel economy. This chapter introduced different strategies of GDI and reviews the developments in the area of GDI technology. This chapter presents the concluding ways for enhancing the performance, way forward for making it more efficient and reliable by overcoming the limitations of GDI engine technologies.

Third chapter discusses about the utilization of alternative fuels in GDI engine and the effect of these alternative fuels on particulate emissions. It is well known fact the addition of oxygenated additives to gasoline reduces the particulate formation tendency compared to gasoline. This chapter discusses the optimization strategies of combustion by varying the parameters such as spark timing, fuel injection quantity, etc. Discussion on several disadvantages of oxygenated additives has been also included in the chapter. Last chapter of this section discusses about the mixed-mode combustion in which engine is operated in both combustion modes namely spark-assisted compression ignition (SACI), pure advanced compression ignition (ACI) and spark-ignited (SI) combustion. This chapter presents challenges involved with such combined mode operation. This chapter presents the addition of ozone (O_3) to avoid excessive knocking at the boundaries of load-speed map. O_3 addition stabilized combustion by enhancing the reactivity of gasoline, which thereby enabled stable auto-ignition with less initial charge heating.

Fourth section of this book is based on emissions and aftertreatment techniques. First chapter is based on the $PM_{2.5}$ bound trace metals and associated health effects. In this chapter, passenger cars of different age group as Bharat Stage (BS) II, III, and IV and different fuel type such as diesel, gasoline and compressed natural gas (CNG) have been used for PM sampling. These samples were analysed using Induced Coupled Plasma-Mass Spectrometry (ICP-MS) and total 17 trace metals (Al, Ag, As, Ba, Co, Cd, Cr, Cu, Fe, Mn, Ni, Pb, Se, Sr, Ti, V, and Zn) were found in PM. Out of these metals, the non-carcinogenic and carcinogenic risks for adults and children were calculated for 5 metals namely Cr, Mn, Ni, Zn, and Pb. This chapter concluded that the human health risks associated with the exposure to $PM_{2.5}$ emitted from gasoline and CNG vehicles were higher as compared to diesel vehicle. Last chapter of this section is based on application of diesel particulate filter (DPF) for reducing PM emissions to achieve Bharat Stage-VI. Bharat Stage-VI requires ~90% reduction of PM compared to Bharat Stage IV, which can be achieved by using DPF. This chapter deals with the challenges involved with application of DPF in which appropriate size, accurate position in the tailpipe and minimum pressure drop are important. This chapter discusses the comprehensive details of material and regeneration processes used in DPF, including action plan for developing it BS-VI compatible.

Last section of this book includes two chapters. First chapter is based on design and development aspects of unmanned aerial vehicles (UAVs), which can be used in numerous applications such as surveillance, communication, terrain mapping, reconnaissance, and attack, etc. This chapter discusses the application of reciprocating engine as a propulsion system for UAVs. Main objective of this chapter is to discuss the challenges involved in development of IC engine based UAV, which can provide more durability, reliability, and enhance the flight duration. Discussion about different aspects such as structural and thermal analysis of engine components is an important feature of this chapter. Second chapter of this section if based on vehicle lightweighting strategy for improving the engine efficiency and for emission reduction. This technique is based on replacing parts made with heavier materials with lighter materials in order to reduce the overall weight of the vehicle.

This monograph presents the different technologies, which can be used for increasing energy efficiency and lowering the exhaust emissions. Specific topics covered in the monograph include:

- Introduction to Advanced Combustion Techniques and Engine Technologies for Automotive Sector
- Development of Methanol Fuelled Two-Wheeler for Sustainable Mobility
- Material Compatibility Aspects and Development of Methanol-Fuelled Engines
- Prospects of Methanol Fuelled Carburetted Two Wheelers in Developing Countries
- Prospects of Gasoline Compression Ignition (GCI) Engine-Fuel System
- Overview, Advancements and Challenges in Gasoline Direct Injection Engine Technology
- Study on Alternate Fuels and their effect on Particulate Emissions from GDI Engines
- Ozone Added Spark Assisted Compression Ignition
- Emissions of $PM_{2.5}$-bound Trace Metals from On-road Vehicles: An Assessment of Potential Health Risk
- Role of Diesel Particulate Filter to Meet Bharat Stage-VI Emission Norms in India
- Design and Development of Small Engines for UAV
- Automotive Lightweighting: A Brief Outline

The topics are organized in five different sections: (i) General, (ii) Methanol utilization, (iii) Advanced engine technologies, (iv) Emissions and aftertreatment systems, (v) Miscellaneous.

References

Burden of disease from ambient air pollution for 2016. Version 2. Summary of results. World Health Organization, Geneva. http://www.who.int/airpollution/data/en/. Last accessed 26 June 2019

Hao H, Liu F, Liu Z, Zhao F (2016) Compression ignition of low-octane gasoline: Life cycle energy consumption and greenhouse gas emissions. Appl Energy 181:391–398, 1 Nov 2016. (https://doi.org/10.1016/j.apenergy.2016.08.100)

Society of Indian automobile manufacturers, New Delhi; Domestics sales trends 2018. Accessed on 13th May 2019. http://www.siamindia.com/statistics.aspx?mpgid=8&pgidtrail=14

Part II
Methanol Utilization

Chapter 2
Development of Methanol Fuelled Two-Wheeler for Sustainable Mobility

Tushar Agarwal, Akhilendra Pratap Singh and Avinash Kumar Agarwal

Abstract With environmental pollution norms becoming increasingly stringent, there is a need for alternate combustion techniques and alternate fuels to keep up with the changing trends. One of the viable solutions for India is the adaptation of methanol as a fuel for automotive sector. Methanol could be produced from stray carbon resources such as high ash coal, municipal solid waste (MSW) and low-value agricultural biomass, and it can be potentially a good substitute for imported petroleum-based fuels. Methanol has a higher Octane number and emits lower hydrocarbon and NOx. Engine noise and vibrations of methanol-fuelled engines are also relatively lesser than equivalent petrol engines. Further, better fuel properties of methanol lead to higher engine efficiency, which in turn lead to higher well-to-wheel efficiency vis-à-vis gasoline. This chapter covers challenges in developing the retrofitment kit for existing electronic fuel injection (EFI) two-wheelers with minimal structural changes for successful M85 adaptation. In a fuel injection system equipped engine, combustion is primarily governed by Electronic Control Unit (ECU) map, which controls the amount of fuel injected in the cylinder and also the spark timings based on various parameters like engine speed, manifold air pressure, throttle position, engine temperature, intake air temperature, acceleration, altitude etc. This chapter primarily deals with the methodology for theoretical and experimental investigations for ECU calibration, which can ensure flawless performance and on-road drivability of M85 fueled motorcycle.

Keywords Methanol · Electronic control unit (ECU) · ECU calibration · Engine performance · Emissions

2.1 Introduction

Majority of fuels currently used worldwide are of fossil origin, mainly derived from petroleum and coal. Electricity production in the world is dominated by coal while the

T. Agarwal · A. P. Singh · A. K. Agarwal (✉)
Engine Research Laboratory, Department of Mechanical Engineering, Indian Institute of Technology Kanpur, Kanpur, Uttar Pradesh 208016, India
e-mail: akag@iitk.ac.in

automotive industry extensively consumes petroleum-based fuels, mainly gasoline and diesel. According to the BP review, global energy consumption increased by 2.2% in 2017, with petroleum being the most dominant fuel resource (Statistical Review of World Energy 2019). Gaseous fuels and renewables are beginning to be adopted on a commercial scale. Global energy demands are also on at an all-time high. Currently, ~80% of the global population lives in countries having per capita annual energy consumption of fewer than 100 GJ (Carley and Spapens 2017; BP Energy Outlook 2019).

According to the U.S. Energy Information Administration (EIA), India has emerged the 3rd largest primary energy consumer in the world after China and USA since 2016 (BP Statistical Review 2018; World Energy Consumption Clock 2019). Total energy consumption of India is ~572.29 million tons of oil equivalent (MTOE). India is the second top consumer of coal and third top consumer of petroleum in the world. The primary energy source for the transport sector in India is petroleum, which provides ~46% (263.25 MTOE) of the entire primary energy demand of the nation. Out of 263.25 MTOE petroleum-based energy, 213.93 MTOE is imported, which means that ~81.26% of transport energy requirements of the country are met by imported petroleum (Total Energy Consumption in India 2013; ET Bureau 2017). However, if we consider the coal reserves of India, the situation is quite different. According to the International Energy Agency (IEA), India has the world's fourth-largest coal reserves (International Energy Agency 2018). The major problem with Indian coal reserves is that although it has low sulphur content (0.2–0.7%), it suffers from high moisture content (4–20%), high ash content (40–50%) and low calorific value (2500–5000 kcal/kg), making it virtually impossible to use in its raw form for electricity generation. Thus, leaving a large untapped primary energy resource, which is not fully exploited.

With increasingly stringent emission norms and ever-increasing energy demand for transport energy, it is extremely important to find alternatives, which can cater to both of these challenges. For any new fuel to be globally acceptable, it has to be readily available and should have sufficient supply at an economical price. Thus, new alternative fuel should also comply with current and upcoming emission norms. Then, the most important factor is its adaptability in existing vehicles and minimal hardware changes required in the existing energy utilization technology to adapt to this new alternative fuel.

2.1.1 Indian Automotive Sector

According to the Transport Research Wing, Ministry of Surface Transport. Government of India, the total number of registered motorized vehicles in India as on 31st March 2016 was 230 million.[1] The report categories these vehicles as Buses,

---

[1]Transport Research Wing, Ministry of Surface Transport. http://www.mospi.gov.in/statistical-year-book-india/2015/189.

Taxies, Light Motor Vehicles (Passengers), Goods Vehicles (multi-axle/Articulated Vehicles/Trucks and Lorries and light), Two–Wheelers, Cars, Jeeps and Miscellaneous consisting of Three wheelers and agricultural vehicles. The population density in each category is shown in Fig. 2.1 (see Footnote 1). As seen from this data, the two-wheelers dominate the automotive sector with more than 73% market share.

Vehicle production statistics (category–wise) for the year 2016, published by Society of Indian Automobile Manufacturers (SIAM), New Delhi is given in Fig. 2.2,
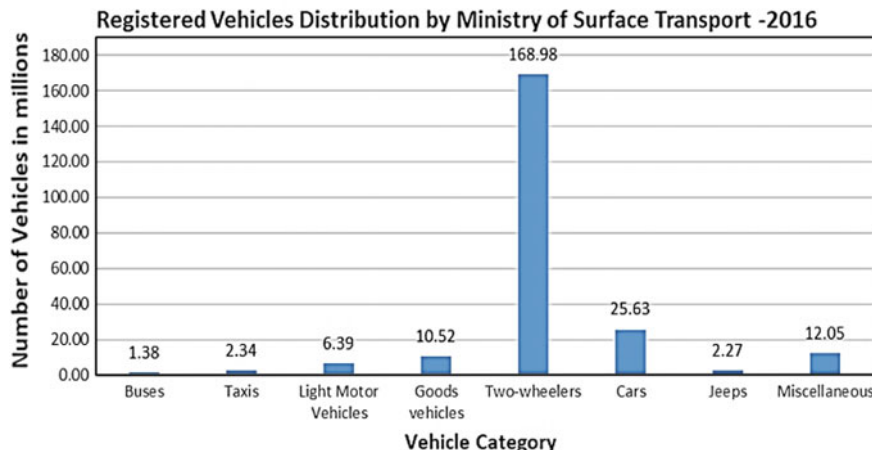

**Fig. 2.1** Registered vehicles in India (2016) (Statistical Review of World Energy 2019)
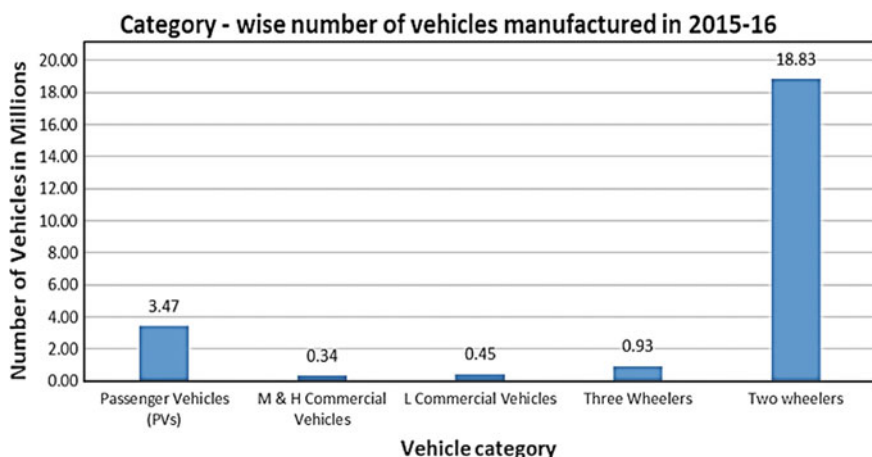
Fig. 2.2 Number of vehicles manufactured in 2015–16 (Society of Indian Automobile Manufacturers 2018)

which shows that at present, the maximum vehicles manufactured and sold in India are two-wheelers (Society of Indian Automobile Manufacturers 2019).

From the above data, it is clear that automotive sector in India is primarily dominated by gasoline-fuelled two-wheelers. Therefore, any reduction in vehicular pollution due to change in existing motorcycle engine technology, or fuel will significantly affect the air ambient air quality in India. Along with this, one has to also keep in mind that the new technology or new fuel should be economical enough to get to the masses and should require minimal changes for retrofitment in the existing engines so that the lead time of changes is relatively small.

2.1.2 Potential Alternative Fuels for Two–Wheelers

Alternative fuels are the fuels, which are not used commercially in the transport sector currently but have potential to be used in the near future. Alternative fuels are non-conventional and advanced fuels, which has constituent substances that can act as an energy carrier for energy conversion in the vehicles. Alternatives to petroleum-based fuels include hydrogen, chemically stored electricity, alcohols etc. A brief description of potential alternative fuels for two-wheelers is given in the following sub-section.

Hydrogen Hydrogen is the cleanest of all fuels. It is a zero-emission fuel, which produces water as a combustion product when burnt in the presence of oxygen. It can be used in internal combustion (IC) engines as a gaseous/liquid fuel and can also be used in electrochemical devices such as fuel cells to produce electricity (Brinner and Philipps 2001). Although hydrogen has many advantages such as clean production from water using renewable primary energy and emissions-free combustion but has several disadvantages and limitations that cannot be ignored. Hydrogen has a very low volumetric energy density of 600 kWh/m^3 at 200 bar storage pressure, which is ~5.5% of gasoline (Brinner and Philipps 2001). Current hydrogen storage methods are very expensive, complicated and unsafe. Hydrogen is an ideal fuel, but it is not freely available. Using current production techniques, hydrogen remains as just an energy carrier and not a primary source of energy. Hence it requires some out of box break through to establish hydrogen as fuel.

Electrical Energy Chemically stored electrical energy in batteries seems to be a potential solution for current transport needs. Renewable energy from solar, wind, hydro etc. can be converted into electricity, which then can be stored in batteries to operate vehicles. However, a major problem with chemically stored electrical energy is the medium of energy storage itself (Brueckner 2018). In India, a company named Ather Energy has successfully launched a battery power scooter with up to 75 km of running a single charge and 0–40 km/h timing just 3.9 s. The company claims a battery life of more than 50,000 km (Hsieh et al. 2002). Worldwide too big giants like Harley Davidson also have come up with their own version of electric motorcycles. In case of the scooter, the vehicle generally uses a hub motor, installed directly on

the wheel of the scooter. While in case of motorcycle, there is a central brushless DC motor (BLDC motor), which is connected to the rear wheel via chain or belt.

Cobalt is an essential part of the lithium-ion batteries used in electric vehicles. Cobalt is available in very few underdeveloped countries, and its resources are rather limited. Cobalt mining heavily relies on child labour in these underdeveloped and poor African countries. Nickel used in battery cells is extremely poisonous to extricate starting from the earliest stage. There are serious environmental concerns and land use clashes associated with lithium mining in nations like Tibet and Bolivia. The metals utilized in battery production are rather limited and in extremely constrained supply. This makes it difficult to cater to any significant number of global transport vehicles using current battery technology. In addition, there is no economical method of reusing and recycling lithium-ion batteries, to recover and recycle scarce metal resources used.

Ethanol Another feasible solution can be the use of primary fuels such as ethanol and methanol. Ethanol can be produced from agricultural products such as sugarcane, corn, potato etc. Advantage of using primary alcohols as fuel is that they can be produced domestically and have the potential to reduce CO and HC emissions (Hsieh et al. 2002). Alcohols tend to be much more efficient and provide cleaner burning characteristics compared to petroleum-based fuels such as gasoline. They have a higher octane rating, which allows dedicated ethanol engines to be designed for higher compression ratios without the fear of knocking. However, the use of ethanol puts additional pressure on the already scarce food availability due to the diversification of land for ethanol feedstock production. Hence, alternate resources to produce alcohols need to be explored for making it a sustainable fuel.

The potential of these alternative fuels for two-wheelers can, therefore, be summarized as follows:

- Hydrogen provides clean burning characteristics, but it is challenging to store and manage and can be potentially unsafe compared to conventional petroleum-based fuels.
- Electric vehicles are zero tailpipe emission vehicles and do not degrade the urban ambient air quality. However, since electricity is mostly produced from the traditional primary source of energy such as coal and gas, the zero-emission claim of EV's is rather meaningless. Also, hazards associated with rare metal mining for manufacturing batteries and hazardous battery disposal pose a significant threat to the environment, making this technology environmentally unsustainable.
- Alcohols seem to be a practical solution for resolving the transport energy crisis. Alcohol adaptation in existing vehicles requires minimal changes in fuel transportation infrastructure as well as in the engine technology. Ethanol seems to be a potential alternative fuel. However, it's limited availability, and agriculture linked production makes it unsuitable for large-scale substitution of petroleum-based fuels such as gasoline.

Above discussion indicates that we can possibly consider primary alcohol, which is not limited by its scarce availability and production for large scale displacement

of gasoline and diesel in the transport sector. One such primary alcohol with large supply potential is methanol. It offers advantages of ethanol in addition to an abundant fuel supply potential. Possibility of methanol as a potential alternative fuel for two-wheelers is discussed in the following section.

2.2 Methanol as a Potential Alternative Fuel for Two-Wheelers

Throughout the history of energy generation from carbon-based sources, there has been a constant move towards low carbon fuels (lower C/H ratio). The transition from firewood to fossilized coal, followed by a transition to petroleum and finally to natural gas currently, suggests the natural adaptation of primary hydrogen-rich fuels such as methanol. Advantages of methanol include lower emissions, improved brake thermal efficiency of the engine and reduced fire hazard due to lower flammability range compared to gasoline. Methanol can be produced from low-value agricultural waste, biomass and other carbon-containing primary sources such as natural gas, coal, etc. Thus, the use of methanol in the transportation sector can potentially reduce India's petroleum imports. According to the Methanol Institute USA, engines operating on methanol show 50% energy-based efficiency gain over gasoline. Methanol is therefore extensively used in motorsports (The Benefits of Methanol as an Alternative Fuel 2019; Ingham 2017).

Surplus methane can be used to produce methanol for transportation while potentially reducing greenhouse emissions (Cheng et al. 2011). The CO_2 produced from methanol combustion is used up by plants and converted back to agricultural waste in a short period of time, which can further be used to produce methanol. Thus, methanol has a much shorter recycling time compared to fossil fuels, making it a renewable fuel. Production of methanol from agricultural and municipal solid waste (MSW) will use these resources, which otherwise are dispensed off to landfills and water bodies or burnt away. All these means are environmentally unfriendly. In addition, ~40% of India's coal reserves consist of high ash coal (40–50%), which cannot be used for power production or any other industrial application (High Ash content 2018; Kurose et al. 2001). This coal can, however, be converted to methanol via gasification process and put to use in the transport sector as fuel.

Unlike CNG or hydrogen, methanol does not require any unique distribution network. It can potentially be dispensed from the existing gasoline and diesel petrol pumps, thus saving a considerable amount of money, circumventing the need to build additional infrastructure. The knowledge of fuel properties is essential to design and engineer the combustion systems, fuel storage systems, and fuel handling and dispensing systems.

Fuel properties affect engine performance, emission and combustion characteristics significantly; hence, it is essential to understand the properties of methanol compared to conventional fuels. Methanol is a colourless, odourless primary alcohol,

Table 2.1 Important fuel properties of methanol compared to other fuels (Man energy solutions, web resource. Accessed on 8 June 2019. https://www.man-es.com/)

Property	Methanol	Ethanol	Diesel	Gasoline
Chemical formula	CH_3OH	C_2H_5OH	C_8-C_{25}	C_4-C_{12}
Carbon (wt%)	38	52	85	86
Hydrogen (wt%)	12	13	15	14
Oxygen (wt%)	50	35	0	0
Molar mass (kg/kmol)	32	56	183	114
Liquid density (kg/m^3)	798	794	840	740
Lower heating value (MJ/kg)	20.1	27.0	42.7	44
Boiling temperature (°C at 1 bar)	65	78	180–360	27–245
Vapour pressure (bar at 20 °C)	0.13	0.059	~0	0.25-0.45
Kinematic viscosity (cSt at 20 °C)	0.74	1.2	2.5–3.0	0.6
Bulk modulus (N/mm^2 at 20 °C, 2 MPa)	823	902	553	1300
Cetane number	<5	8	38–53	–
Octane number	109	109	15–25	90–100
Auto ignition temperature in air (°C)	470	362	250–450	250–460
Heat of vaporization (kJ/kg at 1 bar)	1089	841	250	375
Minimum ignition energy (mJ at $\Phi = 1$)	0.21	0.65	0.23	0.8
Stoichiometric air/fuel ratio	6.5	9.1	14.6	14.7
Peak flame temperature (°C at 1 bar)	1890	1920	2054	2030
Flammability limits (vol.%)	6–36	3–19	0.5–7.5	1.4–7.6
Flash point (°C)	12	14	52	−45

which is a liquid at room temperature and can be handled like other petroleum-based fuels such as gasoline and diesel. Table 2.1 compares some important fuel properties of methanol, diesel, ethanol and gasoline.

Combustion Properties Methanol has a higher auto-ignition temperature compared to gasoline, which makes it safer to transport. Higher auto-ignition temperature means that in case of a CI engine, higher compression ratios can be used, which can potentially lead to a superior BTE (Zhao et al. 2015). The octane rating of methanol (109) is significantly higher as compared to gasoline (90). This allows a dedicated methanol engine to operate at a higher spark advance without knocking. Thus, it can potentially be more thermodynamically efficient and generate higher power output as compared to the similar capacity gasoline engine.

Oxygenated Fuel Methanol has oxygen inherently present in its molecular structure, which is responsible for the reduction in emissions of CO and HC, and it converts them to carbon dioxide (CO_2) and H_2O. Fuel-bound oxygen helps in achieving more complete combustion during expansion stroke (Datta and Mandal 2017).

Latent Heat of Vaporization Methanol has significantly higher latent heat of vaporization compared to gasoline and diesel. Higher latent heat of vaporization of methanol poses some advantages as well as disadvantages. Because of higher latent heat of vaporization, methanol has superior engine cooling characteristics (Wanger et al. 1979). This further improves the fuel efficiency by operating the engine on lean fuel-air mixtures. On the other hand, higher latent heat of vaporization of methanol can potentially lead to poor idling and cold starting issues. If 100% methanol or even methanol-gasoline blends are used in the current generation vehicles without proper adjustments, significant cold starting and drivability issues may be experienced (Hodgson et al. 1998).

Calorific Value Methanol has a lower calorific value compared to baseline gasoline. Thus, higher fuel quantity needs to be injected in order to achieve equivalent brake power output from a similar capacity gasoline engine.

2.3 Challenges of Using Methanol in IC Engines

Although methanol has several advantages over gasoline, its immediate utilization in the IC engines is challenging, since there are several issues, which need to be addressed. In this section, major challenges of using methanol as a fuel in the current generation SI engines are discussed.

Material Compatibility Material compatibility issues of using methanol in the fuel supply systems are prominent (Crowley et al. 1975). Brass and copper containing components are prone to heavy corrosion with the use of methanol. However, synthetic rubber components and seals made of Neoprene and Buna-N are not damaged by methanol (Brinkman et al. 1975). High volatility and affinity of methanol to water hampers engine combustion and performance. When methanol-gasoline blends are stored for extended periods, phase separation of methanol and gasoline can happen, leading to poor drivability of the vehicle (Ingamells and Lindquist 1975). The polarity of methanol is a major reason for its poor material compatibility. Methanol has the tendency to corrode both metals as well as elastomers used in fuel supply systems and engine seals (Crowley et al. 1975). Polarization of methanol molecules causes dry corrosion in metals, which is further reinforced by chloride ion (Cl^-) impurities present in the fuel (Yuen et al. 2010). Methanol is a hygroscopic compound, and after absorbing moisture, it can trigger wet corrosion in metals. Combination of methanol with other impurities such as ethyl acetate, acetic acid and chloride leads to synergistic effects, which may result in a higher degree of corrosion than that from a single impurity (Walker and Chance 1984). Methanol is very aggressive towards copper, aluminum and magnesium, but steel and other ferrous metal are relatively less affected (Bromberg and Cheng 2010). Thus, preferring steel over the aluminum to manufacture components that come in direct contact with methanol, can reduce corrosion related problems to some extent. The Methanol Institute, USA published a

complete list of metals and elastomers that are compatible with methanol and can be used in engines. A careful material selection for manufacturing engine components can resolve the material compatibility issue while using methanol.

Limited Operating Range Methanol (20.1 MJ/Kg) has half the calorific value compared to gasoline (44 MJ/Kg). To quantify, for M85 blend, the engine gets only 52% of the energy of gasoline for the same delivery quantity. This issue can be resolved by using injectors with larger nozzle holes or by injecting a larger fuel quantity per engine cycle to induct the same energy in the engine cylinder. Thus, for the same power output in similar capacity methanol and gasoline-fuelled engines, the quantity of methanol injected should be almost twice as much like that of gasoline injected. To maintain the same range of the vehicle, the fuel tank of a methanol-fuelled vehicle must be about twice as large compared to base gasoline-fuelled vehicle.

Cold Starting Cold starting is another major issue related to methanol utilization. In 1977, Menrad experimented on a single cylinder Volkswagen engine to check the feasibility of methanol fueling of an engine. In this investigation, it emerged that the minimum ambient temperature required for successful methanol (M100) combustion is 10 °C (Menrad et al. 1977). Later, in 1983, Gardiner tried to improve methanol cold-starting by adjusting spark timing and fuel injection phasing. He reported that methanol fuelled engine could not start below 0 °C (Gardiner and Bardon 1983).

Major factors leading to poor cold starting of methanol compared to gasoline are summarized as follows (Nakata et al. 2006; Turner et al. 2012):

Low energy density: Methanol has a lower heating value (20 MJ/kg) as compared gasoline (45 MJ/kg). Hence, compared to gasoline, more methanol quantity needs to be vaporized to form a combustible charge and release an equal amount of heat in an engine cycle.
Latent heat of vaporization: The heat of vaporization of methanol (1089 kJ/kg) is much higher than gasoline (375 kJ/kg). Hence, higher energy investment is required to vaporize methanol for equivalent energy release in an engine cycle.
Single component fuel: Unlike gasoline, methanol is a single component fuel with no presence of readily volatile components. In gasoline, the presence of readily volatile components greatly improves its cold startability.
Electrical conductivity: Methanol is a fairly good conductor of electricity and can cause an electric short-circuit in the spark plug electrodes in case of spark plug wetting, which needs to be taken into account.

Flame Visibility High flame luminosity is one of the major requirements of automotive fuel, from a safety point of view, since it helps in easy detection of flames in case of an accident (Fanick and Smith 1984). Luminosity occurs because of the formation of microscopic soot particles during burning. These carbon particles, when heated to a certain temperature, start emitting light in the visible light region because of 'grey-body' radiation phenomenon (Fanick et al. 1984). During methanol combustion, fewer soot particles are formed as compared to gasoline, due to which it

burns with a very light blue colored flame, which is almost invisible during daylight and therefore it poses significant safety challenge (Keller et al. 1978).

Some of the challenges associated with methanol combustion can be easily resolved by using suitable additives. For example, adding boric acid to methanol gives it a green color to the flame, which is easily visible during daylight (Pearson 1985). Adding volatile compounds like butane or butene can improve also its cold startability (Fanick et al. 1990). Fortunately, both of these issues can be resolved by adding a small quantity of gasoline to the methanol as well. The properties of methanol-gasoline blends in overcoming the limitations of 100% methanol is of great interest and has been discussed in the next section.

2.4 M85: Fuel Properties and Advantages Over M100

Addition of a small quantity of gasoline to methanol, several fuel properties of blend improve, which make methanol fit for use in IC engines. M85 is one such typical and popular methanol—gasoline blend containing 85% v/v methanol and 15% v/v gasoline. In 1990, Fanick conducted a study on the effects of gasoline and other additives on the flame luminosity of methanol (Fanick et al. 1990). He investigated the variations in the luminosity of methanol with increasing concentration of gasoline in methanol-gasoline blends. The flame luminosity of methanol—gasoline blend rapidly increased with increasing gasoline concentration (v/v) beyond 12%. Fanick also compared the luminosity of M85 to other methanol-gasoline blends such as M88, M90 and M92. The luminosity of M85 was significantly higher than 100% methanol, thus making it safe for use in the engines used in the transport sector. M85 has superior visibility even in daylight compared to 100% methanol. Thus M85 is easily detectable in case of an accident.

Apart from increasing the visibility of methanol flame, gasoline also improves its cold startability. Blending gasoline with methanol adds some volatile compounds into the mixture and increases its vapor pressure. On addition of a small amount of methanol to gasoline increases the Reid vapor pressure (RVP) by more than 30%, resulting in values that are higher than those of base gasoline (61 kPa) and 100% methanol (31 kPa) (Andersen et al. 2010). The RVP of methanol blends is higher than that of base gasoline for concentrations up to 80% (v/v). Thus, adding 15% gasoline (v/v) to methanol improves both its flame visibility and cold startability. This makes M85 much safer than methanol to store and transport and also suitable for use in cold climate conditions. Table 2.2 lists the important properties of M85 in comparison with methanol and gasoline.

Table 2.2 Comparative fuel properties of methanol, M85 and gasoline

Property	Methanol	M85	Gasoline
Stoichiometric AFR	6.5	7.62	14.7
Density at 15 °C (g/cm^3)	0.798	0.785	0.753
Latent heat of vaporization (kcal/ kg)	260.7	234	89.96
RON (Research Octane Number)	110	111	100
Reid Vapour pressure (RVP) (kPa)	31	60.4	61

2.5 Methanol Utilization Strategies in Two-Wheelers

Dominance of two-wheelers in Indian automotive market, potentially economical and abundant availability of methanol and clean burning characteristics of methanol clearly show that utilization of methanol in two-wheelers is an effective way for energy diversity in the near future. The next logical question is how to utilize methanol efficiently in two-wheeler engines. Methanol utilization strategy for two-wheelers should preferably be based on light spark-ignited (SI) gasoline engine, which makes it easier to adapt not only to the new generation engines but also to provide a retrofitment solution for the existing engines. Two different fuel injection technologies used in two-wheelers are (a) fuel delivery using conventional carburetors in SI engines, and (b) modern port fuel injected (PFI) electronic fuel injection (EFI) systems. These two technologies are discussed below:

2.5.1 Conventional Carbureted Two-Wheelers

Carburetor is a mechanical device used to mix air and fuel in the required ratio (Air-fuel ratio) in order to prepare suitable charge for combustion in an engine cylinder. A carburetor consists of a float chamber, which acts as a reservoir of fuel at atmospheric pressure. The fuel quantity in the float chamber is maintained at a constant level using a float. As the fuel from the float chamber is consumed, the float comes down, which in turn causes the float valve to open and allow more fuel to flow from the fuel tank to the float chamber.

Once the fuel is in the float chamber, it flows into the venturi through a jet, based on the pressure difference between atmosphere and static pressure inside the venturi. As the engine piston moves from top dead centre (TDC) to bottom dead centre (BDC) during the intake/ suction stroke, vacuum created causes the air to rush into the intake manifold at high velocities depending on the engine speed. Fast-moving air causes reduction in static pressure, leading to fuel flow from the float chamber via venturi to the intake air stream in the carburetor throat.

Although carburetor works well for gasoline engine, it may not be the case for methanol. Technological limitations of carburetor such as lack of dynamic fuel injection timing and absence of temperature or altitude-based compensations, coupled

with poor cold-starting characteristics of methanol may render conventional carbu-
reted vehicles of little application. Another promising technology for utilization of
methanol in two-wheelers is Port Fuel Injection (PFI) System, which is discussed in
the next sub-section.

2.5.2 Modern Port Fuel Injected Two-Wheelers

Modern port fuel injection systems rely on Electronic Control Unit (ECU) for optimal
fuel delivery and spark timings. An ECU is a miniature on-board computer that
controls various actuators of engine. The ECU senses the physical conditions of
the engine and environmental parameters using multiple sensors in the engine bay
and then interprets the data from multi-dimensional performance tables to adjust the
actuators in the engine. Before advent of electronic fuel injection (EFI) systems, air-
fuel mixture, idle speed, ignition timing etc. were mechanically set and controlled
by the carburetor. In EFI systems, airflow continues to be regulated by a butterfly
valve, but the fuel delivery is controlled by the electronic fuel injector. The fuel and
air quantities in an EFI system can therefore be adjusted independently.

As shown in Fig. 2.3, ECU maintains the air/fuel ratio by adjusting various actu-
ators based on the data provided by multiple sensors. These include the inlet air
temperature sensor (IAT), coolant temperature sensor (CT), crank position sensor
(CPS), barometric pressure sensor, manifold pressure sensor (MAP), throttle posi-
tion sensor (TPS) etc. ECU computes the optimum fuel injection duration and the
spark timing. In summary, EFI system enables air—fuel ratio to be adjusted in real
time according to the environmental and the engine power output requirements.

EFI system offers several advantages over conventional carburetors such as lower
fuel consumption, higher power output, enhanced reliability, better cold starting,
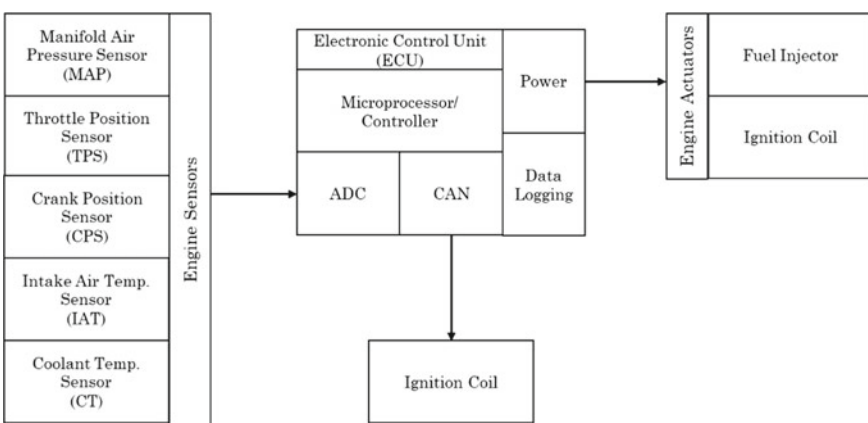
Fig. 2.3 Schematic of an electronic control unit

altitude compensation, etc. The engine management system (EMS) continuously monitors and adjusts the AFR but the carburetors deliver a fuel rich mixture at both low and high-power output. In carburetor, it is challenging to optimize the AFR for all throttle conditions and engine speeds. Altitude/barometric compensation is challenging to achieve with carburetors, whereas in the EFI system, altitude compensation is done by measuring the actual atmospheric pressure using on-board sensors and the injected fuel quantity is accordingly adjusted. EFI systems are significantly reliable as compared to carburetors. Arbitrary engine stops, spark plug wetting, high exhaust emissions and other problems due to sub-optimal AFR are also taken care of by the EFI system. Carburetors tend to go out of tune, which requires periodic adjustments, which induces the risk of failure. EFI systems, on the other hand, continuously adjust themselves and remain tuned.

2.5.3 Case-Study of Carburetor Versus PFI Systems in Two-Wheelers

A comparative study of a 125 cc motorcycle engine equipped with a carburetor and another one with an electronic port fuel injection system is discussed below. In 2012, researchers from Robert Bosch GmbH conducted an experimental and numerical study for comparing carburetor and EFI systems on a motorcycle engine (Schuerg et al. 2012). The experiments were conducted on a single cylinder motorcycle engine with the details given in Table 2.3.

Both engine configurations were tested on four test cycles: World Motorcycle Test Cycle (WMTC), Indian Drive Cycle (IDC), Malaysian Cycle and Bangalore Cycle. The EFI configuration delivered better fuel economy compared to carburetor in both chassis dynamometer tests and simulations at different temperatures. The EFI system had a closed loop lambda control, which adjusted the fuel quantity with changing driving conditions and maintained the air – fuel ratio close to the stoichiometric value at all times.

In a study conducted by Latey et al. a single cylinder carbureted two-wheeler engine was converted into a methanol (M20) fuelled port fuel injection (PFI) engine

Table 2.3 Comparison of electronic fuel injection Versus carburetion systems in a two-wheeler (Schuerg et al. 2012)

	Electronic Fuel Injection	Carburetion
Engine	Single Cylinder, air cooled, four stroke, two valves	
Engine volume	125 cc	
Power Output	11.6 bhp at 8000 rpm	11 bhp at 8000 rpm
Torque generated	11.2 Nm at 6250 rpm	11 Nm at 6500 rpm

(Latey et al. 2005). The experiments were performed on a single cylinder, naturally aspirated, 350 cc motorcycle engine using M20 (20% v/v methanol and 80% v/v gasoline). It was observed that operating engine hardware of the EFI system produced higher power and provides superior fuel economy compared to the carburetor (Latey et al. 2005). EFI system provided significantly higher power than carburation system for the same engine.

2.6   Tools for ECU Calibration

An electronic control unit (ECU) is a mini computer that controls the various actuators in an internal combustion engine to ensure smooth running and optimal performance of the engine. The production vehicles with a locked ECU in which the calibration settings and performance tables come pre-configured by the automobile manufacturer. The user cannot access or modify the program installed in such kind of ECU's. Another category of the electronic control unit is programmable ECUs, which can be reconfigured by the user. When an engine is modified for alternate fuel, stock ECUs can't automatically make the required fuel compensations. To account for the engine modifications, an open ECU is used to replace stock ECU. The performance tables are modified based on engine sensor data, and by monitoring the air/fuel ratio from exhausts using a wideband lambda sensor. This process is carried out at an engine performance facility using engine and chassis dynamometer. Engine dynamometer provides useful data such as engine speed, torque output, power output, gear change events, etc. A chassis dynamometer is used for street and other high-performance applications. Engine calibration parameters include fuel injection duration, fuel injection timing, spark timing, throttle-fuel volume mapping, engine load-fuel volume mapping etc. An open ECU is also equipped with a data logger to record sensor data and ECU out-puts for performance analysis. This is useful to monitor engine stalls, misfires or other undesired behaviors during street trials.

2.6.1   Engine Dynamometer

The overall experimental setup of engine dynamometer was divided into three parts: test engine and dynamometer assembly, instrumentation for generating gasoline base fuel maps and ECU recalibration setup. Experiment setup for engine dynamometer testing and calibration is shown in Fig. 2.4. The test engine was mounted on a three degree of freedom cast iron base and coupled to an eddy current engine dynamometer via chain-sprocket arrangement. The engine is pre-equipped with various sensor such as crank position sensor, throttle position sensor, manifold air pressure sensor, ambient air temperature sensor and engine temperature sensor.

The data from these sensors was used by the stock ECU to adjust the fuel injection duration and spark timings by actuating the fuel injector and ignition coil accordingly.
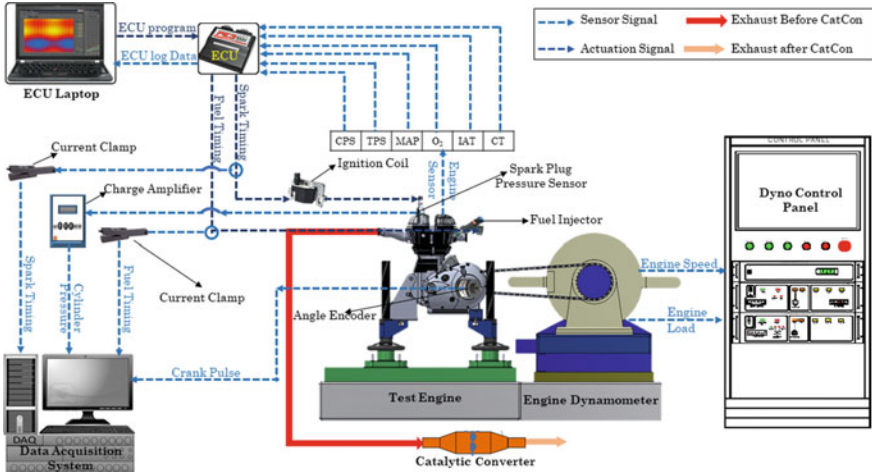
Fig. 2.4 Schematic of engine dynamometer test setup

The dynamometer applied the resistive force on the test engine for simulating the road load driving conditions. To reverse engineer the stock ECU gasoline maps, a combustion analyzer was used to measure various engine parameters such as engine speed, spark timing, fuel injector duration and throttle opening. For interfacing the engine with the combustion analyzer, minor changes were made in the engine. Stock spark plug of engine was replaced with a spark plug pressure transducer to sense the in-cylinder pressure during the intake and power strokes. Crank shaft of the engine was extended out of left-hand side crank case cover (LH cover) in order to facilitate installation of a precision angle encoder for measuring the engine crankshaft rotation. To measure the spark timing and fuel injection duration, spark plug and fuel injector input cables coming from the ECU were tapped using current clamps.

To recalibrate the ECU for M85, stock ECU was replaced with an open ECU. No changes were in the engine wiring harness though. The open ECU was controlled using a laptop connected to the ECU via an ethernet cable. ECU measured the engine speed, throttle opening, intake manifold pressure, lambda value and engine temperature using suitable sensors. Based on these values, it calculates the injector open time and the spark timing, and accordingly actuated the ignition coil and fuel injector.

2.6.2 Chassis Dynamometer

Chassis Dynamometer experimental setup can be divided into three sections: Dynamometer room, Controller room and Underground (Fig. 2.5). Dynamometer
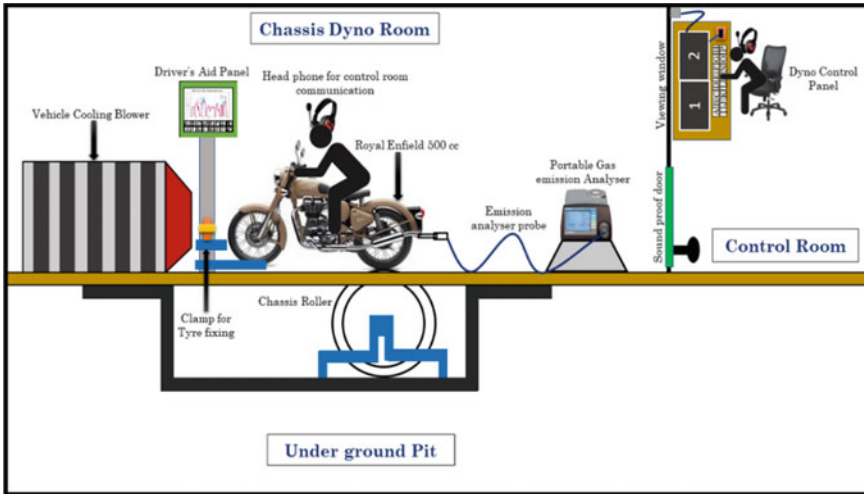
Fig. 2.5 Schematic of chassis dynamometer test setup

room consists of a checkered base plate covering the underground pit. A small portion of classis roller pops out of this checkered base plate, on which the rear/ driving wheel of two-wheeler rest. Front wheel of the motorcycle is pneumatically clamped to the test bed. The motorcycle is securely attached to the test bed using restraining cables at multiple locations for safety. Dynamometer room is equipped with a driver aid panel, which displays important test parameters such as vehicle speed, drive gear and test cycle graph. This information is used by the rider to accordingly control the throttle, brake and drive gear of the motorcycle. To cool the motorcycle and to simulate air resistance to the vehicle during actual road driving condition, a three-phase heavy-duty blower with variable frequency drive is used. The speed of air coming from the blower is synchronized with the motorcycle speed for accurately simulating the road driving conditions. For tailpipe emission analysis, a portable raw emission analyzer is used.

The dynamometer room and the controller room are separated by a double pane glass window for easy communication between the vehicle rider and dynamometer control operator. Rider and dynamometer control operator can additionally communicate via head phones too. The operator feeds testing cycles into dynamometer control panel and logs the test results to the computer.

The underground pit houses an AC regenerative motor for simulating the vehicle load conditions. This regenerative motor is connected to chassis roller, on which the driving wheel of motorcycle rests. All the wirings of the cooling blower, driver aid panel and AC regenerative motor are routed through underground trenches such that the checkered base plate seats are mounted flush with the dynamometer room floor.
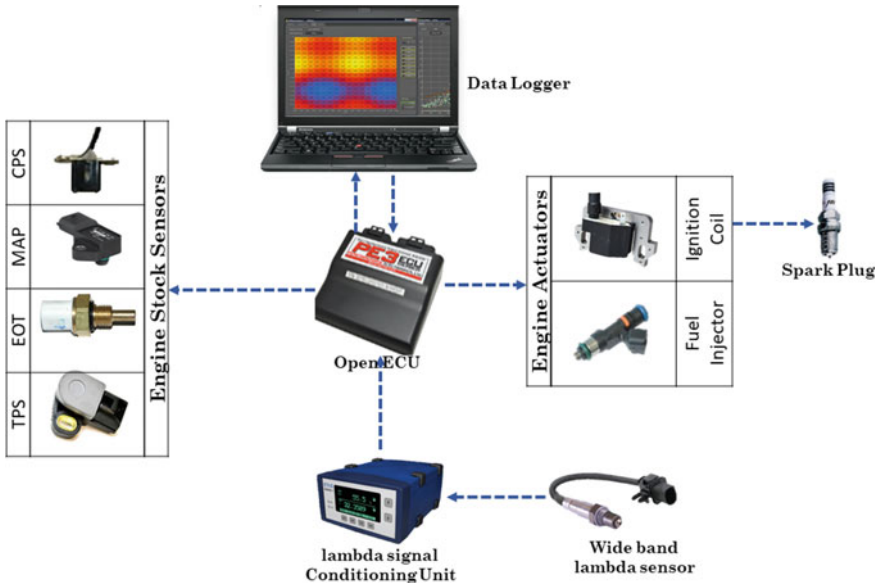
Fig. 2.6 ECU calibration tools

2.6.3   Instrumentation for ECU Calibration

For ECU calibration, most of the stock engine sensors and actuators are used as it is, except ECU and lambda sensor. Narrow band lambda sensor is replaced by a wide band lambda sensor, which is connected to lambda signal conditioning unit. The stock ECU is replaced by reprogrammable open ECU, which is connected to a data logger via an Ethernet cable. The data logger hosts the ECU calibration software required for ECU programming and interfaces with the wideband lambda sensor module and other host of sensors and actuators as shown in Fig. 2.6.

2.6.4   Open ECU

Open ECU is a category of the electronic control units, which is reprogrammable by the user. When an engine is modified for alternate fuel, stock ECUs can't automatically make the required fuel compensation. To account for engine modifications, an open ECU is required to replace stock ECU. Recalibrating an ECU requires interfacing the unit with a data logger; this interfacing is necessary so the data logger can transfer the engine calibration settings to the ECU as well as monitor the engine parameters in real-time. It comes with preview software and calibration tool. The entire unit is protected in a water-resistant aluminum case, with highly rugged automotive-grade connectors.

2.6.5 Wide-Band Lambda Sensor and Conditioning Unit

It is essential to determine the inlet fuel-air mixture strength inside the combustion chamber so that one can get a fair idea about the in-cylinder combustion process and emissions from the engine, which varies with varying λ. For measuring the fuel-air mixture ratio inside the combustion chamber, a wideband lambda sensor is required, which measures the amount of oxygen present in the exhaust gas. A wide-band lambda sensor is a planer zirconium dioxide (ZrO_2) marginal current sensor with integral heater. It consists of a combination of Nernst type potentiometric oxygen concentration cell (sensor cell) and an amperometric oxygen pump cell transporting oxygen ions. Nernst cell has the property that at a higher temperature, as soon as there are partial oxygen pressure differences on both ends of its ceramic, oxygen ion starts diffusing through the ceramic.

The transport of ions results in generation of electrical voltage signal between them, which is measured by the sensor. This voltage signal is then used to determine the amount of unused oxygen present in the engine exhaust. The voltage generated by the sensor cell depends on the difference in the amount of oxygen present in the exhaust with the ambient oxygen. The output from the lambda sensor goes to the lambda signal-conditioning module for calculation of various parameters such as oxygen content, lambda, air-fuel ratio etc.

2.7 ECU Calibration Strategies

ECU calibration is an extensive process of determining the most optimum calibration maps for engine operation. It is a multistep process, which involves designing tests, data collection and analysis, and reconfiguring ECU maps to optimize engine combustion. ECU calibration helps in tuning the engine for optimal performance, emissions and thermal efficiency, creating a balance for best combustion strategy. Figure 2.7 gives a brief outline of the entire ECU calibration process for M85 adaptation

2.7.1 Engine Setup in Calibration Software

Before undertaking the actual calibration of the engine on a chassis or engine dynamometer, there are some essential initial setups required in the ECU calibration software, which are shown in Fig. 2.8.

Engine: In this tab, important physical parameters of the engine such as number of cylinders, primary load control strategy (TPS or MAP), crank position sensor used, cam position sensor used and configuration (Even fire or Odd fire), are defined. In
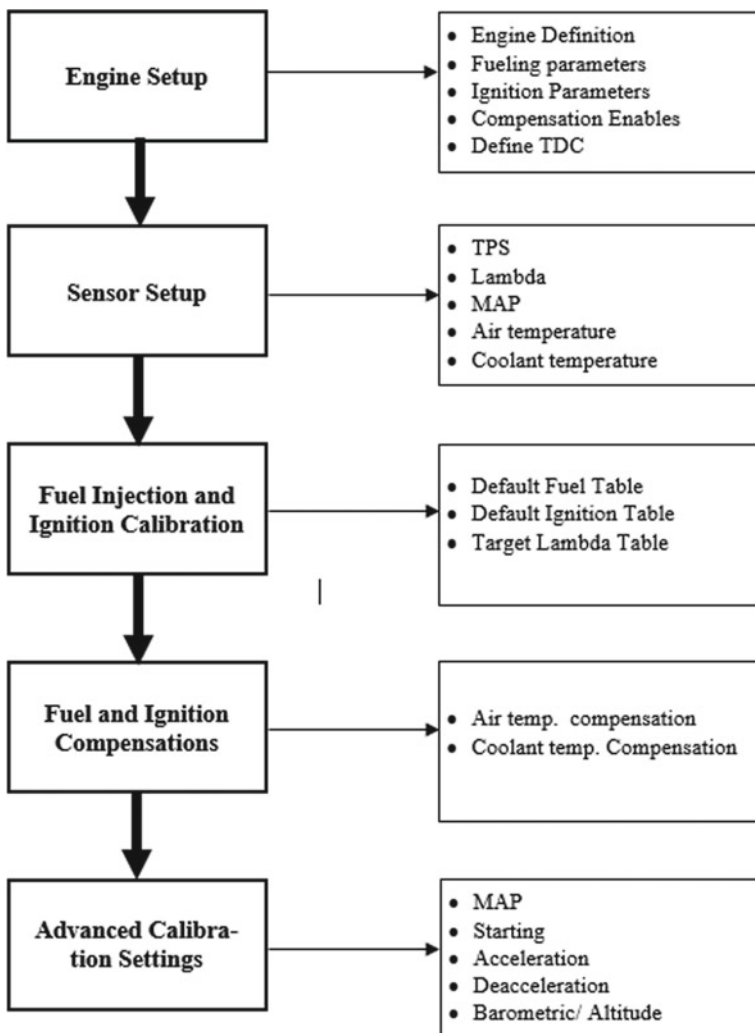
Fig. 2.7 ECU calibration process flow diagram

this study, load control strategy is based on TPS, because in a single cylinder engine, MAP sensor value is highly unstable and cannot be used for calibration.

Fuel: In this tab, fuel injection mode (Sequential, semi sequential, throttle body or random sequential) for engine operation is selected. Since in this study, a single cylinder engine with port fuel injection is used, any injection strategy can be used. Results will be the same for all of them.
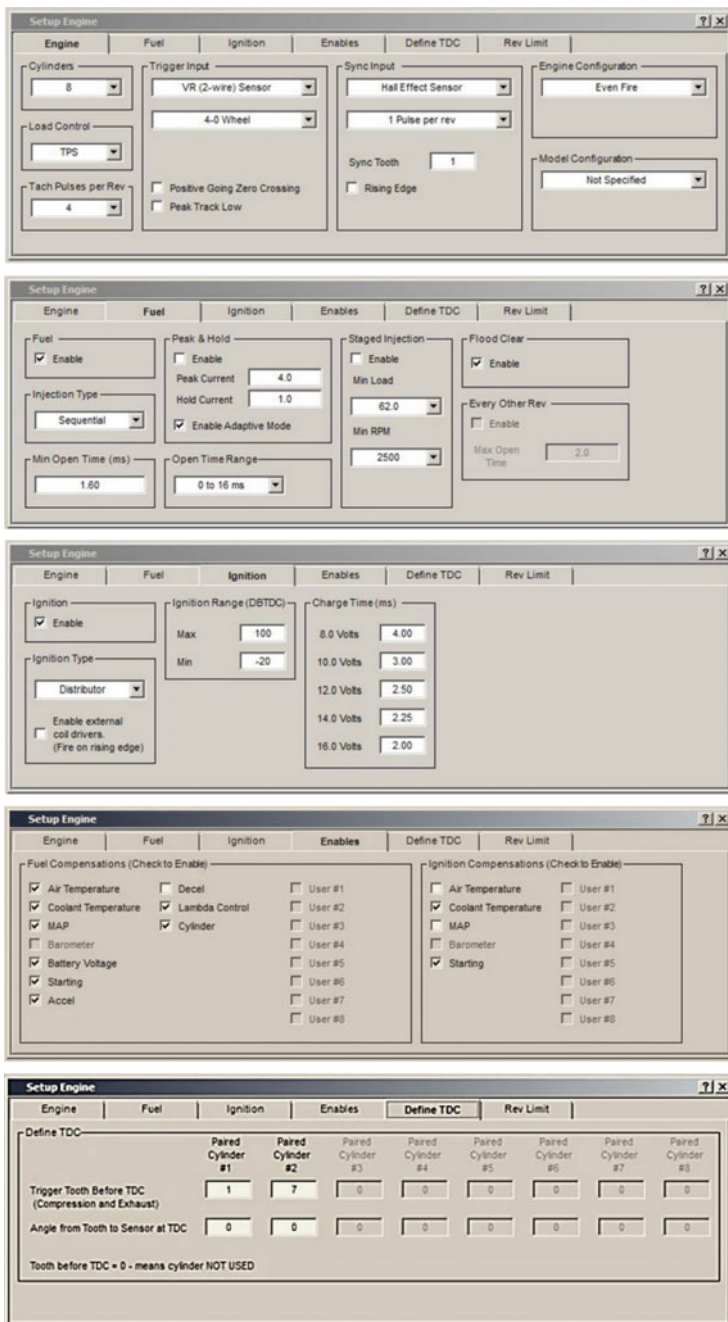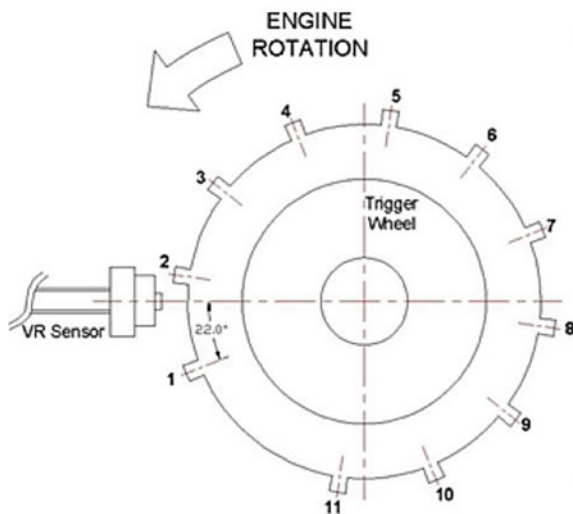
Fig. 2.8 Engine configuration in 'Setup Engine' menu

Fig. 2.9 Crank position
sensor and TDC sensor
configuration

Ignition: The most important parameter of this tab is 'Ignition Type'. The options available in this tab are:

- Distributor: Firing order is controlled by distributer
- Wasted Spark: Ignition coil is fired whenever the ECU sense TDC (both during intake TDC and power stroke TDC); and
- External coil driver: Ignition coil is triggered whenever rising edge of external trigger is sensed at input pin.

Enables: This tab gives centralized location to switch on/off different engine tuning parameters for fuel and ignition compensation. The final injector open time and spark timings are calculated by the ECU based on the settings enabled in this tab. Each of these parameters has to be individually calibrated for the engine.

Define TDC: This tab is used to configure the ECU for different Sync and trigger patterns. By defining 'Angle from tooth to sensor at TDC' and 'Trigger tooth before TDC,' it knows when TDC occurs.

This generally works with missing tooth configuration denoted as m-n, where m is total number of teeth and n is the number of missing teeth. The ECU registers the first tooth after missing tooth as #1 and then counts the subsequent teeth. The trigger wheel and crank position sensor for 12-1 configuration is shown in Fig. 2.9.

2.7.2 Sensor Setup in the Calibration Software

The sensors are electronic devices, which convert the changes in the physical parameter into electrical signals. Prior to use, sensors have had to be calibrated based on
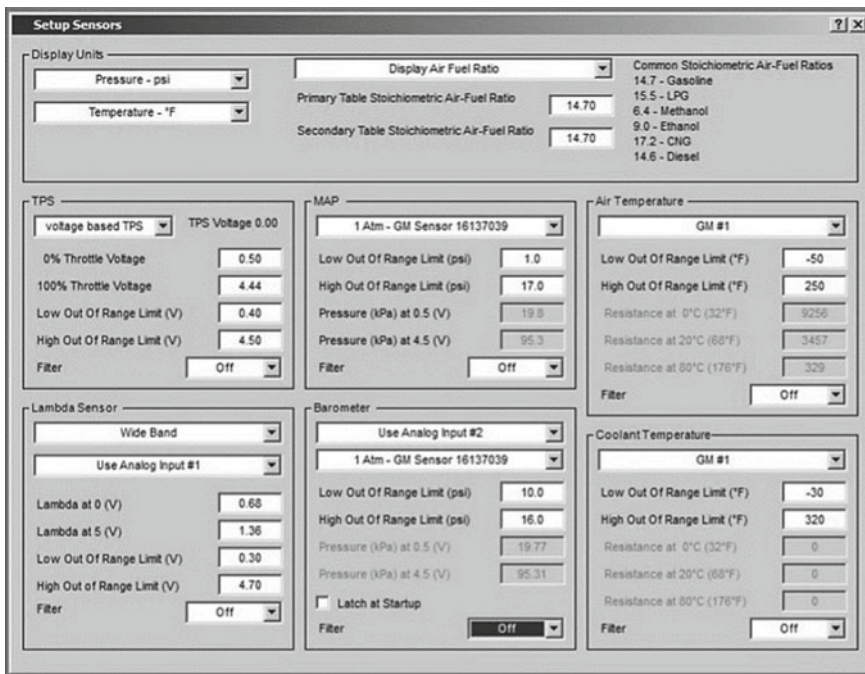
Fig. 2.10 Sensors configuration in 'Setup Sensors' window

known physical principles and its corresponding electrical signals. In this window, the calibration values of all the sensors used in the engine are registered. The ECU contains a directory of commonly used sensors along with their calibration settings. If the calibrator is using one of those sensors, we can choose that sensor from the drop-down menu, otherwise sensor has to be first calibrated on a suitable test rig and then the calibration values are to be entered in the table. PE ECU used for this study has inbuilt signal conditioning algorithms, which are used to filter the sensor data and remove any unwanted noise (Fig. 2.10).

2.7.3 Fuel Injection and Ignition Calibration

The steady state calibration is done by modifying the primary fuel and ignition tables. These look-up tables set the base fuel requirement and spark timings of the engine. These tables are 3-D charts with engine load (in the base table, it is either TPS based or MAP based depending on the calibrator) on the X-axis and engine speed on the Y-axis. Whereas the Z-axis defines the value of injector open time or ignition timing. An example fuel table is shown in Fig. 2.11.

Engine Data												
RPM	0	Water	64 °F	Tps	8 %	Fuel/Rev	0.00 ms	Duty	0 %	U2 Ign	-2°	
Map	14.5 psi	Air	68 °F	Battery	13.9V	Ignition	0.0°	U1 Fuel		U3 Off	Off	

Fuel Table - Injector Open Time per Revolution (ms) of Bank #1

Rpm

	0	1000	2000	3000	4000	5000	6000	7000	8000	9000	10000	11000	12000	13000	14000	15000
15.2	2.438	2.438	2.438	2.438	2.563	2.688	2.813	2.938	3.125	3.250	3.000	2.813	2.625	2.438	2.250	2.000
14.3	2.250	2.250	2.250	2.375	2.500	2.625	2.813	2.938	3.063	2.875	2.625	2.438	2.250	2.063	1.875	
13.4	2.125	2.125	2.125	2.125	2.250	2.375	2.500	2.625	2.750	2.813	2.688	2.500	2.313	2.125	1.938	1.750
12.5	2.000	2.000	2.000	2.000	2.125	2.188	2.313	2.438	2.563	2.625	2.500	2.313	2.125	2.000	1.813	1.625
11.5	1.813	1.813	1.813	1.813	1.938	2.063	2.125	2.250	2.375	2.438	2.313	2.125	2.000	1.813	1.688	1.563
10.6	1.688	1.688	1.688	1.688	1.813	1.875	2.000	2.063	2.188	2.250	2.125	2.000	1.813	1.688	1.563	1.438
9.7	1.563	1.563	1.563	1.563	1.625	1.750	1.813	1.875	2.000	2.063	1.938	1.813	1.688	1.563	1.438	1.313
8.8	1.375	1.375	1.375	1.375	1.500	1.563	1.625	1.688	1.813	1.875	1.750	1.625	1.500	1.375	1.313	1.188
7.9	1.250	1.250	1.250	1.250	1.313	1.375	1.438	1.563	1.625	1.688	1.563	1.438	1.375	1.250	1.125	1.063
7.0	1.125	1.125	1.125	1.125	1.188	1.250	1.313	1.375	1.438	1.500	1.375	1.313	1.188	1.125	1.000	.938
6.1	.938	.938	.938	.938	1.000	1.063	1.125	1.188	1.250	1.313	1.188	1.125	1.063	.938	.875	.813
5.2	.813	.813	.813	.813	.875	.930	.930	1.000	1.063	1.125	1.000	.930	.875	.813	.750	.600
4.2	.688	.688	.688	.688	.688	.750	.813	.813	.875	.875	.875	.813	.750	.688	.625	.563
3.3	.500	.500	.500	.500	.563	.563	.625	.625	.688	.688	.688	.625	.563	.563	.500	.438
2.4	.375	.375	.375	.375	.375	.438	.438	.500	.500	.500	.500	.438	.438	.375	.375	.313
1.5	.313	.313	.313	.313	.313	.313	.313	.313	.313	.313	.313	.313	.313	.313	.313	.313

3.250

0.313

9.7 —— 8.8 —— 7.9 ——

Add | 1.0000 | Subtract | Multiply | 1.20 | Divide | Smooth

Fig. 2.11 Primary fuel table

As seen in the table, the engine speeds and loads are at discrete intervals. All the values in between are calculated based on the four-point interpolation method, as seen in red color. The block moves in the table based on engine speed and load, as sensed by the various engine sensors. This red block along with Cross-hairs (green color cross) aids the calibrator in the tuning process. The values of injector open-time and spark timings BTDC can be modified by the user in many ways. The values can be directly entered by selecting a particular cell. If more than one cell is selected; the same value is set for all those cells. In addition to that, user can also use Multiply, Divide, Subtract and Add buttons from the console. Once the default tables are set, calibration process is started for engine idle tuning and freezing lambda value for Idling, which is generally 0.86–0.88. After that, start ignition timing calibration is done to freeze the ignition timing with highest engine torque output. Along with it, spark plug pressure transducer and combustion analyzer are used to ensure that there is no pinging/ knocking tendency.

Once the ignition map is calibrated for each throttle positions and engine speed, fuel maps are calibrated. For fuel map calibration, vehicle is operated on chassis dynamometer at constant speed. Then injector open time is calibrated for each throttle position at that engine speed to obtain maximum power output. Once the fueling is set for each throttle position for that particular engine speed, one moves to next engine speed in the fuel table and repeat the process. With this, the base engine calibration in completed and calibrator can move to various types of compensations such as lambda, air temperature, altitude, acceleration, deceleration, battery voltage compensations.
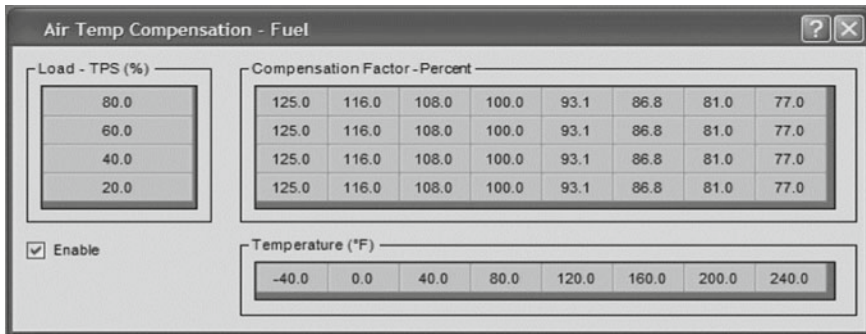
Fig. 2.12 Air temperature compensation tab

2.7.4 Fuel and Ignition Compensations

Air Temperature Compensation (Fuel): With change in air temperature, its density also changes. Cold air is denser; hence requires more fuel quantity for optimal combustion. An example of intake air temperature calibration window is shown in Fig. 2.12. For intake air temperature compensation, the vehicle is operated at Idle below −20 to 120 °C in a temperature-controlled chamber and after every 3 min interval, the value of lambda is logged. Based on the logged AFR, air temperature compensation is such that $\lambda = 1$ for all temperature conditions. Once the temperature calibration is done for idling, the same process has to be repeated for different values of the throttle positions.

Coolant Temperature Compensation (Fuel): For this compensation, the vehicle is operated on the chassis dynamometer at a constant speed of 60 kmph, keeping the throttle value constant at 20, 40, 60 and 80%. For each throttle opening, value of engine temperature is logged at a step of 40oC along with its corresponding lambda value. Now based on the lambda, fuel compensation factor is adjusted in the coolant temp compensation table. Typical coolant temp compensation table is shown in Fig. 2.13.

Starting Compensation: At the time of start, the engines require some extra fuel. For methanol, the cold start is even more important because of its poor vaporization characteristics. For cold start calibration, the vehicle is cranked at pre-defined temperature and maintained at 0% throttle until lambda becomes equal to 1. Then throttle in suddenly increases to 5% and then engine response is noted. This test is performed at −10, −5, 0, 5 and 10 °C. For each test, engine response is qualitatively noted and based on that, fuel compensation factor is adjusted. Starting compensation factors are shown in Fig. 2.14.

Acceleration compensation: Acceleration compensation increases the injector open time, whenever the throttle is increased rapidly. If acceleration compensation is not calibrated, the engine runs lean until steady state is achieved. This results in poor drivability and substandard throttle response. In extreme cases, it may also read to

Coolant Temp Compensation - Fuel

Load - TPS (%)

80.0
60.0
40.0
20.0

Compensation Factor - Percent

160.0	150.0	140.0	130.0	120.0	110.0	100.0	100.0
160.0	150.0	140.0	130.0	120.0	110.0	100.0	100.0
160.0	150.0	140.0	130.0	120.0	110.0	100.0	100.0
160.0	150.0	140.0	130.0	120.0	110.0	100.0	100.0

☑ Enable

Temperature (°F)

-40.0	0.0	40.0	80.0	120.0	160.0	200.0	240.0
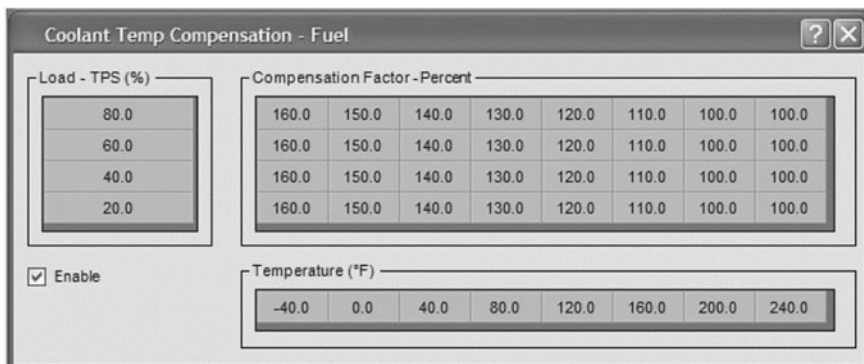
Fig. 2.13 Coolant temperature compensation tab

Starting/Accel/Decel Compensation

Starting - Fuel

☑ Enable

0 °F (%)	300.0
* 80 °F (%)	250.0
160 °F (%)	150.0
240 °F (%)	105.0
Duration (revs)	20
Fuel Starting RPM	400
Initial Fuel Pulse (ms)	5.0

* value used if no sensor defined

Starting - Ignition

☑ Enable

Timing (deg)	10.0
Ignition Starting RPM	400

Accel

☑ Enable

Type	TPS ▼
min TPS rate (%/sec)	20.0
min TPS (%)	2.0
Max Factor (%)	170.0
Duration (sec)	0.5
Max RPM	7000

Decel

☑ Enable

| min TPS (%)	1.0
max RPM	5000
RPM Delta	250

**Fig. 2.14** Starting/Acceleration/Deceleration compensation tab

Fig. 2.15 Battery/Barometer compensation

engine stall. In acceleration compensation, ECU injects extra fuel into the engine, based on the rate of change of throttle. This compensation is calibrated based on the actual driver feedback on the track. Various factors, which need to be addressed in acceleration compensation are shown in Fig. 2.15.

Deceleration compensation: Deceleration compensation has nothing to do with engine performance. It is a feature used to increase the fuel economy of the vehicle. This compensation enables Deceleration Fuel Cut-Off (DFCO), when the throttle is less than 'TPS min', and engine speed is higher than 'Max RPM'.

Altitude Compensation: As the vehicle goes to higher altitudes, the ambient air density decreases, hence engine requires less fuel to operate. To compensate for changing altitudes the ECU needs to be calibrated in a pressure-controlled chamber on an engine/chassis dynamometer.

Battery Voltage: Battery compensation in necessary to account for increasing injector deadtime (time between ECU output pulse and injector opening) with decreasing battery voltage.

References

Andersen VF, Anderson JE, Wallington TJ, Mueller SA, Nielsen OJ (2010) Vapor pressures of alcohol-gasoline blends. Energy Fuels 2010 24(6):3647–3654. Publication Date 21 May 2010. https://doi.org/10.1021/ef100254w

BP Statistical Review (2018). Accessed on 13 May 2019. https://www.bp.com/en/global/corporate/energy-economics/statistical-review-of-world-energy.html

BP Energy Outlook 2019 Edition (2019). Accessed on 13 May 2019. https://www.bp.com/content/dam/bp/business-sites/en/global/corporate/pdfs/energy-economics/energy-outlook/bp-energy-outlook-2019.pdf

Brinkman et al (1975) Exhaust emissions, fuel economy and driveability of vehicles fueled with alcohol-gasoline blends. SAE paper 750120

Brinner A, Philipps F (2001) Hydrogen as the fuel of the future—production; purification; storage. In: Conference proceeding of Motor & Umwelt 2001, Graz, 6–7 Sep 2001

Bromberg L, Cheng WK (2010) Methanol as an alternative transportation fuel in the US: options for sustainable and/or energy-secure transportation. Sloan Automotive Laboratory, Massachusetts Institute of Technology, Cambridge, MA, 02139. Accessed on 24 May 2019. https://afdc.energy.gov/files/pdfs/mit_methanol_white_paper.pdf

Brueckner M (2018) Why the electric vehicle revolution will bring problems of its own (7 Apr 2018). www.phys.org. Accessed on 13 May 2019. https://phys.org/news/2018-04-electric-vehicle-revolution-problems.html

Carley M, Spapens P (2017) Sharing the world sustainable living and global equity in the 21st century

Cheng Y-P, Wang L, Zhang X-L (Jan 2011) Environmental impact of coal mine methane emissions and responding strategies in China. Int J Greenhouse Gas Control 5(1):157–166. https://doi.org/10.1016/j.ijggc.2010.07.007

Crowley AW, Kuebrich JP, Roberts MA, Koehl WJ, Wascher WL, Wotring WT (1975) Methanol-gasoline blends performance in laboratory tests and in vehicles. SAE paper 750419

Datta A, Mandal BK (2017) Effect of alcohol addition to diesel on engine performance, combustion and emission characteristics of a CI engine. In: International conference on advances in mechanical, industrial, automation and management systems (AMIAMS), Allahabad, pp. 110–114. https://doi.org/10.1109/AMIAMS.2017.8069198

ET Bureau (June 2017) Oil consumption grows fastest in India. Accessed on 13 May 2019. https://economictimes.indiatimes.com/industry/energy/oil-gas/indias-oil-consumption-grows-at-fastest-pace-in-14-months/articleshow/62896084.cms

Fanick ER, Smith LR (1984) Survey of safety related additives from methanol fuel. Report No. EPA 46013-84-01 6, Contract No. 68-03-31 62 Work Assignment 5, Nov 1984

Fanick ER, Smith LR, Baines TM (1984) Safety related additives for methanol fuel. SAE paper no. 841378, Fuels and lubricants meeting and exposition, Baltimore, MD, Oct 1984. https://www.osti.gov/biblio/5925150

Fanick ER, Smith LR, Russell JA, Likos WA, Ahuja M (1990) Laboratory evaluation of safety-related additives for neat methanol fuel. Published by SAE International, SAE Transactions 99(Section 4). J Fuels Lubr, pp 992–1002. https://www.jstor.org/stable/44580432

Gardiner DP, Bardon MF (1983) Department of Mechanical Engineering Royal Military College of Canada Kingston, Ontario; Cold starting tests on a methanol fuelled spark ignition engine; SAE International, Technical Paper 831175, ISSN 0148-7191. https://doi.org/10.4271/831175

High Ash content (2018) Ministry of coal, press information Bureau, Government of India, 03 Jan 2018. Accessed on 13 May 2019. http://pib.nic.in/newsite/PrintRelease.aspx?relid=175272

Hodgson JW, Irick DK, Margaret V, Whalen (1998) Improving the cold start performance of alcohol fueled engines using a rich combustor device. Published 4 May 1998 by SAE International in United States. https://doi.org/10.4271/981359

Hsieh WD, Chen RH, Wu TH, Lin TH (Jan 2002) Engine performance and pollutant emission of an SI engine using ethanol-gasoline blended fuels. Atmos Environ 36(3):403–410. https://doi.org/10.1016/S1352-2310(01)00508-8

Ingamells JC, Lindquist RH (1975) Methanol as a motor fuel or a gasoline blending component. SAE paper 750123

Ingham A (2017) Reducing the carbon intensity of methanol for use as a transport fuel. Johnson Matthey Technol Rev 61(4):297. https://doi.org/10.1595/205651317x696216

Keller JL, Nakaguchi GM, Ware JC (July 1978) Methanol fuel modifications for highway vehicle use. U.S. Department of Energy, Washington, D.C., HCPM13683-18, July 2018. https://books.google.co.in/books?id=5qCbrG1cb08C&dq=Methanol+Fuel+Modifications+for+Highway+Vehicle+Use&lr=&source=gbs_navlinks_s

Kurose R, Ikeda M, Makino H (Aug 2001) Combustion characteristics of high ash coal in a pulverized coal combustion. Fuel 80(10):1447–1455. https://doi.org/10.1016/S0016-2361(01)00020-5

Latey AA, Bhatti TS, Das LM, Gajendra Babu MK (2005) Methanol blended fuel investigations on an injected single cylinder spark ignition engine. Published 19 Jan 19 2005 by The Automotive Research Association of India in India, Technical paper 2005-26-031, ISSN 0148-7191. https://doi.org/10.4271/2005-26-031

Market Report Series: Coal 2018 (2018). Analysis and Forecasts to 2023, International Energy Agency. https://webstore.iea.org/market-report-series-coal-2018

Menrad H, Lee W, Bernhardt W, Volkswagenwerk AG (Germany) (1977) Development of a pure methanol fuel car. SAE International, Technical Paper 770790, ISSN 0148-7191. https://doi.org/10.4271/770790

Nakata K, Utsumi S, Ota A, Kawatake K, Kawai T, Tsunooka T (2006) Toyota motor corporation. The effect of ethanol fuel on a spark ignition engine. Published 16 Oct 2006 by SAE International in United States, Technical Paper 2006-01-3380, ISSN 0148-7191. https://doi.org/10.4271/2006-01-3380

Pearson RS (1985) An improved calcium flame test. University of Arkansas at Monticello, Monticello, AR 71655

Schuerg F, Prashanth A, Raatz T—Robert Bosch GmbH, Dani C, Manikandan K, Padmanabhan V–Robert Bosch India Ltd (2012) Experimental and numerical comparison of fuel economy for 125 cc motorcycles with carburettor or electronic port fuel injection based on different drive cycles. Published 23 Oct 23 2012 by SAE International in United States, Technical Paper 2012-32-0067, ISSN 0148-7191. https://doi.org/10.4271/2012-32-0067

Society of Indian Automobile Manufacturers (2019) Domestics sales trends 2018, New Delhi. Accessed on 13 May 2019. http://www.siamindia.com/statistics.aspx?mpgid=8&pgidtrail=14

Statistical Review of World Energy (2019). Accessed on 13 May 2019. www.bp.com

The Benefits of Methanol As An Alternative Fuel (2019). Accessed on 13 May 2019. https://www.methanol.org/automotive-fuel/

Total Energy Consumption in India (2013). https://www.eia.gov/beta/international/analysis.php?iso=IND&src=home-b6

Turner JWG, Pearson RJ, Ramsay JM, McGregor MA—Lotus Engineering, Dekker M—BioMCN, Iosefa B—Methanex Corporation, Dolan GA—Methanol Institute, Johansson K, Bergström Kac—Saab Automobile Powertrain AB (2012) GEM ternary blends: testing iso-stoichiometric mixtures of gasoline, ethanol and methanol in a production flex-fuel vehicle fitted with a physical alcohol sensor. Published 16 Apr 2012 by SAE International in United States, Technical Paper 2012-01-1279, ISSN 0148-7191. https://doi.org/10.4271/2012-01-1279

Walker MS, Chance RL (1984) Corrosion of metals and the effectiveness of inhibitors in ethanol fuels. SAE International, SAE Transactions 92(Section 4):831406–831830, (1983), pp 1170–1174. https://www.jstor.org/stable/44647843

Wanger et al (1979) Practicality of alcohols as motor fuel. SAE Trans 88(Section 2):790267–790526, pp 1591–1607. https://www.jstor.org/stable/44658167

World Energy Consumption Clock (2019). Accessed on 13 May 2019. www.usdebtclock.org/energy.html

Yuen PK, Villaire W, Beckett J (2010) Automotive materials engineering challenges and solutions for the use of ethanol and methanol blended fuels, (General Motors). SAE International, Technical Paper 2010-01-0729. https://doi.org/10.4271/2010-01-0729

Zhao Z, Lakshminarayanan N, Swartz SL, Arkenberg GB, Felix LG, Slimane RB, Choi CC, Ozkan US (2015) Characterization of olivine-supported nickel silicate as potential catalysts for tar removal from biomass gasification. Appl Catalysis A: General 489:42–50

Chapter 3
Material Compatibility Aspects and Development of Methanol-Fueled Engines

Vikram Kumar and Avinash Kumar Agarwal

Abstract   The environmental concern and the financial markets over the global scale, alternative fuels were developed to substitute convention fuel. Methanol is a substitute for conventional fuel which can be used in an Internal Combustion (IC) engine. Methanol is an alternative fuel for IC engines in terms of environment and economical aspect. It is renewable, economically, and environmentally interesting. A sustainable strategy is proposed to use methanol in the internal combustion engine in various ranges of concentration. In this chapter, various research data were studied and cited to understand material compatibility aspects and engineering challenges for engine parts made of metals, elastomers, and plastics. The fuel chemistry and quality effects on the engine are discussed. The effects of methanol on the various components of internal combustion engines are studied. The corrosion and wear of engine components are studied and suggested the suitable material for the engine parts which are coming in contact with methanol. The implementations of methanol in spark ignition engine and compression ignition are studied. The engineering path-way of the implementation and design is explained in detail. The design of different engine components such as engine head, fuel injection system, fuel pump, after treatment for methanol fuelled engines are studied and suggested. The vehicle adaptation for methanol fuel is also studied.

Keywords Methanol · Corrosion · Wear · IC engine

3.1   Introduction

In the contest of the current automotive engine landscape, there is a requirement of an alternative viable source of energy. Alternative fuels are a substitute for the convention source of energy in the global prospects for engines. Alcohols are an alternative renewable source of energy which led to full-scale evolution and implementation as fuel in the engine which can operate at different percentages. Among

V. Kumar · A. K. Agarwal (✉)
Engine Research Laboratory, Department of Mechanical Engineering, Indian Institute of Technology Kanpur, Kanpur, Uttar Pradesh 208016, India
e-mail: akag@iitk.ac.in

the alternative fuels, biofuels are one of the examples of such type of development in the world scenario. Alcohol fueled engine is an IC engine which can run at a different percentage of methanol or ethanol and fuel can be stored in the same tank. These engines can burn any fraction of alcohol with conventional fuel by using controlling fuel injection timing i.e. by varying injection stretegies and methods.

Currently, methanol is used as an alternative fuel in various applications, and its trial was demonstrated in the early nineties. It is composed of coal, biomass, and renewable source of energy by carbon capturing and its scheme of utilization. It is a viable fuel having strong potential to cut down the carbon footprint of fossil fuel in the transport sector. It is used as a fuel blend or pure form in internal combustion engines. Thus methanol is a most attractive fuel as an alternative to conventional fuel as its qualities like making, liquid fuel, easy to store and distribution. The physical and chemical properties of convention fuel (gasoline), methanol, and ethanol are compared, as shown in Table 3.1. Methanol application in internal combustion engine increases the brake thermal efficiency hence enhances the energy utilization (Nichols 2003). It produces higher hydrocarbon and reduced NO_x and soot in exhaust gas

Table 3.1 Physical and chemical properties of gasoline methanol and ethanol (Yates et al. 2010)

Property	Gasoline	Methanol	Ethanol
Chemical formula	C4–C12 and H10–H26	CH_3OH	C_2H_5OH
Density (STP) (kg/m$^{3)}$)	740	790	790
Vapour density (STP) (kg/m^3)	3.88	1.42	2.06
Boiling point at 1 bar (°C)	25–215	65	79
Heat of vaporization (kJ/kg)	180–350	1100	838
Surface tension (@20°C) (mN/m)	21.6	22.1	22.3
Dynamic viscosity (@20 °C) mPas	0.6	0.57	1.2
Molecular weight (kg/kmol)	107.00	32.04	46.07
Oxygen content by mass (%)	0.00	49.93	34.73
Hydrogen content by mass (%)	14	12.58	13.13
Carbon content by mass (%)	86	37.48	52.14
Lower heating value (MJ/kg)	42.90	20.09	26.96
Higher heating value (MJ/kg)	48.00	22.88	29.85
Volumetric energy content (MJ/m^3)	31,745	15,871	21,291
Stoichiometric AFR (kg/kg)	14.70	6.50	9.00
Stoichiometric AFR (kmol/kmol)	54.49	7.33	14.33
Specific CO_2 emissions (g/MJ)	73.95	68.44	70.99
Specific CO_2 emissions relative to gasoline	1.00	0.93	0.96
Autoignition temperature (K)	465–743	738	698
Adiabatic flame temperature (K)	2275	2143	2193

emission than convention fuel (Shamun et al. 2016). Thus it has advantages like sustainability, energy security, and air quality point of view.

Methanol chemical structure (CH_3OH) contains oxygen which separates from convention fuel and causes wear or degradation and corrosion of engine components. Therefore engine parts components which come in contact with fuel are required to upgrade. As the current fuel price increased day-by-day, it is necessary to reduce by applying other fuel without changing the operational cost. The engine parts (fuel pump, engine valves, engine valve seats, fuel, and oil sealing materials) upgradation is necessary for compatibility of methanol (Hagen 1977).

In this study, methanol application as fuel in the internal combustion engine and the effect of methanol on the materials of engine components are elaborated in detail. The engine modification and design of methanol-fueled engine components are also studied.

3.2 Material Compatibility Issues for Methanol

The polarity of methanol leads to the challenge regarding material compatibility, which needs the changes in the fuel system of engines. Metals and elastomers used in fuel systems are attacked by methanol if the proper material selection is not done. Amongst alcohol methanol is most aggressive. Methanol and wet methanol are corrosive to iron, steel, magnesium, aluminum, zinc, copper and their alloys. Anodized aluminum is corrosion resistant to methanol (West and McGill 1992). Some rubber and plastic materials are sensitive to methanol, but there are some polymers which are not affected by methanol.

3.2.1 Fuel Chemistry and Quality Issues

Chemical structure and quality of fuel is important for the compatibility of the fuel delivery systems. Fuel delivery system is affected by the chemistry of fuel. The material testing of the components with methanol is necessary for the durability of the fuel delivery system. Methanol is very reactive with coating materials like aluminum oxide or aluminum. The reactions of methanol with aluminum and their oxides are as follows

$$6CH_3OH + Al_2O_3 \ \rightarrow \ 2Al(OCH_3)_3 \ + \ 3H_2O \tag{3.1}$$

The reaction product, methoxide salts are soluble in methanol. Aluminum also react with methanol to form methoxide.

$$6CH_3OH + 2Al \ \rightarrow \ 2Al(OCH_3)_3 \ + \ 3H_2 \tag{3.2}$$

The quality of fuel is very important for the robustness of the fuel delivery components. Impurities present in fuel would also affect the fuel delivery systems. For example injector operations are very much affected by sulfates, which are recorded as deposits in fuel injector and filter plugging (ASTM Standard 2009; Dumont et al. 2007; Devlin et al. 2005). Corrosion because of impurities like chlorides, and peroxides which are formed due to copper, would affected the elastomers seals and fuel delivery system, fuel economy, and emissions (Dumont et al. 2007; Brinkman et al. 1994). Hence, fuel specification of methanol should be improved.

3.2.2 Corrosion

Alcohols exposed to ferrous metals cause more corrosion than conventional fuels. Generally, corrosion is due to the impurities such as formic acid, acetic acid, and chlorides. Contaminant like chloride ion, formic acids present in alcohols causes enhanced corrosion (Walker and Chance 1983). Ethyl acetate, acetic acid and chloride ion all three together are more prone to corrosion than a single one. Formation of formic acid and acetic acid in alcohol fuel are common during combustion and enhance their corrosiveness. Methanol or ethanol which absorbed water make them electrically conductive, and any contaminant containing ions increases their conductivity, which enhances the electrochemical and galvanic corrosion. Azeotropic water present in alcohol causes the wet corrosion which oxidizes most of the metals (Brink et al. 1986). Methanol or ethanol and absorbed water enhanced the electrical conductivity of alcohol, resulting in higher corrosion. Organic contamination, such as formic acid enhances the corrosiveness of exhaust gases produced by alcohol combustion. Formic acid is an alcohol combustion product which brings down the corrosion temperature below the dew point of the engine exhaust gas. Peroxides are the alcohols combustion product, which increases the corrosion growth due to the alcohol combustion product. Metals like magnesium, aluminum, and lead are more susceptible to alcohol attack, which causes corrosion (Dela Harpe 1988). Contaminant in alcohol fuel enhanced the corrosion of the fuel handling system and also corrosiveness of combustion product. The main corrosion outcome is hydrated ferrous chloride, and it enhances the rust formation (Otto et al. 1986, 1988). Metals in contact with alcohols are prone to stress corrosion failure. The crack formed in fuel line enhances the corrosion possibility as metal exposes to alcohol.

Wing et al. (1993) have studied the corrosion of steel and aluminum substrate and also coated with a moderate and high percentage of phosphorus electroless nickel (chemical plating of nickel) for the gasoline and gasoline/methanol fuel test. The test was carried for the gasoline as reference fuel and gasoline with 15 and 85% of methanol for pure substrate and coatings. The electroless coatings over aluminum and steel and anodized aluminum exhibited the best corrosion protection under test conditions. Anodizing is an electrochemical process in which the metal surfaces are converted into an anodic oxide that is corrosion-resistant and highly durable. So these coatings can be used for methanol-fueled engines (Table 3.2).

Table 3.2 Corrosion performance methanol-fueled engine for different materials and coatings (Saarialho et al. 1982)

Material/fuel	15% Methanol	85% Methanol
1010 steel	Moderate corrosion rate	High corrosion rate
Base 1010 steel coated with phosphorous nickel	Excellent corrosion protection	Excellent corrosion protection
304 stainless steel	Moderate corrosion rate	Higher corrosion rate
356 aluminum	Corroded the substrate	Corroded the substrate
356 aluminum with phosphorous nickel	Protected from corrosion	Little corrosion
Anodized 356 aluminum	Protected from corrosion	Little corrosion

3.2.3   Wear

Alcohols used as an alternative fuel causes the wear of metallic components. Wear of engine component is a very detracting concern, and numerous investigations have been performed to understand their sensitivity. Application of methanol as fuel in IC engine enhanced the wear of engine components. This is due to the formation of corrosive combustion products, which causes a reduction of oil films thickness. The intermediate combustion product such as formic acid promotes the wear of engine cylinder liner and piston ring assembly (Naegeli et al. 1997). Corrosion of piston ring and cam follower with the application of 15% blends of ethanol and methanol with conventional fuel (E15 and M15) is causes a significant amount of wear. The wear of engine components due to gasohol is firmly related to the corrosion of those components.

3.2.4   Components Affected by Methanol

Many engine components are affected by using alcohol and their blends as fuel. The compatibility of components material like metal or plastic or elastomers is studied. These components are fuel pumps, seals, fuel tanks, injectors, piston rings, pistons, engine cylinders, valves and valve seats. Fuel pump material must be changed or upgraded to enhance the fuel flow rate because the alcohols and their blends have lesser heating value. The fuel electrical conductivity increases when alcohol is used, so the fuel level sender (consist of an electrical resister) is upgraded or changed. The fuel line materials (metal or polymer) are affected by alcohols presence in the fuel. The improper material selection causes the wear, degradation, and corrosion of engine components and results in the fuel leaks. Therefore, engines are at higher risk by using alcohol fuel and material compatibility and hardware robustness are under suspects. The materials used in engine components (fuel injectors, fuel rails, and their seals) are influenced by the application of alcohols as a substitute fuels for

IC engine. The other engine parts like cylinder head, piston rings, valve seat, engine valve, intake manifold, intake port, and various oil seals are also affected by the use of alcohols. Wear of some components increases due to combustion characteristics (peak pressure, temperature, emissions etc.) and the use of different fuels.

3.2.5 Fuel Handling

Material selection and design of fuel systems must be taken care when alcohols are used in the engine as fuel. Design of metallic components in contact with alcohol is very critical for fuel composition variation, thermal, and pressure effect. Different metals have been selected for the design of fuel tanks, fuel lines, fuel filters, level sensors, fuel pumps, pressure control valves, the liquid containing sensors, regulators and fuel modules. The metallic components materials and their design have been changed according to materials changing regulations. Many older designs which were according to conventional fuel should be validated for alcohols and modified by protective coating for methanol. So, optimal designs of components for alcohol fuels are taken care for the sustainability of methanol. The review of protective coating and metals used is necessary for the application of alcohols. Compatibility of components material is taken care of all ranges of operating conditions.

3.2.6 Fuel Tank Assembly

Compatibility of material and their corrosion resistance properties was considered for the application of alcohol as a fuel. Fuel tank materials are made of carbon steels, which are corroded by alcohols application. These carbon steels fuel tanks are coated with coating materials which are not reactive with alcohols. The coating materials are compatible and withstand for a long duration. These coatings should also fill the spout and filler pipes. This area is attacked by alcohol fuels.

3.2.7 Fuel Supply Assembly

Fuel tube bundles are another important part of the engine by which fuel is transported to or from the engine. It includes the feed line, the return line, and any other component attached to the fuel pipe bundle. These components are fuel composition sensors, liquid pressure sensors, fuel filters, and quick connect. These components are made of austenitic stainless steel, and also some of them are of made of carbon steel coated with anti-corrosion materials. The small amount of other materials used to the components affects the components when alcohol fuels are used. There may be a chance of corrosion by using alcohol, if interior part of the tube is not taken

care by applying appropriate coatings. Thus the interior parts become an issue of corrosion origination and damage the materials. The coating materials may be nickel or zinc-alloy based.

3.2.8 Fuel Pump Module

Fuel pumps are made of many materials. Fuel pump contains many components such as float arms, springs, fuel filters, pressure regulators, electrical terminals, flanges and polymer flanges filled with metals. Metals used in fuel pump assembly are coated steel, stainless steel, aluminum, copper, silver, gold, palladium, and platinum. Design details and material selection are necessary for the application of alcohol as an alternative fuel. The older fuel pump systems are incompatible for alcohol fuel exposure and affect the performance of the system and greatly reduced the life of the component.

The internal component of the fuel pump system is also considered when alcohol fuel is used in the engine as fuel. It contains electrical contact, armature, motor features, and pumping section. Materials used in these components are aluminum, copper, and zinc and these materials are very reactive with alcohols. The electrical devices used to reduce the electronic noise produced by the electric motor of the fuel pump are a major concern by using alcohols and taken care. These components and their joining (solder or weld) and electrical leads should be protected by a coating or enclosing the whole subassembly into an encapsulation. A compatible coating must be applied to the armature and points where they are attached. The copper commutator face used in brush type motor is replaced with the carbon to avoid degradation in alternator by use alcohol fuels. Another option is the selection of brushless motor for fuel pump systems. Another part of the fuel pump system is pumping section, which is to be studied. Pumping section material is an aluminum plate which is used in turbine style pumping and protected. The application of ionized aluminum which is sealed has no issue degradation with the application of alcohols. Unprotected aluminum causes premature wear and degradation when exposed to alcohol. The old type of pump design (vane style or gear style with unprotected steel pumping section) is modified for the higher durability with the application of alcohol fuels (Galante-Fox et al. 2007).

Materials for fuel filter and pressure regulators are major challenges for the use of alcohol fuel in the engine. The moisture present in the alcohol fuel is accumulating in the fuel filter when the fuel pump system is inactive. There is a generation of the static field in the presence of fuel which is electrically conductive cause corrosion of components. The corrosion of the pressure regulator is avoided by using a good quality seal, and pressure is maintained when the pump is on. Fuel pressure regulator and fuel filters are made of austenitic stainless steel to avoid corrosion. The old design materials of filters and regulator are stainless steel and zinc coated carbon steel respectively which is changed according to the alcohols fuel compatible materials. The other components of fuel pump systems materials are changed according to

alcohol compatible materials. These components are springs, guide rods, float arms, electrical terminals, wires, and level sensor contacts and their compatibility with alcohol fuel must be reviewed. These parts are generally made of austenitic steel and wires and terminals are protected from alcohol by insulation and tin plating, respectively. The terminal of level sensors is also taken care as a small electrical load generates stress on terminals and causes corrosion when exposing to alcohol (Matthias and Thomas 2009). Other challenges of a modern fuel pump are high voltage electrical interface. Improperly timed motor cause the wear of carbon brushes which in contact with carbon or copper commutator of the armature. Thus electrical connector design is such that electrical cross-talk should be avoided which lead to terminal corrosion by application of alcohol fuel.

3.2.9 Fuel Rails and Injectors

Most of the fuels contacting parts are made of stainless steel. These components which handle fuels are fuel injectors and fuel rails. Generally, stainless steel is corrosion resistant but not corrosion proof with alcohol as fuels (Shifler2009; Scholz and Ellermeier 2006). Presence of chloride contamination, which is easily soluble in alcohol may cause the corrosion and at stressed point cause the corrosion cracking. Fuel delivery components experience higher stress in spark ignited direct injection technology than conventional port injection due to higher fuel pressure. Many researchers have studied that aluminum components exposed to alcohol are corroded significantly (Yuen et al. 2010; Priyanto 2017). Thus the improper design of material and aluminum components which are direct contact with alcohol exhibited problem and should be taken care of. Aluminum fuel delivery pipes are corroded in the presence of moisture in alcohol fuels. The rust of corroded components may plug the injectors and causes the rough running of the engine. The continuous operation of the engine, the corrosion of fuel rail increased, and pin holes may develop resulting leakage of fuel rails. The dry corrosion is due to the reaction between aluminum and alcohol. Thus alcohols may cause dry corrosion as well as wet corrosion of the fuel components so, the material robustness is optimized.

3.2.10 Engine Valve and Valve Seat

There is a significant amount of valve wear and increase of insert of the valve seat due to the application of alcohols as a substitute for gasoline. So the appropriate materials for the valve train design and materials are selected to meet the end-user life expectations. Various parameters are taken into account for the selection of materials. These parameters are machinability, wear resistance, tribo-oxidative wear, and corrosion of the metal materials and also have a higher cost. Several paths have been used to make the valve seat. These paths involve higher tool steel percentage in

powder metal mixture and inclusion of powder metal components like molybdenum and cobalt in powder metal technology of sintering. With the use of alcohol, there is a possibility of wear of valve face and valve seat and lead to an engine misfire.

3.3   Methanol-Fueled Engines

Methanol is used in an internal combustion engine as fuel in many ways such as direct injection of methanol in the combustion chamber or by mixing with conventional fuel. Mixing of methanol with convention fuels is taken place inside combustion chamber or outside combustion chamber. Blending of methanol with diesel or gasoline is performed for outside mixing, however methanol is injected in port fuel injection.

3.3.1   Methanol Application in Spark Ignition Engine

As methanol is resistance to auto-ignition due to lower in-cylinder temperature, and also the higher auto-ignition temperature cause resistance to knocking. However, properties of methanol in terms of output power, efficiency, and emission are similar to spark ignited engine. Methanol is suitable fuel for spark ignition engines as it has high heat of vaporization and also high autoignition resistance Table 3.1. It can be used as a blend with gasoline or in pure form. Methanol can also be used as an octane booster for gasoline to avoid the knocking as it has a high octane number and also lowers the combustion temperature. Engine modification for a lower percentage of methanol as blend in spark ignition engine operation is not necessary. Caution is required for using the splash blending of methanol with gasoline as the pump is not tailored for methanol in the fuel blend causes higher volatility and resulting fuel evaporation. The volumetric content of energy is necessary for the design of the fuel injection system and fuel tank. As the methanol volumetric content of energy is half of the gasoline, so injection duration of methanol fuel should be nearly double of the gasoline for the same amount of power generation thus suitable injector design is required. For the similar driving condition as the gasoline vehicle, the larger fuel tank is required for methanol. As methanol is resistance to auto-ignition due to lower in-cylinder temperature, and also the higher autoignition temperature cause resistance to knocking.

3.3.2   Methanol Application in Compression Ignition Engine

Compression ignition engines are most commercially used, so there is a very strong interest of using methanol in compression ignition engine. Methanol has very low cetane numbers, which indicate the autoignibility of methanol. As the methanol has

high autoignition resistance, it is used in diesel engine application and requires major modification in the engine. Use of methanol/diesel mixture requires co-solvent or emulsifier agent as methanol diesel do not mix and also methanol fraction is limited. A simultaneously higher fraction of methanol reduces the volumetric energy content and difficult to maintain the same power applying the same injectors. Lubricity of fuel is also decreased and need some lubricating additives. Dual fuel mode is very common, where diesel and methanol are injected in engine separately. Methanol applications in large diesel engines are as dual fuel mode. Recently dual fuel mode is used in many large ships engines where methanol is injected separately, and diesel is used as a source of ignition. This application required modification in the engine cylinder heads and the fuel injection system. The fuel injection system contains separate direct injection methanol injectors or custom built injectors, which allows injecting diesel and methanol to the cylinder (Bünger et al. 2012). In the dual fuel application in an engine, port fuel injection is used for the injection of methanol, and it improves the emissions. The glow plug is used as an ignition source in place of pilot fuel injection for methanol-fueled compression ignition engine (Verhelst and Wallner 2009). Recently compression ignition research engine fueled with methanol is running in the homogeneous compression ignition (HCCI) mode and partially premixed combustion (PPC) mode (Shamun et al. 2016, 2017). These type of combustion mode reduce the soot formation. Most recent research of methanol used in a compression ignition engine is reactivity control compression ignition, which reduced the NO_x and soot simultaneously by complete combustion of fuel (Dempsey et al. 2013).

3.3.3   Methanol-Fueled Engine Design Customisation

There is a requirement of changes or modifications of the hardware of engines or vehicles due to corrosiveness of methanol and its blends with gasoline or diesel. All the vehicle engines running by using a low percentage of methanol (methanol less than 5%) need not require any modification. Low concentration of methanol increases the vapor pressure of gasoline and requires changing the formulation of the base fuel gasoline. Older vehicles cause the problems even at the low level of methanol blends with conventional fuel because methanol acts as a solvent and dissolve the deposits in the fuel system and blockages the down the line. For the use of a high percentage of methanol or neat methanol, there is a requirement of changing of engine hardware materials. Fuel additives are required to improved lubricity and anti corrosivity property to protect the metals (Xiang 2015).

IC engines running on methanol are specially designed to overcome the corrosiveness of the fuel. The engine components design and materials are customized according to the methanol as a fuel in the engine. The new materials such as polyethylene or stainless steel and chrome or nickel plating are selected for fuel tank and fuel system, respectively. The port fuel injection technique is best for the methanol to achieve better fuel air mixing and vaporization.

3.3.4 Cold Start Challenges

There is a problem of cold start of a high percentage of methanol in gasoline. For the successful cold start of methanol blended gasoline engine, the combustible mixture of fuel-air is required and should generate sufficient heat to retain engine running (Yuen et al. 2010; Pearson et al. 2012). Solutions for the cold start and minimize the addition systems requirement by optimizing the following components:

Engine Block: Cold starts problem can be reduced by heating the engine intake and block electrically (Bergstrom et al. 2007; Cowart et al. 1995).

Injector: Startability issues of an engine can also be suppressed by heating injectors individually or fuel rail to enhance the vapor formation of methanol (Kabasin et al. 2009). Second option to enhance vaporization is by heating the intake air (Gong et al. 2011; Colpin et al. 2009). Another way, the injection pressure is enhanced to improve the vaporization and atomization of spray.

Valve: Some researchers have investigated the valve timing effect on the cold startability and observe that both exhaust and intake valve opening and closing would affect the cold startabilty (Colpin et al. 2009; Nakata et al. 2006).

Ignition: Ignition timing adaptation is very important for the cold start. Sometimes multiple sparks are used. Some researchers have proposed the plasma jet spark to enhance startability (Markel and Bailey 1998).

Direct Injection: Late injection and stratification are an effective way of improving cold start performance. Siewart et al. (1987) investigated cold start successfully at the temperature less than −29 °C for methanol (Marriott et al. 2009).

3.3.5 Fueling Systems Customisation and Ignition

As the volumetric energy content of methanol is lower than the conventional fuel, so injectors and fuel pumps of methanol-fueled engines should be with increased flow rate to achieve peak power. Fuel pumps and injectors have the material compatibility issue with methanol (Galante-Fox et al. 2007; Priyanto 2017).

Methanol has been easily pre-ignited due to the presence of a hot spot in the combustion chamber. Methanol generates no soot in flames causes the overheating of ignition source like spark plug electrode (Kalghatgi and Bradley 2012). The temperature of the electrode is in between 700 and 925 °C and suitable for gasoline. So for reducing the electrode temperature, a low heat grade spark plug is needed (Kabasin et al. 2009). Suga et al. (1989) investigated the pre-ignition tendency using various spark plugs with similar heating range. It was observed that spark plugs with platinum tipped electrodes were prone to pre-ignition. Many other researchers had also investigated the spark plug electrode of noble metal with high pre-ignition temperature tendency (Naegeli et al. 1997; Yuen et al. 2010).

3.3.6   Engine Cylinder Head Modification for Methanol

Methanol has very high heat of vaporization, which causes the cooling of intake port and leads to a low temperature of intake. This starts increasing thermo-mechanical stress in the head, and its measurement is necessary (Bergstrom et al. 2007). Valves seat inserts and valve suffer from higher wear during methanol operation due to non-lubricating nature of alcohols and produces lesser lubricating soot. Inlet valve experience increased contact forces due to enhance combustion pressure and thermal shocks (Bergstrom et al. 2007). Thus selected materials for these components are with higher hardness and chrome content (Giroldo et al. 2005; Bergstrom et al. 2007).

Ignition retard is not necessary for the knock suppression at peak power as methanol is knocked resistance but lead to higher peak cylinder pressure. Thus ignition retard is necessary to suppress peak pressure within the allowable limit. Thus methanol engine should have variable valve timing systems with wider timing window for the advantages of internal exhaust gas recirculation rates.

3.3.7   Vehicle Adaptation and Durability

As the volumetric energy density of methanol is much lower than gasoline and diesel, the larger size fuel tank is required for the same driving range. Thus, the additional weight has to carry the vehicle when it fully fueled. Formaldehyde (HCHO) emission from the methanol-fueled engine is increased as compared to gasoline and concern as these emissions are currently unregulated. It is a human carcinogen and plays a very crucial role in tropospheric photochemistry (Wei et al. 2009). Formaldehyde is an intermediate product during combustion at a temperature around 1000 K (Svensson et al. 2016) and leads to formaldehyde emission in case of port fuel injection (PFI) in which methanol goes to crevices and escapes during the expansion stroke. But in case of direct injection of methanol formaldehyde emission is minimized. For methanol application in the engine, there should be specific after treatment catalyst formulation to reduce the formaldehyde emissions.

Engine durability is the proper functioning and reliability of an engine over a long period of time. Durability of existing engine is major technical hurdle for application of methanol as fuel. This is because of corrosive nature of methanol which causes corrosion and wear of engine components. The durability of methanol fuelled engines is improved by engine modifications like using new materials and design features of the engine. These modifications in the engine components are fuel supply systems, fuel mixture delivery, engine cylinder liner, piston rings and engine oil formulations (Ernst and Pefley 1983).

3.4 Summary

This chapter provides a comprehensive review of materials compatibility for the methanol-fueled engines and design of engine components. The above study covers all the aspect of material compatibility and design are discussed, which are as follows:

- Material compatibility of automotive engines and material selection for that
- Wear and corrosion of engine component due to methanol and prevention
- The storage of methanol fuel and their handling
- Design of engine components and subsystem compatible with methanol

The reality of the study is that automotive engineers have to develop the engine for the methanol application in advance for their use. The consumers need transparency about legality of fuel, economy, and durability of engines. They also keen for the easy modification of the engine for methanol.

References

ASTM Standard (2009) D7318-07 standard test method for total inorganic sulfate in ethanol by potentiometric titration

Bergstrom K, Nordin H, Konigstein A, Marriott D, Wiles MA (2007) ABC-alcohol based combustion engines-challenges and opportunities, vol 16. Aachener Kolloquium Fahrzeug-und Motorentechnik 1031

Bergstrom K, Melin SA, Jones CC (2007) The new ECOTEC turbo Biopower engine from GM Powertrain. In: 28th international Vienna motor symposium, Vienna, pp 1–39

Brink A, Jordaan CF, Le Roux JH, Loubser NH (1986) Carburetor corrosion: the effect of alcohol–petrol blends. In: Proceedings of the VII international symposium on alcohol fuels technology, vol 26. Paris, France, pp 59–62

Brinkman ND, Halsall R, Jorgensen SW, Kirwan JE (1994) The development of improved fuel specifications for methanol (M85) and ethanol (Ed85). SAE technical paper 940764

Bünger J, Krahl J, Schröder O, Schmidt L, Westphal GA (2012) Potential hazards associated with combustion of bio-derived versus petroleum-derived diesel fuel. Crit Rev Toxicol 42(9):732–750

Colpin C, Leone T, Lhuillery M, Marchal A (2009) Key parameters for startability improvement applied to ethanol engines. SAE Int J Fuels Lubricants 2(1):180–188

Cowart JS, Boruta WE, Dalton JD, Dona RF, Rivard FL, Furby RS, Piontkowski JA, Seiter RE, Takai RM (1995) Powertrain development of the 1996 Ford Flexible Fuel Taurus. SAE paper 952751

Dela Harpe ER (1988) Ignition-improved ethanol as a diesel tractor fuel. Unpublished MSc. Eng. Thesis, Department of Agricultural Engineering, University of Natal, Pietermaritzburg, South Africa

Dempsey AB, Walker NR, Reitz R (2013) Effect of cetane improvers on gasoline, ethanol, and methanol reactivity and the implications for RCCI combustion. SAE Int J Fuels Lubricants 6(1):170–187

Devlin MT, Baren RE, Sheets RM, Mclntosh K, Turner TL, Jao TC (2005) Characterization of deposits formed on sequence IIIG pistons. SAE Trans 1534–1543

Dumont RJ, Cunningham LJ, Oliver MK, Studzinski WM, Galante-Fox JM (2007) Controlling induction system deposits in flexible fuel vehicles operating on E85. SAE Trans 978–988

Ernst RJ, Pefley RK, Wiens FJ (1986) Methanol engine durability. SAE technical paper 831704

Galante-Fox J, Von Bacho P, Notaro C, Zizelman J (2007) E-85 fuel corrosivity: effects on port fuel injector durability performance. SAE technical paper 01-4072

Giroldo MB, Werninghaus E, Coelho E, Makant W (2005) Development of 1.6 l flex fuel engine for Brazilian market. SAE technical paper 2245

Gong CM, Li J, Li JK, Li WX, Gao Q, Liu XJ (2011) Effects of ambient temperature on firing behavior and unregulated emissions of spark-ignition methanol and liquefied petroleum gas/methanol engines during cold start. Fuel 90(1):19–25

Hagen DL (1977) Methanol as a fuel: a review with bibliography. SAE technical paper 770792

Kabasin D, Hoyer K, Kazour J, Lamers R, Hurter T (2009) Heated injectors for ethanol cold starts. SAE Int J Fuels Lubricants 2(1):172–179

Kalghatgi GT, Bradley D (2012) Pre-ignition and 'super-knock' in turbocharged spark ignition engines. Int J Engine Res 13(4):399–414

Markel A, Bailey B (1998) Modeling and cold start in alcohol-fueled engines. Technical Report National Renewable Energy Laboratory

Marriott CD, Wiles MA, Gwidt JM, Parrish SE (2009) Development of a naturally aspirated spark ignition direct-injection flex-fuel engine. SAE Int J Engines 1(1):267–295

Matthias S, Thomas L (2009) Investigation of the pitting corrosion behaviour of stainless steels in ethanol containing fuels. In: National association of corrosion engineers international—international corrosion conference series 03614409

Naegeli DW, Lacey PI, Alger MJ, Endicott DL (1997) Surface corrosion in ethanol fuel pumps. SAE technical paper 971648

Nakata K, Utsumi S, Ota A, Kawatake K, Kawai T, Tsunooka T (2006) The effect of ethanol fuel on a spark ignition engine. SAE technical paper 06-01-3380

Nichols R (2003) The methanol story: a sustainable fuel for the future. J Sci Ind Res 62:97–105

Otto K, Carter RO, Gierczak CA, Bartosiewicz L (1986) Steel corrosion by methanol combustion products: enhancement and inhibition. SAE technical paper 861590

Otto K, Bartosiewicz L, Carter RO, Gierczak CA (1988) A simple coupon test for analyzing corrosion caused by combustion products of liquid fuels. SAE technical paper 880039

Pearson RJ, Turner JWG (2012) GEM ternary blends: testing iso-stoichiometric mixtures of gasoline, ethanol and methanol in a production flex-fuel vehicle fitted with a physical alcohol sensor. SAE paper 12-01-1279

Priyanto EM (2017) A strategic development of alternative fuel initiation and its adaptation in a developing country: a feasibility study on methanol fuelled domestic passenger ships in Indonesia

Saarialho A, Juhala M, Leppamaki E, Nylund O (1982) Alcohol gasoline fuels and engine wear in cold climates. In: Proceedings: 19th international FISITA congress: energy mobility—SAE technical paper 82037

Scholz M, Ellermeier J (2006) Corrosion behaviour of different aluminium alloys in fuels containing ethanol under increased temperatures. Materialwiss Werkstofftech 37(10):842–851

Shamun S, Shen M, Johansson B, Tuner M, Pagels J, Gudmundsson A, Tunestal P (2016) Exhaust PM emissions analysis of alcohol fueled heavy-duty engine utilizing PPC. SAE Int J Engines 9(4):2142–2152

Shamun S, Haşimoğlu C, Murcak A, Andersson Ö, Tunér M, Tunestål P (2017) Experimental investigation of methanol compression ignition in a high compression ratio HD engine using a Box-Behnken design. Fuel 209:624–633

Shifler DA (2009) Possible corrosion aspects for the use of alternative fuels. In: National association of corrosion engineers international—international corrosion conference series 03614409

Siewert RM, Groff EG (1987) Unassisted cold starts to -29 °C and steady-state tests of a direct-injection stratified charge (disc) engine operated on neat alcohols. SAE paper 872066

Suga T, Kitajima S, Fujii I (1989) Pre-ignition phenomena of methanol fuel (M85) by the post-ignition technique. SAE paper 892061

Svensson E, Li C, Shamun S, Johansson B, Tuner M, Perlman C, Lehtiniemi H, Mauss F (2016) Potential levels of soot, NOx, HC and CO for methanol combustion. SAE technical paper 16-01-0887

Verhelst S, Wallner T (2009) Hydrogen-fueled internal combustion engines. Prog Energy Combust Sci 35(6):490–527

Walker MS, Chance RL (1983) Corrosion of metals and effectiveness of inhibitors in ethanol fuels. GM research report

Wei Y, Liu S, Liu F, Liu J, Zhu Z, Li G (2009) Formaldehyde and methanol emissions from a methanol/gasoline-fueled spark-ignition (SI) engine. Energy Fuels 23(6):3313–3318

West BH, McGill RN (1992) Oil performance in a methanol-fueled vehicle used in severe short-trip service. SAE technical paper 922298

Wing LM, Evarts GL (1993) Materials selection for gasoline/methanol blend fuel systems. SAE technical paper 930447

Xiang H (2015) Introduction of jet sun methanol fuel additives and engine oils. Technical Report Guangzhou Jetsun Lubrication Technology Co., Ltd.

Yates A, Bell A, Swarts A (2010) Insights relating to the autoignition characteristics of alcohol fuels. Fuel 89(1):83–93

Yuen PK, Villaire W, Beckett J (2010) Automotive materials engineering challenges and solutions for the use of ethanol and methanol blended fuels. SAE technical paper 10-01-0792

Chapter 4
Prospects of Methanol-Fuelled Carburetted Two Wheelers in Developing Countries

Hardikk Valera, Akhilendra Pratap Singh and Avinash Kumar Agarwal

Abstract Most developed countries use indigenous fuels for powering their transport sector, however developing countries have to import transport fuels/petroleum to produce transport fuels and they struggle for fuel production from domestic resources. India is focusing on reduction of fuel import by introducing indigenous transport fuels such as variety of biofuels. High ash content coal is available in India, which cannot be used for electricity generation, however this can be used for methanol production using gasification route that can be used to power the Indian transport sector. Although methanol production is already done in India and the current production capacity cannot fulfil the huge demand of the transport sector currently. However methanol economy initiative is gaining momentum due to active intervention of Government of India (GoI) and the technology is being developed for methanol production from high ash coal, municipal solid waste (MSW) and low value agricultural resides. Methanol has great potential to be utilized in spark ignition (SI) engines. This chapter is explores methanol utilization in small carburetor assisted two-wheelers. Two-wheelers population in Indian road transport sector is more than 70% in terms of number of vehicles registered. Carburetor is used to induct the fuel in these small capacity (100–150 cc) SI engines. Existing engines are designed to operate on gasoline therefore slight modifications become essential for adaptation of methanol in these existing two-wheelers. Currently, India is preparing a road map for large scale adaptation of M15 (15% v/v methanol and 85% v/v gasoline) in the existing SI engines, which has several challenges. This chapter summarises challenges and possible solutions for adaptation of M15 in carburetor assisted two-wheelers.

Keywords SI engine · Methanol · Carburetor · M15

H. Valera · A. P. Singh · A. K. Agarwal (✉)
Engine Research Laboratory, Department of Mechanical Engineering, Indian Institute of Technology Kanpur, Kanpur, Uttar Pradesh 208016, India
e-mail: akag@iitk.ac.in

4.1 Transport Fuel Scenario in Developing Countries

Transport fuels are one of the most important factors affecting the economy of any country. Price of crude oil is increasing and cyclic in nature due to rapid depletion and limited reserves. Increasing crude oil prices lead to increase in price of transport fuels such as gasoline, diesel and natural gas. Statistical data of reserves-to-product ratio of coal, oil and natural gas of 2016 shows that these global reserves will exhaust in next 114 years, 50.7 years, and 52.8 years respectively (BP Statistical Review of World Energy 2016). Increasing fuel prices affect the economy from micro level to macro level. Micro level affects because of the price increase of commodities, used in daily life because transportation cost of these items is dependent on vehicles powered by fossil-fuels. Macro level affects because increased fuel prices increase inflation by increasing the price of manufacturing. Developing countries like India are affected to a greater degree by increasing crude oil prices because their net fuel imports are significantly higher compared to several developed countries. India has to explore more options for alternative fuel production and utilization in transport sector. Crude oil import of India in last five years is shown in Table 4.1 (Indian Petroleum and Natural Gas Statistics 2017).

India is aiming to reduce fuel imports by introducing indigenous transport fuels. Therefore India is looking for a sustainable alternative fuel, which can be utilized in all sectors of the economy. For transport sector, fuel properties become more important because the quality of fuel affects engine performance as well as exhaust emissions (Bharj et al. 2019). Among different options, methanol has shown significant potential to be utilized in transport sector due to triple P factors namely production, pollutants, and price. Methanol can be produced from coal, natural gas, biomass, and atmospheric CO_2. It is a clean burning fuel because it has ~50% inherent fuel oxygen, which helps reduce emissions such as CO, HC, etc. (Valera and Agarwal 2019). Methanol price is approximately one third that of conventional fuels however methanol has ~50% lower energy density. This leads to double the amount

Table 4.1 Crude oil imports (Indian Petroleum and Natural Gas Statistics 2017)

Year	Import crude oil (MMT)	% Growth in import of crude oil	Average crude oil prices (US$/bbl)	% Growth in average crude oil prices
2011–12	171.73	4.97	111.89	31.50
2012–13	184.80	7.61	107.97	−3.50
2013–14	189.24	2.40	105.52	−2.27
2014–15	189.43	0.10	84.16	−20.25
2015–16	202.85	7.08	46.17	−45.14
2016–17	213.93	5.46	47.56	3.02
2017–18 (P)	220.43	3.04	56.43	18.65

MMT million metric tons, *P* provisional

of methanol usage compared to conventional fuels for harnessing the same engine power output. Higher energy-to-cost ratio compared to conventional fuels is the most important feature of methanol i.e. it's per unit energy cost is significantly lower than conventional fuels, which makes it cheaper to operate the vehicles on per km basis. Other developing countries like China have already started mass production of methanol and dimethyl ether (DME) using coal as a feedstock (Yang and Jackson 2012). In China, it is mandatory to blend small fraction of methanol with gasoline for vehicular application and DME is blended with liquefied petroleum gas (LPG) for household stoves and water heaters. There are 44 regional standards already adopted by China by FY 2009 for low methanol blends.[1] In China, several automotive companies participated enthusiastically in this green methanol economy (GME) vision initiative and demonstrated methanol-fuelled models. These include Chery Automobiles, Shanghai Maple Automotive, Chang's Auto Group and Greely Group.

In India, methanol seems to be a better alternate compared to hydrogen, biodiesel and electric batteries and it can reduce 10% crude oil dependency by 2022 and reduce GHG emissions by 33–35% (Natarajan 2018). According to the Geological Survey of India, the country has 315 billion tonnes of coal resources as on April 2017,[2] out of which only less than 25% can be utilised in power plants and for Industrial use. 75% of Indian coal reserves have high ash content, which prohibits its commercial utilisation. Therefore, ministry of road transport and highways, National Institution for Transforming India (NITI Ayog) are preparing a road map to reduce crude import bill by up to US$100 Billion by 2030 by adopting 'Methanol Economy' (Methanol Economy 2018). This vision can be achieved if all segments of road transport shift from conventional fuels to alternative fuel to a large extent. Two-wheelers are the most dominant segment in Indian road transport sector, compared to other segments such as three-wheelers, four-wheelers and heavy-duty vehicles as shown in Fig. 4.1,[3] therefore their methanol adaptation will be crucial for achieving this national mission.

Indian two-wheelers segment is the largest vehicle class with variety of two-wheelers such as mopeds, scooters, and motorcycles. During FY 2017–18, two-wheelers industry showed a total sale of ~20 million units in Indian market with 20% increase in exports. The sales for FY 2017–18 showed that sales of scooters and motorcycles increased by ~20% and ~14% respectively, however sales of mopeds declined by ~3.5% compared to sales in FY 2016–17.[4]

Most two-wheelers in India use small SI engines in which the combustible fuel-air mixture is prepared outside the engine using carburetor. Sometimes these two-wheelers face startability issues due to inferior vaporization characteristics of gasoline in cold climatic conditions due to domination of high boiling point hydrocarbons known as 'heavy ends' (Sharma and Mathur 2012). These hydrocarbons remain

---

[1]Standards for methanol blends. https://www.iea-amf.org.

[2]India's coal reserves estimated at 315 billion tonnes—ministry. https://www.indoasiancommodities.com/2018/03/07/indias-coal-reserves-estimated-315-billion-tonnes/.

[3]Two-wheeler industry. www.fintapp.com.

[4]Two-wheeler statistics. http://www.siamindia.com/pressreleasedetails.aspx?mpgid=48&pgidtrail=50&pid=413.
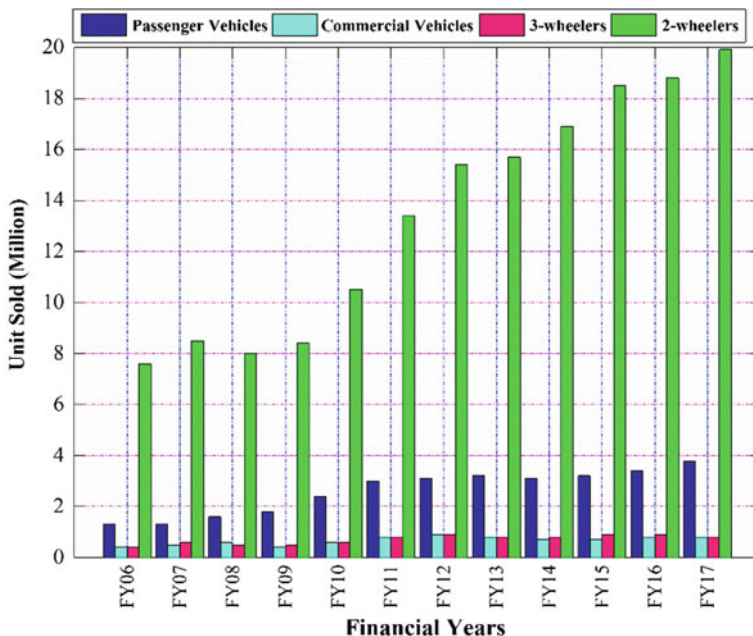
Fig. 4.1 Indian automotive sector (see Footnote 4)

in liquid form and stick inside the combustion chamber walls, leading to startability issues. Therefore, it is important to consider the design aspects of carburetor so that such issues can be avoided. A carburetor is designed to perform three main tasks namely fuel atomization, fuel vaporization, and fuel-air mixing.[5] Following factors are important for these tasks: (i) Time available for fuel-air mixing; (ii) Temperature of the incoming air; (iii) Boiling range of fuel; and (iv) Length of manifold used to connect a carburetor and the test engine.

Primarily, carburetor prepares three types of mixtures: rich mixture for idling condition, lean mixture for superior fuel economy, and stoichiometric mixture for achieving complete combustion. The carburetor has to supply the required air-fuel ratio at steady-state and transient conditions of the vehicle. Steady-state means vehicle can run at a constant speed and achieve constant power output from the engine. Transient condition means speed and load of the vehicle varies continuously, thereby getting variable power from the engine.

---

[5]Fuel system. https://svce.ac.in/departments/auto/Lesson%20plan/II%20YEAR%20CLASS%20NOTES/AT6301/UNIT%20II.pdf.

4.2 Methanol as an Alternative Fuel for Vehicles

Methanol offers numerous advantages over conventional fuels such as gasoline, compressed natural gas (CNG), and diesel. Some of the advantages are:

- Methanol is a colorless, volatile, and flammable liquid, having lower molecular weight compared to conventional fuels.
- Methanol can be produced from coal, biomass, and MSW or from stranded natural gas[6].
- Methanol has inherent fuel oxygen, which reduces harmful tailpipe emissions. Presence of –OH radicals improves the combustion.
- Methanol has higher latent heat of vaporization, which provides extra cooling effects, which improves brake thermal efficiency and reduces the NO_x emissions.
- Methanol is a safer transport fuel due to significantly higher self-ignition temperature, hence is recommended as an alternate to conventional fuels. Due to this, methanol-fuelled engine can be operated at higher compression ratios, which results in higher thermal efficiency compared to gasoline engines.
- Methanol burns without black smoke at high temperatures (Cheng et al. 2008).
- Methanol is a sulfur-free fuel, which results in zero-sulfur based tailpipe emissions such as SO_2 and SO_3.
- Methanol is degradable in aerobic (in the presence of air) and anaerobic (in the absence of air) conditions without any bioaccumulation.
- Accidental methanol release into environment is less harmful compared to spills of crude oil or gasoline.

Due to these advantages, methanol seems to be a strong contender as an alternate fuel for IC engines, especially for SI engines. High octane rating of methanol also makes it more suitable for SI engines, however utilization of pure methanol in an SI engines is a challenging task due to the following reasons.

Methanol Availability: India is in nascent stage of methanol production for fuel use. As of now, only five Indian companies namely Gujarat Narmada Valley Fertilizer and Chemicals Limited, Deepak Fertilizers, Rashtriya Chemicals and Fertilizers, Assam Petrochemicals and National Fertilizers Limited are producing methanol as commodity chemical. Methanol production data from domestic companies of India is given in Table 4.2.

Above data shows that India cannot shift to 100% methanol for transport sector at this stage, without augmenting its methanol production capacity, especially from domestic resources such as high-ash coal, MSW and low value biomass. Therefore, it is logical to utilize low fraction of methanol blends with conventional fuels, until domestic production reaches up to the desired level.

Technological Challenges: Methanol has higher latent heat of vaporization compared to gasoline, which is one of the main reason for modifications in the existing engines. Major modifications for methanol adaptation include advancement in spark

---

[6]Methanol as an alternative transportation fuel in the US: options for sustainable and/or energy-secure transportation. https://afdc.energy.gov/files/pdfs/mit_methanol_white_paper.pdf.

Table 4.2 Domestic methanol production in India[a]

Financial year	Domestic production (MT)	Consumption (MT)	Exports (MT)
2010–11	0.375	1.14	0.044
2011–12	0.360	1.44	0.120
2012–13	0.255	1.47	0.185
2013–14	0.307	1.54	0.082
2014–15	0.210	1.80	0.049
2015–16	0.163	1.83	0.044

[a]India's Leapfrog to methanol economy. http://www.niti.gov.in/writereaddata/files/document_publication/Article%20on%20Methanol%20Economy_Website.pdf
MT million tons

timing for carburetor-assisted vehicles and correction in fuel maps and spark timing for port fuel injected engines/vehicles. Methanol is more corrosive than gasoline, which adversely affects elastomers (soft components used for seals and fuel lines) as well as metal components (pumps, lines, and spigots) (Brinkman et al. 1994). Relatively lower energy density of methanol compared to gasoline is another major concern of methanol, which requires more amount of methanol blend to be injected for producing same power as gasoline. This also requires modifications in fuel injection parameters as well as fuel delivery system. This aspect also supports gradual shift from gasoline to methanol so that modifications can be done in an orderly manner.

Formaldehyde Emissions: Methanol-fuelled vehicles emit higher formaldehyde emissions compared to gasoline-fuelled vehicles. Formaldehyde reacts with the atmospheric gases and forms formic acid which is hazardous for humans and animals.[7] Zhao et al. (2011) performed a comparative study of formaldehyde emissions using four different vehicles of 1.8 L capacity. They reported significantly higher formaldehyde emissions from methanol-fuelled vehicles compared to baseline gasoline fuelled vehicles.

Public Acceptance: Methanol is highly poisonous for the nervous system. Ingestion of 28.5 g methanol can cause irreversible injury to the nervous system, blindness, and even death.[8] It has been reported that a person can die due to consumption of 15 mL liquid containing 40% methanol (Naraqi et al. 1979). Hence lower blend (M15) is a more feasible solution, keeping in mind the public perception of methanol being poisonous. Once public is comfortable using lower methanol blends as fuel, higher blends of methanol could be introduced to power the transport sector.

---

[7]Formaldehyde. https://en.wikipedia.org/wiki/Formaldehyde.

[8]Methanol Institute. https://biodiesel.org/docs/ffs-methanol/faq-about-the-safe-handling-and-use-of-methanol.pdf?sfvrsn=6.

4.3 Construction of Carburetor

The carburetor works on the principle of pressure difference across a throat, in which air exerts a pressure force on its contact surface and pressure difference causes the flow of fuel in the form of spray in depression zone. This pressure difference principle is used in the carburetor to supply the air-fuel mixture as per engine requirement at different engine operating conditions. During suction stroke, piston moves from the top dead center (TDC) to the bottom dead center (BDC), which creates vacuum in the engine cylinder. In a carburetor, intake air passes through a narrow area created by venturi. Venturi is a tube with a continuously decreasing cross-sectional area up to the throat. When air passes through the throat, velocity of air increases, which reduces the pressure (Bernoulli's principle).

$$\frac{P}{\rho g} + \frac{V^2}{2g} + Z = \text{Constant} \tag{4.1}$$

where, $\frac{P}{\rho g}$ = Pressure head

$\frac{V^2}{2g}$ = Velocity head

Z = Potential head

This causes pressure difference between the fuel tank in the carburetor and the throat, which are connected by an orifice, resulting in fuel-flow from the orifice into the incoming air stream (Bansal 2004). Carburetor has a mixture outlet and air inlet area at the same level, which results in zero potential head, therefore maximum pressure head generated at the throat area leads to discharge of fuel into the air stream, as shown in Fig. 4.2.

The pressure difference varies with the engine speeds proportionally. Generally suction pressure (vacuum at the carburetor throat) of a 100 cc engine varies from 36.7 kPa at idling to 2.3 kPa at 90 Kmph vehicle speed. Different parts of carburetor such as air adjusting screw, pilot jet, main jet, jet needle, needle jet, air adjusting screw, rpm screw, float valve and float for delivering required air-fuel ratio are discussed below.[9]

Air Screw: It is a slotted brass screw used to adjust the air-flow rate for idling at the air inlet side of the carburetor. This air screw provides flexibility to adjust the air-flow rate so that required air-fuel ratio for idling during different seasons can be maintained (Table 4.3).

Pilot Jet: It is a medium size jet with metering holes to adjust the required air-fuel ratio. It meters the fuel quantity during starting and idling in the first quarter of throttle opening. It can be used either in a lean pilot jet setting or in a rich pilot jet setting. Lean pilot jet setting is not suitable for engines at low engine speeds, however rich pilot jet setting creates problems in engine starting. Available size for the pilot jet

---

[9]Keihin carburetor jetting. https://static1.squarespace.com/static/5be4d5b35ffd2095efa9bdff/t/5bf1a09b6d2a7391b5a84730/1542561947962/KeihinCarbJetting-2015.pdf.
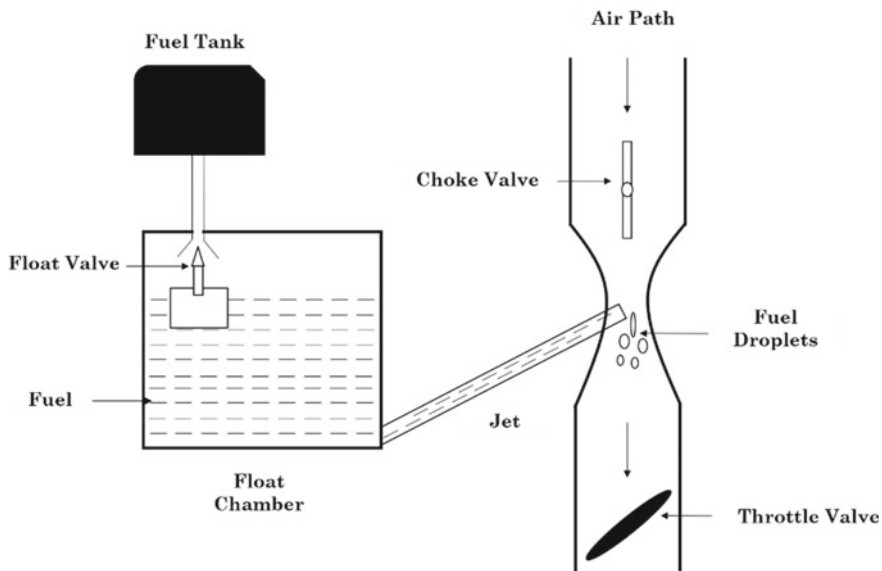
Fig. 4.2 Venturi

Table 4.3 Atmospheric conditions[a]

Seasons	Temperature (°C)	Density (kg/m^3)
Winter	−5 to 25	1.316–1.184
Summer	30–50	1.164–1.093
Rainy	20–40	1.204–1.127

[a]Air density. https://www.engineeringtoolbox.com/air-density-specific-weight-d_600.html

varies from #35 to #80, where the number represents the diameter of the metering hole ($\times 10\ \mu$m) (see Footnote 9).

Needle: It is a most critical part of the carburetor, which affects air-fuel ratio from the first quarter to the third quarter throttle opening. Different geometrical parameters such as diameter, length, and taper section affect the functioning of needle. Needle diameter controls the air-fuel ratio during the first quarter throttle opening position. At lean diameter setting, engine loses power during third quarter throttle opening however rich diameter setting results in choked condition. Needle length is determined by clip position (number of grooves) on the top position of the needle. Needle length ranges from #1 to #5, where #1 corresponds to the leanest setting of the carburetor, and #5 corresponds to the richest setting of the carburetor. The taper section is an angle available on the lower end of the needle, which affects the air-fuel ratio between medium loads to the maximum load range. It affects the size of the main jet since leaner needle taper requires richer main jet to fulfil the engine requirements.

Main Jet: It is a jet having a single metering hole for adjusting the required air-fuel ratio during the third quarter to fourth quarter throttle opening positions. It does not play any significant role during the first quarter to third quarter throttle opening positions. Lean main jet setting causes detonation and rich main jet setting affects the sound quality of vehicle especially from the silencer. Generally available sizes for the main jet ranges from #90 to #230, where the number presents the diameter of the metering hole ($\times 10$ μm) (see Footnote 9).

Float Chamber: It is used to reserve the fuel inside the carburetor at constant level at constant height. High fuel level inside the float chamber discharges more fuel quantity from the jets, and low fuel level discharges lower fuel quantity from the jets. Both conditions adversely affect the engine operation.

Float Valve: It is used to maintain a constant level of fuel in the carburetor during engine operations. It helps during transient driving conditions when the fuel requirement varies continuously.

RPM Screw: It is a slotted brass screw used for adjusting the fuel-air mixture quantity during idling. Its position defines a default jet needle lift position in idling. High jet needle lift results in more quantity of fuel-air mixture supplied to the engine, which increases the engine speed. On the other hand, low jet needle lift results in a less mixture quantity being supplied to the engine, which reduced the engine speed.

Needle Jet Holder/Emulsion Tube: It is used to accommodate jet needle during various throttle positions. In the first quarter throttle opening, emulsion tube accommodates more height of the jet needle, which results in a small fuel quantity emerging from the main jet. In the second quarter throttle opening, emulsion tube accommodates lesser height of jet needle, which results in more fuel quantity emerging from the main jet compared to the first quarter throttle opening. In the third quarter throttle opening with lesser height of the jet, needle accommodates inside the emulsion tube, which results in more fuel quantity emerging from the main jet compared to the second quarter throttle opening. In fourth quarter throttle opening, entire jet needle comes out of the emulsion tube, leading to maximum fuel quantity emerging from the main jet compared to other throttle opening positions.

Choke: It is used for cold starting. During winters, low atmospheric temperature results in inferior spray atomization and vaporization of fuel in the carburetor. This leads to cold startability issues of the engine. This can be resolved by supplying a rich fuel-air mixture using choke.

Needle Jet: It guides the jet needle, and provides a path, through which it enters the emulsion tube.

4.3.1 Conventional Carburetors

There are three types of conventional carburetors namely horizontal draft, updraft and downdraft (Fig. 4.3). In a downdraft carburetor, air flows from upward to the downward direction due to gravity. In an updraft carburetor, air flows from downward to the upward direction, against the gravity. Engine with this type of carburetor
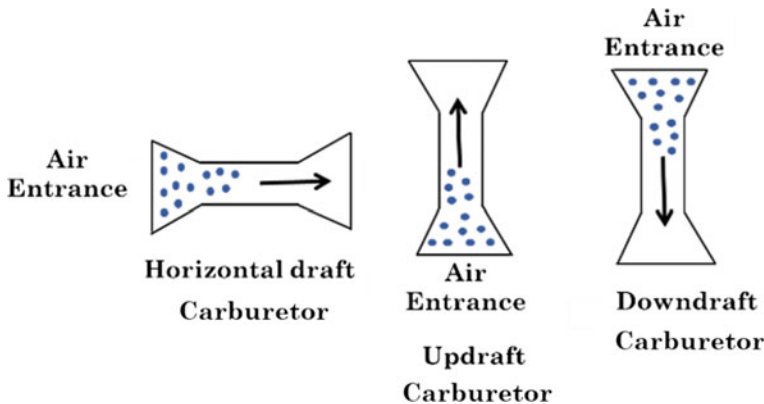
Fig. 4.3 Carburetor based on air supply direction

provides low mechanical efficiency because it requires an additional device to force the air-flow against the gravity. Therefore it has become obsolete now. In a horizontal draft carburetor, air flows in horizontal direction. This type of carburetor is used, where size of the carburetor is rather constrained. Downdraft and horizontal draft carburetors are more popular and widely used for vehicular application. These carburetors give higher mechanical efficiency of the engine compared to the engine equipped with updraft carburetor. Modern carburetors have some unique features, which provide superior fuel economy compared to conventional carburetors. Modern carburetors are explained comprehensively in the next section.

4.3.2   Modern Carburetors

In the modern carburetors, venturi size varies according to throttle position, which makes them different from conventional carburetors. Venturi size increases when the throttle position changes from idle to wide open throttle (WOT) position and decreases when it changes from WOT to idling position; thereby pressure difference remains constant at the throat. Therefore variable venturi type carburetor is called as 'constant velocity' or 'constant vacuum-type' carburetor. Base on variable venturi type, it can be classified as PB type carburetor and CV type carburetor.

4.3.2.1   PB Type Carburetor

PB type carburetor is used in both two-stroke and four-stroke small SI engines, with the engine capacity varying from 50 to 100 cc. It is a lightweight, compact and

(a) Fuel circuit

(b) Pilot circuit

(c) Main circuit

(d) Cold start circuit
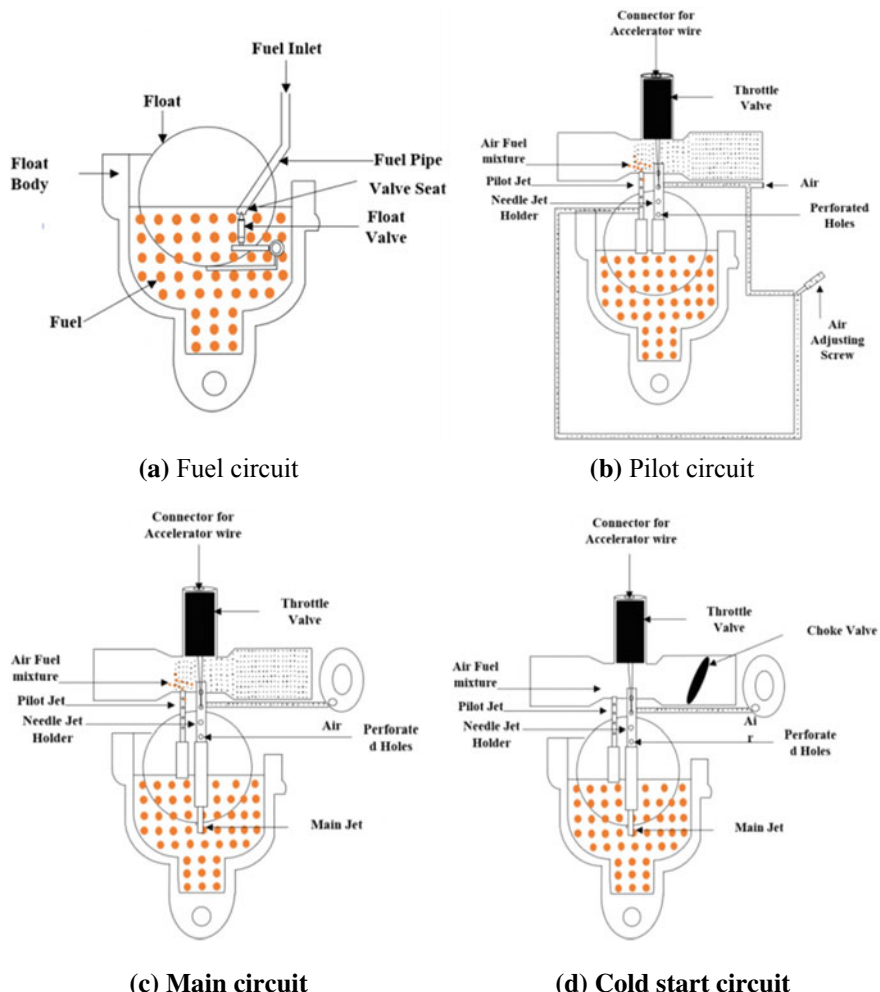
Fig. 4.4 Schematic of various circuits in a PB type carburetor

horizontal draft type carburetor, generally having a mounting angle of 5° to 15°.[10] Air-fuel ratio adjustment can be made by using an air screw. Generally, this type of carburetor is available with different venturi sizes (such as 14, 16, 18 and 20 mm air inlet bore diameter) compatible with atmospheric temperatures varying from −30 to +80 °C.

PB type carburetors have four different circuits namely fuel inlet circuits, pilot circuits, main circuit and cold-start circuit (Fig. 4.4). The drivers use different throttle positions to meet different conditions on the road such as traffic, full speed on

---

[10]PB type carburetor. http://www.keihinfie.com/html/pbtype.htm.

highways, and coast down. As shown in the fuel circuit (Fig. 4.4a), fuel comes from the fuel tank to the float chamber where the float valve maintains a constant fuel level. Drop in fuel level changes the float position thereby float valve opens up for entry of the fuel into the float chamber. Float valve controls the fuel delivery from the fuel tank to the float chamber. Figure 4.4b shows the pilot circuit, which works during idling to the first quarter throttle opening positions. The air-fuel ratio can be adjusted using this circuit, where the air flow can increase or decrease to supply rich/ lean mixture using the air adjustment screw. Figure 4.4c shows the main circuit, which works from the first quarter throttle opening positions to the WOT position. Accelerator wire directly connects to the throttle valve for regulating different throttle positions in order to ensure better drivability. Figure 4.4d shows the cold starting circuit, where the choke valve is used to prepare rich fuel-air mixture via blocking the air passage from the main intake air path. This circuit is usually deployed by the driver during winter season so that the engine starts quickly and cold-starting issues can be tackled.

4.3.2.2 CV Type Carburetor

CV type carburetor is used in both two-stroke and four-stroke small SI engines, with the engine capacity varying from 50 to 200 cc. It is a lightweight, compact, horizontal draft type carburetor. In this type of carburetor, mixture quantity can be adjusted by the mixture screw. Generally, the carburetor is available with different venturi sizes (such as 18, 20, 22, 24 and 26 mm air inlet bore diameter), which are compatible with different atmospheric temperatures ranging from −30 to 80 °C.

CV type carburetor follows four different circuits namely fuel inlet circuit, pilot circuit, main circuit and cold-start circuit, in order to meet different engine requirements as per different load conditions ranging from idle to full load conditions via transient conditions (Fig. 4.5). Figure 4.5a shows the fuel circuit, through which the fuel supply from the fuel tank to the float chamber takes place, essentially for creating a fuel reserve in the float chamber, so that issues with pulsating fuel levels could be avoided, particularly under transient conditions. The float valve is used for maintaining a constant fuel level in the float chamber. Figure 4.5b shows the pilot circuit, which gets activated during idling to first quarter throttle opening position. Here, Pilot jet directly connects to the by-pass holes situated after the butterfly valve, in order to run the engine during idling. Figure 4.5c shows the main circuit, where a diaphragm arrangement is used to lift the jet needle, which gets activated during the first quarter to third quarter throttle opening positions. Here the butterfly valve operates in sync with the accelerator for achieving different throttle positions as per requirements. Figure 4.5d shows a cold-start circuit, where a cold-start valve is used for supplying fuel rich mixtures by blocking the small air passage and utilizing extra jets for making a fuel rich mixture. This circuit helps drivers during winters, when ambient temperatures are significantly lower compared to summer.

(a) Fuel circuit

(b) Pilot circuit

(c) Main circuit

(d) Cold-start circuit
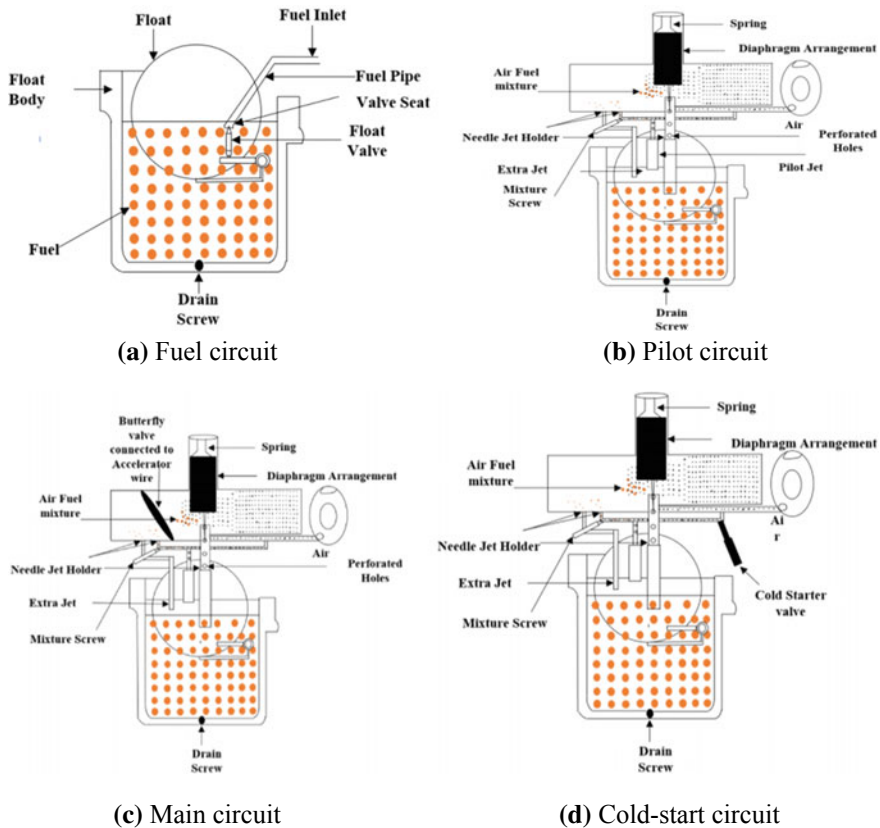
Fig. 4.5 Schematic of various circuits in a CV type carburetor

4.4 Methanol Fueling in Two-Wheelers

Various techniques to induct M15 in carburetor assisted SI engine included blending and fumigation. Blending is most reliable techniques for M15 utilization in IC engines. Both techniques are explained in the following sub-sections.

4.4.1 Methanol Blending

Methanol is blended with gasoline outside the fuel tank to prepare homogeneous miscible blend to supply the carburetor. M15 blend is emerging as a very popular blend for two wheeler applications. M15 induction is the most economical because it does not require any hardware modifications in the engine nor does it require any external device for separate methanol induction. Based on different mixing devices,

blending can be divided into three types namely (i) ultrasonication blending, (ii) mechanical agitator blending, and (iii) magnetic stirrer blending. Ultrasonication blending is a process where sound waves are utilized for agitating the molecules of M15 at micro level for homogeneous mixing of methanol with gasoline such that phase separation can be avoided. In this blending method, a sample of M15 was put in a flask, dipped into the water bath, and sound waves are generated at different frequencies. Frequency defines how often molecules vibrate for preparing homogeneous M15 blend.

Mechanical agitator blending is the blending where a small impeller is used for preparation of M15 blend into a mixing glass/plastic vessel. Centrifugal force is utilized for mixing of molecules of gasoline and methanol. In this blending method, mechanical agitator provides flexibility to utilize different motor rpm for blend preparation.

Magnetic stirrer blending is the one where a rotating magnetic field is enforced by a stirrer bar, which spins quickly for preparation of homogeneous M15 blend. This blending is preferable compared to mechanical agitator blending because it does not have a moving external part, which can damage the mixing glass/plastic vessel.

Further, the blending methods can be divided into four types based on endothermic reactions, used for the preparation of homogeneous blending.[11] These techniques include (i) splash blending, (ii) sequential blending, (iii) ratio blending, and (iv) wild/side stream blending. In splash blending, 85% gasoline and 15% methanol are splashed one after another into the fuel supply tank using fuel meters. In sequential blending, fuels mix sequentially using the same fuel meters. In ratio blending, 85% gasoline and 15% methanol are mixed into the fuel supply tank simultaneously using two flow meters in the downstream connection. In wild/ side stream blending, 85% gasoline is mixed with 15% methanol, and blending occurs upstream of the larger delivery fuel meter. Several researchers have investigated variety of methanol blends for different engines/ vehicles, and their results are summarised in Table 4.4.

Above-mentioned studies showed that M15 can be used as a substitute fuel in SI engines. In general, researchers found that NO_X emissions decreased and CO, HC emissions increase for methanol blends compared to baseline gasoline.

4.4.2 Methanol Fumigation

In this method, M15 is injected into the intake manifold of the engine to prepare homogeneous gasoline-methanol-air mixture for smoother combustion. Homogeneous mixture helps to overcome cold-starting problem, which mostly occurs during the starting of a methanol-fuelled engine. This method is considered as the preferred method for M15 utilization because it reduces the effect of high latent heat of vaporization of methanol due to separate injection in the intake manifold. In fumigation

---

[11]Renewable fuels blending solutions—measurement solutions. http://info.smithmeter.com/literature/docs/tp0a015.pdf.

Table 4.4 Vehicle studies on different methanol blends

Researcher	Fuel used	Engine test bed/vehicle/simulation	Conclusions
Li et al. (2015)	G100 G85M15	Motorcycle	Using G85M15, HC and CO emissions decreased and NO_X emissions increased, compared to G100
Zhao et al. (2011)	G100 G85M15 G80M20 G70M30 G50M50 G15M85	Passenger car	Using methanol blends, CO and HC emissions decreased and NO_x emissions increased compared to G100
Wu et al. (2016)	G100 M100	Engine test bed	M100-fuelled engine showed reduction in CO and HC emissions however NO_x emissions increased compared to G100
Liu et al. (2007)	G100 G90M10 G80M20 G70M30	Engine test bed	Using M30, HC emissions reduced during cold-start and warm up period and CO emission reduced
Elfasakhany (2015)	G100 G97M3 G93M7 G90M10	Engine test bed	CO_2 emissions increased by ~3, 8 and 9.2% for 3, 7 and 10% methanol blended in gasoline. CO emission decreased by ~17.7, 51.5 and 55.5% for 3, 7 and 10% methanol blended in gasoline. HC emissions decreased by ~19.6, 16 and 26% for 3, 7 and 10% methanol blended in gasoline
Vancoillie et al. (2013)	G100 M100	Engine test bed	NOx and CO_2 emissions reduced by 5–10 g/kWh and ~10% compared to gasoline
Iliev (2015)	G95M5 G90M10 G80M20 G70M30 G50M50 G100	Simulation	CO and HC emissions decreased with increasing methanol content compared to G100. Lowest CO and HC emissions were observed for G50M50. NOx emission increased with increasing methanol content in test blend
Canakci et al. (2013)	G95M5 G90M10 G100	Passenger car	**At 80 km/h speed** CO_2 emission decreased by ~11.3 and 3% compared to G100 using M5 and M10. HC emissions decreased by ~35 and 30% compared to G100 using M5 and M10. NOx emissions decreased by ~9 and 1.3% compared to G100 using M5 and M10 **At 100 km/h speed** CO_2 emission increased by ~0.3% using M10 and decreased by ~7% using M5 compared to G100. HC emissions decreased by ~10 and ~17% using M5 and M10 respectively compared to G100. NOx emissions decreased by ~5% using M5 and increased by ~2.8% using M10 compared to G100

Table 4.4 (continued)

Researcher	Fuel used	Engine test bed/vehicle/simulation	Conclusions
Ozsezen and Canakci (2011)	G95M5 G90M10 G100	Passenger car	HC emissions decreased by ~16 and 10% using M5 and M10 compared to G100. CO emission increased by ~1.2% at 80 and 100 km/h vehicle speed using M5 and M10 compared to G100. NO_X emissions decreased by ~1.8 and 2.3% using M5 and M10 compared to G100
Elrod and Bata (1991)	G80M20 G100	Engine dyno	**At 2200 rpm** CO emission decreased by ~18%, HC emissions increased by ~144%, and NO_X emissions decreased by ~14% for M20 compared to G100 **At 2500 rpm** HC emissions decreased by ~143%, and NO_X emissions decreased by ~47% for M20 compared to G100

method, two carburetors are used, where one is used for gasoline and another is used for methanol supply (Fig. 4.6). Fumigation can also be achieved by both mechanical and electronic fuel injection techniques. Mechanical technology is the one where throttle opening of both carburetors was controlled mechanically in such a way that 85% v/v gasoline and 15% v/v methanol is supplied to the manifold to prepare a homogeneous mixture for engine operation. In electronic fuel injection technique, throttle opening position was controlled electronically using either a small circuits or ECU, which control fuel quantities supplied into the manifold to be 85% v/v gasoline and 15% v/v methanol. However, this method increases the net weight of the system since an additional, second carburetor is employed for methanol induction (Abedin et al. 2016). No research has been reported for methanol introduction in SI engine using two carburetors. Globally, this method is in the nascent stage because electronic injectors are preferred for fuel induction these days. Some Indian companies are however considering introduction of this method because Indian market is price sensitive, and carburetor is ~70% cheaper compared to fuel injectors.

Blending is a preferred over fumigation due to following reasons.

Economical: Blending inducts M15 in manifold using existing carburetor whereas fumigation requires an additional carburetor for induction of 15% v/v methanol separately. Further, a separate tank is also required to store methanol for supplying 15% v/v methanol to the additional carburetor. If mechanical fuel induction technology is employed for methanol induction, then additional mechanical components are required. If electronic fuel induction technology is employed, then it requires an additional electronic circuit to ensures required opening of throttle positions for both carburetors. Additional carburetor, additional fuel tank, additional mechanical controls/ electronic circuit results in higher cost for separate 15% v/v methanol supply.
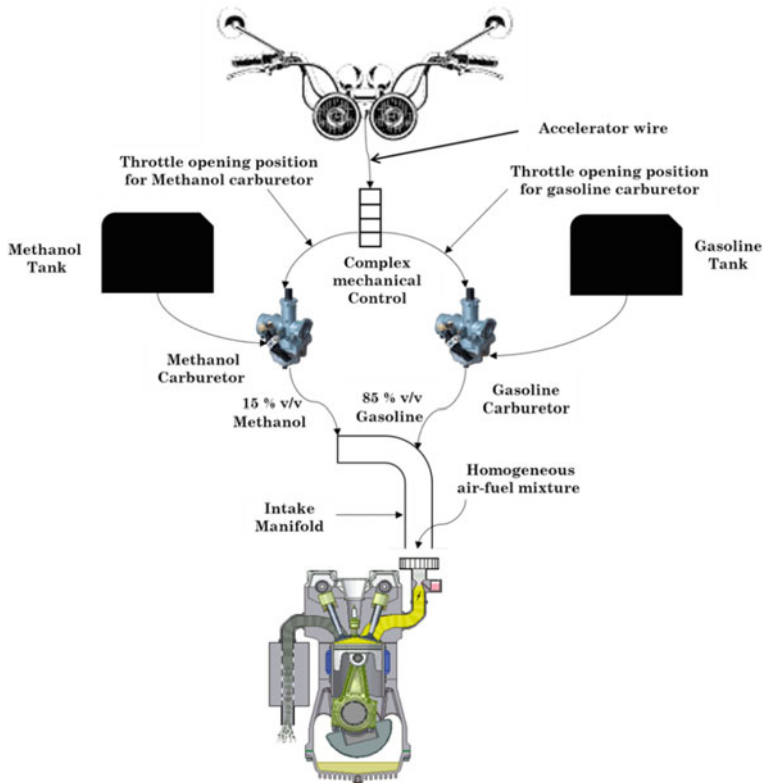
Fig. 4.6 Fumigation technology

Therefore blending method is considered to be economical compared to fumigation technology.

Technical: Blending inducts homogeneous fuel-air mixture (15% v/v methanol and 85% v/v gasoline) into the manifold, which avoids cold-start problems in the vehicle. Fumigation inducts methanol separately in the intake manifold, which creates cold-start issues because methanol has high latent heat of vaporization and during suction stroke, less time is available for homogeneous air-methanol-gasoline mixing, which eventually leads to inferior combustion. Therefore, blending is preferred because homogeneously mixed blends quickly ignite, resulting in higher break thermal efficiency.

Functional: Fumigation requires additional mechanical/ electronic components to induct 15% v/v methanol separately, whereas, blending does not require any additional component for fuel supply. Requirement of additional components in fumigation causes mechanical losses, thereby resulting in lower mechanical efficiency compared to blending. Hence blending is a preferred method for M15 induction into the engine. Existing carburetors are designed optimally for maximum fuel economy

Table 4.5 Properties of gasoline, methanol and M15
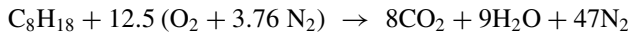
Property	Gasoline	Methanol	M15
Chemical formulae	C_4–C_{12}	CH_3–OH	–
	Incorporate one space before C_{12}	Incorporate one space before OH	
Liquid density (kg/m^3)	740	798	748.7
Lower heating value (MJ/kg)	42	20.1	38.7
Stoichiometric air/fuel ratio	6.5	15.05	14.25
Octane number	90–100	109	–

and minimum tailpipe emissions. However both test fuels have different physico-chemical properties (Table 4.5). Induction of M15 into existing engines using existing carburetors is therefore quite challenging. All these challenges are mentioned in the following section.

4.5 Technical Challenges of Methanol-Fuelled Carburetor Operated Vehicles
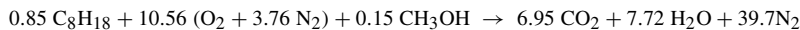
- Introduction of 15% v/v methanol into 85% v/v gasoline makes a leaner mixture for optimally designed existing carburetor because methanol has ~50% inherent oxygen in its molecular structure.
- M15 has ~38.715 kJ/kg energy density whereas gasoline has ~42 kJ/kg energy density, which results in drivability issues.
- Latent heat of vaporization of M15 is higher than baseline gasoline, which causes poor spray atomization of the fuel injected by existing carburetor jets.
- M15 is quite corrosive, and can corrode sensitive carburetor components such as float valve, jet needle, and emulsion tube. Due to its corrosive nature, sometimes it reacts with 'o' rings of the float chamber and makes powdered residues, which can possibly clog the fuel supply.
- M15 has higher latent heat of vaporization, leading to inferior combustion if existing spark timings are used for igniting the fuel.
- For stoichiometric mixtures, complete combustion takes place therefore it is important to compensate for the difference in stoichiometric air-fuel ratio of any new fuel. Stoichiometric air-fuel ratios for gasoline and M15 are 15.05 and 14.25 respectively as calculated subsequently. M15 stoichiometric air-fuel ratio is ~5% lower than baseline gasoline. However due to use of additives, gasoline stoichiometric A/F is considered to be 14.7 generally.

Stoichiometric Air-Fuel ratio calculations for gasoline:

$$C_8H_{18} + 12.5\,(O_2 + 3.76\,N_2) \rightarrow 8CO_2 + 9H_2O + 47N_2$$

$$\frac{ma}{mf} = \frac{12.5(32 + (28 * 3.76))}{96 + 18} = \sim 15.05$$

Stoichiometric Air-Fuel ratio calculation for M15;

$$0.85\,C_8H_{18} + 10.56\,(O_2 + 3.76\,N_2) + 0.15\,CH_3OH \rightarrow 6.95\,CO_2 + 7.72\,H_2O + 39.7N_2$$

$$\frac{ma}{mf} = \frac{10.56(32 + (28 * 3.76))}{0.85(96 + 18) + 0.15(32)} = \sim 14.25$$

Some essential modifications in PB type carburetor (vehicle with 50–100 cc engine capacity) and CV type carburetor (vehicle with 50–200 cc engine capacity) are required to be done for M15 adaption, in order to avoid drivability issues due to above-mentioned challenges.

4.6 Action Plan for Developing M15-Fuelled Dedicated Carburetors for Two-Wheelers

For India, M15 is considered as the best fuel option for small SI engines used in two-wheelers. However there is a need for some design modifications in the existing carburetors. Apart from carburetor, development of the new design of air inlet venturi is also required for adaptation of M15. Few other important steps for adaptation of M15 in two-wheeler sector are given below.

- Development of compatible material for carburetor components
- Development of optimized geometry of main jet and needle jet
- Emission regulations compliances for M15-fuelled vehicles
- Modifications in air bleeder holes and cost reduction
- Reduction in existing venturi dimensions and cost reduction
- Trials of newly designed carburetor on vehicle using M15 and Gasoline
- Durability studies of the carburetor
- Homogeneous blending of 85% v/v gasoline and 15% v/v methanol
- Development of compatible materials for nozzle
- Certification of M15 as automotive fuel based on its physico-chemical properties

4.7 Conclusions

In this chapter, a comprehensive review of the carburetor technology and its classifications are presented. Main objective of this chapter was to explore the scope of methanol as an alternative fuel in carbureted two-wheelers. In India, 100% replacement of gasoline with methanol is very difficult due to very low domestic methanol production compared to potential demands, technical difficulties associated with methanol utilization in existing engines, high formaldehyde emissions and public acceptance. Therefore, M15 has been planned to be introduced as SI engine fuel to start with. M15 would play a vital role to reduce India's high fuel import bill and promote development of indigenous technology for converting waste resources such as MSW, high ash coal and agricultural residues to methanol. M15-fuelled vehicles offer superior economic benefits compared to gasoline-fuelled vehicles. Utilization of M15 in carbureted vehicles has several challenges though, which need to be resolved before its large-scale implementation. Few carburetor components such as metering holes of the main jet and diameter of the jet needle would be required to be optimised. Relatively bigger metering hole diameter compared to existing jets can resolve the issue of lower energy density of methanol. Reduction in the air inlet diameter of the carburetor is necessary to meet the transient conditions by achieving stoichiometric mixture. Overall, M15-fuelled vehicles are capable of offering superior drivability compared to gasoline-fuelled vehicles. M15 is capable of meeting upcoming Bharat Stage-VI emission legislations, which is a quite challenging task for existing gasoline-fuelled vehicles.

References

Abedin MJ, Imran A, Masjuki HH, Kalam MA, Shahir SA, Varman M, Ruhul AM (2016) An overview on comparative engine performance and emission characteristics of different techniques involved in diesel engine as dual-fuel engine operation. Renew Sustain Energy Rev 60:306–316. https://doi.org/10.1016/j.rser.2016.01.118

Bansal RK (2004) A textbook of fluid mechanics and hydraulic machines. Laxmi Publications

Bharj RS, Kumar R, Singh GN (2019) On-board post-combustion emission control strategies for diesel engine in india to meet bharat stage VI norms. In: Agarwal A, Gupta J, Sharma N, Singh A (eds) Advanced engine diagnostics. Energy, environment, and sustainability. Springer, Singapore, pp 105–125. https://doi.org/10.1007/978-981-13-3275-3_6

BP Statistical Review of World Energy (2016). https://www.bp.com/content/dam/bp-country/de_ch/PDF/bp-statistical-review-of-world-energy-2016-full-report.pdf

Brinkman N, Halsall R, Jorgensen SW, Kirwan JE (1994) The development of improved fuel specifications for methanol (M85) and ethanol (Ed 85). SAE Trans 361–374

Canakci M, Ozsezen AN, Alptekin E, Eyidogan M (2013) Impact of alcohol–gasoline fuel blends on the exhaust emission of an SI engine. Renew Energy 52:111–117. https://doi.org/10.1016/j.renene.2012.09.062

Cheng CH, Cheung CS, Chan TL, Lee SC, Yao CD (2008) Experimental investigation on the performance, gaseous and particulate emissions of a methanol fumigated diesel engine. Sci Total Environ 389(1):115–124. https://doi.org/10.1016/j.scitotenv.2007.08.041

Elfasakhany A (2015) Investigations on the effects of ethanol–methanol–gasoline blends in a spark-ignition engine: performance and emissions analysis. Eng Sci Technol Int J 18(4):713–719. https://doi.org/10.1016/j.jestch.2015.05.003

Elrod AC, Bata RM (1991) Exhaust gas emissions of butanol, ethanol, and methanol-gasoline blends. J Eng Gas Turbines Power 113:377

Iliev S (2015) A comparison of ethanol and methanol blending with gasoline using a 1-D engine model. Procedia Eng 100:1013–1022. https://doi.org/10.1016/j.proeng.2015.01.461

Indian Petroleum and Natural Gas Statistics (2017–18) http://petroleum.nic.in/sites/default/files/ipngstat_0.pdf

Li L, Ge Y, Wang M, Li J, Peng Z, Song Y, Zhang L (2015) Effect of gasoline/methanol blends on motorcycle emissions: exhaust and evaporative emissions. Atmos Environ 102:79–85. https://doi.org/10.1016/j.atmosenv.2014.11.044

Liu S, Clemente ERC, Hu T, Wei Y (2007) Study of spark ignition engine fueled with methanol/gasoline fuel blends. Appl Therm Eng 27(11–12):1904–1910. https://doi.org/10.1016/j.applthermaleng.2006.12.024

Methanol Economy (2018) NITI Aayog working on road map for India on World Environment Day. http://pib.nic.in/newsite/PrintRelease.aspx?relid=179785

Naraqi S, Dethlefs RF, Slobodniuk RA, Sairere JS (1979) An outbreak of acute methyl alcohol intoxication. Aust N Z J Med 9(1):65–68

Natarajan R (2018) Methanol as an alternative fuel for India. http://www.cstep.in/uploads/default/files/publications/stuff/CSTEP_Policy_Brief_Methanol_Ramya_Final.pdf

Ozsezen AN, Canakci M (2011) Performance and combustion characteristics of alcohol–gasoline blends at wide-open throttle. Energy 36(5):2747–2752. https://doi.org/10.1016/j.energy.2011.02.014

Sharma RP, Mathur ML (2012) Internal combustion engine, vol 100, pp 200–300. Dhanpath Rai Publications

Valera H, Agarwal AK (2019) Methanol as an alternative fuel for diesel engines. In: Agarwal A, Gautam A, Sharma N, Singh A (eds) Methanol and the alternate fuel economy. Energy, environment, and sustainability. Springer, Singapore, pp 9–33. https://doi.org/10.1007/978-981-13-3287-6_2

Vancoillie J, Demuynck J, Sileghem L, Van De Ginste M, Verhelst S, Brabant L, Van Hoorebeke L (2013) The potential of methanol as a fuel for flex-fuel and dedicated spark-ignition engines. Appl Energy 102:140–149. https://doi.org/10.1016/j.apenergy.2012.05.065

Wu B, Wang L, Shen X, Yan R, Dong P (2016) Comparison of lean burn characteristics of an SI engine fueled with methanol and gasoline under idle condition. Appl Therm Eng 95:264–270. https://doi.org/10.1016/j.applthermaleng.2015.11.029

Yang CJ, Jackson RB (2012) China's growing methanol economy and its implications for energy and the environment. Energy Policy 41:878–884. https://doi.org/10.1016/j.enpol.2011.11.037

Zhao H, Ge Y, Tan J, Yin H, Guo J, Zhao W, Dai P (2011) Effects of different mixing ratios on emissions from passenger cars fueled with methanol/gasoline blends. J Environ Sci 23(11):1831–1838. https://doi.org/10.1016/S1001-0742(10)60626-2

Part III
Advanced Engine Technologies

Chapter 5
Prospects of Gasoline Compression Ignition (GCI) Engine Technology in Transport Sector

Vishnu Singh Solanki, Nirendra Nath Mustafi and Avinash Kumar Agarwal

Abstract Compression ignition (CI) engines are mainly fuelled by diesel-like high cetane fuels, and they have higher overall efficiency due to higher compression ratio compared to their spark ignition (SI) engine counterparts. However, modern diesel engines are more expensive, complicated, and emit high nitrogen oxides (NOx) and particulate matter (PM). Simultaneous control of soot and NOx emissions in diesel engines is quite challenging and expensive. Thermal efficiency of SI engines, on the other hand is limited by the tendency of abnormal combustion at higher compression ratios therefore use of high octane fuel is essential for developing more efficient higher compression ratio SI engines in near future. In the foreseeable future, refineries will process heavier crude oil to produce relatively inferior petroleum products to power the IC engines. Also, fuel demand will shift more towards diesel and jet fuels, which would lead to availability of surplus amounts of low octane gasoline with oil marketing companies, with little apparent use for operating the engines. This low octane gasoline will be cheaper and would be available in excess quantities in foreseeable future as the demand for gasoline will further drop due to increase in the fuel economy of modern generation gasoline fuelled vehicles. For addressing these issues, Gasoline compression ignition (GCI) engine technology is being developed, which is a futuristic engine technology that takes advantage of higher volatility, and higher auto-ignition temperature of gasoline and higher compression ratio (CR) of a diesel engine simultaneously to take care of soot and NOx emissions without compromising diesel engine like efficiency. GCI engines can efficiently operate on low octane gasoline (RON of ~70) with better controls at part load conditions. However cold starting, high CO and HC emissions, combustion stability at part load, and high combustion noise at medium-to-full load operations are some of the challenges associated with GCI engine technology. Introductory sections of this chapter highlights future energy and transport scenario, trends of future fuel demand, availability of low octane fuels and development in advanced engine combustion technologies such as HCCI, PCCI, RCCI, and GDI. GCI engine development, its combustion characteristics and controls are discussed in detail. Particular emphasis is given to the effect

V. S. Solanki · N. N. Mustafi · A. K. Agarwal (✉)
Department of Mechanical Engineering, Indian Institute of Technology Kanpur, Kanpur 208016, Uttar Pradesh, India
e-mail: akag@iitk.ac.in

of various control strategies on GCI combustion, performance and emissions, fuel quality requirement and adaption of GCI technology in modern CI engines. In addition, this chapter reviews initial experimental studies to assess the potential benefits of GCI technology.

Keywords IC engines · GCI engine technology · Combustion control · Low octane gasoline · Oxides of nitrogen (NOx) · Particulates

5.1 Introduction

Growth of transport sector plays a vital role in overall development of the country. At present, ~99% of global transport fleet is powered by internal combustion (IC) engines, in which, liquid petroleum products power ~95% vehicles. This trend would continue to rise due to high energy density, easy processing and transportation of liquid petroleum fuels, and availability of desired infrastructure (Kalghatgi 2018). By the end of 2014, ~910 million passenger cars and ~330 million commercial vehicles were available in the market (Statista 2016). In coming decades, these numbers would continue to rise at a growth rate of 1%, especially in non-OECD (Organization for Economic Co-operation and Development) countries like India and China (U.S. Energy Information Administration 2016; World Economic Forum 2016; Exxonmobil 2019). Transport sector consumes ~20% of global energy and is responsible for ~23% of global carbon di-oxide (CO_2) emissions. However, overall GHG emissions from transport sector are only ~14%, which is comparable to GHG emissions from farming and dairy Industry (U.S. Energy Information Administration 2016; Outlook 2017; IPCC 2019). Figure 5.1 shows sector-wise global GHG emissions.
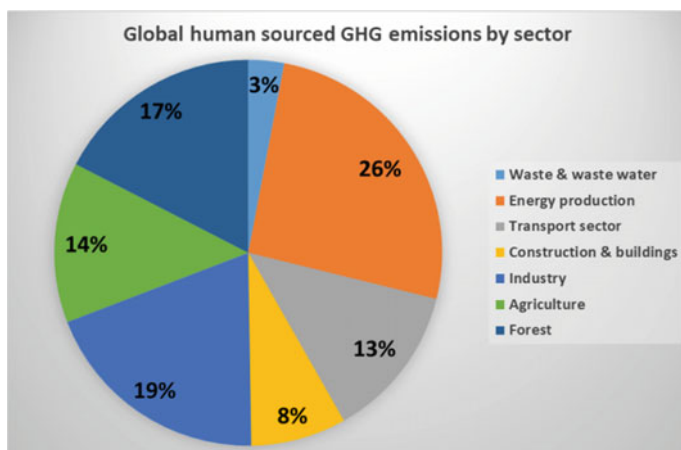
Fig. 5.1 Global anthropogenic GHG emissions sector-wise (*Web Source* http://www.climate-change-knowledge.org/ghg_sources.html)

Global daily consumption of petroleum products in terms of million barrels of oil equivalent (BoE) by the end of 2017 is presented in Table 5.1 (International Energy Agency 2017). By 2040, energy demand for non-OECD countries will be 40% higher than today's demand. Refineries would have no choice but to utilize residual heavier crude oil to meet such a massive demand of fuel in future.

However, now the question is that, is there enough reserves of oil so that the growth of the IC engine will not be affected by the oil demand? Mainly supply of oil depends on the discoveries and efficiency of oil extraction. Since last some decades, the availability of oil is more than the demand. Figure 5.2 (BP Statistical Review of World Energy 2017) shows evolution of oil reserves and the ratio of oil reserves-to-annual production between 1980 and 2010.

Table 5.1 Daily global oil demand at the end of 2017 (International Energy Agency 2017)

	Million Barrels of oil Equivalent (BoE)			Energy, exa-joules	Fuel volume, billion liters
	OECD	Non-OECD	Total		
Gasoline	14.5	11.3	25.8	0.158	4.85
Diesel/Gasoil	13.7	14.6	28.4	0.174	4.83
Jet/Kerosene	4.3	3.2	7.5	0.046	1.27
Residual Oil	2.1	5.4	7.5	0.046	
Others[a]	12.8	16.1	28.9	0.177	
Total	47.4	50.7	98.1	0.601	

[a]Other includes naphtha, LPG and ethane
1 exajoule $= 10^{18}$ Joules $= 277,778$ GWh $= 163.4$ million BoE
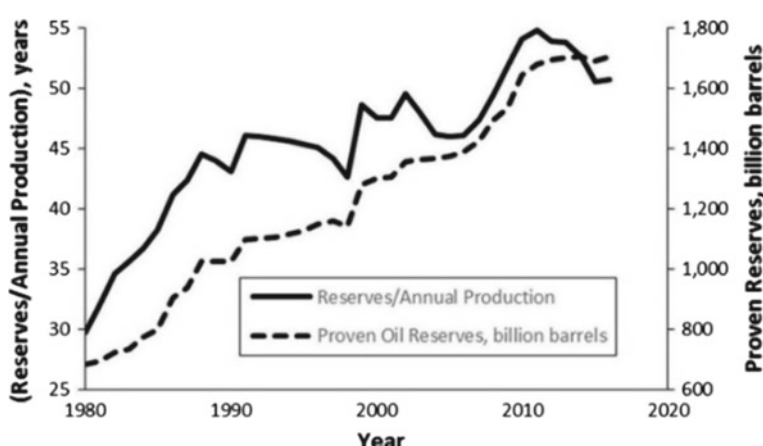
Fig. 5.2 Oil reserves-to-annual production ratio and evolution of proven oil reserves (BP Statistical Review of World Energy 2017)

In 1980, oil reserve capacity was 29 years, which increases to 50 years by 2016. Discoveries and efficient oil extraction techniques would further increase the oil supply in future, hopefully. In 2007, according to worldwide recovery factor, only a small fraction (~27%) of oil could be recovered from the oil wells (Sandrea and Sandrea 2007). Recovery rate can be further enhanced by advanced technologies such as injecting fluid and gas (e.g., CO_2). Introduction of alternative fuels such as shale oil and gas, methanol, and DME will also help the availability of fuel resources for powering IC engines based transport system. Hence the supply of petroleum products will not constrain the growth of engines in foreseeable future.

Currently gasoline-fueled light-duty vehicles (LDV) consume ~44% of total transport energy (U.S. Energy Information Administration 2016). It is easier to replace gasoline-fueled LDV's by the electric, hybrid, fuel-cell vehicles. In future, passenger cars will be travelling relatively shorter distances due to development of smart cities (U.S. Energy Information Administration 2019; World Energy Outlook 2011; U.S. Energy Information Administration 2013; International Energy Agency 2015; Kalghatgi 2014). Hence dependency on gasoline will be relatively lesser in future. Heavy-duty engines will be fueled by more clean fuels than today's diesel. Therefore transport fuel demand domination will shift from light-duty cars to heavy-duty commercial vehicles such as trucks, buses, rail, and marine engines in near future (World Energy Outlook 2011). It would mean that demand for diesel would be higher than that for gasoline in foreseeable future. Projections of gasoline, diesel, and jet fuel demands in the coming decades are captured in Fig. 5.3 (BP Statistical Review of World Energy 2014).

This transition of transport fuel may create abundance/surplus low octane gasoline in refineries and oil marketing companies, which can be used for mitigating the imbalance in future demand for fuel for heavier commercial transport, that uses diesel as of now.
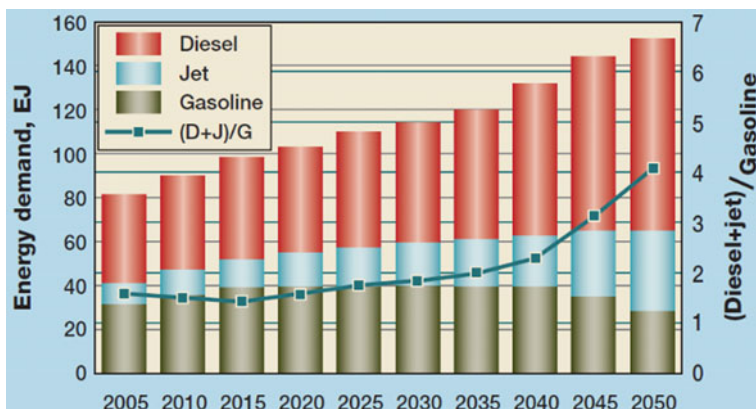

Fig. 5.3 World Energy Council projections for gasoline, jet-fuel and diesel demand up to 2050 (BP Statistical Review of World Energy 2014)
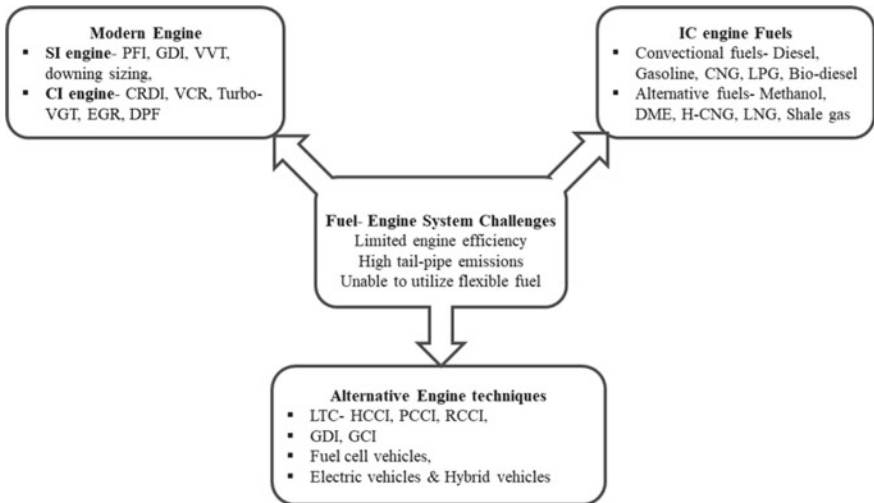
Fig. 5.4 Opportunities and challenges of the fuel-engine system in near future

Current IC engines generally operate on two conventional combustion modes namely spark ignition (SI) and compression ignition (CI) modes. SI engines mainly operate under stoichiometric conditions and utilize 3-way catalytic converters to control high emissions of hydrocarbons (HC), carbon monoxides (CO) and nitrogen oxides (NOx). SI engines would require improvement in fuel's octane rating for further efficiency improvement, which would increase demand for higher octane gasoline. Refineries would therefore require additional investments to produce high-octane gasoline from the heavier crude oil, which is going to be energy-intensive and would entail higher greenhouse gas (GHG) emissions during fuel production process. Opportunities and challenges for the fuel-engine system in near future are captured in Fig. 5.4.

Modern diesel engines are more efficient and emit lower tail-pipe CO and HC emissions than SI engines, but emit higher PM and NOx, which are toxic to human health and the environment. For controlling NOx and PM emissions simultaneously, a diesel engine requires advanced exhaust gas after-treatment system such as diesel particulate filter (DPF) and SCR system, which would increase system complexity and total cost of the vehicle. PM and NOx emissions from CI engines can be controlled by enhancing the fuel-air mixing (turbulence) before the start of combustion (SoC). Gasoline has higher volatility and longer ignition delay than diesel. Higher resistance to auto-ignition allows gasoline more time for mixing with air before the start of combustion (SoC), and higher volatility promotes homogenous mixing of fuel and air. In summary, greater stock of cheaper low octane rating fuel would be available in the market in future to power IC engines, which could be used to reduce GHG emissions as well. GCI engines can operate on low-octane gasoline with a substantial reduction in PM and NOx emissions without compromise in

engine efficiency. Introduction of this new GCI engine-fuel system would reduce capital investments in the refinery, well-to-wheel (WTW) emissions, and total cost of vehicle ownership (Kalghatgi and Johansson 2018).

5.2 Conventional Fuels and Fuel Properties

IC engines mainly operate on petroleum-based liquid or gaseous fuels, which are processed from the crude oil in refineries. As crude oil temperature increases in a fractional distillation column, gas comes out from the crude oil, which is called liquid petroleum gas (LPG). Straight run gasoline (SRG) is recovered between 20 and 200 °C, and diesel is recovered between 160 and 380 °C. The term 'naphtha' is used for the product that lie close to the gasoline boiling temperature range. 40–60% of the petroleum products (by weight) are heavy components, with boiling range higher than 380 °C. Heavy components are further cracked down to light hydrocarbons for improving their cetane or octane rating. Many additives are added to refined products to meet fuel specifications. In addition to petroleum-based fuels, biofuels, alcohols, and other gaseous fuels (such as NG, biogas etc.) are used to power IC engines (Kalghatgi and Johansson 2018). Important fuel properties of diesel and gasoline are listed in Table 5.2 (Web Source: http://large.stanford.edu/courses/2010/ph240/veltman2/docs/Propertiesoffuels.pdf).

Some critical fuel properties, which significantly influence engine combustion, performance and emissions, are discussed.

Auto-ignition Temperature and Volatility These are two crucial fuel properties that play a vital role for air-fuel mixture homogeneity thus strongly influence engine combustion characteristics. Gasoline has higher auto-ignition temperature and volatility than diesel, which facilitates better homogenous mixtures of gasoline.

Octane/Cetane Number Cetane and octane rating measures the ability of spontaneous ignition of fuel. Octane rating expresses gasoline's ignitability and Cetane rating for diesel. In other words, octane rating measures the strength of resistance to auto-ignition/pre-ignition of gasoline. Higher octane number provides greater resistance to auto-ignition/pre-ignition under high combustion temperature and pressure, which enhances combustion efficiency in gasoline engines. Cetane number measures the ignition delay period before the start of combustion (SoC). High cetane number means a shorter delay period, resulting in better combustion efficiency in diesel engines. High octane fuel has a low cetane rating and vice versa.

Molar Mass Gasoline has lower molecular weight compared to diesel (gasoline: 100–105 kg/kmol; diesel: 200 kg/kmol). Due to lower molecular weight, diffusion rate of gasoline is higher than diesel, which helps in reducing tailpipe emissions.

Latent Heat of Vaporization Gasoline has higher latent heat of vaporization than diesel (gasoline: 375 kJ/kg; diesel: 250 kJ/kg). Higher heat of vaporization of gasoline

Table 5.2 Comparison of diesel and gasoline specifications (*Web Source* http://large.stanford.edu/courses/2010/ph240/veltman2/docs/Propertiesoffuels.pdf)

Property	Unit	Diesel	Gasoline
Chemical formula		C_8–C_{25}	C_4–C_{12}
Fuel carbon	wt%	84–87	85–88
Fuel hydrogen	wt%	16–33	12–15
Molecular weight		200	100–105
Density at 15 °C	kg/m^3	810–890	720–780
Lower heating value	MJ/kg	42.7	43.4
Net calorific value	MJ/l	36	32
Research octane number (RON)		–	90–100
Cetane number		40–55	5–20
Boiling temperature	°C	187–343	26–225
Reid vapor pressure	psi	0.2	8–15
Viscosity (at 15 °C)	Centipoise	2.6–4.1	0.37–0.44
Auto ignition temperature in air	°C	210	280
Latent heat of vaporization (at 1 bar)	kJ/kg	250	375
Minimum ignition energy (at $\varphi = 1$)	mJ	0.23	0.8
Stoichiometric air/fuel ratio		14.6	14.7
Flammability limits	vol.%	0.5–7.5	1.4–7.6
Flash point	°C	73	−42

provides better cooling of intake charge compared to diesel, leading to improved engine efficiency and power.

Lower Heating Value The calorific value of gasoline (on mass basis) is slightly higher than diesel (gasoline: 43.4 MJ/kg; diesel: 42.7 MJ/kg). However, diesel has higher density than petrol (gasoline: 750 kg/m^3; diesel: 835 kg/m^3) and have ~12.5% higher energy content per unit volume (gasoline: 32 MJ/m^3; Diesel: 36 MJ/m^3). Apart from difference in energy density, diesel engines are 20% more efficient than gasoline engines and hence more gasoline quantity will be required to be injected for achieving the same power output from a diesel engine.

Lubricity and Viscosity Gasoline provides lower lubrication than diesel and injection of gasoline at high-pressure results in more wear and tear of the fuel injection equipment. Additionally, viscosity of gasoline is also lower than diesel. Therefore suitable additives will be required for utilization of gasoline in CI engines.

5.3   Gasoline and Diesel Spray Characteristics

Fuel spray characteristics are important since they play a vital role in mixing of fuel with air in the combustion chamber (direct injection engines) or in the intake port (port fuel injection engines). Macroscopic spray characteristics include spray penetration length, spray cone angle, spray area and microscopic spray characteristics include droplet size-velocity, and size-number distributions.

Fuel properties significantly affect spray characteristics and consequent fuel-air mixing characteristics. Spray penetration length of gasoline was reported to be shorter than diesel spray due to lower fuel density and viscosity but higher volatility (higher evaporation rate) of gasoline (Kim et al. 2013). It helps in early direct injection of gasoline in CI engines without the wall impingement. However gasoline spray has larger cone angle than diesel sprays due to higher Reynolds number. These effects are more dominant in case of increased fuel injection pressure (FIP) as shown in Figs. 5.5 and 5.6. Results from other studies (Payri et al. 2012) suggested that momentum flux

Fig. 5.5 liquid penetration length traces for **a** diesel and **b** gasoline sprays at different fuel injection pressures and fixed injection timing of −10 CAD aTDC in evaporative conditions. (Kim et al. 2013)
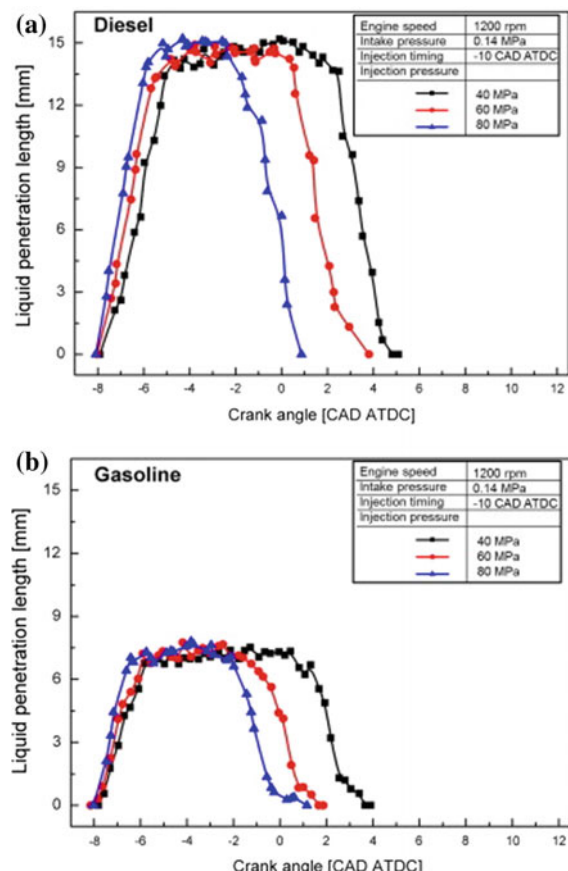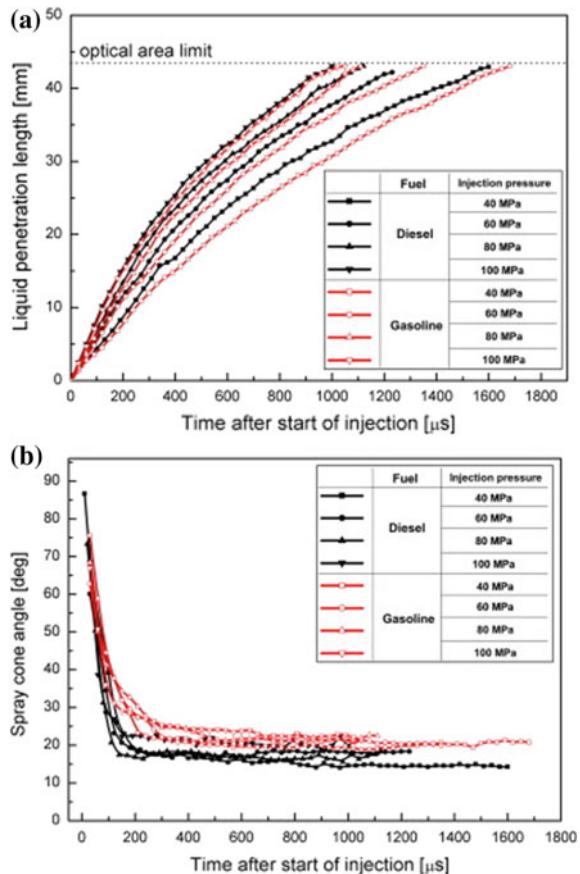
Fig. 5.6 a Spray penetration
length, **b** spray cone angle
for gasoline and diesel at
different fuel injection
pressures according to the
time after the start of the
injection in non-evaporative
conditions (Kim et al. 2013)

was similar for both gasoline and diesel sprays and was independent of fuel density
and injector hole diameter.

5.4 Engine Combustion

SI engines are commonly preferred for light-duty applications and currently, ~80%
of global transport vehicles operate on SI engines, whereas CI engines are mostly
preferred for heavy-duty vehicles such as bus, heavy duty truck, and off-road machin-
ery (OPEC, Organization of the Petroleum Exporting Countries 2013). In SI engines,
premixed fuel-air charge is supplied into the combustion chamber, and a spark plug
is used as an ignition source for initiating the flame propagation. However, in most
diesel engines, fuel is directly injected into the combustion chamber at a high tem-
perature near TDC, just before the end of the compression stroke. Unlike SI engines,

ignition initiates in diesel engines by auto-ignition of combustible charge, once it reaches its self-ignition temperature (Kalghatgi and Johansson 2018). CI engines are characterized by higher compression ratio (CR) and zero throttling losses (Stone 2012). Compression of fuel-air mixture increases pumping losses in a SI engine (OPEC, Organization of the Petroleum Exporting Countries 2013; Heywood 1988; Stone 2012; Boot 2016). SI engine efficiency is usually limited by abnormal combustion or knocking, which is mainly due to pre-ignition of end-gas before flame front reaches to it. SI engines normally operate under stoichiometric to slightly rich fuel-air mixtures, whereas diesel engines always operate under lean condition. Effectiveness of SI engines at low load conditions is inferior because of increase in pumping losses. IC engines are facing huge challenges now-a-days for stringent emission norm compliance. Researchers are focusing on advanced engine combustion techniques, aiming to attain improved engine efficiency, while meeting tail-pipe emission standards. Relative merits, demerits and challenges associated with these combustion techniques are discussed below.

Modern SI engines mostly apply two injection strategies: *Port Fuel Injection* (PFI) and *Gasoline Direct Injection* (GDI) techniques. In PFI system, fuel is injected in the intake port before the intake valve. It leads to fuel metering error, wall wetting, timing lag in fuel delivery, and high unburned hydrocarbon emissions. Direct injection of gasoline inside the combustion chamber can overcome most problems associated with PFI engines, and termed it as gasoline direct injection (GDI) engines. High FIP in GDI engines provides better fuel atomization and lower tailpipe emissions with improved fuel economy (Nohira and Ito 1997; Rottenkolber et al. 2002). However, there are some issues associated with GDI techniques such as high NOx and PM emissions, difficulty in controlling stratified combustion, and high unburned HC and CO emissions at low load (Chincholkar and Suryawanshi 2016).

Low-Temperature Combustion (LTC) technique exhibits relatively lower adiabatic flame temperature than conventional combustion techniques, resulting in lower NOx and PM emissions, while maintaining diesel like high efficiencies. Different LTC techniques are homogenous charge compression ignition (HCCI), reactivity controlled compression ignition (RCCI), and partially premixed charge compression ignition (PCCI). All LTC techniques provide flameless, homogenous combustion of premixed fuel-air mixture ensuring very low NOx formation due to lower adiabatic temperature, and negligible soot formation due to the absence of a fuel-rich zone in the combustion chamber. However, LTC produces higher CO and HC tail-pipe emissions due to reduction in the exhaust gas temperature (EGT) therefore exhaust gas after-treatment devices are essential for controlling CO and HC emissions.

In HCCI engines, fully premixed fuel-air mixture is compressed, and in-cylinder chemical kinetics controls ignition via combustion chamber pressure and temperature. Premixed charge reduces the combustion temperature and local equivalence ratio. Shorter combustion duration leads to a reduction in the heat transfer losses with improved engine efficiency. However high rate of pressure rise (RoPR) and limiting operation under high load range are the main issues encountered in the HCCI engines, which can be manipulated by using combustion phasing.

In RCCI engines, fuels having high auto-ignition temperature such as gasoline, methanol, and ethanol are injected into the port and high reactivity fuels such as diesel or biodiesel is directly injected into the combustion chamber as usual. Best alternative for port injection in RCCI engines is a mixture of alcohols and gasoline. The proportion of each of these two fuels depends on the engine operating condition and other engine parameters. However, only ~10% diesel of total fuel mass is injected into the cylinder to trigger RCCI combustion under most operating conditions. RCCI combustion is capable of achieving near-zero NOx and PM emissions along with high engine efficiency. However requirement of two fuel injection systems increases the cost and complexity of the vehicle significantly.

Premixed Charge Compression Ignition (PCCI) engine (Kimura et al. 1999; Fuerhapter et al. 2003; Cao et al. 2009; Parks II et al. 2010) provides more stable combustion compared to the HCCI engine. It offers more time for mixture preparation before SoC compared to conventional diesel combustion. Ignition of partially premixed fuel-air charge is similar to that of HCCI combustion. Majority of fuel is burned in the premixed phase in PCCI combustion like HCCI combustion, which reduces NOx and PM emissions simultaneously. Similar to other LTC techniques, PCCI combustion faces the same challenges of higher CO and HC emissions compared to diesel engines. However, these CO and HC emissions in PCCI combustion are lower than the HCCI combustion.

5.5 Gasoline Compression Ignition Engine Technology

Gasoline Compression Ignition (GCI) is an advanced engine technology, utilizing low-octane gasoline in place of diesel in CI engines. Gasoline is more volatile with high resistant to auto-ignition, which facilitates homogenous mixing of fuel-air before SoC compared to diesel operation. GCI technology combines the benefits of higher compression ratio (CR) operation of CI engines and positive features of gasoline. It is expected that this new engine-fuel system will be cost-effective because of use of low-octane gasoline, which would be cheaper, and can help reduce exhaust emissions such as NOx and PM simultaneously. Scope of utilizing a higher percentage of exhaust gas recirculation (EGR) exists, which can further help reduce PM and NOx emissions. Mazda recently launched a new car SkyAktiv X, operating on GCI technology (Mazda 2017).

5.5.1 Principle of GCI Combustion

Gasoline compression ignition (GCI) is an advanced LTC technique that can address the problems associated with diesel engines. GCI engine operates on fully pre-mixed homogenous combustion mode (like HCCI) at low load, on partially pre-mixed combustion (PPC) mode at medium load, and on diffusion-controlled combustion (like

a diesel engine) mode at high load condition. Based on the level of mixture homogeneity, partially pre-mixed combustion (PPC) lies in-between the HCCI and CI combustion modes. In PPC mode, fuel-air mixture is burned in combination of both diffusion and pre-mixed mechanisms with bulk auto-ignition. At low loads, fuel is injected in the intake stroke or at the start of compression stroke so that more mixture homogeneity can be achieved whereas at high loads, gasoline is directly injected like diesel near the top dead center (TDC) in the combustion chamber. In GCI engine, level of fuel stratification needs to be improved with increasing engine load, since the ignition delay decreases with increasing load. Therefore, a small amount of combustion takes place by auto-ignition, and the remaining majority of fuel combustion dominated by diffusion process.

5.5.2   GCI Engine Fuel Refining Process

GCI engines can operate efficiently on the low octane gasoline like fuels such as naphtha. Previous studies (Hildingsson et al. 2009) on a single cylinder engine with a compression ratio 16:1 showed that the optimum research octane number (RON) for GCI combustion lies between 75 and 85. Another experimental investigation on a heavy-duty CI engine suggested that optimum RON for GCI combustion should be in the 70's range (Manente et al. 2011). Optimum fuel properties for GCI engines are listed in Table 5.3 (Kalghatgi et al. 2016).

Mixture of diesel and gasoline or low octane gasoline can extend GCI operating range with enhanced fuel stratification (Won et al. 2012a). Gasoline and diesel blend can easily match the required GCI fuel properties although safety and flash point demand of fuel can be an issue. By only adding >25% components from diesel boiling range in the gasoline/diesel blends, GCI fuel can easily meet safety requirement (Algunaibet et al. 2016; Al-Abdullah et al. 2015). Low octane gasoline has a higher hydrogen/carbon ratio and more paraffinic components. Distillation range of GCI fuel is closer to gasoline than diesel, and new fuel has a higher final boiling point

| Table 5.3 Optimum fuel properties for a GCI engine (Kalghatgi et al. 2016)	Properties	Optimum value
	Research octane number (RON)	70–85
	Cetane number	<27
	Density @ 15 °C, kg/m^3	720–800
	Initial Boiling Point, (IBP) °C	28
	Final Boiling Point, (FBP) °C	250
	Olefins, lv%	<18
	Aromatics, lv%	<35
	Sulfur, wt ppm	<10
	Benzene, vol. %	<1
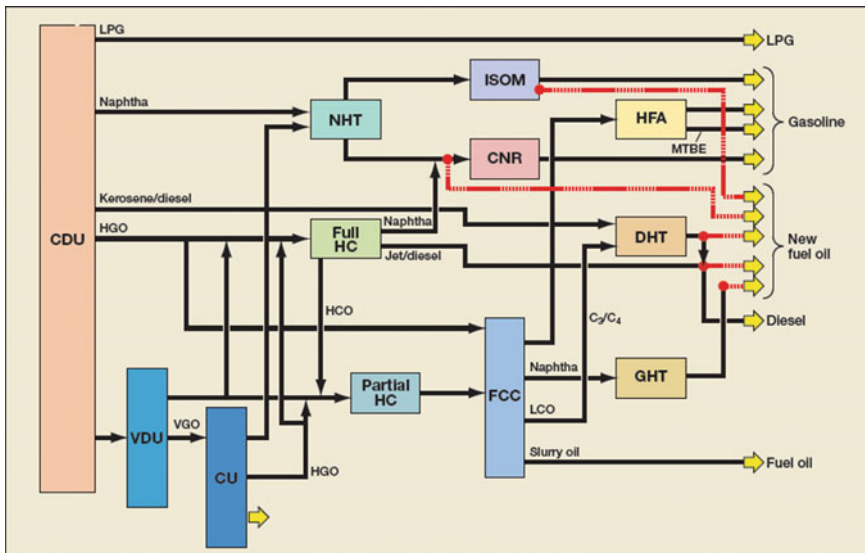
Fig. 5.7 Refinery configuration for new GCI fuel (Kalghatgi et al. 2016) (CDU—crude distillation unit, VDU—vacuum distillation unit, CU—coking unit, HC—hydrocracking unit, DHT—distillate hydrotreating unit, FCC—fluid catalytic cracking unit, HFA—HF alkylation unit, GHT—gasoline hydrotreating unit, NHT—naphtha hydrotreating unit, ISOM—isomerization unit, and CNR—continuous naphtha reforming unit)

compared to baseline gasoline. Refinery configuration for the GCI fuel is almost similar to traditional one except different unit capabilities. Refinery configuration for new GCI fuel is shown in Fig. 5.7 (Kalghatgi et al. 2016).

GHG emissions in refining process for low octane gasoline (12.8 g CO_2-eq/MJ) are lower than that of gasoline (14.8 g CO_2-eq/MJ) and diesel (13.5 g CO_2-eq/MJ) production. Well-to-wheel GHG emissions from a GCI engine is 22% less than an equivalent SI engine and ~9% lower than an equivalent diesel engine. Experimental results of Lu Z. et al. (Lu et al. 2016) suggested that a GCI engine operating on low octane gasoline has 125% higher fuel economy compared to SI engine operating on US gasoline.

5.5.3 GCI Combustion Modes

Depending on engine operating conditions, the level of fuel stratification significantly affects the auto-ignitability, combustion phasing, combustion stability, and emissions in a GCI engine. Fuel stratification can be controlled by using the fuel injection strategy. Due to this, GCI is a more practical technique compared to HCCI and can be utilized in commercial diesel engines for a wider operating range with better-combustion stability (Manente et al. 2011; Dec et al. 2011, 2015; Hao et al.

2016; Borgqvist et al. 2012). GCI combustion modes are classified into three categories according to the level of fuel stratification: partial fuel stratification (PFS), medium fuel stratification (MFS), and high fuel stratification (HFS). Multiple injection strategy is utilized in GCI engines for achieving stable combustion and level of fuel stratification, which is determined by using the injection centroid formula (Dempsey et al. 2016):

$$\theta_{inj} = \frac{\sum_{i=1}^{N_{inj}} Y_i SOI_i}{\sum_{i=1}^{N_{inj}} Y_i} = \sum_{i=1}^{N_{inj}} Y_i SOI_i$$

where N_{inj} = Number of injections, Y_i is the fraction of fuel mass in ith injection, and SOI_i is the start of injection of ith injection.

PFS is used for preparation of homogeneous charge at part-load conditions, in which the first injection takes place either into the port or direct injection in the intake stroke. Main injection takes place in the compression stroke to create desired level of fuel stratification and to auto-ignite the charge so that the engine can achieve low emissions with an acceptable combustion noise. In MFS, level of premixed charge slightly decreases with a slight increase in the fuel stratification level. All injections in MFS mode take place during the compression stroke, in which final injection takes place near TDC to trigger the premixed charge. High level of fuel stratification, with no or very less premixed charge is utilized in the GCI engine at high load condition. In HFS mode, all injection events take place near TDC in the compression stroke (Dempsey et al. 2016). FIP varies to achieve the desired level of fuel stratification in GCI combustion. Higher FIP is utilized in case of HFS compared to MFS and PFS to complete the injection before the SoC. However FIP requirement of HFS is still significantly lower than diesel PCCI due to high self-ignition temperature and high volatility of gasoline. GCI combustion requires lower fuel stratification for the operation with a high level of EGR (Dempsey et al. 2016; Noehre et al. 2006). Effect of different parameters on GCI combustion modes such as PFS, MFS, and HFS are discussed briefly in Table 5.4 (Dempsey et al. 2016). And comparison of various conventional and advanced engine combustion techniques based on the level of fuel stratification before the SoC is captured in Fig. 5.8 (Singh and Agarwal 2019).

5.5.4 GCI Versus Other Combustion Concepts

Implementation of efficient and eco-friendly combustion techniques is the focus of engine researchers at present. Due to increased concerns about emissions and fuel economy, researchers have started to work on alternative combustion technologies such as low temperature combustion (HCCI, PCCI, and RCCI), GDI, and GCI. Comparative analysis of the GCI engine technology with other combustion technologies is discussed in Table 5.5.

Table 5.4 Effects of fuel stratification levels on GCI engine performance, combustion and emissions Parameters (Dempsey et al. 2016)

Parameters	Partial fuel stratification	Medium fuel stratification	High fuel stratification
Injection Period	First injection either in the port or very early in the intake stroke and main injection in the mid-compression stroke θ_{inj}: 320–120°bTDC	All Direct Injection (DI) events take place during compression stroke and main injection near the TDC θ_{inj}: 120°–140°bTDC	Multiple DI events take place near the TDC θ_{inj}: 40°–0°bTDC
FIP	Low	Medium	High, but less than diesel PCCI
Premixing level	Highly premixed before SOC	Medium	No or very less premixed fuel
Combustion and its control	Similar to HCCI combustion with same opportunities and challenges and kinetically controlled combustion identical to HCCI	More closer to diesel PCCI with advanced injection and longer ignition delay, injection driven concept and combustion control mainly by injection near the TDC	Combustion identical to diesel PCCI and injection-induced concept, combustion managed like CDC and diesel PCCI
Opportunities	Ultra-low NOx and soot emissions	Lowest combustion noise and RoPR among all GCI strategies	High combustion efficiency similar to CDC. Low soot emissions
Challenge	Low combustion efficiency, high combustion noise, limited operating range, little control over combustion phasing	Modest combustion efficiency, NOx and soot emissions	High NOx emissions, But lower than diesel PCCI. High RoPR and high combustion noise

5.5.5 Opportunities and Challenges Associated with GCI

High volatility and long ignition delay period of gasoline facilitates superior mixture homogeneity, which eventually allows the GCI engine to operate at lower FIP. Hence, GCI vehicles can be equipped with low-pressure fuel pump, leading to significantly lower cost and complexity of the fuel injection system. Lower FIP improves the GCI combustion stability at part loads and helps in reducing CO and HC emissions as well. By controlling the fuel stratification level, fuel over-mixing and over-leaning of the mixture can be avoided in GCI engine (Kalghatgi and Johansson 2018). GCI technique helps in mitigating the pumping losses and it could be operated at wide-open
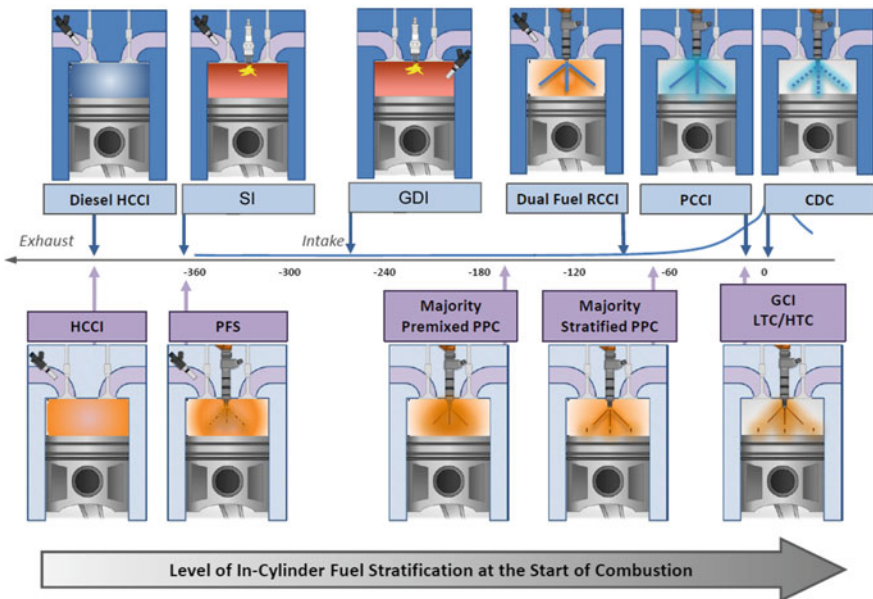
Fig. 5.8 Comparison of various conventional and advanced engine combustion techniques based on the level of fuel stratification before the SoC (Singh and Agarwal 2019)

throttle (WOT) condition at higher compression ratio thus engine can achieve higher efficiency quite similar to conventional diesel engines. Pilot injection is employed in diesel engine at low load condition to reduce combustion noise, but it lowers the engine efficiency and increases the smoke level. This problem can be tackled by GCI fuel, which provides longer ignition delay. Reduced parasitic losses due to lower FIP and less frequently regeneration of particulate filter helps in engine efficiency improvement. However, it is necessary to control high HC and CO emissions of GCI engine by using exhaust gas after-treatment devices. The focus of exhaust gas after-treatment shifts to oxidation of HC and CO in GCI engines, which is much easier and cost-effective compared to controlling NOx and PM emissions in case of a diesel engine. In GCI engines, soot emission increase with increasing engine load. However, its level is always less than that of diesel engine with the same fuel injection system because mixture homogeneity is far better in the previous case. Heavy-duty GCI engine requires a gasoline particulate filter (GPF) to control the soot emissions at high engine load conditions. At high load condition, GPF self-regenerates due to high exhaust gas temperature.

Though a GCI engine produces low NOx emissions, it would require NOx after-treatment device in order to comply with stringent emission norms, however it will be less loaded compared to a DPF. There is scope for developing cost-effective and straightforward after-treatment systems for GCI engines compared to modern diesel engines. Besides, it is necessary to develop oxidation catalysts and GPF that could work at low exhaust temperatures. Figure 5.9 shows that GCI engine technology

Table 5.5 Comparative analysis of different IC engine combustion technologies

Basic Parameters	Conventional Techniques		Low Temperature Combustion			
	SI	CI	HCCI	PCCI	RCCI	GCI
Fuel	Gasoline like fuels	Diesel like fuels	Flexible fuel	Flexible fuel	Combination of fuels	Low octane gasoline
Fuel ignition characteristics	High resistance to auto-ignition (high Octane)	Easy auto-ignition (high Cetane)	Depends upon compression ratio (CR)	Depends upon compression ratio (CR)	High octane fuel in the port and high Cetane fuel via DI	Octane rating in the range of 70–85 (Optimum RON ~70)
Ignition Source	Spark ignition	Auto-ignition	Auto-ignition	Ignited by the main injection	Ignited by the direct injection	Triggered by the main injection
Fuel Injection	PFI/GDI	Direct injection	PFI/DI	Multiple DI	Both Port and DI	Multiple DI
Combustion characteristics and Flame front	Premixed combustion with turbulent flame (homogenous/stratified)	Diffusion combustion without flame (heterogeneous)	Premixed combustion governed by in-cylinder pressure and temp.	Premixed and homogenous combustion without flame front	Premixed combustion controlled by chemical kinetics	Premixed combustion depending upon fuel stratification
Fuel-air ratio	Stoichiometric ($\lambda = 1$), load independent	$\lambda = 1.2$–2.2 linearly dependant on engine load	Lean ($\lambda > 1$)	Lean ($\lambda > 1$)	Lean/stoichiometric ($\lambda > 1$, $= 1$)	Lean ($\lambda > 1$)
Throttling	Throttled/Unthrottled	Unthrottled	Unthrottled	Unthrottled	Unthrottled	Unthrottled
Ignition control	Spark timing	Injection timing	Kinetically controlled	Injection timing and in-cylinder condition	Main injection timing	By Main injection timing
Emissions	High CO and HC, and low NOx and PM	High PM and NOx	Low PM and NOx	Low PM and NOx	Low PM and NOx with high CO and HC	Low PM and NOx with high CO and HC
Efficiency	Poor part load Efficiency	High Efficiency	Depends on CR	High Efficiency	High Efficiency	High Efficiency like CDC

(continued)

Table 5.5 (continued)

Basic Parameters	Conventional Techniques		Low Temperature Combustion			GCI
	SI	CI	HCCI	PCCI	RCCI	
Challenges	Low engine efficiency and high throttling losses	High PM and NOx emissions, high vehicle cost due to installation of expensive exhaust after-treatment system and FIE system	Relativity high CO and HC emissions with poor combustion stability	Relativity high CO and HC emissions	Relativity higher CO and HC emission and complicated and expensive due to addition of a PFI system	High CO and HC emissions, high RoPR at medium and high load, poor combustion stability at low loads
Advantages	Very low emissions using a 3-way catalytic converter	High Efficiency	Improved efficiency with low emissions	High efficiency with little PM and NOx emissions	High thermal efficiency with low PM and NOx emissions and better control on combustion stability	High efficiency, small PM, NOx, and GHG emissions, operates on low octane gasoline, low-cost vehicle
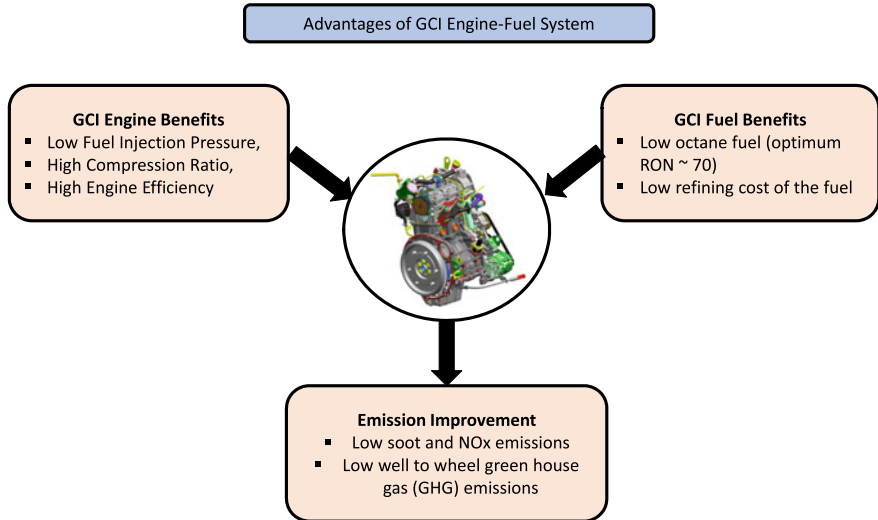
Fig. 5.9   Advantages of GCI engine technology

can reduce vehicle operating cost by using low octane fuel, while maintaining high engine efficiency.

Therefore R&D efforts are required to address the issues associated with GCI engine technology before its adoption in commercial vehicles. Main challenges associated with GCI technology are captured in Fig. 5.10 (Kalghatgi and Johansson 2018). However, most problems can be resolved by optimizing the combustion. It
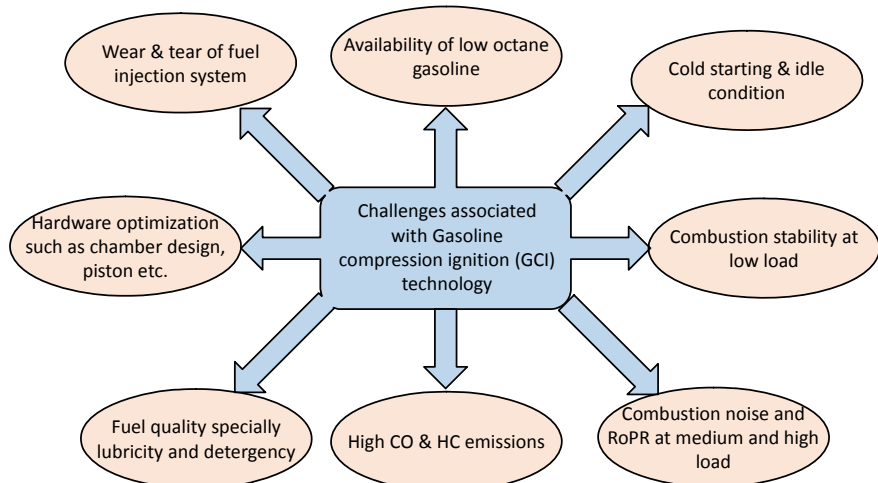
Fig. 5.10   Challenges for GCI engine technology

is much simpler to address the issues associated with GCI engines than the existing diesel engines because diesel engines (CI engines) are the "right engine" operating with the "wrong fuel". Control of PM and NOx emissions from the diesel engine has reached their practical limits. GCI will be an alternative technology to reduce the emissions from CI engines without compromising the engine efficiency. Also it would help in reducing GHG emission footprint (Kalghatgi and Johansson 2018; Mazda 2017). Therefore implementation of GCI technology could be beneficial to both the automotive industry and the oil companies. It opens a path to mitigate imbalance in the future fuel demand for light and heavy fuel oils.

5.6   Effect of Various Control Strategies on GCI Engine

Main issues associated with GCI technique include cold starting problems, high HC and CO emissions, combustion instability at low loads, and high RoPR at medium, and high loads. Like other engine combustion processes, GCI combustion also significantly depends on fuel properties, optimum injection strategies, and engine operating characteristics. GCI technology can be effectively implemented by optimizing injection strategies. Different control strategies that can be employed in GCI combustion towards satisfactory engine performance are described in the following sub-sections.

5.6.1   Injection Strategy

Fuel injection strategies greatly influence engine combustion, performance, and tailpipe emissions. By utilizing split injection strategies in GCI engine, desired level of combustion noise, and knock resistance can be achieved. Split injections (multi-injections) use two or more-injection pulses to control the rate of pressure rise (RoPR), apparent heat release rate (aHRR), and combustion noise. In multi-injection technology, first injection pulse controls the level of premixed charge (mixture homogeneity), and second injection pulse controls the combustion phasing (ignition timing). The effect of pilot injection quantity and fuel quality on mixture condition is shown in Fig. 5.11 (Goyal et al. 2019).

Pilot injection timing and quantity affects the level of fuel stratification and prepares a thermodynamic state for auto-ignition of fuel injected in main injection. It also helps in controlling heat release rate and engine out-emissions (Lu et al. 2011). An optimized injection strategy can help achieve greater productive control on GCI combustion and stretched heat release profile for full engine operating range (Kalghatgi et al. 2007; Sellnau et al. 2012; Manente et al. 2009; Ra et al. 2011; Goyal et al. 2017). Due to long ignition delay of gasoline, injection process and combustion event cannot be easily separated at full load. Extended injection duration and ignition delay result in substantial soot emissions due to diffusion combustion domination at high load (Manente et al. 2010; Lewander et al. 2011). By using multiple injection
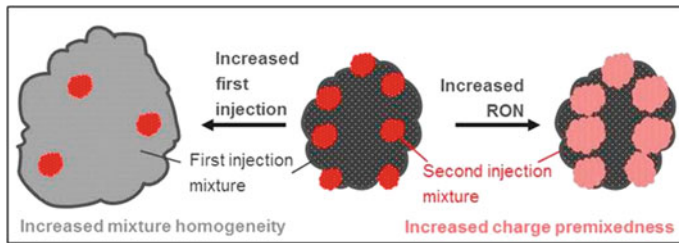
Fig. 5.11 Effect of pilot injection quantity and fuel quality on mixture quality (Goyal et al. 2019)
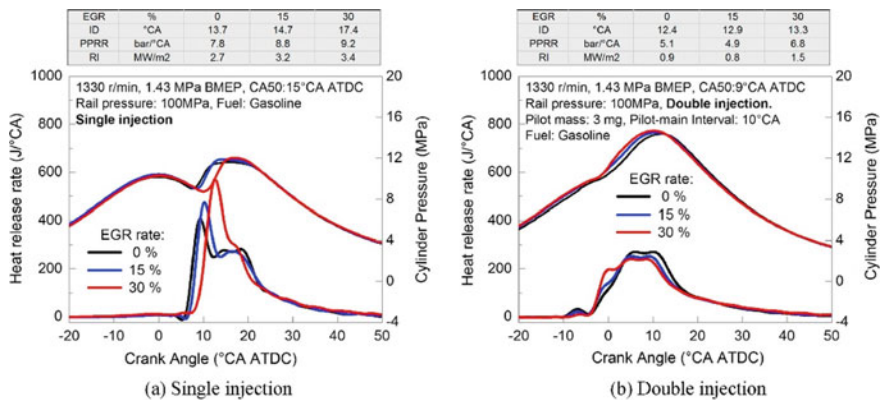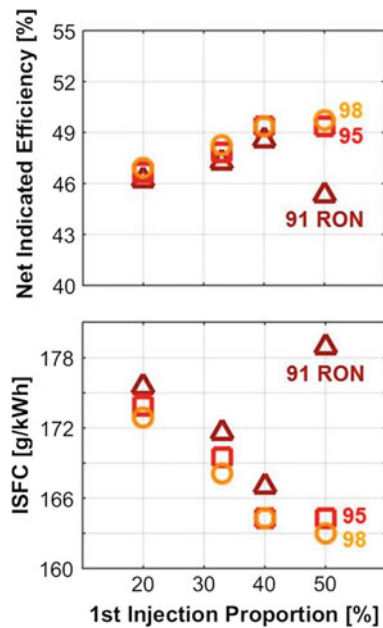

Fig. 5.12 In-cylinder pressure and HRR of GCI combustion engine under **a** single injection and **b** double injection (Mao et al. 2018)

strategy, lower PM and NOx emissions from a GCI engine can be achieved due to improved charge homogeneity, similar to HCCI engines (Kalghatgi et al. 2007; Ra et al. 2012; Zhao et al. 2003; Gray III and Ryan III 1997; Thring 1989), while oxidation of unburned species can lower HC and CO emissions at high temperature due to superior premixing of charge.

Mao et al. (2018) optimized injection strategies of a GCI engine and suggested that a single injection strategy could not be employed effectively in GCI combustion engine due to knocking and substantial reduction in fuel economy (Fig. 5.12). Pilot injection reduced the ignition delay, improved combustion noise and controllability, and reduced the emissions. They achieved a peak brake thermal efficiency (BTE) of ~44% at 1350 rpm in a multi-cylinder GCI engine with Euro-VI NOx emissions.

Goyal et al. (2019) investigated the effect of pilot injection quantity and fuel quality (RON 91, 95 and 98) on a single-cylinder GCI engine operating at 2000 rpm at 940 kPa IMEP. They reported that at fixed RON, an increased proportion of pilot fuel quantity leads to an improvement in mixture homogeneity and slows down initial burning rate, as shown in Fig. 5.13.

Fig. 5.13 Indicated thermal efficiency (ITE) at different pilot/first injection proportion and fuel ignition quality at fixed combustion phasing (CA50 at 10°CA aTDC) (Goyal et al. 2019)

Increased pilot injection quantity provided stretched heat release profile with lower combustion noise. Results suggested that 50% first injection proportion with 91 RON achieved the lowest combustion noise and peak pressure rise rate (PPRR). Enhanced mixture homogeneity reduced the in-cylinder reaction temperature resulting in NOx reductions. However, a more moderate reaction temperature can reduce the oxidation rate, which results in increased emissions of CO, HC, and smoke. Researchers obtained an indicated thermal efficiency (ITE) ranging from 45 to 50% in the GCI engines (Fig. 5.13). Even the lowest efficiency (41%) of GCI engine was relatively higher than the reference diesel engine efficiency.

5.6.2 Fuel Ignition Quality

Gasoline has a lower cetane number (usually <15) which provides longer ignition delay before SoC. It should be injected earlier in the compression stroke at lower in-cylinder pressure and temperature conditions, which are not favorable for auto-ignition of gasoline. Utilization of EGR in GCI combustion further retards the ignition reactions (Cracknell et al. 2008). Ignition delay model was developed for diesel combustion in warmed-up engine conditions (Vallinayagam et al. 2018), and it was extended to estimate ignition delay at lower temperatures or for the fuels having different Cetane ratings. Results showed that ignition delay increased by three times,
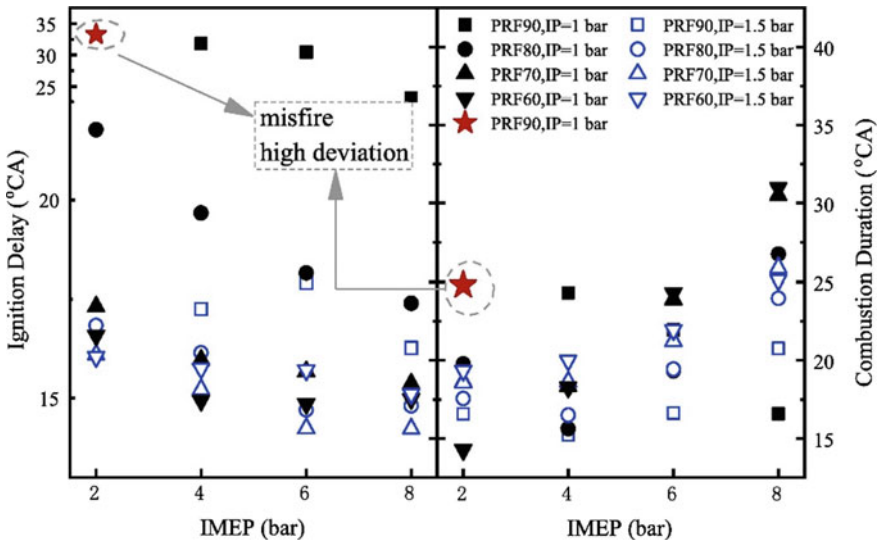
Fig. 5.14 Effect of intake air pressure (IP) on the ignition delay and combustion duration at different engine load conditions (Jiang et al. 2019)

when the engine coolant temperature dropped from 100 to 0 °C and was doubled for gasoline (CN15) as compared to baseline diesel.

Jiang et al. (2019) investigated the performance and emissions characteristics of GCI engine fueled with four different primary reference fuels (PRFs) having research octane number of 60, 70, 80, and 90. Figure 5.14 (Jiang et al. 2019) shows the effects on intake air pressure (IP) on combustion duration and ignition delay. Results showed that combustion was unstable with PRF90 at 2 bar IMEP because of longer ignition delay period. Researchers suggested that GCI engine delivered better performance and engine efficiency using PRF70 with intake air heating at part load (IMEP between 1 and 4 bar). PRF70 provided good results at medium loads (IMEP between 4 and 8 bars) and PRF90 above IMEP of 8 bar without intake air heating. Up to 47% ITE with PRF70 under medium load was observed in this study.

Cho et al. (2017) et al. conducted experiments with the US market gasoline (RON92 E10) and RON80 gasoline on Delphi's 2nd generation GCI engine at different load conditions. GCI engine utilized a high amount of EGR (~44%) with RON80 compared to conventional gasoline (EGR ~39%) for the same combustion phasing at lower temperature and pressure. Due to difference in fuel reactivity, they achieved 10.9% lower BSFC, and improved combustion stability (COV 0.50% for RON80 and 0.99% for conventional gasoline) at part and medium loads. Overall, RON80 was better in terms of efficiency, stability, and emissions compared to RON92 E10 gasoline.

Goyal et al. (2019) reported that higher RON fuels and fixed pilot injection quantity leads to higher premixing of fuel injected during main injection event, which increases combustion noise and peak aHRR. Researchers added that engine efficiency
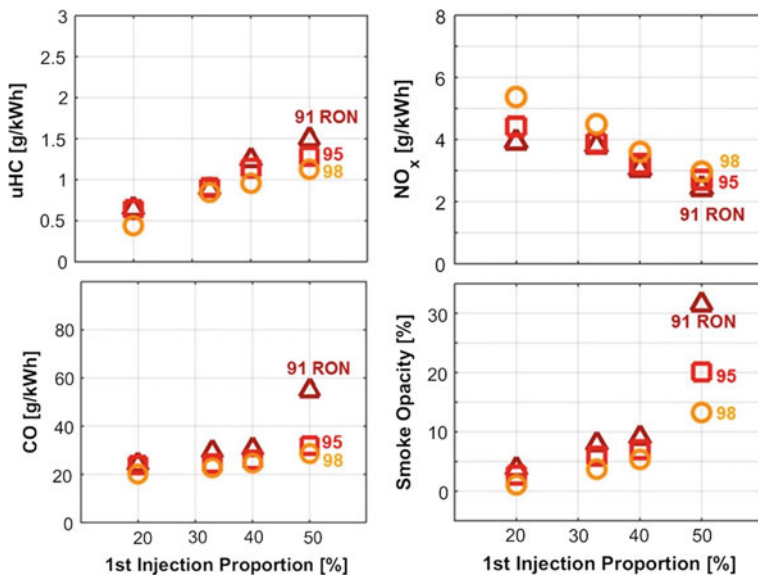
Fig. 5.15 Engine out NOx/HC/CO and smoke emissions at different pilot injection proportions and fuel ignition quality at fixed combustion phasing (CA50 at 10°CA aTDC) (Goyal et al. 2019)

improved with increasing RON of the test fuel but decreased with increasing first injection quantity. However higher RON with fixed mixture homogeneity resulted in over-premixing of the second injection. It increased engine-out NOx emissions due to high reaction temperatures but it reduced the engine-out HC, CO and smoke emissions. Effect of pilot mass and fuel ignition quality is shown in Fig. 5.15 (Goyal et al. 2019) with fixed combustion phasing.

5.6.3 EGR Strategy

Effective control of used EGR reduces NOx emissions by controlling the in-cylinder temperature and oxygen level. Ra et al. (2011) investigated the effect of EGR, injection timing, and fuel split ratio on a light-duty diesel engine in GCI mode at full load (16 bar IMEP, 2500 rpm). They obtained lower PM and NOx emissions (0.1 g/kg-f) and low ISFC (180 g/kWh) due to lower combustion temperature by utilizing high EGR, high volatility and high octane rating of gasoline. Decreasing EGR ratio helped in retarding injection timing for optimum GCI combustion. Similarly Kolodziej et al. (2016) suggested that increased fuel reactivity (lower octane rating) required more EGR for controlled GCI combustion. Yao et al. (2015) reported that lower octane gasoline improved the NOx-PM tradeoff with a high level of EGR. They utilized multiple injection strategy with 50% EGR and demonstrated an ITE of 51.57% with lower maximum RoPR and regulated emissions.

5.6.4 Other Control Techniques

5.6.4.1 Negative Valve Overlapping

Higher RON gasoline has longer ignition delay that creates a problem in combustion at low loads in GCI engine. This can be resolved by a strategy called negative valve overlapping (NVO), i.e. closing the exhaust valve very early in the cycle. Vallinayagam et al. (2018) extended idle and low load stability of GCI combustion using NVO strategy. They varied the exhaust cam phasing so that exhaust valve closes very early. Recompression of hot gases took place before opening of intake valves, which helped in auto-ignition of charge and improved the combustion stability at low loads. With NVO, intake air temperature requirement decreased by 15–20 °C. NVO reduced engine efficiency at low loads due to more heat losses, but it helped in reduction of CO and HC emissions.

5.6.4.2 Controlling Intake Temperature and Pressure

Jiang et al. (2019) investigated the effect of intake temperature and pressure on the GCI engine combustion and emissions. Increasing intake pressure to 8 bar enhanced GCI engine fuel economy by 20 g/kWh at low RON of 70. They reported that increasing intake pressure advanced the combustion and the combustion phasing. Supercharging helped reduce HC and CO emissions due to proper burning and led to a reduction in NOx emissions. However total PM increased at part load conditions. Increasing intake temperature decreased engine's volumetric efficiency, and HC and CO emissions at part load but increased NOx emissions due to relatively higher peak in-cylinder temperature. ITE improved by 16% using PRF70 at intake temperature of 50 °C compared to PRF90 at 30 °C.

5.6.4.3 Effect of Ozone Seeding on GCI Engine

Seeding ozone in intake air improves gasoline reactivity thus can enhance the low load limit of a GCI engine as reported by Pinazzi and Foucher (2017). Ozone seeding reduces the intake air temperature, and subsequently lowered the combustion temperature, resulting in reduction of NOx emissions. Researchers suggested that first injection should be in intake stroke so that ozone get more residence time, and second injection should be in compression stroke to control the level of fuel stratification, avoiding excessive heat release rate. However overall combustion and indicated efficiency can be affected because of large time gap in the injection events.

5.7 Critical Parts of a GCI Engine

GCI technique can be adopted in modern CI engines with minimal modifications in engine design and fuel injection system. It requires a simple fuel injection system and exhaust after-treatment system that can reduce vehicle cost and complexity. In this section, adoption of GCI technique in the contemporary CI engines is summarized.

5.7.1 Fuel Injection System

Fuel injection system is a critical part of a CI engine that affects engine performance, combustion, and tail-pipe emissions. High FIP is required for adequate atomization and mixing of the charge. As the FIP increases, cost, and complexity of the system increases simultaneously. In case of GCI engine, FIP depends on the operating condition and desired level of fuel stratification. Even with high volatility of gasoline, FIP can go up to 1000 bar at full capacity of a GCI engine. CRDI fuel injection system would be a better choice for GCI engine with minor modifications in fuel injector geometry. Fuel injector design should be such that it can provide sufficient fuel quantity at desired FIP. Lower FIP helps reduce power requirement for the fuel pump. For example, reducing FIP from 1460 bar to 960 bar reduces fuel pump power by about 100 W. GCI engines can operate at half of diesel engine's FIP. A GCI engine can achieve the lowest BSFC in between 80 and 110 MPa injection pressure. Gasoline has lower density and calorific value (by volume) compared to diesel, hence more quantity is required to be injected to achieve diesel-like power output. Therefore gasoline fuel injector holes for a GCI engine would be slightly larger than the diesel injector holes. Otherwise, fuel injection period needs to be increased, if a diesel injector is to be used to inject gasoline in a GCI engine.

Lubricity of market gasoline is not adequate to protect the fuel injection system from wear and tear. Hence it requires either a careful selection of material for the fuel injection system or addition of suitable additives in gasoline for improving its lubricity (Rose et al. 2013). Won et al. (2012) suggested that large injector hole and lower FIP could be beneficial for GCI combustion. In contrast to these results, Rose et al. (2013) reported that a smaller injector diameter performs better at full operating range of the engine. With a fixed nozzle size, it is better to utilize multiple fuel injections at low FIP in GCI combustion in order to control the combustion noise.

5.7.2 Compression Ratio

Compression ratio (CR) dramatically changes the ignition delay period. Previous studies (Stone 2012; Al-Abdullah et al. 2015; Ra et al. 2011) confirmed that GCI

engines can work efficiently using similar compression ratios, ranging from 16.5 to 19, as that of conventional diesel engines. Rose et al. (2013) investigated the effect of two different compression ratios (CR17 and CR19) in a GCI engine. Higher CR (19:1) provided shorter ignition delay period, allowing better control on GCI combustion at low engine loads. At full capacity, CR19 provided better efficiency due to reduced losses. However, use of higher CR was limited by smoke emission, noise, and exhaust gas temperature. Researchers concluded that utilization of variable compression ratio (VCR) could be beneficial for GCI engines. However, another study showed that lowering CR of heavy-duty Cummins engine from 18.9 to 15.7 improved soot-NOx tradeoff at the expense of engine efficiency (Won et al. 2012b), without altering the bowl geometry.

5.7.3 Engine Management System

Optimum performance of an engine depends on different operating parameters such as FIP, injection timing, injection quantity, intake air conditions, and EGR. These parameters must be controlled simultaneously in order to achieve optimum engine performance at given operating conditions. Automobile companies use a preset non-programmable electronic control unit (closed ECU) in vehicle for attaining optimum performance of the engine. As mentioned previously, GCI engines would require multiple injections strategy for achieving better combustion stability and engine performance. Therefore, an open ECU (programmable ECU) has to be used instead of a closed ECU to control and optimize different influencing parameters mentioned earlier. Different sensors and actuators such as lambda sensor, cam sensor, crank sensor, and various temperature and pressure sensors are usually connected to an open ECU and a user can reprogram the ECU as per requirement. Thus an optimized engine management system can effectively and efficiently control in-cylinder conditions by varying the EGR rate, boost level, and valve timing (Fig. 5.16).

5.7.4 GCI Exhaust After-Treatment System

GCI engine emits lower tailpipe NOx and PM emissions but higher HC and CO emissions than diesel engine. Fortunately, it is much simpler to control NOx and PM emissions in GCI engines (Rose et al. 2013). However, GCI will require efficient oxidation catalyst to control the HC and CO emissions at low exhaust gas temperature and gasoline particulate filter (GPF) in order to comply with emission regulations. Regeneration interval of GPF in GCI vehicles will increase and save ~1.5% fuel compared to diesel DPF equipped vehicles.
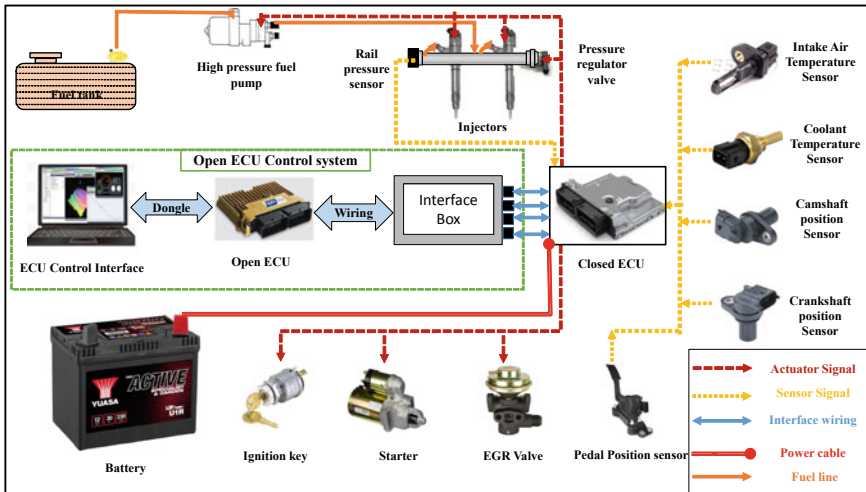
Fig. 5.16 Open ECU interface and engine management system

5.8 Path Forward for GCI Engine Technology

Gasoline compression ignition (GCI) offers an efficient and eco-friendly combustion technique at a reasonable cost. GCI engine can operate efficiently with low octane fuels (RON 70) in the diesel boiling range. Straight run gasoline after the first distillation can be utilized in GCI engines without any post-processing. In initial phase, GCI vehicles can be operated with gasoline-diesel blend in case of unavailability of low octane fuel. However, in order to commercialize GCI vehicles in the current market, significant R&D efforts are needed in the following directions:

(i)   GCI engines need to improve combustion stability at part loads. GCI engine fuelled with conventional gasoline has poor combustion stability at low loads due to higher ignition delay, lower cylinder pressure and temperature. Operating parameters such as fuel injection strategy, fuel ignition quality (octane rating), EGR rate, intake pressure and temperature, and piston bowl geometry need to be optimized for effective control of combustion at low loads. Strategies like advanced fuel injection, multiple-injection, low octane fuel usage, negative valve overlap, intake air heating, and EGR usage effectively addresses this issue.

(ii) Combustion control at cold start and idle condition is still an issue with GCI technology. In-cylinder environment at this condition (i.e. low pressure and temperature) is not favorable to auto-ignition of low reactive fuels. To overcome this problem, a suitable combination of fuel ignition quality, advanced injection timing, preheating of intake air, EGR, and NVO can be employed. Glow plug or spark plug can also be used to address the issue of cold start.

(iii) Optimized injection strategies would be needed to control high noise and high rate of pressure rise (RoPR) at medium and high engine loads. Double and triple fuel injections, optimized injection timing and fuel quantity can be beneficial, depending on engine operating conditions.

(iv) GCI engines emit lower NOx and PM emissions but higher HC and CO emissions than a diesel engine. Therefore development of an exhaust gas after-treatment system consisting of efficient oxidation catalysts to control HC and CO emissions at low exhaust gas temperature is essential. Additionally, development of particulate filter will also be required to capture fine soot particles coming out from the engine tailpipe.

 (v) Development of close-loop control and sophisticated engine management system can help GCI engine to operate efficienctly in transient operating conditions. Close loop control can help optimize the operating parameters as per driving cycle requirements instantaneously.

(vi) Fuel injector (with optimum hole size and number), fuel pump, piston geometry, and inlet port are some of the crucial parts, that are needed to be designed properly for effective implementation of GCI technique. R&D efforts are needed to develop suitable additives to improve gasoline lubricity without affecting engine tailpipe emissions.

(vii) Availability of low octane fuel in the market is a major concern associated with implementation of GCI fuel-engine system. A blend of iso-octane and n-hexane with suitable additives can be a suitable test fuel for GCI engine.

In addition to the points mentioned above, R&D efforts should be directed towards the reduction of overall system complexity, and costs, while ensuring easy adaptability of GCI technique to existing CI engines.

5.9 Summary

GCI is an advanced engine combustion technology, which improves engine efficiency, while maintaining low levels of tail-pipe NOx and PM emissions. The issues of high PM and soot formation in diesel engines can be minimized by substituting diesel injection quantity by more volatile and medium reactivity fuels such as low octane gasoline. Investigations of microscopic and macroscopic spray characteristics show that gasoline has a lower spray penetration length than diesel under evaporative ambient conditions, which reduce the chances of wall-wetting in GCI engines. GCI engine can therefore operate efficiently with low octane gasoline fuels. Low octane requirement of GCI engine is beneficial since it can reduce well-to-wheel GHG emissions as well as refining costs. GCI engine operates on three levels of fuel stratification such as partial, moderate, and high, which facilitate optimization of vehicle's performance and emissions under variable operating conditions. Opportunities and challenges associated with all combustion modes like PFS, MFS, and HFS have been discussed in detail.
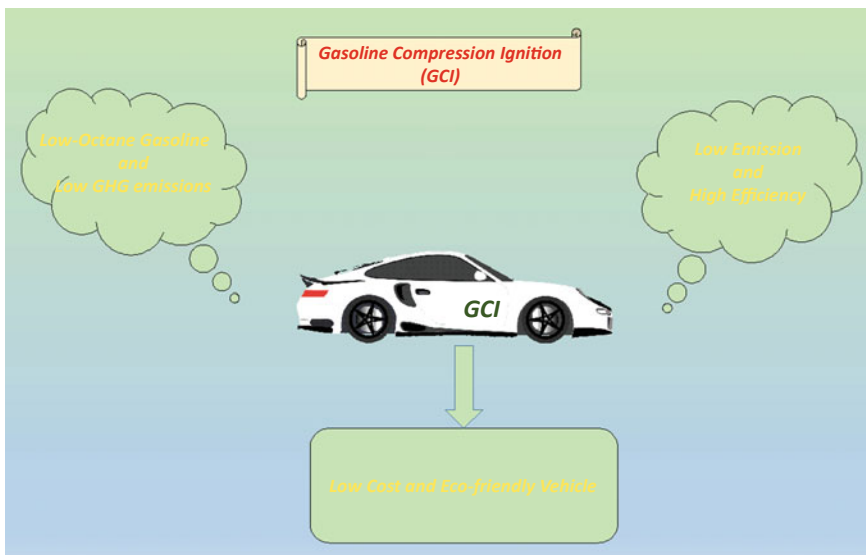
Fig. 5.17 Future of GCI fuel-engine system

Spilt fuel injections strategy can help reduce the combustion noise to a desired level in a GCI engine. Part-load stability of GCI engines can be improved by using NVO, early first injection, EGR and glow-plug. GCI engines would require a robust fuel injection system with a slightly larger injector hole diameter. Maximum compression ratio of a GCI engine depends on operating conditions but is usually between 16:1 to 19:1. Although remarkable progress has been made in the field of GCI technology, high RoHR and combustion noise at medium and full loads, high HC and CO emissions, combustion stability at low loads, cold and idle conditions, and unavailability of low octane fuel are the major obstacles in adoption of GCI technology commercially. Proper optimization of different key influencing parameters discussed in this chapter as well as continuous R&D efforts are quite crucial to address these challenges associated with GCI engines. It can be concluded that it would be easier to work with GCI fuel-engine systems rather than controlling the emissions from diesel engines, hence GCI technology has a bright future in transport sector, as shown in Fig. 5.17.

References

Al-Abdullah MH, Kalghatgi GT, Babiker H (2015) Flash points and volatility characteristics of gasoline/diesel blends. Fuel 153:67–69. https://doi.org/10.1016/j.fuel.2015.02.070

Algunaibet IM, Voice AK, Kalghatgi GT, Babiker H (2016) Flammability and volatility attributes of binary mixtures of some practical multi-component fuels. Fuel 172:273–283. https://doi.org/10.1016/j.fuel.2016.01.023

Boot M (2016) Fuels and combustion. In: Boot M (ed) Biofuels from lignocellulosic biomass. Wiley–VCH, Weinheim, pp 1–27

Borgqvist P, Tunestal P, Johansson B (2012) Gasoline partially premixed combustion in a light duty engine at low load and idle operating conditions. SAE Technical Paper. https://doi.org/10.4271/2012-01-0687

BP Energy Outlook (2017) https://www.bp.com/content/dam/bp/pdf/energy-economics/energy-outlook-2017/bp-energy-outlook-2017.pdf. Accessed 5 Mar 2019

BP Statistical Review of World Energy (2014) https://www.bp.com/en/global/corporate/energy-economics/statistical-review-of-world-energy.html. Accessed 11 May 2015

BP Statistical Review of World Energy (2017) https://www.bp.com/content/dam/bp-country/de_ch/PDF/bp-statistical-review-of-world-energy-2017-full-report.pdf. Accessed 25 Feb 2019

Cao L, Bhave A, Su H, Mosbach S, Kraft M, Dris A, McDavid RM (2009) Influence of injection timing and piston bowl geometry on PCCI combustion and emissions. SAE Intl J Eng 2(1):1019–1033. https://www.jstor.org/stable/26308451

Chincholkar SP, Suryawanshi JG (2016) Gasoline direct injection: an efficient technology. Energy Procedia 90:666–672. https://doi.org/10.1016/j.egypro.2016.11.235

Cho K, Latimer E, Lorey M, Cleary DJ, Sellnau M (2017) Gasoline fuels assessment for Delphi's second generation gasoline direct-injection compression ignition (GDCI) multi-cylinder engine. SAE Intl J Eng 10(4):1430–1442. https://doi.org/10.4271/2017-01-0743

Cracknell RF, Rickeard DJ, Ariztegui J, Rose KD, Muether M, Lamping M, Kolbeck A (2008) Advanced combustion for low emissions and high efficiency. Part 2: impact of fuel properties on HCCI combustion. SAE Technical Paper. https://doi.org/10.4271/2008-01-2404

Dec JE, Yang Y, Dronniou N (2011) Boosted HCCI-controlling pressure-rise rates for performance improvements using partial fuel stratification with conventional gasoline. SAE Intl J Eng 4(1):1169–1189. https://doi.org/10.4271/2011-01-0

Dec JE, Yang Y, Dernotte J, Ji C (2015) Effects of gasoline reactivity and ethanol content on boosted, premixed and partially stratified low-temperature gasoline combustion (LTGC). SAE Intl J Eng 8(3):935–955. https://www.jstor.org/stable/26277996

Dempsey AB, Curran SJ, Wagner RM (2016) A perspective on the range of gasoline compression ignition combustion strategies for high engine efficiency and low NOx and soot emissions: effects of in-cylinder fuel stratification. Intl J Eng Res 17(8):897–917. https://doi.org/10.1177/1468087415621805

Exxonmobil (2019) Outlook for Energy: a view to 2040. https://www.capp.ca/~/media/capp/customerportal/publications/317291.pdf?modified=20180526153435. Accessed 16 June 2019

Fuerhapter A, Piock WF, Fraidl GK (2003) CSI-controlled auto ignition—the best solution for the fuel consumption—versus emission trade-off? SAE Trans 1142–1151. https://doi.org/10.4271/2003-01-0754

Goyal H, Kook S, Hawkes E, Chan QN, Padala S, Ikeda Y (2017) Influence of engine speed on Gasoline Compression Ignition (GCI) combustion in a single-cylinder light-duty diesel engine. SAE Technical Paper. https://doi.org/10.4271/2017-01-0742

Goyal H, Kook S, Ikeda Y (2019) The influence of fuel ignition quality and first injection proportion on gasoline compression ignition (GCI) combustion in a small-bore engine. Fuel 235:1207–1215. https://doi.org/10.1016/j.fuel.2018.08.090

Gray III AW, Ryan III TW (1997) Homogeneous charge compression ignition (HCCI) of diesel fuel. SAE Trans 1:1927–1935. https://www.jstor.org/stable/44730808

Hao H, Liu F, Liu Z, Zhao F (2016) Compression ignition of low-octane gasoline: life cycle energy consumption and greenhouse gas emissions. Appl Energy 181:391–398. https://doi.org/10.1016/j.apenergy.2016.08.100

Heywood JB (1988) Internal combustion engine fundamentals. McGraw-Hill, New York

Hildingsson L, Kalghatgi G, Tait N, Johansson B, Harrison A (2009) Fuel octane effects in the partially premixed combustion regime in compression ignition engines. SAE Technical Paper. https://doi.org/10.4271/2009-01-2648

International Energy Agency (2015) Oil market report, 15 April 2015. https://www.iea.org/media/omrreports/fullissues/2015-04-15.pdf. Accessed 11 May 2015

International Energy Agency (2017) Oil Market Report, 14 December 2017. https://www.iea.org/media/omrreports/fullissues/2017-12-14.pdf. Accessed 22 Jan 2019

IPCC (2019) Chapter 8: Transport IPCC WGIII fifth assessment report. https://www.ipcc.ch/site/assets/uploads/2018/02/ipcc_wg3_ar5_chapter8.pdf. Accessed 1 Mar 2019

Jiang C, Li Z, Liu G, Qian Y, Lu X (2019) Achieving high efficient gasoline compression ignition (GCI) combustion through the cooperative-control of fuel octane number and air intake conditions. Fuel 242:23–34. https://doi.org/10.1016/j.fuel.2019.01.032

Kalghatgi GT (2014) The outlook for fuels for internal combustion engines. Int J Engine Res 15(4):383–398

Kalghatgi G (2018) Is it really the end of internal combustion engines and petroleum in transport? Appl Energy 1(225):965–974

Kalghatgi G, Johansson B (2018) Gasoline compression ignition approach to efficient, clean and affordable future engines. Proc. Instit. Mech. Eng. Part D: J. Automob. Eng. 232(1):118–138. https://doi.org/10.1177/0954407017694275

Kalghatgi GT, Risberg P, Ångström HE (2007) Partially pre-mixed auto-ignition of gasoline to attain low smoke and low NOx at high load in a compression ignition engine and comparison with a diesel fuel. SAE Technical paper. https://doi.org/10.4271/2007-01-0006

Kalghatgi G, Gosling C, Weir MJ (2016) The outlook for transport fuels: part 2. Petrol Technol Quart Q2:17–23

Kim K, Kim D, Jung Y, Bae C (2013) Spray and combustion characteristics of gasoline and diesel in a direct injection compression ignition engine. Fuel 109:616–626. https://doi.org/10.1016/j.fuel.2013.02.060

Kimura S, Aoki O, Ogawa H, Muranaka S, Enomoto Y (1999) New combustion concept for ultra-clean and high-efficiency small DI diesel engines. SAE Technical Paper. https://doi.org/10.4271/1999-01-3681

Kolodziej CP, Sellnau M, Cho K, Cleary D (2016) Operation of a gasoline direct injection compression ignition engine on naphtha and e10 gasoline fuels. SAE Intl J Eng 9(2):979–1001. https://www.jstor.org/stable/26284873

Lewander CM, Johansson B, Tunestal P (2011) Extending the operating region of multi-cylinder partially premixed combustion using high octane number fuel. SAE Technical Paper. https://doi.org/10.4271/2011-01-1394

Lu Y, Yu W, Su W (2011) Using multiple injection strategies in diesel PCCI combustion: potential to extend engine load, improve trade-off of emissions and efficiency. SAE Technical Paper https://doi.org/10.4271/2011-01-1396

Lu Z, Han J, Wang M, Cai H, Sun P, Dieffenthaler D, Gordillo V, Monfort JC, He X, Przesmitzki S (2016) Well-to-wheels analysis of the greenhouse gas emissions and energy use of vehicles with gasoline compression ignition engines on low octane gasoline-like fuel. SAE Intl J Fuels Lubr 9(3):527–545. https://www.jstor.org/stable/26273484

Manente V, Johansson B, Tunestal P (2009) Partially premixed combustion at high load using gasoline and ethanol, a comparison with diesel. SAE Technical Paper. https://doi.org/10.4271/2009-01-0944

Manente V, Johansson B, Tunestal P, Cannella W (2010) Effects of different type of gasoline fuels on heavy duty partially premixed combustion. SAE Intl J Eng 2(2):71–88. https://www.jstor.org/stable/26275408

Manente V, Johansson B, Cannella W (2011) Gasoline partially premixed combustion, the future of internal combustion engines? Intl J Eng Res 12(3):194–208. https://doi.org/10.1177/1468087411402441

Mao B, Chen P, Liu H, Zheng Z, Yao M (2018) Gasoline compression ignition operation on a multi-cylinder heavy duty diesel engine. Fuel 215:339–351. https://doi.org/10.1016/j.fuel.2017.09.020

Mazda (2017) Skyaktiv technology. https://www.mazda.com/en/innovation/technology/skyactiv/skyactiv-g. Accessed 8 Apr 2019

Noehre C, Andersson M, Johansson B, Hultqvist A (2006) Characterization of partially premixed combustion. SAE Technical Paper. https://doi.org/10.4271/2006-01-3412

Nohira H, Ito S (1997) Development of Toyota's direct injection gasoline engine. In: Proceedings of AVL engine and environment conference, pp 239–249

OPEC, Organization of the Petroleum Exporting Countries (2013) World Oil Outlook. https://www.opec.org/opec_web/static_files_project/media/downloads/publications/WOO_2013.pdf. Accessed 16 June 2019

Parks II JE, Prikhodko V, Storey JM, Barone TL, Lewis Sr SA, Kass MD, Huff SP (2010) Emissions from premixed charge compression ignition (PCCI) combustion and affect on emission control devices. Catalysis Today 151(3–4):278–284. https://doi.org/10.1016/j.cattod.2010.02.053

Payri R, García A, Domenech V, Durrett R, Plazas AH (2012) An experimental study of gasoline effects on injection rate, momentum flux and spray characteristics using a common rail diesel injection system. Fuel 97:390–399. https://doi.org/10.1016/j.fuel.2011.11.065

Pinazzi P, Foucher F (2017) Potential of ozone to enable low load operations of a gasoline compression ignition (GCI) engine. SAE Technical Paper 2017-01-0746. https://doi.org/10.4271/2017-01-0746

Ra Y, Loeper P, Reitz R, Andrie M, Krieger R, Foster D, Durrett R, Gopalakrishnan V, Plazas A, Peterson R, Szymkowicz P (2011) Study of high speed gasoline direct injection compression ignition (GDICI) engine operation in the LTC regime. SAE Intl J Eng 4(1):1412–1430. https://www.jstor.org/stable/26278232

Ra Y, Loeper P, Andrie M, Krieger R, Foster D, Reitz R, Durrett R (2012) Gasoline DICI engine operation in the LTC regime using triple-pulse injection. SAE Intl J Eng 5(3):1109–1132. https://www.jstor.org/stable/26277529

Rose KD, Ariztegui J, Cracknell RF, Dubois T, Hamje HD, Pellegrini L, Rickeard DJ, Heuser B, Schnorbus T, Kolbeck AF (2013) Exploring a gasoline compression ignition (GCI) engine concept. SAE Technical Paper. https://doi.org/10.4271/2013-01-0911

Rottenkolber G, Gindele J, Raposo J, Dullenkopf K, Hentschel W, Wittig S, Spicher U, Merzkirch W (2002) Spray analysis of a gasoline direct injector by means of two-phase PIV. Exp Fluids 32(6):710–721. https://doi.org/10.1007/s00348-002-0441-8

Sandrea I, Sandrea R (2007) Global oil reserves—recovery factors leave vast target for EOR technologies. Oil Gas J. https://www.ogj.com/drilling-production/production-operations/ior-eor/article/17227761/global-oil-reserves1-recovery-factors-leave-vast-target-for-eor-technologies. Accessed 8 Apr 2018

Sellnau MC, Sinnamon J, Hoyer K, Husted H (2012) Full-time gasoline direct-injection compression ignition (GDCI) for high efficiency and low NOx and PM. SAE International Journal of Engines. 5(2):300–314. https://www.jstor.org/stable/26278360

Singh AP, Agarwal AK (2019) Characteristics of particulates emitted by ic engines using advanced combustion strategies. In: Advanced engine diagnostics 2019. Springer, Singapore, pp 57–71. https://doi.org/10.1007/978-981-13-3275-3_4

Statista (2016) The statistics portal. Number of passenger cars and commercial vehicles in use worldwide from 2006 to 2014 in (1,000 units). http://www.statista.com/statistics/281134/number-of-vehicles-in-use-worldwide/. Accessed 5 May 2019

Stone R (2012) Introduction to internal combustion engines, 4th edn. Palgrave Macmillan, Basingstoke

Thring RH (1989) Homogeneous-charge compression-ignition (HCCI) engines. SAE Technical Paper. https://doi.org/10.4271/892068

U.S. Energy Information Administration (2013) International energy outlook 2013. DOE/EIA-0484. https://www.eia.gov/outlooks/ieo/pdf/0484(2013).pdf. Accessed 11 May 2019

U.S. Energy Information Administration (2016) International Energy Outlook. https://www.eia.gov/outlooks/ieo/pdf/0484(2016).pdf. Accessed 13 July 2019

U.S. Energy Information Administration (2019) Frequently asked questions. https://www.eia.gov/tools/faqs/faq.php?id=447&t=1. Accessed 11 May 2019

Vallinayagam R, AlRamadan AS, Vedharaj S, An Y, Sim J, Chang J, Johansson B (2018) Low load limit extension for gasoline compression ignition using negative valve overlap strategy. SAE Technical Paper. https://doi.org/10.4271/2018-01-0896

Won HW, Pitsch H, Tait N, Kalghatgi G (2012a) Some effects of gasoline and diesel mixtures on partially premixed combustion and comparison with the practical fuels gasoline and diesel in a compression ignition engine. Proc Inst Mech Eng Part D: J Autom Eng 226(9):1259–1270. https://doi.org/10.1177/0954407012440075

Won HW, Peters N, Tait N, Kalghatgi G (2012b) Sufficiently premixed compression ignition of a gasoline-like fuel using three different nozzles in a diesel engine. Proc Inst Mech. Eng. Part D: J. Automob. Eng. 226(5):698–708. https://doi.org/10.1177/0954407011423453

World Economic Forum (2016) https://www.weforum.org/agenda/2016/04/the-number-of-cars-worldwide-is-set-to-double-by-2040. Accessed 13 June 2019

World Energy Outlook (2011) International Energy Agency, OECD/IEA, Paris. https://www.iea.org/publications/freepublications/publication/WEO2011_WEB.pdf. Accessed 11 May 2019

Yao C, Yang F, Wang J, Huang H, Ouyang M (2015) Injection strategy study of compression ignition engine fueled with naphtha. SAE Technical Paper. https://doi.org/10.4271/2015-01-1797

Zhao F, Asmus TN, Assanis DN, Dec JE, Eng JA, Najt PM (2003) Homogeneous charge compression ignition (HCCI) engines. SAE Technical Paper

Chapter 6
Overview, Advancements and Challenges in Gasoline Direct Injection Engine Technology

Ankur Kalwar and Avinash Kumar Agarwal

Abstract Gasoline direct injection engines have become the popular powertrain for commercial cars in the market. The technology is known for its characteristics of high power output, thermal efficiency and fuel economy. Accurate metering of fuel injection with better fuel utilization makes the engine possible to run on lean mixtures and operation under higher compression ratio relatively makes it of greater potential than PFI engines. Due to its capability of being operated under dual combustion mode by varying fuel injection timing, it can be realized as a cornerstone for future engine technology. Under mode switching, the homogeneous mixture for higher power output at medium and high load-rpm conditions, and stratified mixture for greater fuel economy at low load-rpm conditions are achieved respectively. It can be considered as the technology having the benefits of both diesel engine of higher thermal efficiency and gasoline engine of higher specific power output. But, with the growing concerns towards the limited fuel reserves and the deteriorated environment conditions, strict norms for tail-pipe emissions have been regulated. And considering the higher particulate matter and particle number emissions as a major drawback for GDI engine, upgradation and improvement in designs is needed to meet the required norms of emissions. In the initial section, the chapter gives a brief idea of the overview of the GDI combustion system and its operating modes. Subsequently, the improvements and researches in various aspects like fuel injection parameters and strategies, dual fuel utilization, mixture formation, lean burn control and application of providing turbocharging and residual gas fraction, are elaborately discussed in the direction of optimizing the performance of the engine. Further, the following section explains the major challenges and overcoming of this technology. Review of the work done by various researchers is discussed, focussing on the effect of operating parameters on particulates emissions, injector deposits and knocking in GDI engine.

A. Kalwar · A. K. Agarwal (✉)
Engine Research Laboratory, Department of Mechanical Engineering, Indian Institute of Technology Kanpur, Kanpur, Uttar Pradesh 208016, India
e-mail: akag@iitk.ac.in

A. Kalwar
e-mail: ankurkalwar810@gmail.com

111

Finally, the chapter presents the concluding ways for enhancing the performance, way forward for making it more efficient and reliable by overcoming the limitations of GDI engine technologies.

Keyword Gasoline direct injection technology · Homogenous charge · Lean-burn mixture · Fuel economy · PM emissions

Abbreviations

ATDC	After top dead centre
BMEP	Brake mean effective pressure
BSFC	Brake specific fuel consumption
BTDC	Before top dead centre
CAD	Crank angle division
CFD	Computational fluid dynamics
CO	Carbon monoxide
CR	Compression ratio
DI	Direct injection
DISI	Direct injection spark ignition
DNA	Deoxyribonucleic Acid
EGR	Exhaust gas recirculation
GDI	Gasoline direct injection
GPF	Gasoline particulate filter
HC	Hydrocarbons
IC	Internal combustion
IMEP	Indicated mean effective pressure
ITE	Indicated thermal efficiency
MPFI	Multi-point fuel injection
NEDC	New European driving cycle
PFI	Port fuel injection
PM	Particulate matter
PN	Particulate number
RON	Research octane number
SI	Spark Ignition
TEM	Transmission electron microscope
THC	Total hydrocarbon
TRF	Toluene reference fuel
TWC	Three-way catalyst
VCR	Variable compression ratio
WLTC	Worldwide harmonized light vehicles test cycles

6.1 Introduction

Rising consumption of petroleum products and deteriorating condition of the environment has caused the implementation of the stringent emission standards globally and the development of notable engine technology. The research in engine technology focuses on meeting the objectives of minimizing the fuel consumption and engine emissions, and maximizing combustion efficiency and specific power output of the engine. All these parameters are directly or indirectly influenced by the process of mixture formation which can be either external, internal or both. Gasoline direct injection technology involves creating an air-fuel mixture inside the cylinder by injecting high pressure gasoline fuel directly into the air present in cylinder unlike port fuel injection and ignited with a spark plug. Thus, we get the combined advantages of both diesel and petrol engine i.e., brake specific fuel consumption approaches that of diesel engine and specific power output of petrol engine (Blair 1996). Formation of air-fuel mixture externally using carburetor and injection of fuel in low-pressure manifold has totally occupied 20th century for SI engine development. It has benefits of allowing larger time for mixture formation as it is independent of phase transformation inside the cylinder, thus leads to better fluid dynamic condition and control (Zhao et al. 1999). But still, it has disadvantages of throttling, inlet valve-wetting and charge loss due to valve overlap. GDI overcomes these limitations and its unthrottled operation during part-load conditions significantly improve fuel economy, cause fewer emissions and allow for leaner combustion. Early fuel injection for homogeneous condition results in charge cooling which certainly allows provision for higher compression ratio and lower octane rating fuels as comparison to that of PFI engines.

   With the benefits of high thermal efficiency and substantially less HC and NO_x emissions, GDI engines are likely to dominate the powertrains of passenger cars. Although significant work in research and design is required for tackling the challenges of high particulate matter (PM) emissions and knocking tendency. Worldwide, countries have formulated strict legislations towards exhaust emissions from vehicles. In Europe, the target of approaching CO_2 emission of 95 g/km by 2020 for major light-vehicles has to be achieved. Average annual reductions in CO_2 emissions have to be 3.5 and 5% from 2017 to 2021 and 2022 to 2025 respectively, in the USA. India has decided to adopt Bharat stage 6 (BS-VI) from April 2020 directly from Bharat stage 4 (BS-IV) countrywide in order to curb the pollutant level. Euro 6 emission norms with 0.0045 g/km of particulate matter and the particulate number of 6×10^{11} particle number per km, are some of the examples showing stringent norms for emissions globally (China 2016). It requires more advancement in GDI technology, keeping in view of these regulations. Mazda SKYACTIV sets an example in this direction.[1] In Japan, industry-academia initiative of Research Association of Automotive Internal Combustion Engines aims at achieving the thermal efficiency up to 50% for GDI engine by 2020 (Aubernon 2014).

---

[1]Mazda Corporation, Skyactiv Technology. http://www.mazda.com/en/innovation/technology/skyactiv/.

Thus, examining the developments of GDI technology will be beneficial as the technology has significantly evolved and it has the potential of improvements in energy efficiency and emission reductions.

6.1.1 Evolution of Gasoline Induction Technologies

The strategies of mixture formation differentiate PFI from GDI engine as shown in Fig. 6.1. In PFI, fuel injection takes place over the back face of the inlet valve when it is in a closed state during exhaust stroke. Thus, it leads to the formation of liquid film on the back side of the inlet valve and on the walls of the intake port, causing wall-wetting phenomenon. These are the major concerns of the PFI engine which creates an error in metering and delay in fuel delivery. Injecting the fuel directly into the cylinder overcomes the problem of wall-wetting in the port; thus, much lesser time is required for fuel to transport. Also, better control of fuel to be injected helps the mixture burn leaner. Although, the port injection has the advantage of washing out the carbon deposits build up on the back of inlet valve due to positive crankcase ventilation and EGR. This trouble is mainly faced by GDI engines. Higher fuel injection pressure (4–15 MPa) in case of GDI enables the spray to atomize properly compared to PFI, where injection pressure is in range of 0.3–0.6 MPa. Better atomization of fuel results in a higher vaporization rate thus helps in tackling cold-start problems. Other advantages include fuel cut-off during deceleration and cooling effect by absorbing enthalpy of vaporization during phase change of liquid droplets. This increases the volumetric efficiency if fuel is injecting during the intake stroke (Chincholkar and Suryawanshi 2016).
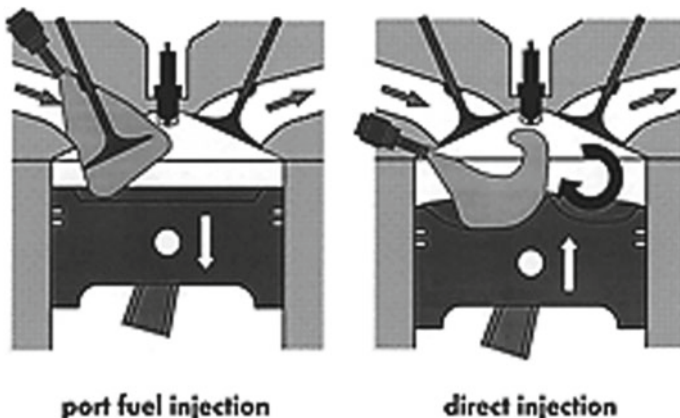
Fig. 6.1 PFI versus GDI engine configurations (Chincholkar and Suryawanshi 2016)

6.2 Overview of GDI Engine Technology

GDI technology allows the engine performance to vary according to the driving requirements. Its capability to operate in different modes according to user demand makes it efficient powertrain among SI engines. Broadly, there are two operating modes of GDI engines with three combustion system configurations.

6.2.1 GDI Operating Modes

The engine management system chooses the operating modes which are categorized by air-fuel ratio. Comparing the air-fuel ratio with the stoichiometric mixture of 14.7:1 for gasoline, the leaner mode can take the air-fuel ratio up to 65:1. Running the engine on the leaner composition of mixture helps in reduction of fuel consumption to a greater extent. There are two operating modes in the GDI engine.

(1) Stratified mode—It operates with overall leaner mixture and utilized during low load and low speed requirements. In this, fuel injection takes place late during the compression stroke, thus stratified layers of charge of different equivalence ratio are formed within the combustion chamber with the rich combustible mixture near the vicinity of spark plug and leaner mixture away from the spark plug. The toroidal or ovoidal cavity on the piston is used where combustion takes place as shown in Fig. 6.2. The location of the cavity on piston is according to the injector position and is used to create the swirl during the injection of fuel so that mixture having optimal air-fuel ratio gets located near spark plug when firing occurs. As a result, it can generate the flame and burn the overall lean mixture, hence gives better fuel economy (Nakashima et al. 2003). To a large extent, air and residual gases surround the stratified layers of charge, thus

Fig. 6.2 Piston showing swirl cavity (https://en.wikipedia.org/wiki/Gasoline_direct_injection)
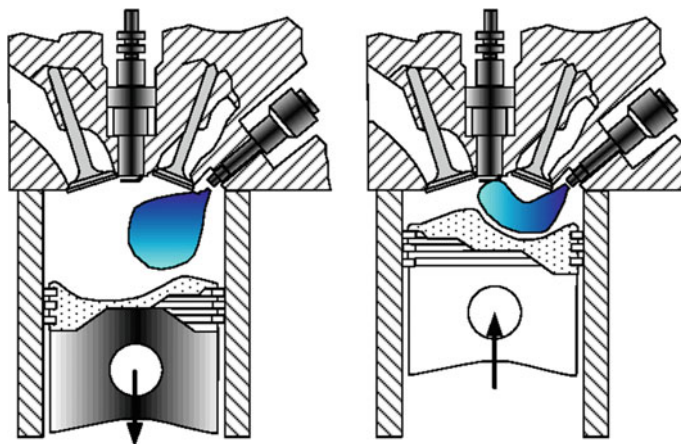
Fig. 6.3 Injection timing under homogeneous (left) and stratified (right) mode (Chincholkar and Suryawanshi 2016)

minimizes the heat loss during combustion by keeping the flames away from the walls and lower emissions due to less combustion temperature.

(2) Homogenous mode—This mode operates on stoichiometric composition at all loads and speeds. It involves the injection of fuel during suction stroke, thus gets sufficient time to form a homogeneous mixture and results in complete combustion and lesser emissions. Early injection cools the charge as the droplet absorbs heat of vaporisation from the air present inside the cylinder, thereby increasing the volumetric efficiency of the engine. Cooling of the charge allows for operating under higher compression ratio with greater knock tolerances.

Figure 6.3 shows the fuel injection timing for achieving homogeneous and stratified composition of air-fuel mixture. GDI engine with mixed operating mode has the best fuel economy. But mode switching in GDI is a very complex mechanism and a massive hurdle in the pathway of GDI development.

6.2.2   GDI Combustion Systems

GDI combustion systems are classified into three types as air-guided, wall-guided and spray-guided. These configurations are used for operating in the homogeneous and stratified mode as shown in Fig. 6.4. These are differentiated on the basis of injector position and piston cavity for in-cylinder motion. In air guided and wall guided systems, injector position is away from the spark plug and mixture formation is created by well-defined in-cylinder motion or by spray interaction with the cavity. In spray-guided, the injector is placed near the spark plug so that rich combustible mixture can be formed in the proximity of the spark plug. Spray-guided system is of
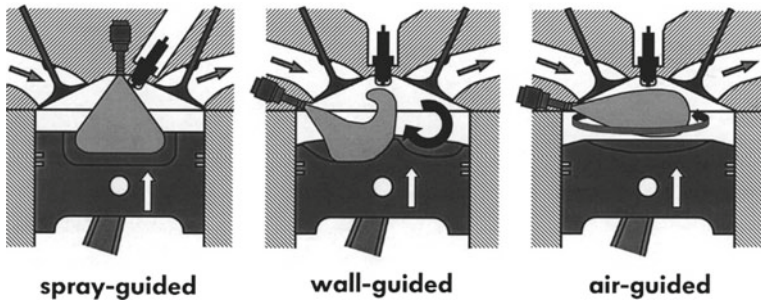
Fig. 6.4 Combustion systems of GDI (Chincholkar and Suryawanshi 2016)

second-generation type and has advantages of greater combustion efficiency which leads to improvement of the fuel economy. Wall-guided and spray-guided configurations are used for a stratified mode of mixture formation. Wall-guided system makes the use of piston bowl to guide the injected fuel to locate around the spark plug at the time of ignition while spray-guided make the use of its location to locate the spray near the spark plug.
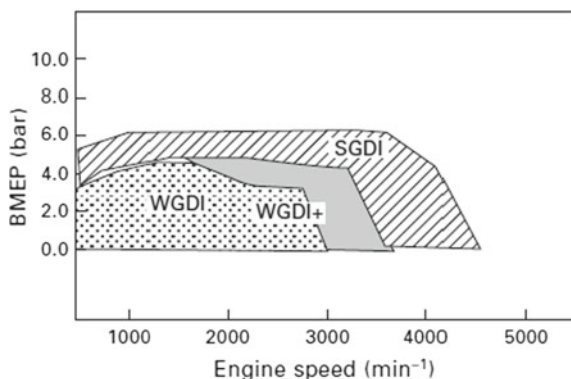
6.3   Recent Progress in GDI Engine Technology

GDI technology has been evolved to a significant extent for the past two decades. Automotive engineers and researchers have been continuously improving the areas such as injection system optimization, mixture preparation, combustion system etc., in order to achieve good performance and lower emissions. Various areas of improvement are discussed below, along with the recent progress and work done in the area.

6.3.1   Injector Location

The wall guided configuration has limitations of fuel impingement and emissions of particulate and THC, thus is at least priority in recent engine production (Park et al. 2012). However, with a combination of air-guided system, the wall-guided system is still used to cut down cost in some systems (Yu et al. 2009). GDI combustion system employing a combination of air-guided and spray-guided have shown satisfactorily outcome in recent studies (Tang et al. 2018; Eichhorn et al. 2012). Spray-guided motion is used for stratified mode operation by incorporating late injections to reduce fuel impingement and also turbulence caused by in-cylinder air motion is considered to be significant while designing combustion system (Itabashi et al. 2017). In a spray-guided combustion system, the engine can be operated at a higher range of load and speed than that of wall-mounted combustion system as shown in Fig. 6.5.

Fig. 6.5 Comparison of
performance between
wall-guided (WGDI) and
spray-guided direct injection
(SGDI) system (Zhao 2010)
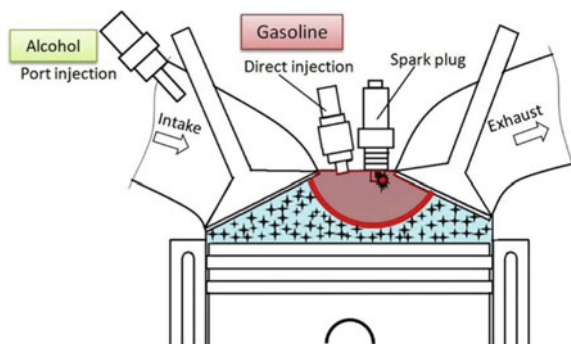
In wall-guided and air-guided configurations, injectors are located on the side wall
while, in spray-guided configuration, the injector is located centrally. Side-mounted
injector results in enhanced tumble factor, reduction in thermal load, greater thermal
efficiency and preignition suppression in comparison to central-mounted injector
(Sevik et al. 2016). However, there are more chances of impingement which has its
own drawbacks. Central injector offers greater flexibility and simplifies the design of
the combustion chamber, while attempting to avoid wall-wetting in order to reduce
emissions of PM/PN. It is situated centrally near the spark plug so as the spray easily
reaches the vicinity of the spark plug in order to operate the engine in stratified mode.
Also, piezoelectric injectors (Skogsberg et al. 2007) are centrally mounted for multi-
injection operation in short intervals for obtaining a desired air-fuel composition for
improved performance.

6.3.2 Dual Fuel Injection

Using gasoline blended with ethanol as a single fuel in fixed proportion limits the
potential of ethanol to improve the engine performance under varying operating con-
dition. For making flexible and efficient use of ethanol, a system having dual injection
was introduced which covers the advantages of both port and direct injection. The
dual fuel injection system is becoming an important trend in GDI combustion system
by making the use of port fuel injection and direct injection as shown in Fig. 6.6.

Ikoma et al. (2006) initially proposed the use of dual injector which provides the
advantages of achieving highest power output among similar displacement engines,
better fuel economy and lowest emissions. They used dual fan-shaped spray DI
injector to eliminate the limitation of a heterogeneous mixture in the absence of any
devices for creating in-cylinder motion. Port fuel injector improved the homogeneity
of the mixture during high load and low speed conditions.

Fig. 6.6 Dual-injection system (PFI and DI) (Liu et al. 2015)

Many studies have employed the use of dual fuel combinations (mainly alcohol and gasoline) for port and direct injection application. Feng et al. (2018) evaluated the combustion performance using n-butanol as direct injection fuel and gasoline as port-fuel injection fuel. Different injection ratio of these two fuels was used by varying the mass fraction of gasoline in PFI from 100 to 0%. Dual fuel injection strategy using n-butanol with optimum spark timing benefitted in extending the engine load and higher IMEP with early rise in combustion pressure as compared to gasoline PFI and GDI. However, indicated specific energy consumption decrement showed better fuel energy conversion efficiency when fuelling with n-butanol dual injection. In contrast, despite cooling effects, knock propensity for smaller ratios of DI of n-butanol are increased as compared to butanol direct injection and GDI relatively due to low RON and increasing engine load. In an experimental study (Zhuang et al. 2017), the author found that ethanol direct injection with gasoline port injection is more effective than gasoline port injection and GDI in eliminating engine knock with more spark advance and thereby enhancing the thermal efficiency of small engines.

Authors have also experimented with port injection of alcohol and direct injection of gasoline. He et al. (2016) studied the combustion performance taking ethanol and n-butanol as the port injected fuel and gasoline as direct injected fuel. He found better efficiency and lesser emissions for the dual fuel strategy of port injection of n-butanol and direct injection of gasoline than gasoline direct injection only. Also, the highest thermal efficiency was observed for ethanol and gasoline combination as a port and direct injected fuel respectively.

These results were justified by the work of many researchers in a direct or indirect way. Qian et al. (2019) found the similar indicated thermal efficiency in the dual fuel system when 35% of ethanol is port injected and gasoline surrogates (TRF) of RON of 75 is direct injected, compared with direct injection of TRF of RON 95 under knock limited spark timing. Thus, the same combustion characteristics and efficiency can be obtained with fuel having less RON if operated with an optimal amount of ethanol in port injection, to that of operating solely on fuel having high RON. The results also accounted for longer flame development duration (about 2°CA) and rapid combustion duration (about 3°CA) and lesser emissions on increasing the ethanol

injection ratio with direct injection of fuel of RON 90. Increasing the proportion of ethanol for the dual-fuel injection strategy (DI of gasoline and port injection of ethanol) could increase the compression ratio of the engine leading to rise in engine efficiency and could help in extending the knock-limit effectively (Liu et al. 2014) while reducing the particulate matter emissions (Liu et al. 2015).

Gasoline/alcohol blended fuels have also been tested for their combustion, performance and emissions characteristics and the results were positive in terms of efficiency and emissions (Turner et al. 2011). However, Storch et al. (2015) found the presence of diffusion flames during combustion in the gaseous phase and improper evaporation of droplets for gasoline blended with 20% ethanol by volume as compared to iso-octane. Also, there is more susceptibility of higher unregulated emissions for ethanol-gasoline blended fuels, especially carbonyls (Clairotte et al. 2013). Qian et al. (2019) investigated the combustion and emissions in a GDI engine for C3-C5 alcohol blended with TRF, resulting in the mixture of fixed RON of 95. He found the advancing of knock-limiting spark timing on blending with alcohols where ethanol/TRF and n-propanol/TRF showed more advancing than remaining one. Blend of n-butanol/TRF showed the highest ITE among other blends at the same blending ratio while n-propanol/TRF mixture showed the highest indicated thermal efficiency for the same oxygen content. Considering the combustion and emissions results, n-propanol and n-butanol are reported to be more suitable alternative fuels than ethanol and n-pentanol. Increasing the ethanol percentage lead to a significant rise in HC and NO_x emissions while the reduction in PM emissions (Costagliola et al. 2013).

From the previous studies and all the results discussed above, it can be justified that addition of ethanol as fuel can improve combustion efficiency of SI engine (Balki et al. 2014). Presence of inherent oxygen molecules can widen flammability limit which helps in lean burn combustion (Koç et al. 2009) and higher-octane rating of ethanol can improve the compression ratio. On the other hand, limitations like lower heating value of ethanol, higher latent heat of vaporization and lower saturated vapour pressure may result in cold-start issues.

6.3.3   Split Injection Strategy

In split injection strategy, primary injection is done during the intake stroke to give sufficient time for forming a lean homogeneous mixture; then the secondary injection is done while compression happens such that stratified mixture is formed. Thus, it is used for obtaining overall lean homogeneous stratified charge at the start of ignition (Song et al. 2015; Costa et al. 2016).

Many investigations have been done on split injection of GDI engine. In the researches carried out by Song et al. (2015), Kim et al. (2015), improvement in mixture quality and combustion characteristics were observed due to split injections, one

is done at the middle of induction and other at the starting of compression. Retarding the injection timing for the second injection of gasoline results in the greater turbulence intensity inside the cylinder. This results in shorter combustion duration with higher in-cylinder pressure since turbulence created due to faster movement of spray increases the flame propagation speed. However, the local regions of rich-fuel mixture cause an increase in higher emissions. Clark et al. (2016, 2017) analyzed the combustion performance under the effect of different split injection timings using the optical engine. An increase in indicated mean effective pressure (imep) was observed on retarding the second gasoline injection or advancing first gasoline injection. The highest imep was obtained for the primary injection at 300 CAD BTDC (suction stroke) and secondary injection at 110 CAD BTDC (compression stroke), considering the starting of power stroke at 0 CAD at TDC. The eccentricity of flame boundary tends to increase on retarding second injection timing because of the decrease in homogeneity with regions having variable laminar burning speed. On the other hand, greater particle emissions, fuel film formation due to spray impact and incomplete evaporation were still to be the areas of study for GDI engines (2016).

Ji et al. (2018) performed the investigation for varying second gasoline direct injection timings in hydrogen-blended gasoline direct injection engine. Hydrogen is blended by hydrogen port injection system during intake. The blending of hydrogen results in minimizing the variations in the performance of engine caused by parameters affected by different second injection timing, when compared to operate with pure gasoline. Hydrogen blended mode leads to higher brake thermal efficiency and maximum pressure rise due to rapid combustion. Hydrogen addition had resulted in a significant reduction in HC, CO_2 emissions and particulate number while greater NO_x percentage was observed.

6.3.4 Fuel Injection Parameters

Fuel injection pressure and fuel injection timing are considered to be among the most influential parameters affecting the combustion performance of the engine. Huang et al. (2016) analyzed the impact of injection timing on the mixture formation and combustion results for a dual fuelled engine having direct injection of ethanol and port injection of gasoline. They justified the results with the help of CFD simulation studies. Retarding direct injection timing of ethanol proved effective in producing a greater cooling effect and mitigating knock tendency, however, combustion and emissions results of late injection were very degenerated. The results found that late direct injection of ethanol leads to form richer composition opposite spark plug and leaner mixture near spark plug which retards the combustion speed. Severe problem of fuel impingement on piston occurs due to reduced volume of the combustion chamber at the time of compression stroke and this causes slower in-cylinder motion and incomplete evaporation. Thus, higher HC and CO emissions resulting from incomplete combustion are major concerns though NO_x was in less percentage due to reduced volume of the combustion chamber.

Song et al. (2018) investigated the effect of injection pressure and coolant temperature for two fuel injection timings on THC and particle emissions. As higher injection pressure gives better atomization and reduces particulate emissions, while the increasing temperature of coolant during cold-start could effectively improve engine efficiency and reduce emissions. His results stated that for wall wetting condition (injection at 330° CAD bTDC), increasing injection pressure up to 50 MPa from 10 MPa can lead to the reduction of particulate emissions by 90% due to the formation of a thinner film. For non-wall wetting condition (injection at BTDC 270), an increase in injection pressure didn't have much effect on particulate emission. Also, minute reduction in THC was observed on increasing fuel injection pressure. However, the increment in coolant temperature from 40 to 80 °C during cold start reduced the soot and THC substantially along with better thermal efficiency.

6.3.5 Injector Design

Typical designs of different kind of injectors, namely, swirl, outward opening and multi-hole injectors are shown in Fig. 6.7. Multi-hole nozzle is more popular because jet orientation control can be easily achieved with this. Toyota made use of the slit
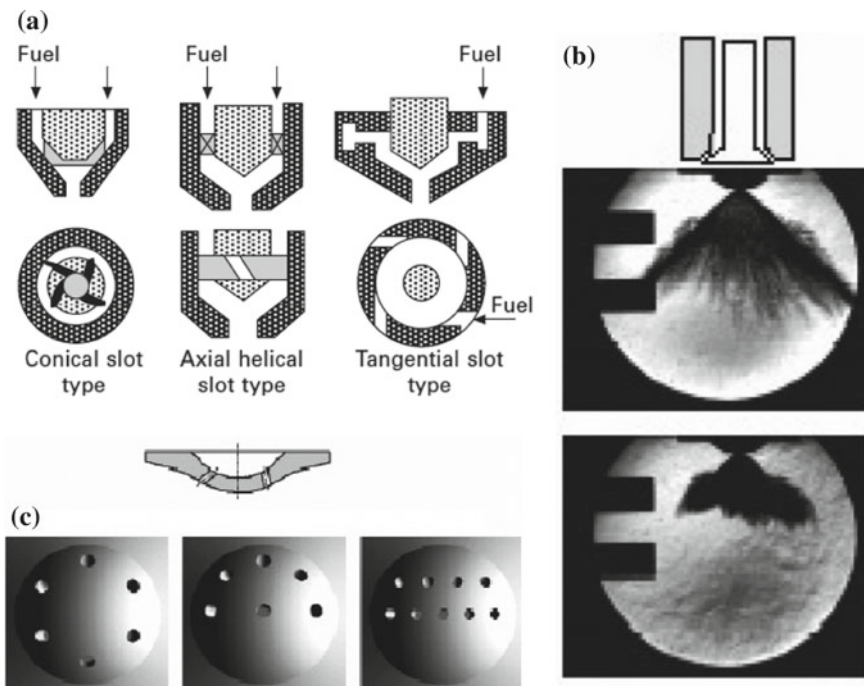
Fig. 6.7 **a** Swirl injector **b** outward opening injector **c** multi-hole injectors (Zhao 2010)

nozzle due to its fan-shaped spray which results in wider dispersion and proper atomization (Matsumura et al. 2013). Features like fast response time with better accuracy and control put the piezo-driven injector on the upper side as compared to solenoid-driven injectors (Dahlander et al. 2015), however, their applications are restricted due to high cost.

Recently, the utilization of outward-opening piezo driven injectors in stratified mode has been increased as it produces a spray of relatively shorter penetration length which eliminates the trouble of wall-wetting (Dahlander and Hemdal 2015; Stiehl et al. 2013). Additionally, it results in more ignition stability because of slower flow velocity in vortex than mainstream spray.
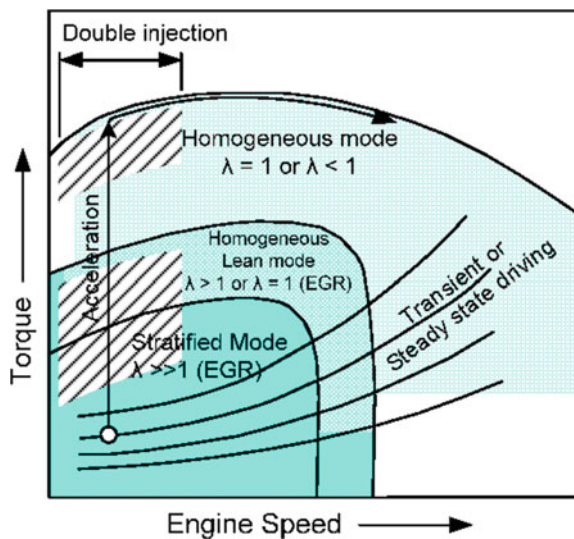
6.3.6 Application of Turbo-Boost, VCR and EGR in GDI Engine

For achieving higher thermal efficiency while developing GDI combustion system, larger compression ratio (CR) and minimal heat losses play a vital role in fulfilling the requirements. For natural aspirated GDI engine, the value of CR can lie in the range of 11–13 (Lee et al. 2017; Hwang et al. 2016) while for turbo boost engine, CR reduces to 9.5–11 (Wada et al. 2016; Yamazaki et al. 2018) as it is limited by knocking phenomenon. The highest CR of 15 is achieved in the development stage (Lee et al. 2017). Thus, naturally aspirated engines enjoy the advantage of better thermal efficiencies. But boosting helps in attaining higher mean effective pressure and higher power output with downsized engines.

Incorporating variable compression ratio (VCR) (Kojima et al. 2018) or variable valve timing (VVT) (Lee et al. 2017; Yamazaki et al. 2018) resulted in attaining CR above 13. Asthana et al. (2016) designed seven different configurations for VCR, but mostly lacking the adaptability for high speed, robustness and cost. The Nissan developed the world's first production-ready VCR turbo engine in 2017 (Kojima et al. 2018). It covers the range of CR 8.0 to 14.0 with the help of multi-link rod crank and servo motor for continuous variation. Different design models have been adopted for VCR adaptability by AVL and FEV, where the variation of rod length was done (Wolfgang et al. 2017; Kleeberg et al. 2013). Honda utilizes dual piston system (Kadota et al. 2009). Studies suggested that the VCR system resulted in a rise in fuel economy by 8% (Wolfgang et al. 2017).

Applying exhaust gas recirculation (EGR) helps in minimizing combustion temperature by increasing the specific heat of gaseous mixture, thus reduces NO_x and also improves fuel economy. EGR contribution in improving thermal efficiency can be understood by the effect of two factors. Firstly, EGR minimizes the pumping loss due to availability of less oxygen in the cylinder; throttle needs to be opened more and second, it reduces the heat loss from the engine because of less combustion temperature. Thus, at higher loads, knock suppression and less heat loss due to EGR improves the thermal efficiency (Cairns et al. 2006; Potteau et al. 2007). As shown in Fig. 6.8,

stratified mode and lean homogeneous mode are applied for low load-rpm and part load-rpm conditions respectively, but the lean mixture combustion leads to high NO_x emissions. Thus, EGR addition is done to limit NO_x levels in the exhaust. In high load and low rpm conditions, stratification results in high soot formation due to availability of highly rich-mixture. And in high load and high rpm conditions, stratification of the charge cannot be maintained due to high turbulence. Thus, it is limited to low load and low rpm conditions, while homogeneous mode with the stoichiometric mixture is used for high load and rpm conditions. The double injection is used during accelerating conditions while taking the transition from stratified to homogeneous mode at low rpm conditions. It results in forming stratified with the overall lean homogeneous mixture. In high load and low rpm conditions, large combustion duration and high in-cylinder temperature increase the chances of knocking. It can be inhibited by the application of double injection strategy. However, applying high EGR rates worsen the combustion stability of the engine (Yu and Shahed 1981). Hydrogen can be used as an additive for gasoline fuel as it improves the combustion stability due to faster flame speed, brings homogeneity in mixture due to larger diffusion coefficient and reduces the chances of knocking due to higher ignition temperature (Kim et al. 2015). Hence, hydrogen can be used to enhance combustion stability at high EGR rates. In the study done by Kim et al. (2017), it was found that hydrogen exhibited an important role in improving the combustion and emission characteristics of turbo GDI engine with EGR. They found that the addition of hydrogen results in faster combustion with less cycle-to-cycle variations and provides stability in combustion performance. Thus, the engine can be operated under high EGR rates with improved thermal efficiency. Reduction in HC and CO emissions were observed, but NO_x was higher due to higher adiabatic flame temperature.

But these desired requirements can only be fulfilled by cooled EGR which not only reduces NO_x but also help in knock suppression, especially at higher loads. On the other hand, hot EGR reduces the volumetric efficiency of the engine but decreases HC emissions during cold-start and low load. The study suggested that hot EGR can greatly affect the combustion duration and efficiency of the engine as compared to cooled EGR (Toulson et al. 2007). It is reported (Wei et al. 2012) that, with cooled EGR there was a reduction up to 90% in NO_x and 50% in CO, and also lowers the brake specific fuel consumption by 11%. But the THC emissions shoot up significantly. Hot EGR can result in four times NO_x emissions than cooled EGR, while cooled EGR can produce 1.5 times THC emissions than hot EGR.

6.3.7 Lean-Burn Strategy

Several pieces of research have been done for lean combustion in GDI engine operating under stratified mode. Though the results proved effective in increasing fuel economy, high engine NO_x emissions and low exhaust temperature have always been an obstacle in emission control and after-treatment devices. Earlier, Toyota, Nissan and Volkswagen have proposed for first-generation lean-burn engines which were based on wall-guided combustion type having side mounted injector. Spray utilizes the shape of the piston cavity to deflect its movement such that spark plug get surrounded by the rich mixture. The mixture development is easier but depends on the in-cylinder flow which gets influenced by various operating conditions (Kim et al. 2009; Lee and Lee 2006). Thus, combustion of the stratified mixture is limited by a particular range of operating conditions, and also wall-wetting conditions lead to emissions of higher unburnt hydrocarbons. BMW and Daimler-Benz have manufactured commercial lean-burn GDI engine with spray-guided combustion system. Although, the high cost of injection system and after treatment devices has demolished the wider utilization of these engines. However, with an increase in cost of fuel and burden of CO_2 emission regulation, the lean-burn engine may find applications to a greater extent.

Park et al. (2014) evaluated the combustion and emissions characteristics along with visualization studies of ultra-lean gasoline DI engine operating under stratified mode. With spray-guided configuration, they were able to improve fuel economy up to 23% for excess air-ratio of 4. They optimized the event timing for injection delay and ignition advance taking the stoichiometric conditions as reference. Flame visualization was also carried out along with in-cylinder measurements. Under lean operating conditions, combustion phasing occurred earlier till BTDC 41 CAD with maximum pressure in the cylinder was attained at ATDC 2 CAD as shown in Figs. 6.9 and 6.10. Despite stable combustion at an excess ratio of 4, there were an increased amount of NO_x and HC emissions due to the presence of over-rich mixture near the spark plug and more fuel impingement on piston respectively. As shown in Figs. 6.9 and 6.10, the blue flame can be realized as a result of premixed combustion and are
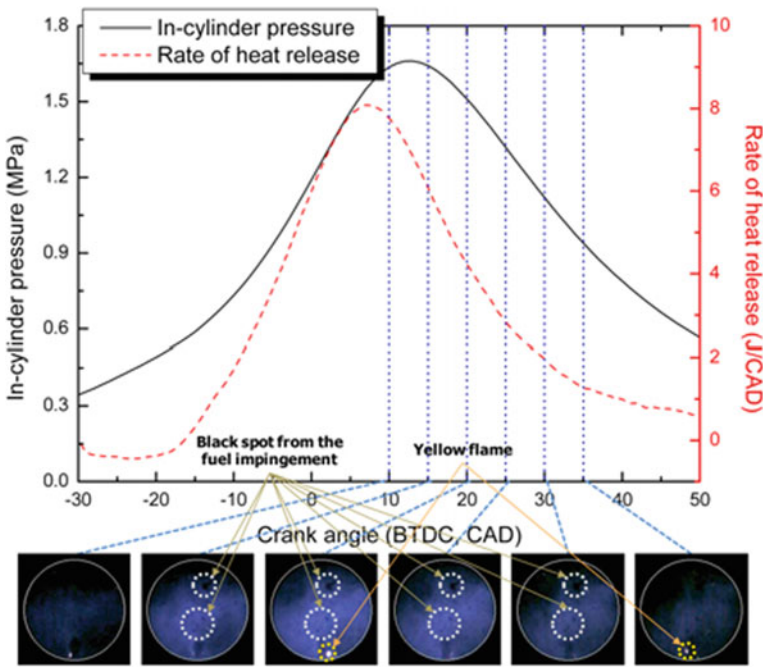
Fig. 6.9 Pressure and heat release curves with flame images for stoichiometric conditions having injection at BTDC 330 CAD and spark advance timing at BTDC 50 CAD (Park et al. 2014)

of less intensity. On the other hand, diffusion combustion near spark plug can result in higher luminosity due to residual fuel on electrodes while operating in stratified mode.

In many studies (Park et al. 2014; Matthias et al. 2014), it is reported that lean burn combustion can minimize BSFC to a great extent along with minimizing the coefficient of variance and knocking. Iida (2017) achieved the burning of the super lean mixture ($\lambda = 1.92$) by utilizing highly energized ignition system and complying large tumble ratio of 2.5, thereby getting an indicated thermal efficiency up-to 46% in single cylinder engine. However, large PM/PN emissions are the disadvantages of the stratified mode operation. It has been found that particle concentration from lean stratified combustion is much higher than the conventional stoichiometric and lean homogeneous combustion, whereas lean homogeneous condition produced minimum particulate number and soot (Bock et al. 2018). Figure 6.11 reports the similar results of higher PM emissions for the lean-burn case.
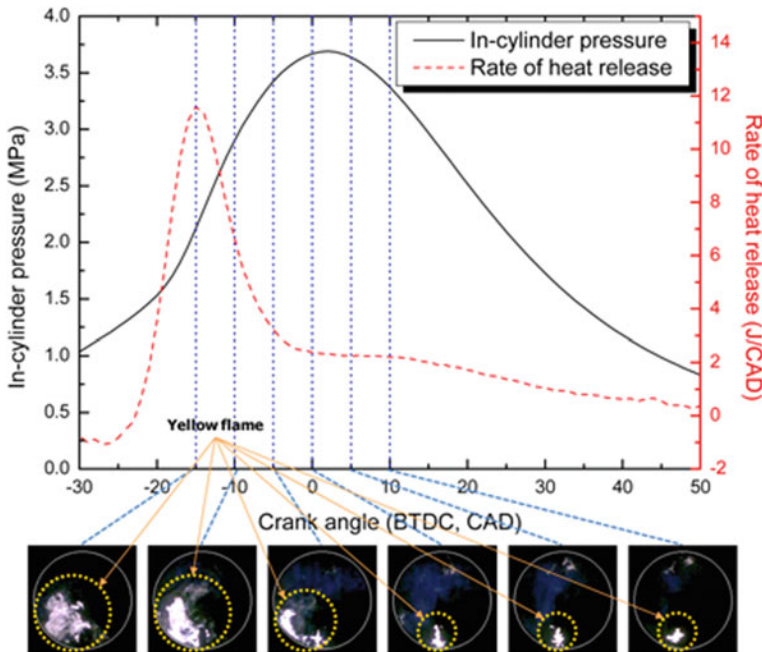
Fig. 6.10 Pressure and heat release curves with flame images for lean combustion conditions having injection at BTDC 31 CAD and spark advance timing at BTDC 35 CAD. (Park et al. 2014)
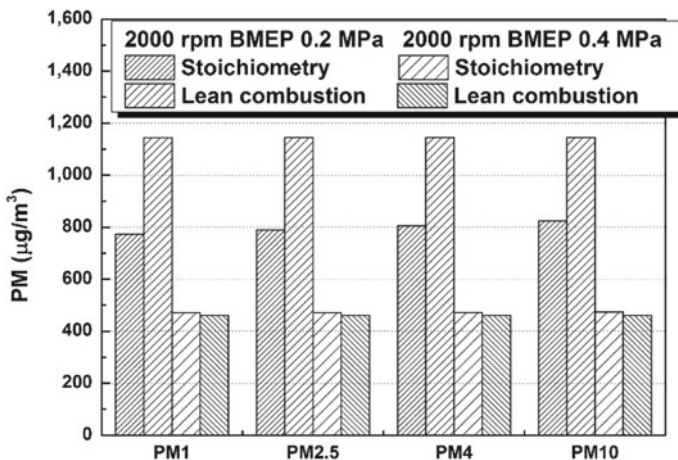

Fig. 6.11 Effects of engine load and combustion strategy on particulate matter (PM) mass concentration having excess air ratio of 3.6 and 2.1 for 0.2 MPa and 0.4 MPa respectively (Park et al. 2016)

6.4 Challenges in GDI Engine Technology

Despite having several best-in technology features, GDI engines are facing major challenges of high particulates emissions, injector fouling due to deposits and deto-knock. Injector deposits ultimately hinder the proper mixture formation, as a result, large PM emissions can be observed in the exhaust. Deto-knock occurs due to pre-ignition of charge and causes large pressure oscillation during combustion. It has a very damaging effect on engine components and performance. The factors responsible for these limitations of GDI engines along with the preventive measures are explained elaborately in the subsequent sections.

6.4.1 Particulates and Soot Formation in GDI Engine

6.4.1.1 Causes and Sources

Although GDI engines are very popular due to various advantages such as high thermal efficiency and lower BSFC, however large soot and particulate emissions is one of their major limitations. The process of soot formation is initiated by the soot precursors like C_2H_2 (ethylene) and PAH (polyaromatics hydrocarbons), then the growth of nucleates takes place by agglomerating particles and their coalescence, and finally followed by their oxidation (Tree and Svensson 2007). The gaseous and semi-volatile hydrocarbons from engine exhaust get adsorbed on these solid particles and coagulate into larger particles. Formation of soot in GDI engines can be attributed to mainly three sources, namely, pool fire due to fuel impingement (Velji et al. 2010), improper mixing in stratified combustion of the charge (Lucchini et al. 2014) and the diffusion combustion of fuel jet near injector (Berndorfer et al. 2013). In homogeneous mode, pool fire and diffusion combustion are dominant, while the presence of rich-mixture locally and pool fire are the major factors in stratified mode. The exhaust particles are classified based on their sizes and also divided into nucleation and accumulation mode as shown in Fig. 6.12 (Kittelson 1998).

In a report published in June 2014, the World Health Organisation (WHO) officially classified engine soot particles as carcinogenic. Research has established that material found in PM 2.5 is water soluble and can form droplets under certain conditions. PM 2.5 can penetrate the cardiovascular system of the human body which results in pulmonary diseases and can affect DNA (Short et al. 2015). Thus, institutional bodies across the world have set stringent emissions norms to curb the ill-effects of emissions on the environment. As per application of Euro 6 standards in Europe, particulate mass emission is restricted to 4.5 mg/km and particulate number emissions are limited to 6.0×10^{11} particles/km from 2017 (Euro 6c). The limiting values for particulate mass and number are shown in Fig. 6.13 for PFI and GDI engines with their current emission levels.
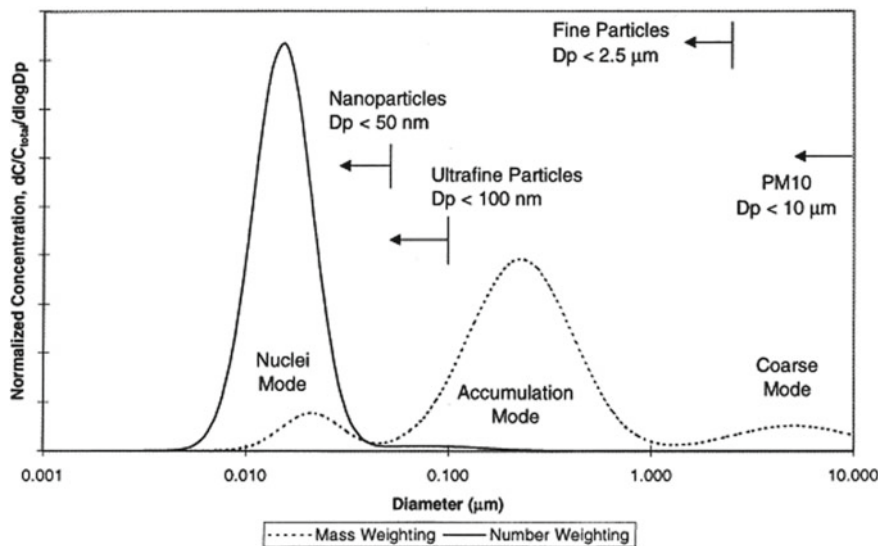
Fig. 6.12 Size distribution of engine exhaust particles on mass and number basis (Kittelson 1998)
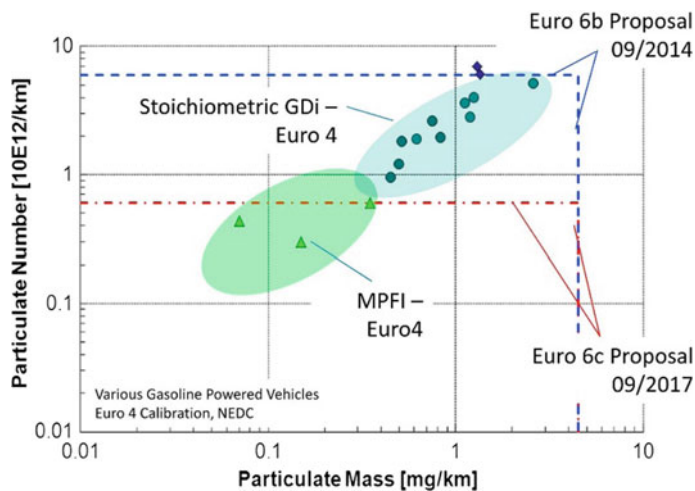

Fig. 6.13 Euro 6 standard for PM and PN emissions (Qian et al. 2019)

6.4.1.2 Responsible Operating Parameters and Controlling Measures

Researchers have been studying particle emissions under different combustion modes of an IC engine. Their formation, size and number distribution are largely dependent on the fuel composition, mixture preparation, ignition mechanisms and operating

conditions of the engine. Many studies have been conducted to improve the atom-
ization of fuel spray for proper mixing by increasing the injection pressure, which
can greatly inhibit the formation of soot. Injection pressures up to 35 MPa have been
used for refining the spray. Hoffmann et al. (2014) reported a decrease in Sauter
mean diameter (SMD) i.e., D_{32} of spray droplets with increase in injection pressure.
However, atomization can be largely influenced by injector design parameters; thus
in-depth research is needed in this aspect.

It is stated that the New European Driving Cycle results in approximately ten
times higher concentration of particle number for GDI engine than that of PFI, while
particle mass emissions lie between that for PFI and diesel engines. Hence, it is
very crucial for the GDI engine to limit their particulates emissions to meet the pre-
scribed emissions standard. It can be done in two ways, either by using after-treatment
systems like gasoline particulate filter (GPF) and three-way catalyst (TWC) or by
reducing in-cylinder particle emission. Aftertreatment devices generate exhaust back
pressure. Hence, optimizing the different factors responsible for in-cylinder parti-
cle generation will certainly limit the emission. For this, multiple injection strategy,
injection parameters, fuel type and combustion mode are some of the factors to
be optimized. Also, understanding soot particles characteristics, structure and mor-
phology will help to get better insight for its controlling actions. Particles from GDI
engine mostly contain soot as compared to organic particles than PFI engines as
shown in Fig. 6.14. Figure 6.15 shows the TEM images of soot and organic particle
from gasoline engine illustrates the chain and agglomerates structures of soot with
darker regions of organic particles which are lighter and inhomogeneous (Xing et al.
2017).
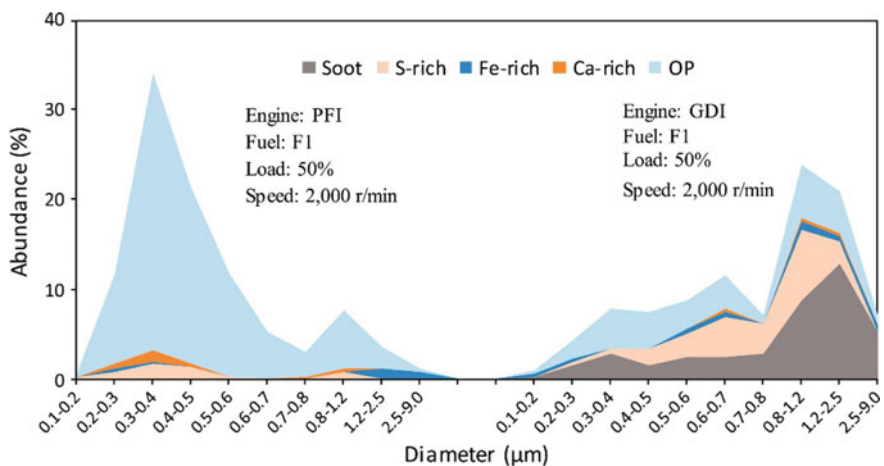
Fig. 6.14 Number size distribution of different particles types in PFI and GDI engines (Xing et al. 2017)
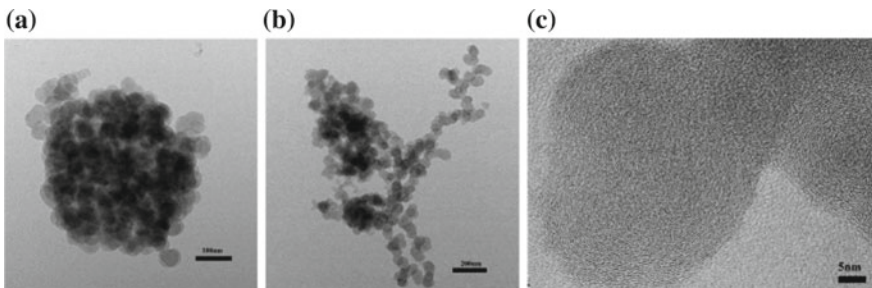
Fig. 6.15 Soot particles images from TEM **a** Cluster-like soot, **b** chain-like soot **c** high-resolution TEM image of soot (Xing et al. 2017)

It is reported that the injection timing of fuel has a significant effect on particulate emissions characteristics. Ketterer and Cheng (2014) found that more fuel impingement occurs when fuel is injected either at the early induction or at the late compression, which certainly leads to more PM emissions. If injection happens early in the compression stroke, droplets get more time to evaporate and film formation occurs in much less quantity. Hence, particle number and size reduce than at late injections. Moreover, fuel impingement characteristics are found to be directly influenced by injection timing (Beavis et al. 2017). The film formation location has also been noticed to be different for different fuels by many studies which can be stated as a probable reason for higher particulates for heavier fuels.

Based on the endoscopy studies done on a single cylinder engine, Berndorfer et al. (2013) concluded that diffusion combustion of fuel jet near injector is a major cause of particulate formation. As early injection was done during suction stroke, the blue flame radiation above piston indicates the well-mixed homogeneous mixture. However, the diffusion flame resulting from the injector tip can be observed as highly luminous, indicating rich mixture condition. The results showed a clear correlation of injector diffusive flame and PN with soot mass emissions.

In a report given by the Japan Petroleum Energy Centre with other agencies, particulate emissions from different engines with the varying after-treatment system were collected and analyzed. It can be inferred that particle number size distribution from DISI engine is unimodal having peak concentration of particle size of around 85 nm. Local availability of rich-fuel mixture in lean-burn DISI engine resulted in 10 times higher emissions compared to stoichiometric DISI engines. Overall the PN distribution for both cases of DISI engine lies much higher than that of MPFI gasoline and diesel particulate filter (DPF) vehicles.

Location of injector also plays a vital role in mixture preparation as there are fewer chances of spray impingement on the wall for spray-guided arrangement than wall-guided arrangement. Consequently, diffuse combustion seldom occurs during combustion. Thus, particulate matter is emitted in less quantity in spray-guided DI engine than that of wall-guided (Price et al. 2006).

As port fuel injection systems are believed to emit fewer particulates, thus several automobile companies turned for dual injection systems (port and direct injection) (Trimbake and Malkhede 2016). Toyota bought PFI and GDI dual injection system in 2005, to improve mixture quality and reduce emissions, and similar strategies later followed by Nissan, Suzuki and Honda. Audi bought the similar strategy recently, reducing particulate emissions and meeting the standards of Euro 6 without using gasoline particulate filter. Daniel et al. (2013) investigated the PM emissions using dual injection strategy. And found to have higher in-cylinder temperature due to dual injection which enhances the burning of fuel droplets and eliminates soot formation to a good scale. The PFI also provides more time for mixture preparation than solely DI, thereby reducing the problem of wall-wetting. In dual injection mode, the average size of PM is comparably smaller than DI mode and the accumulation mode particles are negligible.

Additionally, two fuels can be used in a dual injection system for better control of engine performance and emissions by varying the mixture properties. In the study done by Liu et al. (2015), it was reported that as compared to alcohol-gasoline duel fuel SI mode, gasoline-alcohol duel fuel SI mode was more efficient in fuel economy due to the utilization of the higher latent heat of vaporization of alcohol. With the increase in alcohol percentage, a significant reduction in PN was observed under all combustion strategies.

Various physical and chemical properties of the fuel like viscosity, boiling point, surface tension, distillation curve, vapour pressure, molecular structure (length of carbon chain, branching, unsaturated bonds, rings, etc.) largely affect the particulate emissions (Chapman et al. 2016). Jiang et al. (2018) discovered that three surrogates fuels of the same RON have lower particulates number than gasoline due to the presence of heavier molecules in gasoline.

The engine operating conditions like load, equivalence ratio, injection parameters, charge boosting, EGR, ignition timing etc. certainly influence the particulate emissions as justified by several studies. Bonatesta et al. (2014) observed higher soot mass emissions under high load-low speed and medium load-medium speed condition as a result of high nucleation rates, in the homogeneous stoichiometric mode of combustion. According to a study (Pei et al. 2014), the air-fuel ratio is likely to affect the particle number concentration and causes decrement in particle number on increasing the air-fuel ratio for a rich mixture. It is also believed that lean burn gasoline DI engines emit a larger amount of ultra-fine particulates than a conventional engine. Further increase in air ratio beyond 2 leads to increment in particulate number and PM emissions, which could be likely due to increased air pressure and a decrease in combustion temperature. High ambient pressure results in lower penetration of spray, forming local rich-mixture in the cylinder.

High fuel injection pressure leads to finer droplets, high spray velocity i.e., more penetration length, and shorter duration of injection. All these parameters enhance proper combustion by restricting the formation of locally rich mixture composition and wall-wetting trouble (Chung et al. 2016).

De Boer et al. (2013) varied fuel temperature and studied its effects on mixture formation and particulate emissions. They operated the engine with injection pressure in the range of 150–300 bar and fuel temperature of 320 °C which is above the supercritical condition of gasoline (45 bar and 280 °C). The results showed a significant reduction in particulate number, ranging from 47 to 98%. It dictates the potential of fuels in the supercritical state for PN reduction than liquid fuels.

Few studies have been done which quantify the EGR on PM emissions from SI engines. It is believed that EGR can affect the engine combustion and emissions by (a) heating intake charge (b) increasing heat capacity (c) diluting the charge and (d) changing chemical aspects (Zhao et al. 2001). Hedge et al. (2011) concluded from their study on light-duty GDI engine that cooled EGR can bring down the particle mass by 65% and particle number by 40% in most of the conditions. Wide EGR range can result in a decrease in combustion temperature and can lead to a higher number of accumulation mode particles, while nucleation mode particles showed a decreasing trend (Lattimore et al. 2016).

Turbocharging results in improved performance of the vehicle, higher thermal efficiency, reduced fuel consumption and exhaust emissions, thus are widely used in GDI engines. Although Cucchi and Samuel (2015) observed that there was a clear difference in particle concentration before and after the turbocharger. The centrifugal motion of the exhaust gas particles enhanced the nucleation of particles and agglomeration, which are fragmented into micro-scale particles. Thus, the particles size was seemed to be larger after the passing through the turbine. Whelan et al. (2013) studied the particulate emissions from wall-guided turbo-charged DI engine running in transient conditions of cold-start and warm-up. Total particle count was found to decrease during cold start transient and was tend to increase with higher coolant and oil temperature of the engine.

Jiang et al. (2017) studied the variation in spray and emission due to injector deposits. Deposits on the injector tip increased the penetration length and mean droplet size of spray, which was mainly responsible for a larger amount of PM emissions. The deposits accumulation on injector can deteriorate the particulate emissions by these possible sources (a) fuel impingement due to larger penetration length (b) incomplete combustion due to large size droplets (c) leaking of fuel due to imperfect closing and (d) adsorption of fuel on the deposits tends to increase diffusion combustion.

Pirjola et al. (2015) studied the effect of using different lubricating oil with low sulphur gasoline on the particulates emissions and found that the results were affected during cold-start and warm-up phase. The emissions were increased during acceleration and steady-state than deceleration condition. Lubricating oil having metal content are found to emit more PM emissions.

The blended fuel may have different physical and chemical properties, depending on the amount of blending done. These properties affect the injection characteristics, mixture composition and overall combustion process, thus cause variation in soot formation and particulate emissions. Hence, it cannot be directly concluded that alcohol blended gasoline fuels result in the increase or decrease in PM emissions as
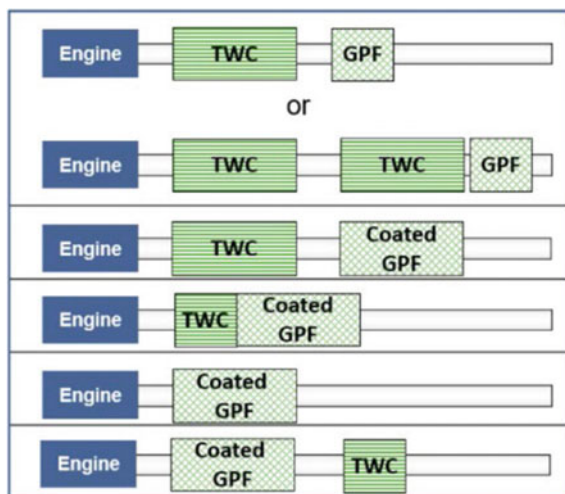
the parameters for injection strategy of ethanol/gasoline blends are not optimized for the overall operating range of engine (Storch et al. 2015).

PM emissions are also very sensitive to driving cycle on which vehicle is running. As tested under the NEDC cycle, particle concentration during cold start was very high and decreased during warm-up conditions (up to 300 s) for PFI engine. However, particulate concentration for GDI engine was high in warm-up conditions too and during the transition from one operating condition to other (Chen et al. 2017).

Hence, the gasoline particulate filter optimization is of uttermost need due to large particulate emissions from GDI and strict emission limit of WLTC cycle. Considering after-treatment technologies for PM reduction in GDI engines for meeting the limit of exhaust particles in Euro 6, gasoline particulate filter (GPF) and three-way catalyst (TWC) are unavoidable. Figure 6.16 shows various arrangements for location of GPF coupled with TWC or GPF in the underfloor position (AECC Technical Summary 2017). For underfloor position, bare GPFs are used while coated GPFs are usually placed in close-coupled position after TWC. GPF with the underfloor position was found to have 15% more filtration efficiency than that when placed in close-coupled position, due to reduced exhaust gas temperature resulting in the decrease in the volumetric flow rate of gas.

GPF with coating positioned at the under-floor location is capable of converting the exhaust gases by catalytic activity along with increased filtration efficiency of particulate number (Inoda et al. 2017). A system of coated GPF (CGPF) with TWC was demonstrated using two GDI vehicles and found to have improved tailpipe emissions, particularly the NO_x emissions (Richter et al. 2012). However, CGPF cannot replace the application of TWC as CGPF requires comparatively more time to light-off in cold starting than conventional TWC (Opitz et al. 2014).

Fig. 6.16 Possible layouts of a GPF and TWC (AECC Technical Summary 2017)

## *6.4.2 Injector Deposits*

6.4.2.1 Causes of Formation
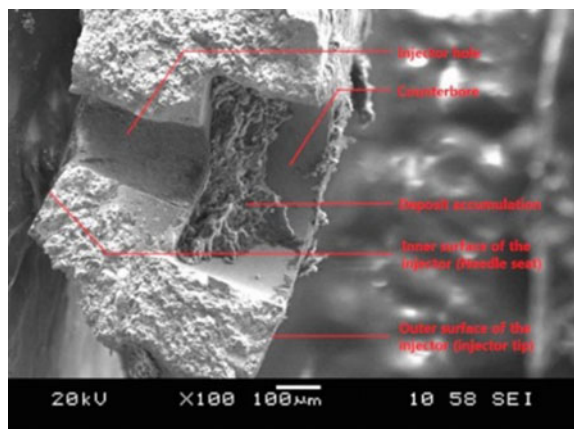
The deposits on injector were considered to be majorly dependent upon the temperature of the nozzle tip and the rate of deposits build-up increased when the temperature of the tip goes beyond 150 °C (Kinoshita et al. 1999). In the study, the mechanism behind the rapid accumulation of deposits after reaching 150 °C was described as thermal condensation and cracking reaction kinetics of gasoline. Although this growth was only limited to a range of temperature, as on exceeding a specific higher temperature (dependent on fuel and deposit composition), the self-cleaning phenomenon started (Stępień 2015). Kinoshita et al. (1999) formulated the relation between the temperature of the injector tip and T90 temperature of the fuel (temperature at 90% volume distillation) for GDI injector deposition. And concluded that when injector tip temperature is less than T90 temperature of the fuel, fuel present on the tip remains in the liquid state and washes away the deposit's precursors by next injection. On the other hand, if the tip temperature is more than T90 temperature, liquid fuel will be in the vapour state, which makes the deposits precursor adhere and will form agglomeration near the nozzle wall. EGR and intake-air cooling have a certain influence on injector deposits as they determine the in-cylinder charge temperature (Zhao et al. 1999). Carbon deposition can be routed from two factors, namely, high-temperature decomposition of hydrocarbons and generation of poly-aromatic hydrocarbons (PAHs), which latter nucleate and grow to form carbonaceous deposits.

6.4.2.2 Examining Techniques and Consequences of Deposits

Scanning Electron Microscope (SEM) (Imoehl et al. 2012; Jiang et al. 2017) has been used as an effective tool by many researchers for investigating the deposits around GDI injector, as shown in Fig. 6.17. Song et al. (2016) examined the deposits at the orifice of the choked injector with the help of photographs of SEM. There were loose deposits at the outer surfaces which were easy to remove, while deposits formed inside the holes were thick and distributed axially at the aperture with more density along a particular side of the hole. However, the depositions were radially distributed at an external aperture. Dearn et al. (2014) conducted the investigation of deposits distribution and composition at injector tip by mechanically cracking the injector. The deposits were formed at different levels over the injector with the proportion of its constituents varying with location. Their elemental study revealed that C, O, S and Ca were the elements with the largest proportion in the deposit. Moreover, there was a reduction in the amount of S and Ca, while increment in C in the deposits as location approaches towards the combustion chamber.

Deposits are most likely to form near the regions of metering of the fuel and where atomization takes place due to the constricted passage of the nozzle. It can distort the fuel injection spray by altering its shape and penetration length. It also results in

Fig. 6.17 SEM image of injector deposits (Jiang et al. 2017)

the reduction of fuel to be injected per pulse width. These modifications can affect the mixture formation and combustion characteristics adversely. Anbari et al. (2015) analyzed the spray structure of choked multi-hole injector using high-speed camera imaging and concluded that spray penetration length of spray plume increased and cone angle decreased due to choking effect. Also, the effect of choking was not same on all the plumes emerging from the injector. Similar results were derived from the work of Yiqiang et al. (2015), due to poor atomization of fuel by the choked injector. In contrast to this, Song et al. (2016) conducted the study on GDI injector and stated that penetration length and droplet size decreased while cone angle of spray increased. Thus, it can be inferred that spray characteristics would behave differently from different injectors due to deposits. Wang et al. (2014) compared the performance of fouled injector against that of clean injector in spray-guided DISI engine and came with results of higher emissions produced by fouled injector continuously, reaching the peak at maximum engine load condition of 8.5 bar IMEP. The PM emissions were 200% higher and PN emissions were 58% higher in the case of fouled injector. Badawy et al. (2018) investigated the effect of choking GDI injector on spray structures and engine performance of multi-cylinder engine. The choking process of injector was achieved in a consistent way by undergoing the fouling cycle. The spray characteristics like penetration length, cone angle, droplet diameters and velocity distribution were obtained using high-speed imaging and Phase Doppler Particle Analyser (PDPA). With higher penetration length of spray from choked injector as compared to the clean injector, the rear plume accounted for higher penetration as compared to ignition and side plume, and greater penetration observed with higher injection pressure among all plumes. Similarly, among smaller plume angles of choked injector, rear and side jets reported for maximum reduction in plume angle. Deposition distribution was studied using SEM and X-ray 3D microtomography as shown in Fig. 6.18. For visual scanning and composition analysis, Energy Dispersive X-ray Spectroscopy (EDS) was employed. Flame propagation characteristics revealed the occurrence of diffusion flame near the injector

Fig. 6.18 X-ray microtomography of **a** clean and **b** choked injector (Badawy et al. 2018)
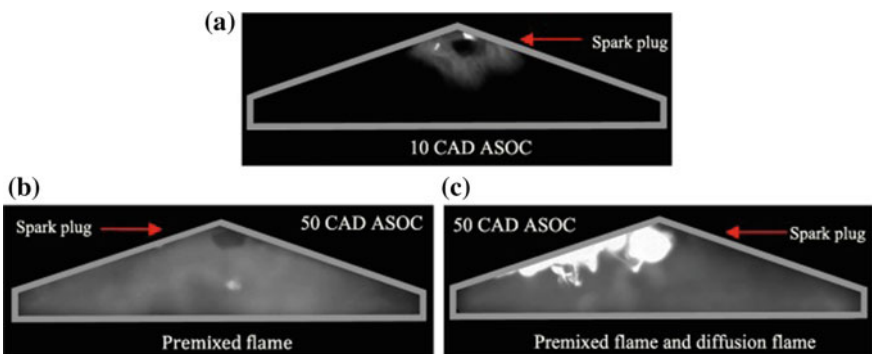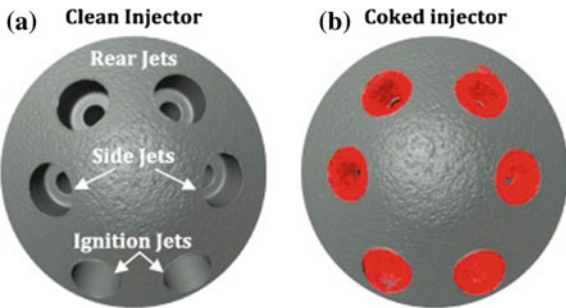

Fig. 6.19 Flame development with increasing crank angles, **a** early flame development of both clean and coked injectors, **b** clean injector and **c** coked injector, using gasoline (Badawy et al. 2018)

tip as shown in Fig. 6.19. In addition, with lower in-cylinder pressure and poorer combustion stability, choking in injector proved to be a crucial factor in affecting the engine performance. Inhomogeneity of charge and poor-repeatability of the mixture, lower load observation, higher unburnt HC emissions and particulates concentration are the major consequences of injector choking in GDI engine (Badawy et al. 2018).

6.4.2.3 Preventive Measures

The studies involving the methods for minimizing the formation of deposits include: (1) fuel detergents (Aradi et al. 2000), (2) coating of the injector with lower thermal conductivity material to reduce the injector tip temperature (Green et al. 2001) and (3) injection of fuel with high pressure (Von Bacho et al. 2009). These practices reduced the deposits formation in an efficient manner. Outward opening piezo-driven injector having a smooth surface, sharp inlet of the nozzle and counterbore design was proved significant in controlling deposit formation (Xu et al. 2015).

6.4.3 Pre-ignition and Deto-Knock

6.4.3.1 Causes

Several approaches like downsizing, high intake-boosting and direct injection have resulted in enhancing the fuel economy and power output of the engine. Although, higher boosting results in the engine knock condition which leads to an increment of developed pressure by one order magnitude as compared to the conventional knocking (Shuai et al. 2018). It is also termed as a super knock, mega knock or low-speed pre-ignition (LSPI) and is usually triggered at low-speed high-load conditions with the occurrence of pre-ignition prior to spark in the combustion chamber. The turbo-boosting in GDI engines is mainly restricted by deto-knock. As pressure and temperature of the charge attain the values of the deto-curve regime, the pre-ignition takes place at any hot spot inside the charge. The combustion flame front and wave propagated due to pre-ignition induce the ignition of the unburnt charge, resulting in high-pressure pulse with oscillating magnitude. It can cause severe damage to the liner and piston ring, and lead to the melting of exhaust valves.

Although pre-ignition induces the deto-knock, it is rare that pre-ignition will always lead to deto-knock as it occurs randomly with natural combustion and extinct naturally (Dahnz and Spicher 2010). It is measured by the number of its occurrences during certain completion of cycles, with a typical frequency of less than one in a thousand (Wang et al. 2017). Thus, investigation for the mechanism becomes difficult.

In the study, Wang et al. (2015) analysed the process involving the phenomenon of pre-ignition due to local hot-spot. This causes the rise in pressure and temperature of the charge, subsequently leading to deflagration of charge. This further induces the secondary hot spot at near-wall end-charge, causing a substantial increase in pressure trace with oscillating magnitude as shown in Fig. 6.20. This whole process is examined by synchronizing with high speed camera along with rapid compression machine (RCM) for pressure traces. It was concluded that the second hot spot situated in unburned charge was responsible for the detonation, which was induced by the deflagration (pre-ignition) due to primary hot spot.

Lubricating oil is considered to be a major source for pre-ignition that can lead to deto-knock condition due to higher tendency of auto-ignition (Amann and Alger 2012). The Dahnz and Spicher (2010) stated that wall-wetting due to spray and dilution of charge with oil present on the liner wall cause the oil droplets deposition in piston crevices. During deceleration of piston while moving towards TDC (top dead centre), less viscous diluted oil droplets enters the combustion chamber by virtue of inertia forces. In the optical study done by Lauer et al. (2014), oil droplets were found to be the initiator of pre-ignition. The pressure oscillations during auto-ignition release the deposits from the combustion chamber wall into the charge which act as ignition sources and subsequently leading to deto-knock. The diluted oil droplets and deposits require considerable time to accumulate, thus causing the event of deto-knock occasionally.
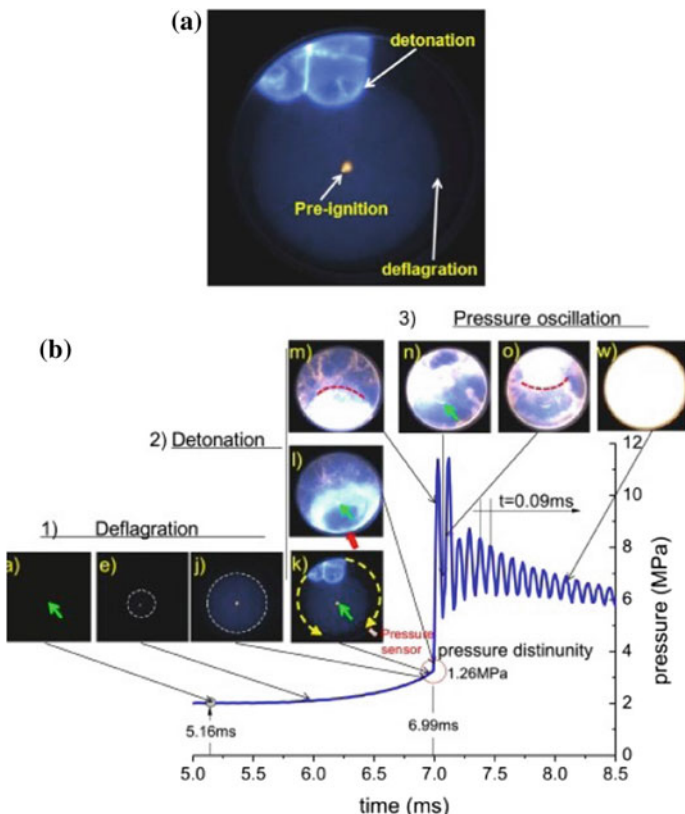
Fig. 6.20 Process showing the detonation induced by pre-ignition (Wang et al. 2015) **a** luminosity image showing pre-ignition, deflagration and detonation **b** synchronous pressure traces

6.4.3.2 Preventive Measures

The main approach for eliminating the trouble of deto-knock is to suppress pre-ignition. Various factors can be considered to diminish the chances of pre-ignition like oil and fuel properties, design and operational parameters of engines.

It has been established that oils with base stock having less reactivity and longer ignition delay, have less tendency towards auto-ignition (Welling et al. 2014). The metal elements used as additives in engine oil also influence the pre-ignition tendency of the charge. Calcium (Ca) based oil additives are found to enhance the phenomenon of pre-ignition (Kassai et al. 2016), whereas Zinc (Zn) and Molybdenum (Mo) based additives are reported to decrease the chances of pre-ignition. Similarly, fuel properties like lower aromatic content (Amann et al. 2011) and high volatility (Chapman et al. 2014) have led to decrease the frequency of pre-ignition. Designing and operating the engine with parameters such that it inhibits the wall-wetting and oil-diluted fuel deposition in crevices, can limit the chances of pre-ignition. As liner wetting

is more prone to pre-ignition than piston wetting (Zahdeh et al. 2011), in-cylinder motion of mixture can help to reduce the liner wetting issues by limiting the penetration length of spray and washing deposited droplets off the liner (Palaveev et al. 2013). Moreover, split-injection strategy by optimizing the timing has shown an effective reduction in pre-ignition frequency (Wang et al. 2014). Avoiding the condition of auto-ignition of the mixture by controlling the pressure, temperature and composition of the charge is a good approach for reducing the reactivity of mixture. With the aid of EGR, a significant reduction in pre-ignition can be observed because of lower in-cylinder temperature (Zaccardi and Escudié 2015) without compromising the BMEP.

Thus, many factors are helpful in reducing the phenomenon of pre-ignition. However, the phenomenon is specific to the particular engine configuration, and so are the parameters for controlling it. Thus, these factors should be considered on the engine-to-engine basis.

6.5   Conclusions

A thorough analysis of the work done in the area of gasoline direct injection technology reveals that the technology has evolved in large proportions. The automotive engineers are trying to make it more reliable and efficient, along with solving critical issues related to DISI engines. We have discussed various works in the direction of improving the performance and fulfilling the required objectives of this notable technology.

The fuel injection system is the heart of the GDI technology which prepares the required mixture according to load and rpm conditions. From the research conducted, it can be concluded that spray-guided combustion system is best suited for running the engine on ultra-lean charge as well as stoichiometric charge. For this, injection timing, parameters and in-cylinder motion need to be optimized for avoiding the spray-impingement problem and obtaining proper mixture preparation and charge cooling benefits. Utilizing alcohol in port injection and gasoline in direct injection (dual fuel injection) has resulted in achieving better thermal efficiency and reducing emissions. Also, it decreases the tendency of knocking with the provision of greater spark advance timing. This strategy is helpful in utilizing alcohol as alternate fuel along with performance benefits. The characteristics of different injector designs are also discussed; out of which piezo-driven outward opening injectors are best suited for stratified operating mode due to lower spray penetration length. By optimizing the fuel injection timing for split-injection, successful operation of the overall lean homogeneous mixture has been observed in GDI engine. Further, higher injection pressure for better atomization, with lower coolant temperature during cold-start conditions have efficiently reduced the HC and PM emissions from the GDI engine. All these strategies are to be considered for optimizing the injection system of the GDI engine.

Additionally, with the advantages of downsizing the engine, boosting help in improving the power output of the engine, though it limits the operating compression ratio of the engine. Thus, the provision of variable compression ratio accommodates the engine operation according to the required load and rpm condition. Further, addition of EGR helps to reduce the NO_x emissions, minimize the heat loss and improve thermal efficiency of the engine.

We also discussed the particulate matter characteristics of GDI engine and its dependence on various operational factors. Improving atomization and eliminating fuel-film formation issues by running the engine with optimized fuel injection parameter helps to reduce high PM emissions. Likewise, supplying cooled EGR has reported a significant reduction in PM emissions. The issue of injector deposits is also seen as major concerns in GDI engine operation. Avoiding injector deposits by adopting the aforementioned measures and using suitable additives with engine oil can bring down the levels of particulate emission. Furthermore, the role of after-treatment devices such as TWC and GPF are discussed for limiting the tail-pipe emissions.

Finally, the occurrence of deto-knock due to pre-ignition of charge is discussed. The causes of pre-ignition like presence of oil-diluted fuel droplets and operating conditions like temperature, pressure and mixture composition leading to auto-ignition of charge, should be avoided in order to eliminate the chances of deto-knock. Here also, inhibiting wall-wetting conditions, utilizing split-injection strategy, enabling EGR and controlling operational parameters has proved beneficial for reducing the menace of deto-knock in engines.

Although GDI engines operating on homogeneous mode are available in the market, the stratified mode is still in the development phase. Studies of optical diagnostics and CFD simulation have literally helped to optimize the operating parameters for achieving stratified mode operation to some extents, but not completely. Hence, a full-fledged GDI system with mode-switching technology remains a promising field for the research community.

References

AECC technical summary (2017) Gasoline particulate filter (GPF), How can the GPF cut emissions of ultrafine particles from gasoline engines

Amann M, Alger T (2012) Lubricant reactivity effects on gasoline spark ignition engine knock. SAE Int J Fuels Lubric 5(2):760–771

Amann M, Mehta D, Alger T (2011) Engine operating condition and gasoline fuel composition effects on low-speed pre-ignition in high-performance spark ignited gasoline engines. SAE Int J Engines 4(1):274–285

Anbari AM, Badawy T, Xu H (2015) Optical investigation of influence of injector nozzle deposit on particulate matter emissions drift. IMechE, London, Internal Combustion Engines

Aradi AA, Colucci WJ, Scull HM, Openshaw MJ (2000) A study of fuel additives for direct injection gasoline (DIG) injector deposit control. SAE technical paper, 19 June 2000

Asthana S, Bansal S, Jaggi S, Kumar N. A comparative study of recent advancements in the field of variable compression ratio engine technology. SAE Technical Paper; 2016 Apr 5

Aubernon C (2014) Japanese automakers form alliance to develop next-gen fuel-efficient engines. http://www.thetruthaboutcars.com/2014/05/japanese-automakers-formalliance-to-develop-next-gen-fuel-efficient-engines/#more-826666.%202014

Badawy T, Attar MA, Hutchins P, Xu H, Venus JK, Cracknell R (2018a) Investigation of injector coking effects on spray characteristic and engine performance in gasoline direct injection engines. Appl Energy 15(220):375–394

Badawy T, Attar MA, Xu H, Ghafourian A (2018b) Assessment of gasoline direct injector fouling effects on fuel injection, engine performance and emissions. Appl Energy 15(220):351–374

Balki MK, Sayin C, Canakci M (2014) The effect of different alcohol fuels on the performance, emission and combustion characteristics of a gasoline engine. Fuel 1(115):901–906

Beavis NJ, Ibrahim SS, Malalasekera W (2017) Impingement characteristics of an early injection gasoline direct injection engine: A numerical study. Int J Engine Res 18(4):378–393

Berndorfer A, Breuer S, Piock W, Von Bacho P (2013) Diffusion combustion phenomena in GDI engines caused by injection process. SAE technical paper, 8 Apr 2013

Blair GP (1996) Design and simulation of two-stroke engines. Society of Automotive Engineers, Warrendale, PA

Bock N, Jeon J, Kittelson D, Northrop WF (2018) Solid particle number and mass emissions from lean and stoichiometric gasoline direct injection engine operation. SAE technical paper, 3 Apr 2018

Bonatesta F, Chiappetta E, La Rocca A (2014) Part-load particulate matter from a GDI engine and the connection with combustion characteristics. Appl Energy 1(124):366–376

Cairns A, Blaxill H, Irlam G (2006) Exhaust gas recirculation for improved part and full load fuel economy in a turbocharged gasoline engine. SAE technical paper, 3 Apr 2006

Chapman E, Davis R, Studzinski W, Geng P (2014) Fuel octane and volatility effects on the stochastic pre-ignition behavior of a 2.0 L gasoline turbocharged DI engine. SAE Int J Fuels Lubric 7(2):379–389

Chapman E, Winston-Galant M, Geng P, Konzack A (2016) Global market gasoline range fuel review using fuel particulate emission correlation indices. SAE technical paper, 17 Oct 2016

Chen L, Liang Z, Zhang X, Shuai S (2017) Characterizing particulate matter emissions from GDI and PFI vehicles under transient and cold start conditions. Fuel 1(189):131–140

China (2016) Limits and measurement methods for emissions from light duty vehicles (CHINA 6)

Chincholkar SP, Suryawanshi JG (2016) Gasoline direct injection: an efficient technology. Energy Procedia 1(90):666–672

Chung J, Kim N, Choi H, Min K (2016) Study on the effect of injection strategies on particulate emission characteristics under cold start using in-cylinder visualization. SAE technical paper, 5 Apr 2016

Clairotte M, Adam TW, Zardini AA, Manfredi U, Martini G, Krasenbrink A, Vicet A, Tournié E, Astorga C (2013) Effects of low temperature on the cold start gaseous emissions from light duty vehicles fuelled by ethanol-blended gasoline. Appl Energy 1(102):44–54

Clark LG, Kook S, Chan QN, Hawkes ER (2016) Multiple injection strategy investigation for well-mixed operation in an optical Wall-Guided Spark-Ignition Direct-Injection (WG-SIDI) engine through flame shape analysis. SAE technical paper, 17 Oct 2016

Clark LG, Kook S, Chan QN, Hawkes ER (2017) Influence of injection timing for split-injection strategies on well-mixed high-load combustion performance in an optically accessible Spark-Ignition Direct-Injection (SIDI) engine. SAE technical paper, 28 Mar 2017

Costa M, Sorge U, Merola S, Irimescu A, La Villetta M, Rocco V (2016) Split injection in a homogeneous stratified gasoline direct injection engine for high combustion efficiency and low pollutants emission. Energy 15(117):405–415

Costagliola MA, De Simio L, Iannaccone S, Prati MV (2013) Combustion efficiency and engine out emissions of a SI engine fueled with alcohol/gasoline blends. Appl Energy 1(111):1162–1171

Cucchi M, Samuel S (2015) Influence of the exhaust gas turbocharger on nano-scale particulate matter emissions from a GDI spark ignition engine. Appl Therm Eng 5(76):167–174

Dahlander P, Hemdal S (2015) High-speed photography of stratified combustion in an optical GDI engine for different triple injection strategies. SAE technical paper, 14 Apr 2015

Dahlander P, Iemmolo D, Tong Y (2015) Measurements of time-resolved mass injection rates for a multi-hole and an outward opening piezo GDI injector. SAE technical paper, 14 Apr 2015

Dahnz C, Spicher U (2010) Irregular combustion in supercharged spark ignition engines–pre-ignition and other phenomena. Int J Engine Res 11(6):485–498

Daniel R, Xu H, Wang C, Richardson D, Shuai S (2013) Gaseous and particulate matter emissions of biofuel blends in dual-injection compared to direct-injection and port injection. Appl Energy 1(105):252–261

De Boer C, Bonar G, Sasaki S, Shetty S (2013) Application of supercritical gasoline injection to a direct injection spark ignition engine for particulate reduction. SAE technical paper, 8 Apr 2013

Dearn K, Xu J, Ding H, Xu H, Weall A, Kirkby P, Cooper B, Edington I, Krueger-Venus J (2014) An investigation into the characteristics of DISI injector deposits using advanced analytical methods. SAE Int J Fuels Lubric 7(3):771–782

Eichhorn A, Lejsek D, Kulzer A, Kufferath A, Wizgall E, Centmayer R (2012) Design of a boosted 2-cylinder SI-engine with gasoline direct injection to define the needs of future powertrains. SAE technical paper, 16 Apr 2012

Feng D, Wei H, Pan M, Zhou L, Hua J (2018) Combustion performance of dual-injection using n-butanol direct-injection and gasoline port fuel-injection in a SI engine. Energy 1(160):573–581

Green AC, DAVID M, Lambert MDD, Nandy M (2001) Injection nozzle. Delphi Technologies Inc. Patent EP1081374 A2 patent application, 2001. https://patents.google.com/patent/EP1081374A2/en

He BQ, Chen X, Lin CL, Zhao H (2016) Combustion characteristics of a gasoline engine with independent intake port injection and direct injection systems for n-butanol and gasoline. Energy Convers Manag 15(124):556–565

Hedge M, Weber P, Gingrich J, Alger T, Khalek I (2011) Effect of EGR on particle emissions from a GDI engine. SAE Int J Engines 4(1):650–666

Hoffmann G, Befrui B, Berndorfer A, Piock WF, Varble DL (2014) Fuel system pressure increase for enhanced performance of GDi multi-hole injection systems. SAE Int J Engines 7(1):519–527

Huang Y, Hong G, Huang R (2016) Effect of injection timing on mixture formation and combustion in an ethanol direct injection plus gasoline port injection (EDI + GPI) engine. Energy 15(111):92–103

Hwang K, Hwang I, Lee H, Park H, Choi H, Lee K, Kim W, Kim H, Han B, Lee J, Shin B (2016) Development of new high-efficiency Kappa 1.6 L GDI engine. SAE technical paper, 5 Apr 2016

Iida N (2017) Research and development of super-lean burn for high efficiency SI engine. In: The proceedings of the international symposium on diagnostics and modeling of combustion in internal combustion engines 2017.9, The Japan Society of Mechanical Engineers, pp PL-1

Ikoma T, Abe S, Sonoda Y, Suzuki H, Suzuki Y, Basaki M (2006) Development of V-6 3.5-liter engine adopting new direct injection system. SAE technical paper, 3 Apr 2006

Imoehl W, Gestri L, Maragliulo M, Del-Frate L, Klepatsch M, Wildeson R (2012) A DOE approach to engine deposit testing used to optimize the design of a gasoline direct injector seat and orifice. SAE Int J Fuels Lubric 5(3):1078–1095

Inoda S, Nomura Y, Ori H, Yabuzaki Y (2017) Development of new coating technology optimized for each function of coated GPF. SAE technical paper, 28 Mar 2017

Itabashi S, Murase E, Tanaka H, Yamaguchi M, Muraguchi T (2017) New combustion and power-train control technologies for fun-to-drive dynamic performance and better fuel economy. SAE technical paper, 28 Mar 2017

Ji C, Cong X, Wang S, Shi L, Su T, Wang D (2018) Performance of a hydrogen-blended gasoline direct injection engine under various second gasoline direct injection timings. Energy Convers Manag 1(171):1704–1711

Jiang C, Xu H, Srivastava D, Ma X, Dearn K, Cracknell R, Krueger-Venus J (2017) Effect of fuel injector deposit on spray characteristics, gaseous emissions and particulate matter in a gasoline direct injection engine. Appl Energy 1(203):390–402

Jiang C, Li Z, Qian Y, Wang X, Zhang Y, Lu X (2018) Influences of fuel injection strategies on combustion performance and regular/irregular emissions in a turbocharged gasoline direct injection engine: commercial gasoline versus multi-components gasoline surrogates. Energy 15(157):173–187

Kadota M, Ishikawa S, Yamamoto K, Kato M, Kawajiri S (2009) Advanced control system of variable compression ratio (VCR) engine with dual piston mechanism. SAE Int J Engine 2(1):1009–1018

Kassai M, Shiraishi T, Noda T, Hirabe M, Wakabayashi Y, Kusaka J, Daisho Y (2016) An investigation on the ignition characteristics of lubricant component containing fuel droplets using rapid compression and expansion machine. SAE Int J Fuels Lubric 9(3):469–480

Ketterer JE, Cheng WK (2014) On the nature of particulate emissions from DISI engines at cold-fast-idle. SAE Int J Engines 7(2):986–994

Kim S, Nouri JM, Yan Y, Arcoumanis C (2009) Effects of intake flow on the spray structure of a multi-hole injector in a DISI engine. Int J Automot Technol 10(3):277–284

Kim T, Song J, Park S (2015a) Effects of turbulence enhancement on combustion process using a double injection strategy in direct-injection spark-ignition (DISI) gasoline engines. Int J Heat Fluid Flow 1(56):124–136

Kim J, Chun KM, Song S, Baek HK, Lee SW (2015) Effect of hydrogen as an additive on lean limit and emissions of a turbo gasoline direct injection engine. SAE technical paper, 1 Sept 2015

Kim J, Chun KM, Song S, Baek HK, Lee SW (2017) The effects of hydrogen on the combustion, performance and emissions of a turbo gasoline direct-injection engine with exhaust gas recirculation. Int J Hydrogen Energy 42(39):25074–25087

Kinoshita M, Saito A, Matsushita S, Shibata H, Niwa Y (1999) A method for suppressing formation of deposits on fuel injector for direct injection gasoline engine. SAE Trans 1:2177–2184

Kittelson DB (1998) Engines and nanoparticles: a review. J Aerosol Sci 29(5–6):575–588

Kleeberg H, Tomazic D, Dohmen J, Wittek K, Balazs A (2013) Increasing efficiency in gasoline powertrains with a two-stage variable compression ratio (VCR) system. SAE technical paper, 8 Apr 2013

Koç M, Sekmen Y, Topgül T, Yücesu HS (2009) The effects of ethanol–unleaded gasoline blends on engine performance and exhaust emissions in a spark-ignition engine. Renew Energy 34(10):2101–2106

Kojima S, Kiga S, Moteki K, Takahashi E, Matsuoka K (2018) Development of a new 2L gasoline VC-Turbo engine with the world's first variable compression ratio technology. SAE technical paper, 3 Apr 2018

Lattimore T, Wang C, Xu H, Wyszynski ML, Shuai S (2016) Investigation of EGR effect on combustion and PM emissions in a DISI engine. Appl Energy 1(161):256–267

Lauer T, Heiss M, Bobicic N, Holly W, Pritze S (2014) A comprehensive simulation approach to irregular combustion. SAE technical paper, 1 Apr 2014

Lee CH, Lee KH (2006) Experimental study on the stratified combustion characteristics according to compression ratio and intake temperature in a DIG engine. Int J Automot Technol 7(6):675–680

Lee B, Oh H, Han S, Woo S, Son J (2017) Development of high efficiency gasoline engine with thermal efficiency over 42%. SAE technical paper, 8 Oct 2017

Liu H, Wang Z, Wang J (2014) Methanol-gasoline DFSI (dual-fuel spark ignition) combustion with dual-injection for engine knock suppression. Energy 14(73):686–693

Liu H, Wang Z, Long Y, Wang J (2015a) Dual-Fuel Spark Ignition (DFSI) combustion fuelled with different alcohols and gasoline for fuel efficiency. Fuel 1(157):255–260

Liu H, Wang Z, Long Y, Xiang S, Wang J, Wagnon SW (2015b) Methanol-gasoline Dual-fuel Spark Ignition (DFSI) combustion with dual-injection for engine particle number (PN) reduction and fuel economy improvement. Energy 1(89):1010–1017

Liu H, Wang Z, Long Y, Xiang S, Wang J, Fatouraie M (2015c) Comparative study on alcohol—gasoline and gasoline–alcohol Dual-Fuel Spark Ignition (DFSI) combustion for engine particle number (PN) reduction. Fuel 1(159):250–258

Lucchini T, D'Errico G, Onorati A, Bonandrini G, Venturoli L, Di Gioia R (2014) Development and application of a computational fluid dynamics methodology to predict fuel–air mixing and sources of soot formation in gasoline direct injection engines. Int J Engine Res 15(5):581–596

Matsumura E, Kanda M, Hattori F, Nomura H, Hashimoto S, Yoshimaru K (2013) Development of DISI engine utilizing a fan-shaped spray jet. SAE technical paper, 8 Apr 2013

Matthias N, Wallner T, Scarcelli R (2014) Analysis of cyclic variability and the effect of dilute combustion in a gasoline direct injection engine. SAE Int J Engines 7(2):633–641

Nakashima T, Basaki M, Saito K, Furuno S (2003) New concept of a direct injection SI gasoline engine: a study of stratified charge combustion characteristics by radical luminescence measurement. JSAE Rev 24(1):17–23

Opitz B, Drochner A, Vogel H, Votsmeier M (2014) An experimental and simulation study on the cold start behaviour of particulate filters with wall integrated three way catalyst. Appl Catal B 1(144):203–215

Palaveev S, Magar M, Kubach H, Schiessl R, Spicher U, Maas U (2013) Premature flame initiation in a turbocharged DISI engine-numerical and experimental investigations. SAE Int J Engines 6(1):54–66

Park C, Kim S, Kim H, Moriyoshi Y (2012) Stratified lean combustion characteristics of a spray-guided combustion system in a gasoline direct injection engine. Energy 41(1):401–407

Park CW, Oh HC, Kim SD, Kim HS, Lee SY, Bae CS (2014) Evaluation and visualization of stratified ultra-lean combustion characteristics in a spray-guided type gasoline direct-injection engine. Int J Automot Technol 15(4):525–533

Park C, Lee S, Yi U (2016) Effects of engine operating conditions on particle emissions of lean-burn gasoline direct-injection engine. Energy 15(115):1148–1155

Pei YQ, Qin J, Pan SZ (2014) Experimental study on the particulate matter emission characteristics for a direct-injection gasoline engine. Proc Inst Mech Eng, Part D-J Automob Eng 228:604–616

Pirjola L, Karjalainen P, Heikkilä J, Saari S, Tzamkiozis T, Ntziachristos L, Kulmala K, Keskinen J, Rönkkö T (2015) Effects of fresh lubricant oils on particle emissions emitted by a modern gasoline direct injection passenger car. Environ Sci Technol 49(6):3644–3652

Potteau S, Lutz P, Leroux S, Moroz S, Tomas E (2007) Cooled EGR for a turbo SI engine to reduce knocking and fuel consumption. SAE technical paper, 29 Oct 2007

Price P, Stone R, Collier T, Davies M (2006) Particulate matter and hydrocarbon emissions measurements: comparing first and second generation DISI with PFI in single cylinder optical engines. SAE technical paper, 3 Apr 2006

Qian Y, Liu G, Guo J, Zhang Y, Zhu L, Lu X (2019a) Engine performance and octane on demand studies of a dual fuel spark ignition engine with ethanol/gasoline surrogates as fuel. Energy Convers Manag 1(183):296–306

Qian Y, Chen F, Zhang Y, Tao W, Han D, Lu X (2019) Combustion and regulated/unregulated emissions of a direct injection spark ignition engine fueled with C3-C5 alcohol/gasoline surrogate blends. Energy, 5 Mar 2019

Qian Y, Li Z, Yu L, Wang X, Lu X (2019c) Review of the state-of-the-art of particulate matter emissions from modern gasoline fueled engines. Appl Energy 15(238):1269–1298

Richter JM, Klingmann R, Spiess S, Wong KF (2012) Application of catalyzed gasoline particulate filters to GDI vehicles. SAE Int J Engines 5(3):1361–1370

Sevik J, Pamminger M, Wallner T, Scarcelli R, Boyer B, Wooldridge S, Hall C, Miers S (2016) Influence of injector location on part-load performance characteristics of natural gas direct-injection in a spark ignition engine. SAE Int J Eng 9(4):2262–2271

Sharma N, Agarwal AK. Gasoline direct injection engines and particulate emissions. In: Air pollution and control 2018. Springer, Singapore, pp 87–105

Short D, Vu D, Durbin TD, Karavalakis G, Asa-Awuku A (2015) Particle speciation of emissions from iso-butanol and ethanol blended gasoline in light-duty vehicles. J Aerosol Sci 1(84):39–52

Shuai S, Ma X, Li Y, Qi Y, Xu H (2018) Recent Progress in Automotive Gasoline Direct Injection Engine Technology. Automot Innovation. 1(2):95–113

Skogsberg M, Dahlander P, Denbratt I (2007) Spray shape and atomization quality of an outward-opening piezo gasoline DI injector. SAE technical paper, 16 Apr 2007

Song J, Kim T, Jang J, Park S (2015) Effects of the injection strategy on the mixture formation and combustion characteristics in a DISI (direct injection spark ignition) optical engine. Energy 15(93):1758–1768

Song H, Xiao J, Chen Y, Huang Z (2016) The effects of deposits on spray behaviors of a gasoline direct injector. Fuel 15(180):506–513

Song J, Lee Z, Song J, Park S (2018) Effects of injection strategy and coolant temperature on hydrocarbon and particulate emissions from a gasoline direct injection engine with high pressure injection up to 50 MPa. Energy 1(164):512–522

Stępień Z (2015) Deposits in spark ignition engines–formation and threats. Combust Engines, vol 54

Stiehl R, Schorr J, Krüger C, Dreizler A, Böhm B (2013) In-cylinder flow and fuel spray interactions in a stratified spray-guided gasoline engine investigated by high-speed laser imaging techniques. Flow Turbul Combust 91(3):431–450

Storch M, Hinrichsen F, Wensing M, Will S, Zigan L (2015) The effect of ethanol blending on mixture formation, combustion and soot emission studied in an optical DISI engine. Appl Energy 15(156):783–792

Tang Y, Deng W, Liu B, Hu TG, Wang X, Yang Q, Jiang B, Lin L, Zhan ZS, Min L (2018) The new Chang An inline 4 cylinder 1.6 L gasoline naturally aspirated GDI engine. SAE Technical Paper, 3 Apr 2018

Toulson E, Watson HC, Attard WP (2007) The effects of hot and cool EGR with hydrogen assisted jet ignition. SAE technical paper, 5 Aug 2007

Tree DR, Svensson KI (2007) Soot processes in compression ignition engines. Progr Energy Combust Sci 33(3):272–309

Trimbake S, Malkhede D (2016) Investigations of Port Dual Injection (PDI) strategies in single cylinder SI engine fueled with ethanol/gasoline blends. SAE technical paper, 5 Apr 2016

Turner D, Xu H, Cracknell RF, Natarajan V, Chen X (2011) Combustion performance of bio-ethanol at various blend ratios in a gasoline direct injection engine. Fuel 90(5):1999–2006

Velji A, Yeom K, Wagner U, Spicher U, Roßbach M, Suntz R, Bockhorn H (2010) Investigations of the formation and oxidation of soot inside a direct injection spark ignition engine using advanced laser-techniques. SAE technical paper, 12 Apr 2010

Von Bacho PS, Sofianek JK, Galante-Fox JM, McMahon CJ (2009) Engine test for accelerated fuel deposit formation on injectors used in gasoline direct injection engines. SAE technical paper, 20 Apr 2009

Wada Y, Nakano K, Mochizuki K, Hata R (2016) Development of a new 1.5 L I4 turbocharged gasoline direct injection engine. SAE technical paper, 5 Apr 2016

Wang C, Xu H, Herreros JM, Wang J, Cracknell R (2014a) Impact of fuel and injection system on particle emissions from a GDI engine. Appl Energy 1(132):178–191

Wang Z, Liu H, Song T, Xu Y, Wang JX, Li DS, Chen T (2014) Investigation on pre-ignition and super-knock in highly boosted gasoline direct injection engines. SAE technical paper, 1 Apr 2014

Wang Z, Qi Y, He X, Wang J, Shuai S, Law CK (2015) Analysis of pre-ignition to super-knock: hotspot-induced deflagration to detonation. Fuel 15(144):222–227

Wang Z, Liu H, Reitz RD (2017) Knocking combustion in spark-ignition engines. Prog Energy Combust Sci 1(61):78–112

Wei H, Zhu T, Shu G, Tan L, Wang Y (2012) Gasoline engine exhaust gas recirculation–a review. Appl Energy 1(99):534–544

Welling O, Collings N, Williams J, Moss J (2014) Impact of lubricant composition on low-speed pre-ignition. SAE technical paper, 1 Apr 2014

Whelan I, Timoney D, Smith W, Samuel S (2013) The effect of a three-way catalytic converter on particulate matter from a gasoline direct-injection engine during cold-start. SAE Int J Engines 6(2):1035–1045

Wolfgang S, Sorger H, Loesch S, Unzeitig W, Huettner T, Fuerhapter A (2017) The 2-Step VCR conrod system-modular system for high efficiency and reduced CO_2. SAE technical paper, 28 Mar 2017

Xing J, Shao L, Zheng R, Peng J, Wang W, Guo Q, Wang Y, Qin Y, Shuai S, Hu M (2017) Individual particles emitted from gasoline engines: impact of engine types, engine loads and fuel components. J Clean Prod 15(149):461–471

Xu H, Wang C, Ma X, Sarangi AK, Weall A, Krueger-Venus J (2015) Fuel injector deposits in direct-injection spark-ignition engines. Progr Energy Combust Sci 1(50):63–80

Yamazaki D, Mori A, Murase E (2018) The development of a new V6 3.5 L turbocharged gasoline engine. SAE technical paper, 3 Apr 2018

Yiqiang P, Hao CH, Jing Q, Jianwei Z, Xiang L, Bin L (2015) Effect of GDI engine injector coking on spray. J Tianjin Univ, vol 48

Yu RC, Shahed SM (1981) Effects of injection timing and exhaust gas recirculation on emissions from a DI diesel engine. SAE Trans 1:3873–3883

Yu CH, Park KW, Han SK, Kim WT (2009) Development of theta II 2.4 L GDI engine for high power and low emission. SAE Technical Paper, 20 Apr 2009

Zaccardi JM, Escudié D (2015) Overview of the main mechanisms triggering low-speed pre-ignition in spark-ignition engines. Int J Engine Res 16(2):152–165

Zahdeh A, Rothenberger P, Nguyen W, Anbarasu M, Schmuck-Soldan S, Schaefer J, Goebel T (2011) Fundamental approach to investigate pre-ignition in boosted SI engines. SAE Int J Engines 4(1):246–273

Zhao H (2010) Overview of gasoline direct injection engines. In: Advanced direct injection combustion engine technologies and development 1 Jan 2010, Woodhead Publishing, pp 1–19

Zhao F, Lai MC, Harrington DL (1999) Automotive spark-ignited direct-injection gasoline engines. Prog Energy Combust Sci 25(5):437–562

Zhao H, Peng Z, Ladommatos N (2001) Understanding of controlled autoignition combustion in a four-stroke gasoline engine. Proc Inst Mech Eng Part D J Automob Eng 215(12):1297–1310

Zhuang Y, Qian Y, Hong G (2017) The effect of ethanol direct injection on knock mitigation in a gasoline port injection engine. Fuel 15(210):187–197

Chapter 7
Study on Alternate Fuels and Their Effect on Particulate Emissions from GDI Engines

Sreelekha Etikyala and Vamshi Krishna Gunda

Abstract With strict environmental legislations and to reduce related health hazards, there is immense focus on reducing particulates from gasoline direct injection engines. With increasing use of biofuels in the market, their blends with hydrocarbon fuels are also being considered as cleaner alternatives to gasoline. This chapter confers the addition of oxygenates to gasoline and their capacity to reduce sooting tendency compared to gasoline. Challenges related to optimizing combustion by appropriately choosing engine parameters such as start of ignition, duration of injection, etc. have been addressed. Optimizing combustion can reduce the particulate emissions, by sometimes increasing efficiency. Oxygenated fuels always have the advantage of higher oxidation of soot formed inside the cylinder, which further reduces particulate emissions. Towards the end of this chapter, disadvantages of using oxygenated fuel blends or alternate fuels are discussed.

Keywords Particulate matter · Legislation · Gasoline blends · Renewable fuels

7.1 Introduction

Almost a quarter of particulate emissions into the environment are caused by transportation in the world (Indicator Assessment 2015). Conventionally, world's demand for energy is mostly met from combusting fossil fuels. Fossil fuel combustion generates global warming pollutants such as CO, CO_2 and NO_x along with soot and hydrocarbons including polycyclic aromatic hydrocarbons (PAHs) that affect human health (Liu et al. 2015). Particulate matter, formed due to incomplete combustion, is a carbonaceous material. Upon inhalation, being carcinogenic, particulate matter may lead to pulmonary and respiratory diseases (Claxton 2015). Soot is also one on the contributors to global warming due to its role in regional warming and the faster melting of polar icecaps (Maione et al. 2016). It is essential to regulate soot

S. Etikyala (✉) · V. K. Gunda
Chalmers University of Technology, Gothenburg, Sweden
e-mail: etikyala@chalmers.se

Volvo Cars Corporation, Gothenburg, Sweden

formation in engines to abide by emission regulations and also towards controlling health effects (Überall et al. 2015).

Compared to diesel engines, gasoline engines emit higher number of particulates, sometimes even more than the prescribed limit (Myung et al. 2012). Moreover, this problem of soot has intensified with gasoline direct injection (GDI) engines taking over the market with their benefits compared to port fuel injection (PFI) engines (Zimmerman et al. 2016). GDI engines prevailed in the automotive industry as it offers relatively higher BSFC, volumetric efficiency and for their superior knock resistance compared to PFI. GDI engines also plays a major role in reducing CO_2 emissions from gasoline-powered engines. However, the particulate mass and the number of large particulates emitted by GDI is higher than PFI (Saliba et al. 2017). Thus, during gasoline combustion there is still a greater need to address the higher particulate emissions by reducing soot formation. Detailed discussion on health effects related to soot emissions from GDI can be found in Sharma and Agarwal (2018).

Some of the existing techniques to reduce particulate emissions include fuel reformulation, addition of metal catalysts to fuels, and methods for after-treatment of exhaust. For instance, one of the widely implemented after-treatment system, gasoline particulate filters (GPF) are used to filter out soot from entering into atmosphere from engine exhaust (Chan et al. 2014). Especially in Europe due to the upcoming stringent regulations on the number of particulates that can be emitted from gasoline engines (Johnson and Joshi 2017). GDI engines with GPF produce more ultrafine particulates compared to diesel engines fitted with diesel particulate filter (DPF) (He et al. 2012). These ultrafine particulates with sizes less than 100 nm, are found to cause adverse impacts on human health and environment (Bernstein 2004). This chapter focusses on particle number (PN) rather than particulate mass (PM) emitted from an engine as health impact of PN emissions can be strongly correlated to PN. Especially, particles as fine as ultrafine particles contribute little to the PM while being a significant part of the total PN. Finer the particulates get, deeper becomes their penetration into the lungs and therefore increased are the chances of passage into the human bloodstream (Eastwood 2008).

Moreover, these metal catalysts that are added to fuels which reduce soot, end up being more harmful to the environment and human health (Cassee et al. 2011). There are promising results from fuel blends that could lower soot emissions without the need for modifying the engine technologies (Guerrero Peña et al. 2018).

Fuel reformulation facilitates increase in the amount of oxidizer inside the combustion chamber by blending oxygenated and conventional fuels that leads to reduction in soot formation. Quite a lot of oxygenated compounds such as methanol (Wang et al. 2015), ethanol (Masum et al. 2013), butanol (Gu et al. 2012), furans (Tanaka et al. 2015), dimethyl carbonate (Schifter et al. 2016), ethers (Cataluña et al. 2008) and ketones (Elfasakhany 2016) have been found to decrease soot emission when blended with gasoline (Guerrero Peña et al. 2018). The reduction in sooting tendency of such blended fuels comes from the fact that the oxygen atoms present in these fuels present favorable chemical or dilution effects (Lemaire et al. 2010, 2015), or makes soot particles more susceptible towards oxidation (Gogoi et al. 2015). Such high soot oxidation can also help with the rapid regeneration of GPFs at low temperatures.

This chapter describes the characteristics of PN emitted from GDI engines from the view point of impact of fuel composition, in terms of oxygenates blended with gasoline making it an alternative to the existing engine technology. Many studies have tested individually on the application and possible benefits of such alternate fuels. This study provides a comprehensive report on recent progress in reducing PN from GDI research using alternate fuels including gasoline blended with renewable fuels.

7.2 PN from GDI Engines and Alternate Fuels

Particulates are usually formed from GDI engines during fuel combustion in the combustion chamber. The ones that exit the engine can also originate from nucleation of supersaturated vapors in the exhaust gas after-treatment systems (Heywood 1988). Formation of fuel films on the combustion chamber walls contribute significantly to the PN formation since fuel deposited this way form fuel-rich areas. From these locally rich areas, soot can easily be formed and subsequently emitted. Many studies recently looked at improving mixture quality that promote soot reduction. For available engine technology fuel reformulation and alternate fuels provide an easily adaptable alternative.

A variety of fuel properties affect PN formation in an engine including aromatic content and oxygenate content, enthalpy of vaporization and boiling points of individual components. Soot formation is highly affected by the existence of aromatic fuel rings as combustion researchers believe that gaseous polycyclic aromatic hydrocarbons (PAHs) act as precursors for soot. As expected, it was found in research that higher amount of aromatics in the fuel would lead to a higher level of PN (Raza et al. 2018).

The impact of fuel volatility on PN emissions comes from the fact that slower evaporation of a fuel due to its lower vapor pressure produce a relatively poorer mixture formation leading to higher PN. Pool fires that occur due to higher impingement on walls and piston that cause significantly higher PN making their occurrence a case of extremity. However, higher volatility in a fuel can also cause higher PN with flash evaporation leading to a mixture with locally rich zones causing incomplete combustion.

Of all the available fuel blends, E5 (5% of ethanol and 95% of gasoline by volume) is now common in Europe (European Committee for Standardization 2008); blends of E10 are ubiquitous, and E15 is on its way to the market for newer vehicles in the USA (U.S.C. §7546). Introducing ethanol into gasoline fuel blends tends to increase the enthalpy of vaporization for the fuel. Higher enthalpies of vaporization in a way, increase the charge cooling effect for the fuel and improve volumetric efficiency. However, charge cooling and lower boiling point of ethanol that promote less production of soot can sometimes play the opposite role and have competing effect which could lead to the formation of soot (Leach et al. 2018).

In general, addition of ethanol helps with soot reduction. However, some studies have found that under certain conditions, ethanol blended with gasoline can increase particulate emissions, while other studies have shown a reduction in PN emissions with increasing levels of ethanol. Thus, there is still a need for clear distinction of points where presence of oxygen in fuel can help reduce soot formation. After several attempts made to link the fuel composition and particulate emissions, the Honda Particle Matter Index (PMI) has shown a very good correlation with emissions for gasoline engines (Wittmann and Menger 2017). Researchers are still searching for such an index to provide a robust prediction to PN emission from a gasoline fuel blend. However, PMI is still used for comparative purposes (Bock et al. 2019).

7.3 Impact on PN

Alternate fuels are oxygenated fuel blends, having a great potential to reduce well-to-wheel CO_2 emissions from vehicles. Ethanol is the most commonly added oxygenate component to gasoline; other oxygenates include alcohols such as methanol, butanol and ethers such as methyl tert-butyl ether (MTBE), ethyl tert-butyl ether (ETBE) formed out of etherification of respective alcohols. E5 with 5% (v/v) ethanol blended in gasoline is everywhere in Europe, with E10 and E15 prevailing in the USA; E85 and E100 are also available, although requires vehicles to acquire special adaptation.

Compared to pure gasoline, oxygenated fuels are found to have higher vapour pressures, significantly higher heat of vaporization, and significantly lower LHVs. These characteristics most likely affect the amounts of fuel injected into the cylinder. Thus, also affecting the spray evaporation once after the fuel has been injected. These affected phenomena in turn result in higher or lower PN depending on engine operating conditions. Due to the presence of the –OH bond in almost all oxygenates, it increases the reactivity towards oxidation of soot precursors, which reduce PN emissions.
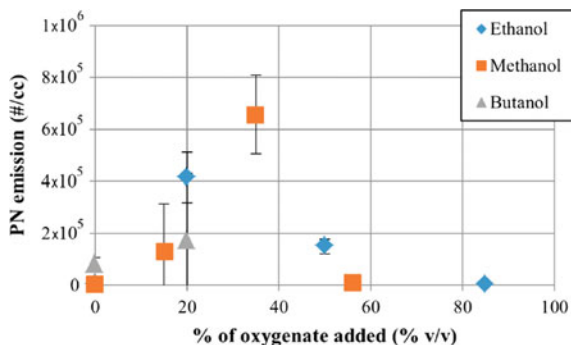
What makes alcohols such great oxygenates that are commonly available these days? Some factors include:

(a) they can be produced from renewable feedstocks (Bae and Kim 2017),
(b) have low water solubility, posing less impact to our water supply,
(c) can be blended with gasoline and burned directly as a neat fuel, and
(d) reduces carbon monoxide emissions forcing leaner combustion than pure gasoline (Fig. 7.1).

7.3.1 Effect of Ethanol on PN

Since, ethanol is produced from renewable sources, most of the times recycled, ethanol utilization doesn't contribute to possible global warming and pollution

Fig. 7.1 PN emissions from a single cylinder optical engine for fuel blends with pure components having varying levels of oxygenates (Leach et al. 2013)

(Wyman and Hinman 1990). Hence, making ethanol a sustainable drop-in fuel for spark ignition engines.

Using ethanol to reduce PN has already been established in PFI engines reduces PN. However, studies show mixed behavior in GDI engines, i.e., adding ethanol can both increase and decrease. As in the case of GDI, quality of combustion and engine operating conditions are deemed important for PN. Liquid fuel impingement on cylinder walls, valves and piston is one of the major causes of particulate formation, and it is rather prevalent at cold start and transients. With ethanol blends, spray formation is relatively challenging which may lead to higher PN compared to gasoline. However, in case where impingement can be compensated by time and energy for relatively better mixture formation, PN reduces.

Once, the level of blended ethanol increases there is a decrease in PN emissions reported. The presence and dominance of the chemically bonded oxygen and much diluted aromatics, there is a reduction in formation of PAHs, soot precursors which in turn reduces soot. However, recently Burke et al. (2017) found that high levels of ethanol can stratify the aromatics within the evaporated mixture and lead to higher PN although certain amount of dilution of aromatics in the fuel with blended ethanol.

Some investigations with ethanol blended with gasoline include Storey et al. (2010) who used E10 and E20 and measured reduced PN from GDI engine over FTP75 and US06 cycle. Zhang et al. (2014) studied the impact E10 and E20 on PN and found that the PN before the catalyst (TWCs) decreased from a GDI engine, while some others reported contrary results. In general, ethanol reduces PN emissions at low and part load conditions. However, in some cases, liquid fuel impingement arises, then ethanol generates more PN emissions as compared to gasoline. This increase in PN may be attributed to the higher heat of vaporization of ethanol.

7.3.2 Effect of Methanol on PN

Sometimes, methanol can be used instead of ethanol as a blend-in fuel with its lower costs of production compared to ethanol. Using methanol is not as common as

ethanol, however in China one can find M100 (100% methanol) and is widely used in their transportation. Like ethanol, methanol has a lower volumetric energy density and higher RON compared to gasoline.

Following its predecessor, methanol, like ethanol, when blended with gasoline has similar effect on PN. One of such effect from methanol is that it promotes fuel evaporation by reducing the final boiling point of the fuel that helps in reducing PN. Also, there is increased heat of vaporization and high volatility which may cause poorer mixtures leading to higher PN. In a study, Qin et al (2014) investigated the impact of gasoline, 100% methanol, and other combinations of methanol-gasoline blends and found that with increase of methanol concentration in gasoline, PN emissions decreased significantly. As expected, neat methanol produced even fewer PN compared to gasoline. Also supported by another study that reported compared to gasoline, methanol blends (M15, M25, and M40) reduced PN (Turner et al. 2013). However, studies like Mohd Murad et al. (2016) reported that M15 does not consistently lower PN from gasoline engines. There is a recent interest in mixed blends of gasoline, ethanol and methanol.

7.3.3   Effect of Butanol on PN

Compared to ethanol and methanol, butanol is a higher alcohol containing four-carbon (C4) molecules (Jin et al. 2011). Butanol has higher energy density among the mentioned alcohols, smaller latent heat of vaporization and is comparatively less corrosive. Both *n*-butanol and isobutanol isomers are commonly used as blend-ins for gasoline. Butanol, having higher energy density among other benefits compared to other alcohol blend-ins is now being considered as the next major oxygenate to blend-in with gasoline. Having higher energy density shows promise towards minimal increase in fuel consumption as opposed to its competitors. *N*-butanol is also produced from a fermentation process. From the recent research on the effect of butanol on PN, the trend reported is similar to ethanol which showed a modest increase in PN with butanol levels (Jin et al. 2011; Tao et al. 2014).

7.4   Conclusions

Particulate matter emissions from GDI engines comprise of complex mix of volatile and solid components containing soot, organic carbon and hydrocarbons. Nucleation mode (<50 nm) particles have often been considered as volatiles, but recently studies have reported to find solid particles in nucleation mode as well. Accumulation mode (50–200 nm) particles include black carbon, carbonaceous soot particles with a rudimentary carbon structure and adsorbed volatiles.

In general, homogeneous operation in GDI engines have fully vaporized fuel-air mixture and give low levels of PN compared to other charge compositions. Any

diffusion flames caused by liquid fuel remains at ignition, particularly on combustion chamber surfaces, leads to PN, also known as pool fire. Many injection strategies have been developed and investigated addressing such liquid fuel impingement. This phenomenon is also prevalent at cold starts with cold conditions inside the cylinder.

Type of fuel is very essential to engine-out PN emissions. In general, effect of fuel is often masked by other dominating engine operating parameters. It has been made possible to compare the effect of fuel while running at stoichiometric operation. Aromatics, the most commonly PN attributed fuel property typically promote formations of PAHs, soot precursors which in turn increases PN. Some other fuel properties do influence PN but are dependent on engine design and load point.

Adding oxygenated to a fuel dilutes the aromatic content of the fuel, theoretically leading to lower PN compared to the fuel in its pure form. Since aromatics is not the only influencing property of a fuel towards PN, there is a mixed trend that is reported for oxygenated blends. Although, lower levels of oxygenates in the blends show promise for reducing PN at lower loads, they fail to reduce PN at higher loads. Coming to higher levels of oxygenates, overall the PN emitted from the GDI engines have reduced almost to 0 (i.e., not detectable by measurement instrument) in some cases.

PN from GDI engines still stands as one of the complex physiochemical phenomena with many parameters and variables affecting the engine out performance. However, with increased levels of understanding now available of PN formation in GDI engines from research it is possible to take measures to reduce PN and its formation. Certainly, this chapter has only focused on engine-out PN emissions, many aftertreatment devices, such as gasoline particulate filters are available, and are only delivering better performance with time.

References

Bae C, Kim J (2017) Alternative fuels for internal combustion engines. Proc Combust Inst 36(3):3389–3413

Bernstein JA et al (2004) Health effects of air pollution. J Allergy Clin Immunol

Bock N, Jeon J, Kittelson D, Northrop W (2019) Effects of fuel properties on particle number and particle mass emissions from lean and stoichiometric gasoline direct injection engine operation. SAE Tech Pap Ser 1:1–13

Burke SC, Ratcliff M, McCormick R, Rhoads R, Windom B (2017) Distillation-based droplet modeling of non-ideal oxygenated gasoline blends: investigating the role of droplet evaporation on PM emissions. SAE Int J Fuels Lubr 10(1):69–81

Cassee FR et al (2011) Exposure, health and ecological effects review of engineered nanoscale cerium and cerium oxide associated with its use as a fuel additive. Crit Rev Toxicol 41(3):213–229

Cataluña R, da Silva R, de Menezes EW, Ivanov RB (2008) Specific consumption of liquid biofuels in gasoline fuelled engines. Fuel 87(15–16):3362–3368

Chan TW, Meloche E, Kubsh J, Brezny R (2014) Black carbon emissions in gasoline exhaust and a reduction alternative with a gasoline particulate filter. Environ Sci Technol 48(10):6027–6034

Claxton LD (2015) The history, genotoxicity, and carcinogenicity of carbon-based fuels and their emissions: part 5. Summary, comparisons, and conclusions. Mutat Res Rev Mutat Res 763:103–147

Eastwood P (2008) Particulate emissions from vehicles

Elfasakhany A (2016) Performance and emissions analysis on using acetone–gasoline fuel blends in spark-ignition engine. Eng Sci Technol Int J 19(3):1224–1232

European Committee for Standardization (2008) European standard EN 228

Gogoi B et al (2015) Effects of 2,5-dimethylfuran addition to diesel on soot nanostructures and reactivity. Fuel 159:766–775

Gu X, Huang Z, Cai J, Gong J, Wu X, Lee CF (2012) Emission characteristics of a spark-ignition engine fuelled with gasoline-n-butanol blends in combination with EGR. Fuel 93(2012):611–617

Guerrero Peña GDJ, Hammid YA, Raj A, Stephen S, Anjana T, Balasubramanian V (2018) On the characteristics and reactivity of soot particles from ethanol-gasoline and 2,5-dimethylfuran-gasoline blends. Fuel 222:42–55

He X, Ratcliff MA, Zigler BT (2012) Effects of gasoline direct injection engine operating parameters on particle number emissions. Energy Fuels 26(4):2014–2027

Heywood JB (1988) Internal combustion engine fundamentals. McGraw Hill, New York, NY, USA

Indicator Assessment (2015) Emissions of primary particles and secondary particulate matter precursors. European Environment Agency

Jin C, Yao M, Liu H, Lee CFF, Ji J (2011) Progress in the production and application of *n*-butanol as a biofuel. Renew Sustain Energy Rev 15(2011):4080–4106

Johnson T, Joshi A (2017) Review of vehicle engine efficiency and emissions. SAE technical papers 2017-01-0907

Leach F, Stone R, Richardson D (2013) The influence of fuel properties on particulate number emissions from a direct injection spark ignition engine

Leach FCP et al (2018) The effect of oxygenate fuels on PN emissions from a highly boosted GDI engine. Fuel 225:277–286

Lemaire R, Therssen E, Desgroux P (2010) Effect of ethanol addition in gasoline and gasoline-surrogate on soot formation in turbulent spray flames. Fuel 89(12):3952–3959

Lemaire R, Lapalme D, Seers P (2015) Analysis of the sooting propensity of C-4 and C-5 oxygenates: comparison of sooting indexes issued from laser-based experiments and group additivity approaches. Combust Flame 162(9):3140–3155

Liu Y et al (2015) Particulate matter, gaseous and particulate polycyclic aromatic hydrocarbons (PAHs) in an urban traffic tunnel of China: emission from on-road vehicles and gas-particle partitioning. Chemosphere 134:52–59

Maione M et al (2016) Air quality and climate change: designing new win-win policies for Europe. Environ Sci Policy 65:48–57

Masum BM, Masjuki HH, Kalam MA, Rizwanul Fattah IM, Palash SM, Abedin MJ (2013) Effect of ethanol-gasoline blend on NO_x emission in SI engine. Renew Sustain Energy Rev 24:209–222

Mohd Murad SH, Camm J, Davy M, Stone R, Richardson D (2016) Spray behaviour and particulate matter emissions with M15 methanol/gasoline blends in a GDI engine. SAE International

Myung CL, Park S, Myung CL, Park S (2012) Exhaust nanoparticle emissions from internal combustion engines: a review. Int J Automot Technol 13(1):9–22

Qin J, Li X, Pei Y (2014) Effects of combustion parameters and lubricating oil on particulate matter emissions from a turbo-charged GDI engine fueled with methanol/gasoline blends. SAE International

Raza M, Chen L, Leach F, Ding S (2018) A review of particulate number (PN) emissions from gasoline direct injection (GDI) engines and their control techniques. Energies 11

Saliba G et al (2017) Comparison of gasoline direct-injection (GDI) and port fuel injection (PFI) vehicle emissions: emission certification standards, cold-start, secondary organic aerosol formation potential, and potential climate impacts. Environ Sci Technol 51(11):6542–6552looseness-1

Schifter I, González U, González-Macías C (2016) Effects of ethanol, ethyl-tert-butyl ether and dimethyl-carbonate blends with gasoline on SI engine. Fuel 183:253–261

Sharma N, Agarwal AK (2018) Gasoline direct injection engines and particulate emissions, pp 87–105

Storey JM, Barone T, Norman K, Lewis S (2010) Ethanol blend effects on direct injection spark-ignition gasoline vehicle particulate matter emissions. SAE Int J Fuels Lubr 3(2):650–659

Tanaka K et al (2015) Ignition characteristics of 2,5-dimethylfuran compared with gasoline and ethanol. SAE Int J Engines 9(1):39–46

Tao L et al (2014) Techno-economic analysis and life-cycle assessment of cellulosic isobutanol and comparison with cellulosic ethanol and *n*-butanol. Biofuels Bioprod Biorefin 8(1):30–48

Turner JWG, Pearson RJ, Dekker E, Iosefa B, Johansson K, ac Bergström K (2013) Extending the role of alcohols as transport fuels using iso-stoichiometric ternary blends of gasoline, ethanol and methanol. Appl Energy

Überall A, Otte R, Eilts P, Krahl J (2015) A literature research about particle emissions from engines with direct gasoline injection and the potential to reduce these emissions. Fuel 147(2015):203–207

Wang X et al (2015) Evaluation on toxic reduction and fuel economy of a gasoline direct injection-(GDI-)powered passenger car fueled with methanol-gasoline blends with various substitution ratios. Appl Energy 157:134–143

Wittmann J-H, Menger L (2017) Novel index for evaluation of particle formation tendencies of fuels with different chemical compositions. SAE Int J Fuels Lubr 10(3):690–697

Wyman CE, Hinman ND (1990) Ethanol. Appl Biochem Biotechnol 24(1):735–753

Zhang Z, Wang T, Jia M, Wei Q, Meng X, Shu G (2014) Combustion and particle number emissions of a direct injection spark ignition engine operating on ethanol/gasoline and *n*-butanol/gasoline blends with exhaust gas recirculation. Fuel 130(2014):177–188

Zimmerman N, Wang JM, Jeong CH, Wallace JS, Evans GJ (2016) Assessing the climate trade-offs of gasoline direct injection engines. Environ Sci Technol 50(15):8385–8392

Chapter 8
Ozone Added Spark Assisted Compression Ignition

Sayan Biswas and Isaac Ekoto

Abstract The mixed-mode engine combustion strategy where some combination of spark-assisted compression ignition (SACI) and pure advanced compression ignition (ACI) are used at part-load operation with exclusive spark-ignited (SI) combustion used for high power-density conditions has the potential to increase efficiency and decrease pollutant emissions. However, controlling combustion and switching between different modes of mixed-mode operation is inherently challenging. This chapter proposes to use ozone (O_3)—a powerful oxidizing chemical agent—to maintain stable and knock-free combustion across the load-speed map. The impact of 0–50 ppm intake seeded O_3 on performance, and emissions characteristics was explored in a single-cylinder, optically accessible, research engine operated under lean SACI conditions with two different in-cylinder conditions, (1) partially stratified (double injection—early and late injection) and (2) homogeneous (single early injection). O_3 addition promotes end gas auto-ignition by enhancing the gasoline reactivity, which thereby enabled stable auto-ignition with less initial charge heating. Hence O_3 addition could stabilize engine combustion relative to similar conditions without O_3. The addition of ozone has been found to reduce specific fuel consumption by up to 9%, with an overall improvement in the combustion stability compared to similar conditions without O_3. For the lowest loads, the effect of adding O_3 was most substantial. Specific NO_x emissions also dropped by up to 30% because a higher fraction of the fuel burned was due to auto-ignition of the end gas. Measurement of in-cylinder O_3 concentrations using UV light absorption technique showed that rapid decomposition of O_3 into molecular (O_2) and atomic oxygen (O) concurred with the onset of low-temperature heat release (LTHR). The newly formed O from O_3 decomposition initiated fuel hydrogen abstraction reactions responsible for early onset of LTHR. At the beginning of high-temperature heat release (HTHR), end gas temperatures ranged from 840 to 900 K, which is about 200 K cooler than those found in previous studies where intake charge heating or extensive retained residuals were used to preheat the charge. An included analysis indicates that in order to achieve optimal auto-ignition in our engine, the spark deflagration was needed to add

S. Biswas (✉) · I. Ekoto
Sandia National Laboratories, Livermore, CA 94550, USA
e-mail: sayanbiswas@ieee.org

159

10–40 J of additional thermal energy to the end gas. We have leveraged these results to broaden our understanding of O_3 addition to different load-speed conditions that we believe can facilitate multiple modes (SI, ACI, SACI, etc.) of combustion.

Keywords O_3 addition · Spark assisted compression ignition (SACI) · Low-temperature heat release (LTHR) · Homogeneous versus stratified combustion · Advanced plasma ignition

Definitions/Abbreviations

ϕ	Equivalence ratio
σ_{O_3}	Ozone absorption cross-section
ACI	Advanced compression ignition
AHRR	Apparent heat release rate
B	Bore diameter
BDI	Barrier discharge igniter
CA	Crank angle referenced to main TDC
CA50	50% cumulative burn angle
CO	Carbon monoxide
CO_2	Carbon dioxide
CoV	Coefficient of variation
C_p	Constant pressure specific heat
DI	Direct injection
E	Energy
EGR	Exhaust gas recirculation
EI	Emission index
EVC/EVO	Exhaust valve close/open
DI	Direct injection
GCI	Gasoline compression ignition
H/C	Hydrogen-to-carbon ratio
H_2O	Water
HO_2	Hydroperoxyl
H_2O_2	Hydrogen peroxide
HC	Hydrocarbon
HTHR	High-temperature heat release
I_{ref}	Reference intensity
IMEP	Indicated mean effective pressure
ISFC	Indicated specific fuel consumption
ITE	Indicated thermal efficiency
ITHR	Intermediate-temperature heat release
IVC/IVO	Intake valve close/open
LHV	Lower heating value
LTC	Low-temperature combustion

LTHR	Low-temperature heat release
LTP	Low-temperature plasma
m	Mass
MBT	Maximum brake torque
N_2	Nitrogen
NO	Nitric oxide
NO_2	Nitrogen dioxide
NO_x	Nitrogen oxide
NVO	Negative valve overlap
O	Atomic oxygen
O_2	Molecular oxygen
O_3	Ozone
OH	Hydroxyl
OS	Octane sensitivity
P	Pressure
PID	Proportional, Integral, Derivative
PM	Particulate matter
PMT	Photomultiplier tube
ppm	Parts per million
PVO	Positive valve overlap
R	Alkyl radical
R	Gas constant
RGF	Residual gas fraction
RI	Ringing intensity
ROOH	Alkylhydroperoxide
RON	Research octane number
rpm	Revolutions per minute
SACI	Spark assisted compression ignition
SI	Spark ignition
SOI	Start of injection
ST	Spark timing
T	Temperature
T10/T50/T90	10, 50, and 90% boiling points
TDC	Top dead center
TPI	Transient plasma ignition
UHC	Unburned hydrocarbon
UV	Ultraviolet

Subscripts

1, **2**	First injection, second injection
b	Burned
bulk	Bulk/Averaged

exh	Exhaust
f	Fuel
int	Intake
r	Residual
ref	Reference
u	Unburned

8.1 Introduction

Conventional compression-ignition (CI) engines provide a plausible solution to light-duty vehicle manufacturers due to their improved efficiency operating at higher compression ratio compared to spark-ignition (SI) gasoline engines (Dec 2009). However, controlling the emissions of nitrogen oxide (NO_x) and particulate matter (PM) are the biggest challenges for CI engines (Stone 1999; Biswas 2018). As emission standards continue to become stricter, future engine control strategies will be a combination of combustion optimization, fuel refinement, and aggressive exhaust after-treatment technologies—all of which add significant cost and complexity to the engine architecture (United States, Environmental Protection Agency, Office of Transportation and Air Quality 2012; Graham et al. 2009; United States Environmental Protection Agency, Office of Policy and Evaluation 2016; Biswas et al. 2016; Biswas and Qiao 2016). On the other hand, even though homogeneous charge compression ignition (HCCI) combustion offers high thermal efficiency and ultra-low NO_x and PM emissions (Stanglmaier and Roberts 1999; Christensen et al. 1997; Weinrotter et al. 2005; Srivastava et al. 2009), it is limited by a lack of a direct control mechanism for ignition timing and combustion phasing (Zhao et al. 2003). One way to address this control issue is to explore mixing controlled advanced compression ignition (ACI) strategies such as gasoline compression injection (GCI), and spark-assisted compression ignition (SACI) that use some amount of bulk-gas auto-ignition of gasoline-like fuels. Within controlled laboratory environments, mixing controlled ACI strategies have demonstrated the efficiency benefits of CI and the low engine-out emissions of SI (Saxena and Bedoya 2013).

The main challenge for ACI approaches is to keep stable and knock-free operation throughout the entire load-speed map. Poor combustion stability at low load conditions can be improved by tailoring the charge reactivity through some combination of injection strategy, intake heating, excessive usage of retained residual, charge motion, and piston bowl design (Fitzgerald and Steeper 2010; Kolodziej et al. 2015; Wolk et al. 2016a, b). These solutions for improved stability come at the cost of increased heat transfer losses (Ekoto et al. 2017) and more complex valve train requirements. For high load conditions, heavy use of exhaust gas recirculation (EGR) is required to slow heat release rates (Dec et al. 2015; Dernotte et al. 2015) and to reduce engine knock propensity, which then requires heavy intake boosting to meet load demands. Consequently, expansion efficiency is reduced, and mechanical losses

are increased due to the higher peak cylinder pressure requirements. Each of these alternatives contributes to the price and complexity that should have been avoided by using ACI.

A practical near-term alternative to ACI engine combustion is the so-called dual- or mixed-mode combustion strategy, where the idea is to run the engine in SI mode for high power-density conditions (Lawler and Filipi 2013; Manofsky et al. 2011) and in SACI mode at low and part load to keep up efficiency. The SACI strategy differs from conventional SI engines in that elevated unburned gas temperatures induced by compression heating from an expanding spark initiated flame kernel (Persson et al. 2007; Reuss et al. 2008; Lavoie et al. 2010; Benajes et al. 2013, 2014; Olesky et al. 2013, 2014, 2015; Ortiz-Soto et al. 2014; Middleton et al. 2015) are utilized to promote end gas auto-ignition. Moderate to high EGR dilution is used to limit adiabatic flame temperatures and heat release rates. Turbo- and super-charging can recover part of the power density losses due to EGR dilution at high load results peak cylinder pressures very near to knocking conditions. Although SACI benefits from higher compression ratios, high-power-density SI conditions dictate that compression ratios should be set to below 14 to avoid knock. This is significantly below 16+ compression ratios commonly employed for conventional ACI. Therefore, some combination of mixture stratification and charge heating becomes unavoidable to ensure enhanced gasoline reactivity sufficient for end gas auto-ignition.

However, charge reactivity can be increased by seeding a small amount (less than 50 ppm) of Ozone (O_3)—a powerful oxidizing chemical agent to the intake charge. Compared to other additives, O_3 is a particularly promising candidate that can be generated onboard via increasingly inexpensive and compact O_3 generators or even by low-temperature plasma discharges from advanced ignition systems (Uddi et al. 2009). Thus, O_3 addition enables stable auto-ignition with lower intake heating or complex valve train adjustments (Masurier et al. 2013, 2015a, b; Truedsson et al. 2017; Pinazzi and Foucher 2017; Ekoto and Foucher 2018). The idea of adding O_3 to improve fuel reactivity is not new (Ombrello et al. 2010; Zhang et al. 2016). Masurier et al. (2015b) compared various oxidizing species such as nitric oxide, nitrogen oxide, and O_3 affecting engine performance and O_3 found to be the most effective additive among them. Truedsson et al. (2017) demonstrated that O_3 addition could facilitate ignition of high octane rating fuels blended with ethanol that are otherwise difficult to ignite in HCCI combustion.

Ozone-assisted oxidation—'ozonolysis,' has lately drawn considerable interest in low-temperature combustion research due to the increase of plasma-assisted combustion methods and chemically controlled engine designs. Rousso et al. (2018) studied ethylene oxidation in a jet-stirred reactor and observed ozonolysis below 600 K. However, the O_3 decomposition rate increases rapidly above 600 K. Above 600 K temperature, O_3 rapidly decomposes into molecular and atomic oxygen (O) (Masurier et al. 2013; Depcik et al. 2014). The O radical then initiates heat release through fuel hydrogen (H) abstraction reaction to form alkyl (R) and hydroxyl (OH) radicals (Ekoto and Foucher 2018; Smekhov et al. 2007). The OH radical further reacts with fuel and continues the H abstraction reaction. This initiates low-temperature heat release (LTHR) pathways that occurs at temperatures below ~800 K. Furthermore, R

combining with molecular oxygen (O_2) forms peroxy radicals (RO_2). Then RO_2 participates in ongoing fuel H abstraction reaction through $RO_2 + RH \rightarrow ROOH + R$. The breakdown of alkyl hydroperoxide (ROOH) into alkyloxy radical (RO) and OH then becomes a sustainable source of LTHR radicals (Zádor et al. 2011). These early LTHR reactions can progress combustion phasing by more than 20 crank angles (CA) depending on the initial O_3 concentrations.

In this chapter, the effect of intake seeded O_3 was investigated as a way to replace charge pre-heating for stable lean SACI operation with two different injection strategies, (1) Partially stratified: double injection—early (75–90% fuel) and late DI (10–25% fuel), and (2) Homogeneous: single early direct injection (DI). Experiments have been carried out in an optically accessible single-cylinder spray-guided research engine. For the partially stratified double injection strategy, O_3 concentrations required to achieve stable combustion were lower at between 30 and 34 ppm. Low to moderate engine loads of between 1.5 and 5.5 bar IMEP and speeds of between 800 and 1600 rpm were examined. For all single injection homogeneous conditions, moderate engine loads of between 4 and 5 bar indicated mean effective pressure (IMEP) and speeds of between 800 and 1400 revolution per minute (rpm) were examined. O_3 concentrations were set at 50 ppm—the peak attainable concentration at the highest 1400 rpm engine speed assessed with the current O_3 generator. Note that the O_3 concentration was reduced from 50 to 31 ppm for a single low speed and high intake temperature due to excessive knocking with higher O_3 concentration. For both fueling strategies, a naturally aspired intake pressure was maintained, with internal residual gas fractions (RGF) between 10 and 20% achieved by combining positive valve overlap (PVO) with moderate exhaust backpressures. For the homogeneous strategy intake temperatures were swept between 42 and 80 °C, while for partially stratified strategy a constant 42 °C intake temperature was maintained for all conditions. Each load/speed operating condition was optimized to maximize engine performance while maintaining NO_x emissions and ringing intensity (RI) below 5 g/kg-fuel and 1 MW/m^2 respectively. Performance and engine-out emissions measurements were complemented by CA resolved O_3 measurements performed via ultraviolet (UV) light absorption and single-zone chemical kinetic modeling of end gas LTHR.

8.2 Experimental Methods

8.2.1 Sandia Single-Cylinder Research Engine

All engine testing was conducted in a single-cylinder engine that featured a Bowditch piston, four-valve pent-roof, spray-guided injection, and optical access as shown schematically in Fig. 8.1. The optical access into the engine cylinder was provided via diametrically opposed wall-mounted quartz windows (12.7 mm aperture). Research-grade RD587 gasoline was directly injected into the cylinder via a centrally located
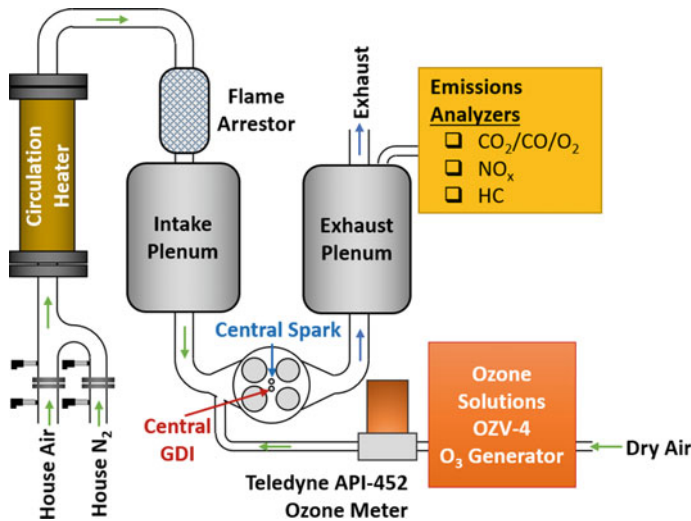
Fig. 8.1 Schematic of the Sandia light-duty optical gasoline engine, gas supply system, O_3 generator, and emissions measurement setup

Bosch HDEV1.2 injector with eight uniformly distributed 125 μm diameter nozzles forming a 60° umbrella angle. The ignition system consisted of a long-reach resistor type spark plug (NGK 12 mm nominal thread), and a Bosch 93 mJ ignition coil. Intake and exhaust cams were set to create a positive valve overlap (PVO) of 34 crank angles at TDC. An engine dynamometer was used to vary engine speeds. An optical encoder (BEI sensors) with 0.1 CA resolution was used to locate the crank angle position. Intake port and runner designs are optimized to limit swirl and tumble flows to reduce heat transfer losses via in-cylinder turbulence. An Aquatherm heat exchanger was used to maintain a constant cylinder wall temperature to 90 °C.

A Tescom ER5000 PID (Proportional, Integral, Derivative) pneumatic actuator was used to precisely regulate the intake air supply. In both the intake and exhaust runners, pressure and temperature were measured. The exhaust runner was heated using wire-wrapped resistive heaters and fiberglass insulation to minimize the heat transfer losses. A Chromalox circulation heater located between the intake plenum and air supply was used to heat the intake charge up to 80 °C. A piezoelectric pressure sensor (Kistler 6125A) was used to measure cylinder pressure history. Heat release and load in every cycle were estimated from the in-cylinder pressure trace.

A two-zone pressure-based heat release assessment was conducted where the cylinder volume was divided into burned and unburned regimes so that unburned temperatures could be estimated at the onset of end gas LTHR and HTHR. The onset of LTHR was estimated from apparent heat release rate (AHRR) profile difference with and without O_3 addition operating at the identical conditions. In the burned gas region, the two-zone model presumed complete combustion of the fuel. The burned gas temperature was calculated from the heat of combustion of the consumed fuel.

Since major portion of heat release was from the end gas auto-ignition, a modified Woschni correlation for ACI combustion (Chang et al. 2004) served best to estimate the heat loss.

Ozone generated by an external O_3 generator (Ozone Solutions OZV-4) directly seeded into the intake runner. The O_3 concentration was varied by changing the amount of dry air using a mass flow controller (MKS GE50) passing through the O_3 generator. An O_3 meter (Teledyne API 452) was used to monitor the O_3 concentration out of the O_3 generator. Table 8.1 summarizes significant details on engine geometry, valve timings, and operating conditions, and fueling strategies.

For all experiments, research-grade RD587 gasoline with a RON of 92.1 and octane sensitivity of 7.3 was used. Table 8.2 summarizes the essential physical and chemical properties of RD587.

Pollutant emissions from the exhaust plenum were sampled for fired cycles using heated sampling lines to minimize condensation of water and fuel. A CAI 600

Table 8.1 Engine specifications and operating conditions

Engine specifications		
Displaced volume (L)	0.551	
Bore/stroke/connecting rod (mm)	86/95.1/166.7	
Geometric compression ratio	13:1	
Intake valve open/close (CA)[a]	343/−145	
Exhaust valve open/close (CA)[a]	160/−343	
Valve lift (mm)	9.7	
Fuel pressure (bar)	100	
Injector hole number	8	
Injector cone angle (°)	60	
Injector orifice diameter (μm)	125	
Operating conditions		
	Partially stratified	Homogeneous
Intake/exhaust pressure (kPa)	100/105	100/110
Intake temperature (°C)	42	42–80
Intake O_3 concentration (ppm)	0–34	0–50
Engine speed (rpm)	800, 1000, 1200, 1400, 1600	800, 1000, 1200, 1400
Cycle fueling rates (mg/cycle)	8.1–17.9	13.4–16.9
Equivalence ratio	0.27–0.56	0.37–0.45
RGF (%)	10–18	12–20
Spark timing (CA)	−70 to −28	−60 to −55
Main start of injection (SOI) (CA)[a]	−230	−330
2nd injection SOI (CA)	−64 to −36	–
2nd injection fueling fraction (%)	10–25	0

[a]0 CA corresponds to TDC of the compression stroke

Table 8.2 Physical and chemical properties of RD587 gasoline

Liquid density @ 15 °C (g/L)	748
LHV (kJ/mg)	41.9
H/C ratio	1.972
O/C ratio	0.033
Research octane number	92.1
Octane sensitivity	7.3
T10/T50/T90 (°C)	57/98/156

NDIR/Oxygen Multi-Component analyzer was used to measure the dry engine out emission of carbon monoxide (CO), carbon dioxide (CO_2), and oxygen (O_2). A CAI 600 HFID was employed to measure hydrocarbon (HC) emissions. Measurements of CO and HC measurements were used in conjunction along with measured airflow and fuel injection rates to estimate combustion efficiency. A CAI 600 HCLD NO/NO_x chemiluminescence analyzer was used to measure oxides of Nitrogen (NO_x).

8.2.2   Partially Stratified Versus Homogeneous SACI

Figure 8.2 illustrates the injection strategies along with the in-cylinder combustion processes for partially stratified and homogeneous conditions. For partially stratified SACI, each cycle featured an early direct injection with a fixed SOI at −230 CA and a late second injection with the SOI timed just after ST. The second injection SOI was varied between −64 and −36 CA. While a greater quantity of fuel 75–90%
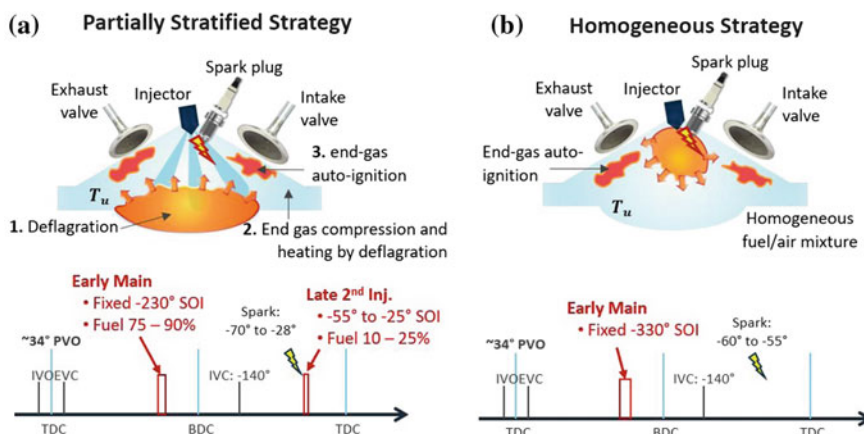
Fig. 8.2 Schematic of in-cylinder combustion processes and cycle events for **a** partially stratified, **b** homogeneous SACI

was injected in the early cycle, a small quantity of late-cycle injection 10–25% helped stabilize the combustion. Two of the fuel sprays straddle the spark plug gap with virtually all of the fuel spray for injections later than -80 CA entering the piston bowl. The initial deflagration is believed to be confined to the piston bowl where mixtures are fuel-rich. Compressive heating by the deflagration then leads the leaner end gas mixtures to transition to auto-ignition. To find the optimum operating points for partially stratified SACI, ST and second injection timing/quantity were adjusted for each operating point until MBT conditions were reached provided that ringing intensity values and engine-out NO_x emissions remained below 1 MW/m^2 and 5 g/kg-fuel respectively.

For homogeneous SACI, an early DI with SOI set at -330 CA created a homogeneous charge in the cylinder. The initial deflagration created by the spark ignition propagated into the cylinder and led to an end gas auto-ignition. The intake seeded 50 ppm O_3 along with the moderate RGF of between 12 and 20% tailored the end gas reactive enough to auto-ignite. However, slight intake heating 42–80 °C was necessary to stabilize combustion. The engine speed was a key factor that affected the O_3 decomposition and end gas auto-ignition behavior. To locate the optimum operating conditions for homogeneous SACI, the fueling rate at maximum brake torque (MBT) spark timing (ST) was adjusted until the minimum achievable load was met, provided that the coefficient of variation (CoV) of IMEP was below 3%, the ringing intensity (RI) was below 1 MW/m^2, and NO_x emissions were below 1 g/kg-fuel.

The intake seeded O_3 concentration (30–34 ppm) for partially stratified SACI was lower than that was required for homogeneous SACI. Note that intake temperature was fixed at 42 °C in partially stratified SACI. Similar to the homogenous SACI, an exhaust pressure of 1.05 bar in conjunction with the use of PVO produced moderate RGF of between 10 and 18%. The engine was motored for approximately 30 s for each experiment with the O_3 generator switched on to accumulate uniform and constant O_3 levels in the intake runner. Using a predefined spark timing, the engine was then fired for about 90 s. The injection quantity and ST were adjusted gradually to the desired set point after the 90-s warm-up period. Once combustion and engine-out emissions readings become steady, a 100-cycle dataset was collected for every operating point. Before the engine was stopped to oil the rings, O_3 generator was switched off and the engine was motored to clear out residual emission in the exhaust runner. This entire process was repeated for the next experimental condition.

8.2.3   In-Cylinder O_3 Measurement

The in-cylinder-averaged O_3 concentrations were estimated using UV light absorption on a CA basis, as shown in Fig. 8.3. This in-cylinder O_3 measurement technique has been discussed in detail in our earlier work (Biswas and Ekoto 2019a, b). Hence a brief description is presented here for the readers' convenience. Partly collimated 250-Watt continuous broadband light generated from a Xenon arc lamp (Spectra physics 66924-250XV) was transmitted through the optical engine into an integrating
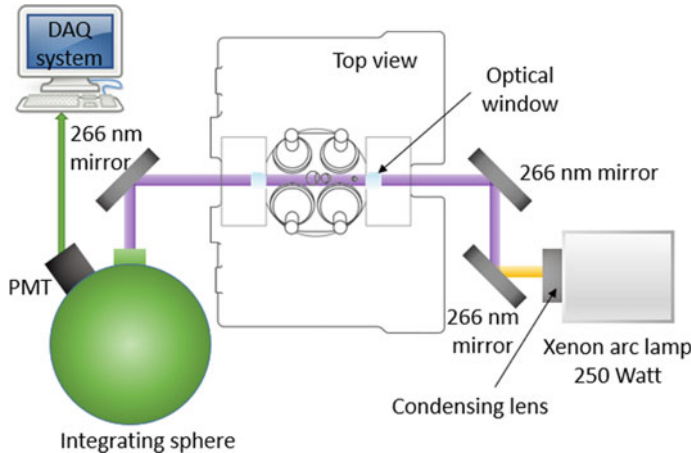
Fig. 8.3 Schematic representation of the O_3 absorption diagnostic

sphere followed by a photomultiplier tube (PMT, Pacific Instruments 3150RF) using several Nd: YAG 4th harmonic laser line mirrors that reflected only the 266 nm light. The absorption cross-section of O_3 (σ_{O_3}) at 266 nm is 9.37×10^{-18} cm^2/molecule (Gorshelev et al. 2014). The optical setup is shown in Fig. 8.3 minimized beam steering effect attributed to the thermal gradients within the combustion chamber. Finally, the Beer-Lambert law was used to calculate the CA resolved O_3 mole fraction, X_{O_3}.

$$X_{O_3} = \frac{k_B T_{bulk}}{p B \sigma_{O_3}} \ln \frac{\mathbb{I}_{ref}}{\mathbb{I}} \qquad (8.1)$$

Here, $\mathbb{I}$ is the light intensity, B is the cylinder bore diameter, T_{bulk} is the in-cylinder bulk-gas temperature, p is the cylinder pressure, and k_B is the Boltzmann constant $(1.381 \times 10^{-23} J/K)$. Based on the recorded cylinder pressure, the bulk gas temperature was estimated assuming isentropic compression.

Three different datasets, namely "background", "reference", and "target", each containing 100 cycles were acquired to estimate the in-cylinder O_3. The "background" dataset accounted for the noise signal coming from the ambient light in the absence of the lamplight. The "target" and "reference" datasets were acquired with and without O_3 addition. Note that only the closed part of the cycle was considered in the O_3 measurement. During O_3 measurement, the fuel was added but the spark was kept inactive to avoid combustion in "reference" and "target" cycles. Enhanced combustion stability with O_3 addition in the "target" cycle would have led to a high amount of residual CO_2 that absorbs 266 nm light (Schulz et al. 2002). Also, the presence of combustion intermediates that absorbs UV light like hydroperoxyl (HO_2) and hydrogen peroxide (H_2O_2) (Ekoto and Foucher 2018; Kijewski and Troe 1971; Molina and Molina 1981) during LTHR and HTHR can differ in "reference" and "target" cycles. Thus, to have a correct O_3 measurement—free from absorption

error by other species, combustion was suppressed by keeping the spark inactive. To compensate for the effect of combustion, the intake temperatures were increased to match the intake valve closing (IVC) temperatures of the corresponding fired cycles.

8.2.4 Single Zone Chemical Model

Chemkin-Pro 0D homogeneous reactor simulations were conducted to assess chemical kinetic pathways responsible for the fuel oxidation with O_3 addition (Ansys 2017). Several experimental parameters were matched or used during simulations to capture the relevant processes related to O_3 decomposition, radical formation, and fuel oxidation. The experimentally measured pressure and unburned gas temperature during the compression stroke were kept constrained throughout the simulation. IVC temperature and species compositions obtained from the experiments were used to initialize the simulation. O_3 oxidation chemistry from Masurier et al. (2013) added to the Lawrence Livermore National Laboratory's gasoline surrogate mechanism (Mehl et al. 2011) that yielded a total of 2028 species and 8636 reactions was used for simulations. A five-component gasoline surrogate (46.6% iso-octane, 17.8% n-heptane, 9.9% ethanol, 6.0% 1-hexene, and 19.7% toluene by liquid volume) was used to match the overall molecular composition and reactivity characteristics of RD587 gasoline (Wolk et al. 2016a).
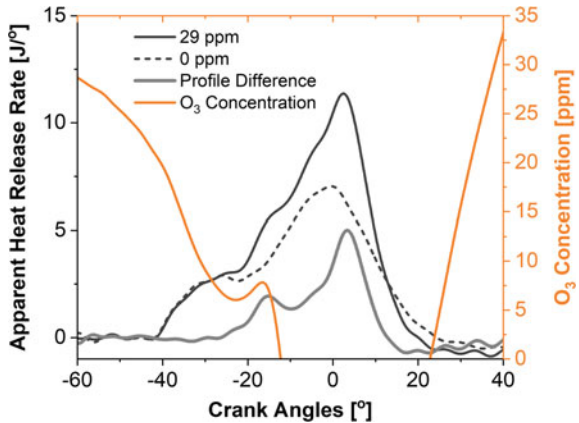
8.3 Results and Discussion

8.3.1 Effect of O_3 on Combustion Performance and Emissions

O_3 addition enabled stable combustion relative to similar conditions without O_3 by promoting end gas reactivity. AHRR profiles are shown in Fig. 8.4 for a baseline 1000 rpm, 2.8 bar IMEP, partially stratified operating condition with and without 29 ppm of added O_3 to showcase the impact of O_3 addition on heat release characteristics. The total fueling rate was 12 mg/cycle, with ~20% of the fuel injected during the second injection. The spark timing was at -54 CA, and the second injection occurred 7 CA later. To investigate the effect of O_3 decomposition on end gas auto-ignition behavior, a measured O_3 profile was plotted in Fig. 8.4 for similar non-fired operating conditions. However, to capture the correct O_3 decomposition rate, the IVC temperatures between fired and non-fired cycles were closely matched.

For both conditions, the first noticeable heat release occurred around -42 CA as the stratified mixture created from the second injection was ignited. The authors speculate that this heat release is the result of a deflagration confined to the piston bowl where the second injection produced rich stratified mixtures. Until -25 CA,

AHRR profiles of with and without O_3 for a 1000 rpm, 2.8 bar IMEP, partially stratified operating condition
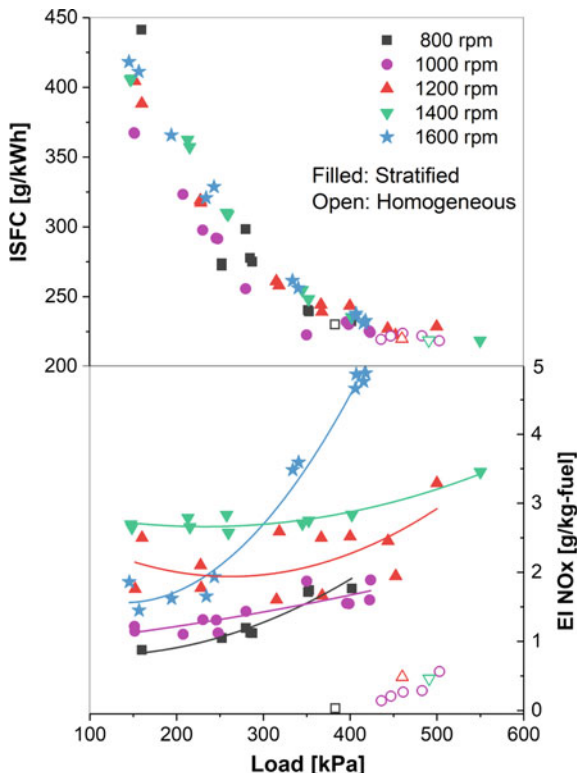

AHRR values remained closely matched for conditions with and without O_3 addition. Beyond this point, the O_3 added AHRR profile increasingly separated from the condition without O_3. The sharp increase in AHRR is not consistent with the consumption of lean end gas mixtures by deflagration alone, suggesting that additional heat release occurred because of auto-ignition of the end gas.

To illustrate more clearly the occurrence of the end gas auto-ignition, the AHRR profile for the condition without O_3 addition has been subtracted from the condition with O_3 addition and is plotted as the 'Profile Difference' in Fig. 8.4. The addition of O_3 resulted in an increase of 31% in total heat release. The profile resembles low-temperature combustion (LTC) auto-ignition, with an LTHR period starting around −25 CA and a larger high-temperature heat release (HTHR) period near TDC. The thermal decomposition of O_3 into O and O_2 began around −60 CA and almost ended with the initiation of LTHR. Secondary absorbance, which was started around −22 CA, was probably from the HO_2 formed during LTHR reactions.

Figure 8.5 plots the indicated specific fuel consumption (ISFC) and NO_x emission index (EI) for a range of engine speeds (800–1600 rpm) as a function of engine load. The O_3 concentrations were fixed at 50 ppm for homogeneous SACI and 30 ppm for partially stratified SACI. For the partially stratified SACI results, the largest declines in ISFC were observed for the lowest engine loads and speeds. Moreover, ISFC data from the homogeneous SACI had a more limited range of achievable loads and speeds similarly collapsed to the same curve. These findings show that there is no obvious punishment with stratified operation due, for instance, to a change in the features of total heat transfer.

In partially stratified SACI, NO_x emissions had a weak positive correlation with increased engine load and a much stronger positive correlation with an increased engine speed for engine speeds of 1400 rpm and lower. These trends reversed for the load sweep of the highest speed (1600 rpm) condition, which had a much stronger dependence on increased engine load. Homogeneous SACI NO_x emissions were

Fig. 8.5 ISFC and NO$_x$ emissions as a function of load at engine speeds of 800–1600 rpm for O$_3$ seeded homogeneous versus partially stratified SACI (Biswas and Ekoto 2019b)

about an order of magnitude lower than comparable partially stratified SACI conditions, probably due to the significant reduction of high-temperature deflagration in fuel-rich stratified regions existed in the piston bowl.

Contour maps of indicated thermal efficiency (ITE), combustion efficiency, coefficient of variation (COV) of IMEP, and 50% burn angle (CA50) are plotted in Fig. 8.6 as a function of engine speed and load for partially stratified SACI. For the range of operating conditions examined, ITE values ranged from 20 to 40%. As anticipated, enhanced ITE was heavily associated with enhanced load for a specified engine speed due to a combination of greater combustion efficiency and more optimal phasing of combustion which reduced cycle-to-cycle variability. Increased ITE for a given load was also observed for a decrease in engine speeds resulting solely from higher combustion efficiency. Longer cycle durations permitted more time for lean mixture combustion to occur for the slower engine speeds.

Similar contour maps of engine-out NO$_x$, unburned hydrocarbon (UHC), and CO emissions are plotted in Fig. 8.7. Although the NO$_x$ emission limit was 5 g/kg-fuel, only the highest load and speed conditions (5+ bar IMEP and 1400+ rpm) approached this limit. For higher loads and lower engine speeds, UHC and CO emissions were typically low, which is unsurprising considering that these are the regions where
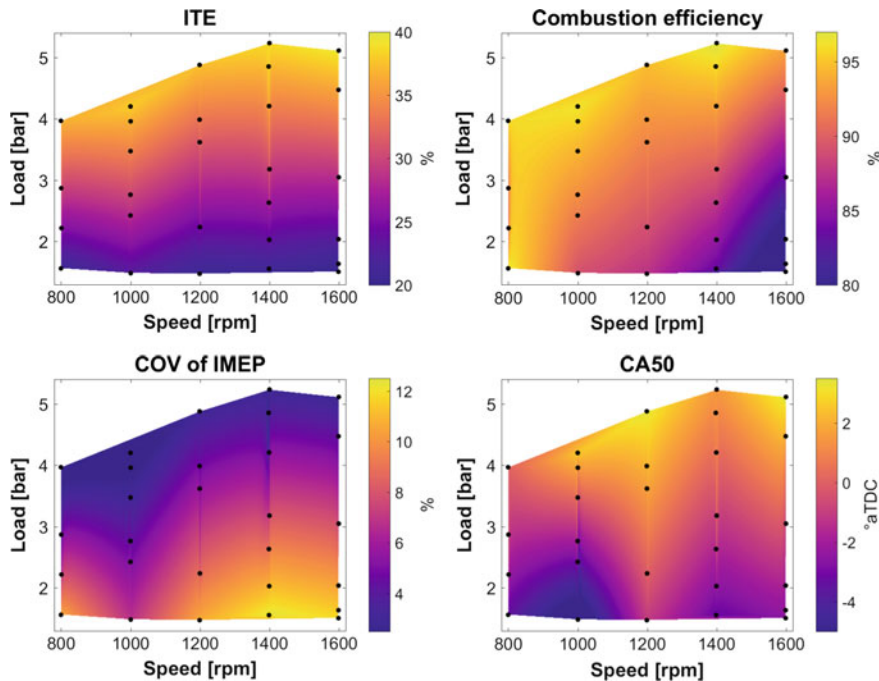
Fig. 8.6 Contour maps of ITE, combustion efficiency, CoV of IMEP, and CA50 from partially stratified SACI for a range of engine speeds (800–1600 rpm) and loads (1.5–5.5 bar IMEP)

combustion efficiency was high. As loads dropped and engine speeds increased, UHC emissions increased steadily. While CO emissions likewise increased with decreased engine load, peak values occurred at lower speeds due to a substantial conversion of hydrocarbons to CO, but the final oxidation step of CO to CO_2 being rate limited.

8.3.2 Intake Temperature and Engine Speed on O_3 Decomposition

To examine the impact of intake temperature on O_3 decomposition kinetics, measured O_3 profiles with IVC temperatures of 361 and 384 K are plotted in Fig. 8.8a alongside AHRR profiles zoomed in on the LTHR period. O_3 profiles are plotted on a semi-log scale to more clearly highlight when rapid thermal decomposition into O and O_2 occurs. Note that there was increased absorbance starting around −25 °aTDC that was not present in the reference datasets. As stated in the introduction, this increased absorbance was likely from HO_2 formed during LTHR reactions. Although the spurious absorbance was not desired, it nonetheless is a convenient marker of
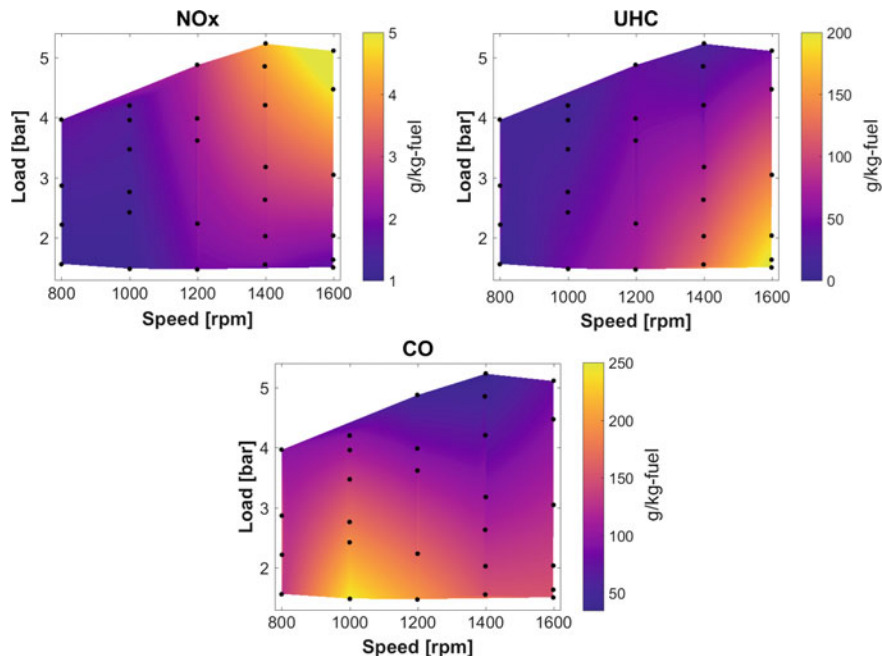
Fig. 8.7 Contour maps of engine-out NO_x, UHC, and CO emissions from partially stratified SACI for a range of engine speeds (800–1600 rpm) and loads (1.5–5.5 bar IMEP)

LTHR onset. For both profiles, rapid O_3 thermal decomposition started around $-40\,°aTDC$, and was nearly complete by $-20\,°aTDC$. Thermal O_3 decomposition for the higher IVC temperature condition (384 K) concluded just before the appearance of LTHR for the fired conditions with the highest intake temperature (i.e., 70 and 80 °C).

Figure 8.8b shows the in-cylinder O_3 concentration for the range of engine speeds (800–1400 rpm) along with a close-up view of LTHR period heat release rates for the fired conditions. In-cylinder O_3 concentrations gradually declined early in the cycle before the start of rapid O_3 decomposition, which occurred around -45 CA irrespective of engine speeds. Note that the only major difference for the different engine speeds was that O_3 decomposition occurred earlier in the cycle with lower engine speeds. This behavior can be attributed to the longer residence times at lower speeds that enabled a greater amount of decomposition during the cooler early portion of the cycle. Rapid thermal O_3 decomposition of O_3 ended by around -25 CA, which is about the time of LTHR onset for all fired conditions.

O_3 addition reduces the intake heating requirement and hence enables wide CA50 control for LTC. Contour plot in Fig. 8.9 shows a non-linear dependence of CA50 on intake O_3 concentration and engine temperature. The reduction in intake heating requirement is highest for smaller concentrations of O_3. The return of O_3 addition slowly diminishes with an increase in O_3 concentrations. An addition of 25 ppm of O_3

Fig. 8.8 Effect of **a** intake temperature and **b** engine speed on in-cylinder O_3 decomposition
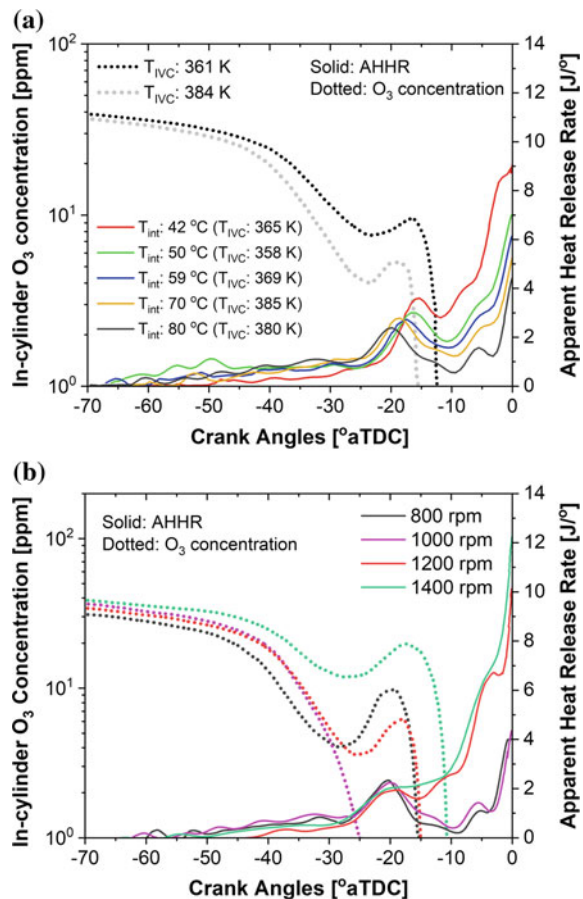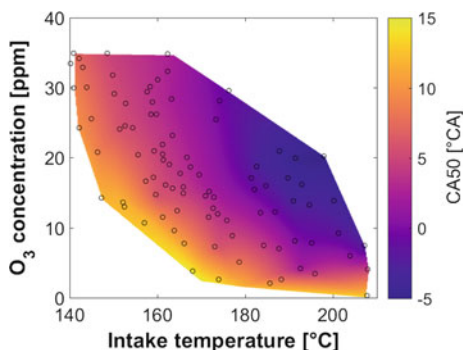

Fig. 8.9 Contour maps of CA50 as a function of intake O_3 concentration and temperature for a fixed operating point (-230 CA SOI, 1000 rpm, $\phi = 0.3$)

can considerably lower the intake temperature by 65 K. A lower intake temperature also implies that achieving a stable point was possible without adding O_3. Hence, O_3 provides an additional control knob to adjust the combustion phasing in ACI operation.

8.3.3 Kinetic Study of LTHR Pathway

To recognize key reaction pathways for enhanced auto-ignition chemistry with O_3 addition, 0D chemical kinetic simulations with detailed gasoline chemistry were performed. At the beginning of the simulations, experimentally estimated IVC conditions were imposed. The simulations were carried out through main compression stroke to capture relevant physics of O_3 decomposition, radical formation, and fuel oxidation. Figure 8.10 illustrates a schematic of the dominant LTHR response paths outlined in the introduction. It shows O_3 decomposed O leads to various sustainable production pathways for R and OH. Note that an additional pathway is included for completeness in which RO_2 undergoes inner isomerization to create hydroperoxyalkyl radical (QOOH).

Simulations were carried out with and without 50 ppm O_3 addition, with all other boundary conditions fixed to explore the most sensitive reactions to LTHR chemistry as illustrated in Fig. 8.10. The following engine operating condition: 1400 rpm, T_{intake} 80 °C, IMEP 4.9 bar, ST −54 °aTDC, T_{IVC} 383 K, RGF 12.5%, was chosen for this purpose. Figure 8.11 plots AHRR profiles of this operating condition along with the corresponding simulation results with and without the addition of O_3. The onset of LTHR with O_3 addition from the simulations closely matches the respective outcomes of the experiment. On the contrary, simulations without O_3 addition did not show any evidence of LTHR. Early in the cycle, O_3 concentrations are stable; however, start

Fig. 8.10 Schematic of LTHR reaction pathways initialized by O formed from thermal decomposition of O_3. Violet and red arrows highlight the sustained source of R and OH radicals, respectively (Biswas and Ekoto 2019a)
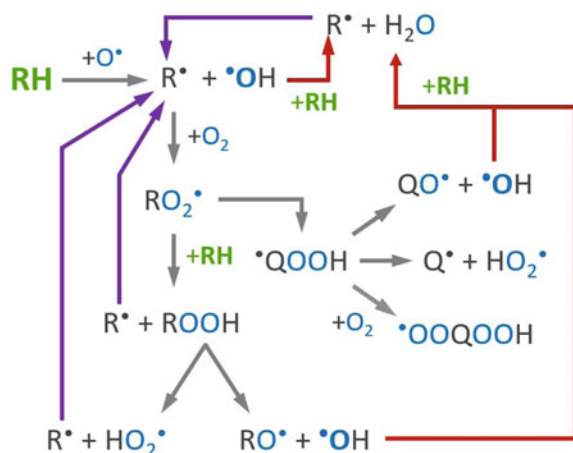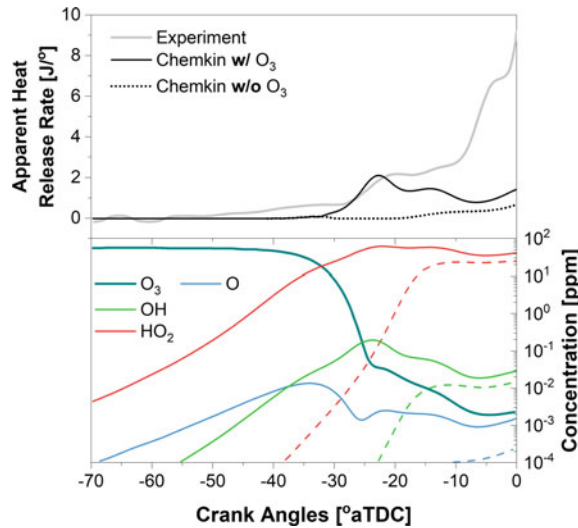
Fig. 8.11 AHRR profiles from the engine experiment and 0D Chemkin simulations with (solid) and without (dotted) O_3 (top). Cycle evolution of O_3 and important fuel oxidation radicals highlighted in Fig. 8.10 (bottom) (Biswas and Ekoto 2019a)
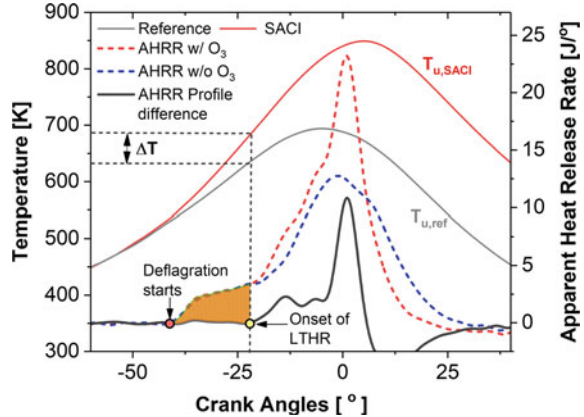

to decline rapidly at $-40\,°aTDC$ and finally reaches a negligible concentration by $-25\,°aTDC$. These findings are well in agreement with the experimental findings shown in Fig. 8.8b. O concentrations did not exceed 0.01 ppm since it quickly consumed by fuel molecules. However, rapid decomposition of O_3 leads to the creation of O, OH, and HO_2 much sooner.

8.3.4 Energy Requirements for End Gas Auto-ignition

While end gas reactivity increased with O_3 addition, it was not sufficient on its own to lead to auto-ignition for the fuel-lean conditions examined in this study. Additional thermal energy supplied by the fuel-rich bowl deflagration was needed to accelerate end gas auto-ignition reactions. However, results from the previous section demonstrated that the second injection was the primary source of NO_x emissions. Thus, it is imperative to minimize the second injection fueling fraction while preserving good combustion stability and efficiency for a given condition, which requires new design tools. In this section, a simplified analysis is presented to evaluate the end gas thermal energy deficit needed to initiate sufficiently strong auto-ignition. Optimized conditions used to generate performance and emissions maps in Figs. 8.6 and 8.7 were used as the reference points.

It was observed earlier that heat release rates from the initial bowl deflagration were well-matched, regardless of the amount of in-cylinder O_3 concentration. Accordingly, the increased thermal energy from the early deflagration can be estimated from the integrated heat release up to the onset of LTHR. The beginning of LTHR for each condition was identified from the 'profile difference' between the

Fig. 8.12 Schematic used to
illustrate the methods used to
estimate energy requirement
for end gas auto-ignition

same operating conditions with and without O_3 addition as illustrated in Fig. 8.12.
The orange hatched area represents the integrated energy that is attributed exclusively
to the early deflagration heat release.

While the integrated heat release provides an estimate for thermal energy addition,
it is not very predictive. An alternate method that is potentially more predictive is
to evaluate the auto-ignition energy using cycle thermodynamic parameters. For this
method, a simple two-zone system was assumed, with deflagration in the piston bowl
growing outwardly and end gas mixture getting compressed by this deflagration, as
shown in Fig. 8.2. Deflagration and end gas zones were assumed to be quasi-steady
and homogenous, with each zone identified by a single burned or unburned tem-
perature. Thus, the energy required for auto-ignition was the difference in unburned
end gas enthalpies for an operating condition relative to a reference motored condi-
tion without deflagration. The estimated energy deficit required to initiate end gas
auto-ignition can then be written as,

$$E = m_u C_{p,u}\left(T_{u,SACI} - T_{u,ref}\right) \tag{8.2}$$

where m_u is the end gas mass of, $C_{p,u}$ is the end gas constant pressure specific heat,
$T_{u,SACI}$ is unburned end gas temperature for stratified SACI condition, i.e., with O_3
seeding and the presence of deflagration providing additional energy, and $T_{u,ref}$ is
the reference temperature from a corresponding motored condition.

A map of the calculated thermal energy deficit (integrated heat release up to LTHR
onset) required for end gas auto-ignition is plotted in Fig. 8.13a for the full range of
load and engine speed conditions evaluated in the present study. The energy deficit
varied from 10 J for highest load and lowest speed conditions (4 bar IMEP, 800 rpm)
to 40 J for the lowest loads and highest engine speed conditions (1.5 bar IMEP,
1600 rpm). These results are unsurprising given the longer residence times and more
reactive mixtures for the highest load and lowest speed conditions. Indeed, it was
often observed that these conditions could sustain auto-ignition without a spark,

(a)

Energy required for end gas auto-ignition

(b)

Difference in energies from two methods
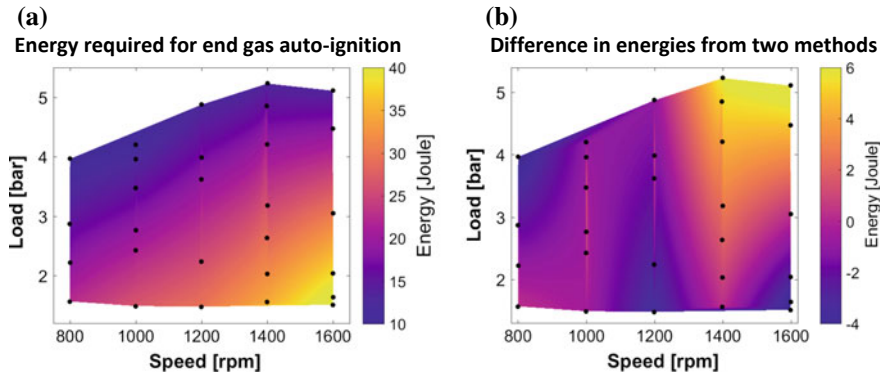
Fig. 8.13 End gas auto-ignition energy **a** estimated from the integrated heat release up to LTHR onset, **b** difference estimated from two methods, i.e. energy integrated heat release (method 1) and Eq. (8.2) (method 2)

utilizing only energy addition from retained residual heating. The maps illustrate a fairly linear transition between these two extreme regions.

A map illustrating the difference in thermal energies estimated by integrated heat release (method 1) and from Eq. (8.2) (method 2) is plotted in Fig. 8.13b. It is immediately apparent that energy trends for both methods are remarkably well matched. The largest differences between the two methods were observed for the highest load conditions. Relative to the end gas thermal energy deficit calculation that used the integrated heat release, the method that used the difference in end gas temperatures at the onset of LTHR predicts modestly higher values for the lowest engine speeds (0–4 J) and modestly lower values (0–6 J) for the highest speeds. Potential reasons for the discrepancy include: (a) errors in the estimated temperature calculation at LTHR onset, (b) end gas thermal stratification that would have led to reduced thermal energy requirements for local hot spots, and (c) potential fuel stratification from the second injection that likewise would have led locally rich regions that ignite earlier. Future work will evaluate each of these sensitivity parameters in greater detail.

8.3.5   Development of Advanced Ignition System

O_3 added homogeneous SACI failed to operate at lower loads compared to stratified SACI which enabled stable combustion across the entire load speed map. However, partially stratified SACI operation was responsible for a 3–5 folds increase in NO_x emissions. Thus, an optimum combustion strategy is crucial to enable stable combustion with lesser emission. The advanced ignition system has the potential to bridge these two requirements—stable combustion with lower emissions.

Transient Plasma Ignition (TPI) is a promising advanced ignition technology that utilizes short pulse (~10 s of nanoseconds), high-voltage (15 kV+) electrical

discharges to generate highly energized low-temperature plasma (LTP). Our preliminary study (Biswas et al. 2018) shows that TPI extends the lean limit and increase the dilution tolerance of propane/air mixture compared to conventional inductive spark. TPI promotes faster flame propagation rates through a combination of larger volume ignition kernels and the generation of active radicals that enhance flame speeds. Visualization of ignition event and early flame propagation by transient plasma was performed within a custom-built optically accessible spark calorimeter for near-atmospheric, 1.3 bar, $\phi = 0.41–1.0$ propane/air mixtures. A barrier discharge igniter (BDI) with an anode tip covered by high-temperature, high-dielectric strength epoxy was used for TPI.

Figure 8.14 compares the pressure and heat release rate of TPI with an inductive spark. Figure 8.14a shows that for $\phi = 0.6$ the ignition delay was shorter for TPI. Also, a steeper slope in TPI pressure profile indicates that combustion by transient plasma happens faster than an inductive spark. To compare the performance of lean TPI, pressure history of stoichiometric spark ignition is also plotted in Fig. 8.14a. The pressure rise rate is nearly identical for TPI $\phi = 0.6$ to stoichiometric spark ignition. This indicates that plasma ignition produces stronger ignition kernels and faster flame propagation even at the leaner operating condition. This is also evident from the heat release rate (HRR) profiles shown in Fig. 8.14b. At $\phi = 0.6$, the peak heat release rate doubled for TPI compared to inductive spark. TPI had a burn duration of 10 ms, compared to a burn duration of 23 ms for inductive spark. This shows that the flame growth rate in TPI is much faster compared to spark ignition for $\phi = 0.6$. The HRR at $\phi = 0.6$ for TPI matched closely with stoichiometric HRR from spark ignition.

Transient plasma discharges lead to increased ionization and dissociation. Previous studies (Wolk et al. 2013; Cathey et al. 2008) have shown that TPI generates radicals and other electronically excited species over a relatively large volume. Plasma discharges dissociate O_2 to create O which again combines with O_2 to produce O_3. We measured LTP generated O_3 in desiccated air at different pressure and voltage
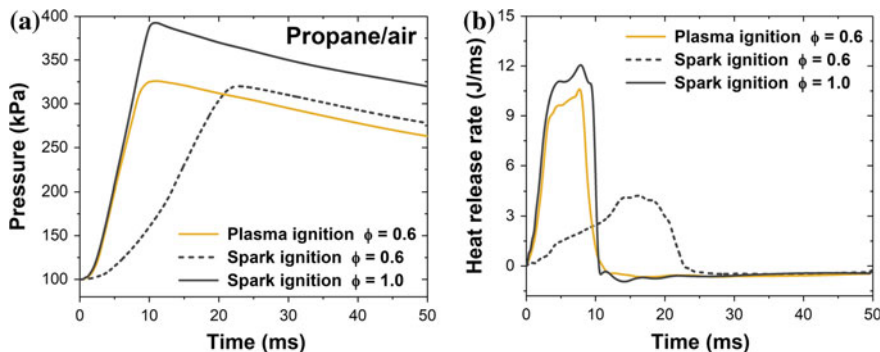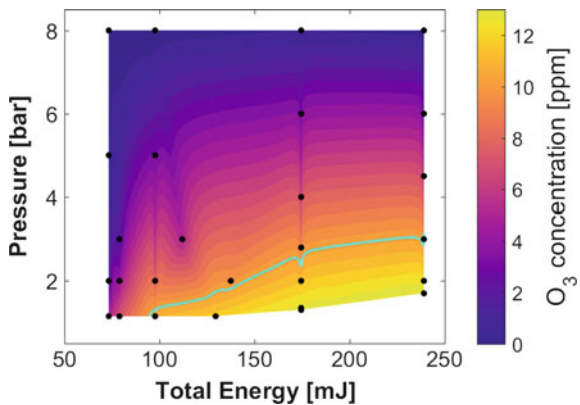

Fig. 8.14 **a** Pressure history and **b** heat release rate from low-temperature plasma and inductive spark ignition in stoichiometric and $\phi = 0.6$ propane/air

Fig. 8.15 The contour plot of O_3 generated by low-temperature plasma discharges (10 pulses) in desiccated air at engine condition. The cyan line represents an O_3 concentration of 10 ppm

conditions in a 29 cc optically accessible spark calorimeter. Then the estimated O_3 concentrations were converted to engine conditions of 0.55 L volume and 1 bar intake pressure. The contour map of generated O_3 at the engine condition is shown in Fig. 8.15. The cyan line represents 10 ppm of O_3. Note that these 10 ppm O_3 was generated by a discharge of 10 pulses with the time difference between each pulse was 100 microseconds. Thus, to reach an O_3 concentration of 50 ppm, 5 such discharges will be necessary. However, the rate of O_3 generation decreases at higher pressure. Sine in-cylinder pressure changes in non-linear fashion during the compression stroke, an optimum pulsing strategy need to be utilized to achieve the target amount of O_3 necessary for end gas auto-ignition.

8.4 Summary

In the present study, performance and emissions characteristics were investigated for 0–50 ppm O_3 added lean SACI operation with two different injection strategies, (1) partially stratified: double injection—early (75–90% fuel) and late DI (10–25% fuel) and (2) homogeneous: single early direct injection (DI) in an optically accessible single-cylinder research engine. Significant findings are as follows:

- O_3 addition stabilized engine combustion relative to comparable conditions without O_3 by increasing end gas reactivity. Increased intake O_3 addition—and hence late-cycle O—led to a corresponding increase in end gas LTHR that accelerated the onset of HTHR.
- The addition of O_3 was most useful for the lowest engine speeds due to the longer cycle residence times for kinetically controlled heat release to occur. The impact of O_3 addition decreased with increased engine speed due to shorter residence times available for auto-ignition.

- Increased fueling fractions in the late second injection likewise increased the strength of the early deflagration, which generally increased combustion stability but led to rapid increases in NO_x emissions.
- Lower loads were more challenging to achieve in O_3 enhanced homogeneous SACI relative to partially stratified SACI. However, homogeneous SACI approach generated higher efficiencies and lesser emissions.
- A simplified thermodynamic analysis method was developed to calculate the energy deficit that used either the integrated heat release up to the onset of LTHR or the difference in the end gas temperatures for cycles with and without combustion. Both methods exhibited excellent agreement with each other. For the conditions examined here, roughly 10–40 J of thermal energy was needed from the early deflagration to lead to optimized end gas autoignition. Higher speed and lower load conditions required the most energy due to the shorter residence times and leaner end gas mixtures.

The present study demonstrates that the best way to dramatically reduce NO_x emissions is to eliminate the late second injection altogether. O_3 addition helps with this by increasing the strength of end gas LTHR reactions and thus requiring a weaker bowl deflagration. While further reductions of second injection fueling fraction are likely possible with even higher O_3 concentrations, this is like not sufficient to entirely eliminate the second injection. It would be desirable to have a strong deflagration without the second injection, which highlights how the current strategy could be augmented by some form of the advanced ignition system (e.g., pre-chamber, low-temperature plasma).

References

Ansys (2017) CHEMKIN-PRO

Benajes J, García A, Domenech V, Durrett R (2013) An investigation of partially premixed compression ignition combustion using gasoline and spark assistance. Appl Therm Eng 52(2):468–477

Benajes J, Molina S, García A, Monsalve-Serrano J, Durrett R (2014) Performance and engine-out emissions evaluation of the double injection strategy applied to the gasoline partially premixed compression ignition spark assisted combustion concept. Appl Energy 134:90–101

Biswas S (2018) Physics of turbulent jet ignition: mechanisms and dynamics of ultra-lean combustion, 1st edn. Springer

Biswas S, Ekoto I (2019a) Detailed investigation into the effect of ozone addition on spark assisted compression ignition engine performance and emissions characteristics. SAE Technical Paper 2019-01-0966

Biswas S, Ekoto I (2019b) Spark assisted compression ignition engine with stratified charge combustion and ozone addition. JSAE 20199089

Biswas S, Qiao L (2016) Prechamber hot jet ignition of ultra-lean H_2/air mixtures: effect of supersonic jets and combustion instability. SAE Int J Engines 9(3)

Biswas S, Tanvir S, Wang H, Qiao L (2016) On ignition mechanisms of premixed CH_4/air and H_2/air using a hot turbulent jet generated by pre-chamber combustion. Appl Therm Eng 106:925–937

Biswas S, Ekoto I, Scarcelli R (2018) Transient plasma ignition (TPI) for automotive applications. In: 4th international conference on ignition systems for gasoline engines. Berlin

Cathey C, Cain J, Wang H, Gundersen MA (2008) OH production by transient plasma and mechanism of flame ignition and propagation in quiescent methane-air mixtures. Combust Flame 154(4)

Chang J, Güralp O, Filipi Z, Assanis D, Kuo T-W, Najt P, Rask R (2004) New heat transfer correlation for an HCCI engine derived from measurements of instantaneous surface heat flux. SAE Technical Paper 2004-01-2996

Christensen M, Johansson B, Einewall P (1997) Homogeneous charge compression ignition (HCCI) using isooctane, ethanol and natural gas—a comparison with spark ignition operation. SAE Technical Paper 972874 106(4)

Dec JE (2009) Advanced compression-ignition engines—understanding the in-cylinder processes. Proc Combust Inst 32(2):2727–2742

Dec JE, Yang Y, Dernotte J, Ji C (2015) Effects of gasoline reactivity and ethanol content on boosted, premixed and partially stratified low-temperature gasoline combustion (LTGC). SAE Int J Engines 8(3)

Depcik C, Mangus M, Ragone C (2014) Ozone-assisted combustion—part I: literature review and kinetic study using detailed n-heptane kinetic mechanism. J Eng Gas Turb Power 136(9)

Dernotte J, Dec JE, Ji C (2015) Energy distribution analysis in boosted HCCI-like/LTGC engines—understanding the trade-offs to maximize the thermal efficiency. SAE Int J Engines 8(3)

Ekoto I, Foucher F (2018) Mechanisms of enhanced reactivity with ozone addition for advanced compression ignition. In: SAE world congress experience. SAE International, Detroit, MI

Ekoto I, Wolk B, Northrop W (2017) Energy analysis of low-load low-temperature gasoline combustion with auxiliary-fueled negative valve overlap. SAE Int J Engines 10(3):1238–1255

Fitzgerald RP, Steeper R (2010) Thermal and chemical effects of NVO fuel injection on HCCI combustion. SAE Int J Engines 3(1):46–64

Gorshelev V, Serdyuchenko A, Weber M, Chehade W, Burrows JP (2014) High spectral resolution ozone absorption cross-sections—part 1: measurements, data analysis and comparison with previous measurements around 293 K. Atmos Meas Tech 7(2):609–624

Graham LA, Belisle SL, Rieger P (2009) Nitrous oxide emissions from light duty vehicles. Atmos Environ 43(12):2031–2044

Kijewski H, Troe J (1971) Study of the pyrolysis of H_2O_2 in the presence of H_2 and CO by use of UV absorption of HO_2. Int J Chem Kinet 3(3):223–235

Kolodziej C, Kodavasal J, Ciatti S, Som S, Shidore N, Delhom J (2015) Achieving stable engine operation of gasoline compression ignition using 87 AKI gasoline down to idle. SAE Technical Paper 2015-01-0832

Lavoie GA, Martz J, Wooldridge M, Assanis D (2010) A multi-mode combustion diagram for spark assisted compression ignition. Combust Flame 157(6):1106–1110

Lawler BJ, Filipi ZS (2013) Integration of a dual-mode SI-HCCI engine into various vehicle architectures. J Eng Gas Turb Power Trans ASME 135(5)

Manofsky L, Vavra J, Assanis DN, Babajimopoulos A (2011) Bridging the gap between HCCI and SI: spark-assisted compression ignition. SAE Int

Masurier JB, Foucher F, Dayma G, Dagaut P (2013) Homogeneous charge compression igni-
tion combustion of primary reference fuels influenced by ozone addition. Energy Fuels
27(9):5495–5505

Masurier JB, Foucher F, Dayma G, Dagaut P (2015a) Ozone applied to the homogeneous charge
compression ignition engine to control alcohol fuels combustion. Appl Energy 160(Supplement
C):566–580

Masurier J-B, Foucher F, Dayma G, Dagaut P (2015b) Investigation of iso-octane combustion in
a homogeneous charge compression ignition engine seeded by ozone, nitric oxide and nitrogen
dioxide. Proc Combust Inst 35(3):3125–3132

Mehl M, Pitz WJ, Westbrook CK, Curran HJ (2011) Kinetic modeling of gasoline surrogate com-
ponents and mixtures under engine conditions. Proc Combust Inst 33:193–200

Middleton RJ, Olesky LKM, Lavoie GA, Wooldridge MS, Assanis DN, Martz JB (2015) The effect
of spark timing and negative valve overlap on spark assisted compression ignition combustion
heat release rate. Proc Combust Inst 35(3):3117–3124

Molina LT, Molina MJ (1981) UV absorption cross-sections of HO_2NO_2 vapor. J Photochem
15(2):97–108

Olesky LM, Martz JB, Lavoie GA, Vavra J, Assanis DN, Babajimopoulos A (2013) The effects of
spark timing, unburned gas temperature, and negative valve overlap on the rates of stoichiometric
spark assisted compression ignition combustion. Appl Energy 105:407–417

Olesky LM, Lavoie GA, Assanis DN, Wooldridge MS, Martz JB (2014) The effects of diluent
composition on the rates of HCCI and spark assisted compression ignition combustion. Appl
Energy 124:186–198

Olesky LKM, Middleton RJ, Lavoie GA, Wooldridge MS, Martz JB (2015) On the sensitivity of
low temperature combustion to spark assist near flame limit conditions. Fuel 158:11–22

Ombrello T, Won SH, Ju YG, Williams S (2010) Flame propagation enhancement by plasma exci-
tation of oxygen. Part I: effects of O_3. Combust Flame 157(10):1906–1915

Ortiz-Soto EA, Lavoie GA, Martz JB, Wooldridge MS, Assanis DN (2014) Enhanced heat release
analysis for advanced multi-mode combustion engine experiments. Appl Energy 136:465–479

Persson H, Hultqvist A, Johansson B, Remón A (2007) Investigation of the early flame development
in spark assisted HCCI combustion using high speed chemiluminescence imaging. SAE Int

Pinazzi PM, Foucher F (2017) Potential of ozone to enable low load operations of a gasoline com-
pression ignition (GCI) engine. In: SAE world congress experience. SAE International, Detroit,
MI

Reuss DL, Kuo T-W, Silvas G, Natarajan V, Sick V (2008) Experimental metrics for identifying
origins of combustion variability during spark-assisted compression ignition. Int J Engine Res
9(5):409–434

Rousso AC, Hansen N, Jasper AW, Ju Y (2018) Low-temperature oxidation of ethylene by ozone
in a jet-stirred reactor. J Phys Chem 122:8674–8685

Saxena S, Bedoya ID (2013) Fundamental phenomena affecting low temperature combustion and
HCCI engines, high load limits and strategies for extending these limits. Prog Energy Combust
Sci 39(5)

Schulz C, Koch JD, Davidson DF, Jeffries JB, Hanson RK (2002) Ultraviolet absorption spectra of
shock-heated carbon dioxide and water between 900 and 3050 K. Chem Phys Lett 355(1–2):82–88

Smekhov GD, Ibraguimova LB, Karkach SP, Skrebkov OV, Shatalov OP (2007) Numerical simu-
lation of ignition of a hydrogen-oxygen mixture in view of electronically excited components.
High Temp 45(3):395–407

Srivastava DK, Weinrotter M, Kofler H, Agarwal AK, Wintner E (2009) Laser-assisted homogeneous
charge ignition in a constant volume combustion chamber. Opt Lasers Eng 47:680–685

Stanglmaier RH, Roberts CE (1999) Homogeneous charge compression ignition (HCCI): benefits,
compromises, and future engine applications. SAE Int J Engines 108(3):2138–2145

Stone R (1999) Compression ignition engines. In: Introduction to internal combustion engines.
Springer, Palgrave, London

Truedsson I, Rousselle C, Foucher F (2017) Ozone seeding effect on the ignition event in HCCI combustion of gasoline-ethanol blends. In: SAE world congress experience. SAE Technical Paper 2017-01-0727. SAE International, Detroit, MI

Uddi M, Jiang NB, Mintusov E, Adamovich IK, Lempert WR (2009) Atomic oxygen measurements in air and air/fuel nanosecond pulse discharges by two photon laser induced fluorescence. Proc Combust Inst 32:929–936

United States Environmental Protection Agency, Office of Policy and Evaluation (2016) Inventory of U.S. greenhouse gas emissions and sinks: 1990–2014. U.S. Environmental Protection Agency, Washington, DC

United States, Environmental Protection Agency, Office of Transportation and Air Quality (2012) Non-conformance penalties for heavy-duty diesel engines subject to the 2010 NO_x emission standard. U.S. Environmental Protection Agency, Office of Transportation and Air Quality, Washington, DC

Weinrotter M, Wintner E, Iskra K, Neger T, Olofsson J, Seyfried H, Aldén M, Lackner M, Winter F, Vressner A, Hultqvist A, Johansson B (2005) Optical diagnostics of laser-induced and spark plug assisted HCCI combustion. SAE Technical Paper 2005-01-0129

Wolk B, DeFilippo A, Chen JY, Dibble R, Nishiyama A, Ikeda Y (2013) Enhancement of flame development by microwave-assisted spark ignition in constant volume combustion chamber. Combust Flame 160(7):1225–1235

Wolk B, Ekoto I, Northrop W (2016a) Investigation of fuel effects in negative valve overlap reforming chemistry using gas chromatography. SAE Int J Engines 9(2)

Wolk B, Ekoto I, Northrop WF, Moshammer K, Hansen N (2016b) Detailed speciation and reactivity characterization of fuel-specific in-cylinder reforming products and the associated impact on engine performance. Fuel 185:348–361

Zádor J, Taatjes CA, Fernandes RX (2011) Kinetics of elementary reactions in low-temperature autoignition chemistry. Prog Energy Combust Sci 37(4):371–421

Zhang Y, Zhu M, Zhang Z, Shang R, Zhang D (2016) Ozone effect on the flammability limit and near-limit combustion of syngas/air flames with N_2, CO_2, and H_2O dilutions. Fuel 186(Supplement C):414–421

Zhao F, Asmus TN, Assanis DN, Dec JE, Eng JA, Najt PM (2003) Homogeneous charge compression ignition (HCCI) engines: key research and development issues. Society of Automotive Engineers International, Warrendale, PA

Part IV
Emissions and Aftertreatment Systems

Chapter 9
Emissions of PM$_{2.5}$-Bound Trace Metals from On-Road Vehicles: An Assessment of Potential Health Risk

Jai Prakash and Gazala Habib

Abstract The present study elucidates on PM$_{2.5}$ (particle aerodynamic diameter $\leq 2.5\,\mu$m) bound trace metals characterization from on-road light-duty vehicles during on-road operation and their health risk assessment for adults and children. The vehicles assessed in present work included 4-wheelers passenger cars with a different age group of Bharat Stage (BS) II, III, and IV and different fuel type [diesel, gasoline and compressed natural gas (CNG)]. To understand the particle losses, particle formation, and homogenous mixing, firstly, a new portable dilution system (PDS) was designed for diluting the exhaust with adequate aerosol formation and growth, and evaluated beforehand under controlled condition in laboratory for diesel vehicles over a wide range of dilution ratio (30:1, 60:1, and 90:1). For on-road experiments, a PDS, a heated duct, a gas analyzer, an exhaust velocity probe, a temperature, and relative humidity probe were mounted on Aerosol Emissions Measurement System (AEMS) and it was towed behind the vehicle. Total 46 experiments were performed on a mixed traffic route in Delhi city, and PM$_{2.5}$ mass was collected on Teflon and quartz filter using multi-stream PM$_{2.5}$ sampler. Total 17 trace metals (Al, Ag, As, Ba, Co, Cd, Cr, Cu, Fe, Mn, Ni, Pb, Se, Sr, Ti, V, and Zn) were characterized on Teflon filters using Induced Coupled Plasma-Mass Spectrometry (ICP-MS). Out of these metals, the non-carcinogenic and carcinogenic risks for adults and children were calculated for 5 metals namely Cr, Mn, Ni, Zn, and Pb. Trace metals concentration was highest in exhaust emitted from 4W-diesel followed by 4W-gasoline, 3W-CNG, and 2W-gasoline. Trace metals such as Cr, Mn, Ni, Zn, and Pb were present in high amount ($25.2 \pm 8.6\,\mu$g m^{-3}). The carcinogenic risk from Cr was considerably higher than tolerable risk (10^{-4}), while the risk from other metals such as Ni, As, Cd, and Pb was within the range of safe (10^{-6}) and tolerable (10^{-4}) level. Overall, the human health risks associated with the exposure to PM$_{2.5}$ emitted from gasoline and CNG vehicles were higher than that from diesel vehicle. This estimated risk in this work can help in refining the burden of disease and crafting policy to help reduce the exposures. This study is limited only for PM$_{2.5}$ bound trace metals and associated

J. Prakash
Aerosol and Air Quality Research Laboratory, Washington University, St. Louis, MO, USA

G. Habib (✉)
Department of Civil Engineering, Indian Institute of Technology Delhi, New Delhi, India
e-mail: gazalahabib@gmail.com

health risk from on-road vehicle emissions. However, poly-aromatic hydrocarbons (PAHs), perfluorinated compounds (PFCs), and semi-volatile compounds in vehicular exhaust can also impose a severe risk to human health which needs to be assessed to evaluate combined risk.

9.1 Introduction

On-road vehicle emissions are the significant source of air pollution especially in urban cities of India and expected rapid growth due to economic growth in India (Reynolds et al. 2011; Grieshop et al. 2012). Several toxicological studies have discussed public-health associated problems such as cardiovascular, cellular inflammation, and lung cancer risk on exposure to exhaust particle emission from on-road vehicles (Xu et al. 2013; Schwarze et al. 2013; Vreeland et al. 2016; Geller et al. 2006; Grahame et al. 2010). Recent studies have been also found that the inhalation of fine particles (PM$_{2.5}$) emitted from vehicles initiate several biochemical reactions within the body (Verma et al. 2015; Lovett 2018) leading to oxidative stress. Vehicle emission contains polycyclic aromatic hydrocarbons (PAHS), metals, carbonaceous constituents [black carbon (BC), organic carbon (OC)], inorganic acidic species (chloride, and nitrate), and complex organic compounds. However, these chemical species, especially particle-bound transition metals, have associated with oxidative stress in the human respiratory tract by reactive oxygen species (ROS) (Zhou et al. 2018; Kelly 2003; Betha and Balasubramanian 2011, 2013). Some studies have investigated particle-bound PAHs and trace metal emissions of diesel, gasoline, biodiesel vehicles using engine dynamometer in controlled laboratory conditions and during on-road operation (Betha and Balasubramanian 2011, 2013; Betha et al. 2012; Shukla et al. 2017a, b; Alves et al. 2015a). Some other studies have described the chemical composition of exhaust emission from diesel and gasoline vehicles in the European and USA fleets (Alves et al. 2015a, b). However, the particle-bound composition of European and USA fleets could be different as compared to Indian fleets, possibly due to driving conditions, road characteristics, vehicle age and category, fuel, lubricant, after-treatment technology, etc. (Jaiprakash and Habib 2017, 2018). Vehicle emission characteristics of particle-bound metals via chassis dynamometer and in tunnel experiment do not reflect the real on-road driving conditions. Therefore, in recent years, the on-road measurement directly from the tail pipe has been greatly emphasized by researchers (Wu et al. 2015, 2016). In this regard, the challenge involves in simulating the atmospheric process of gas-to-particle partitioning before collection of particle mass. Earlier studies have used a portable dilution system (PDS) and portable emission measurement system (PEMS) to carry out vehicle emission measurement under real driving conditions (Wu et al. 2015, 2016; Wang et al. 2014). However, the studies using a PDS to measure the emissions from vehicles during

on-road operation are limited (Hao et al. 2018), in addition, the characterization of particle-bound trace metals and their associated risk have not been reported in the Indian context. Therefore, this study focuses on emissions of particle-bound metals from diesel, gasoline, and CNG powered vehicles during on-road operation of mixed traffic route in Delhi city. In present work, a new Aerosol Emission Measurement System (AEMS) was used as detailed in Jaiprakash and Habib (2017). The non-carcinogenic and excess cancer risk (ECR) of particle-bound metals were estimated and presented here.

9.2 Materials and Methods

Portable dilution system (PDS) simulates the rapid cooling and dilution of exhaust a happens in the atmosphere to achieve complete gas-to-particle partitioning. The partial exhaust sample withdraws from a combustion source sampling probe and entrains into dilution tunnel, where it dilutes rapidly and homogenous with the particle and VOC free dry air (described as zero air). The dilution allows to lessen the particle number concentration inside the dilution tunnel and therefore, it avoids unwanted condensation and nucleation (Betha and Balasubramanian 2011; Betha et al. 2012; Lipsky and Robinson 2005, 2006) of the particles. In the present work, a PDS was designed following Lipsky and Robinson (2005). For on-filed measurement of any combustion sources, new PDS was subjected to reduce their compactness, incessant zero air and power supply.

9.2.1 Design of Portable Dilution System (PDS)

Figure 9.1 shows a schematic diagram of PDS, which contains 0.4 m length, and 0.1 m-diameter stainless steel dilution tunnel, 0.06 m diameter and 1.0 m length stainless duct, a heated stainless sampling probe, zero air assembly, and power supply with inverter (3 kW) and four 12 V batteries for continuous power supply for an hour. The heated sampling probe and the duct is maintained at a temperature above (~10 °C) the sample exhaust temperature (~150 °C) to avoid the thermophoresis and condensation losses (Zhang and McMurry 1992; Baron and Willeke 1993). The zero-air generation system comprised of a filter holder, an activated carbon cartridge, and molecular sieves to remove particles, volatile organic compounds, and the moisture, respectively, and the atmospheric air is stored in a reservoir (volume of 40 L) to produce continuous zero air. A dual-stage tower automatically regenerates zero air by the principle of Pressure Swing Adsorption (PSA), where the total pressure of assembly "swings" between high pressure in feed and low pressure in regeneration (Ruthven et al. 1994; Rezaei and Webley 2009). The particle sampling probe extracts a portion of the exhaust sample directly from the exhaust tailpipe by the principle of eductor technique. In eductor technique, the pressurized zero air flows at high speed
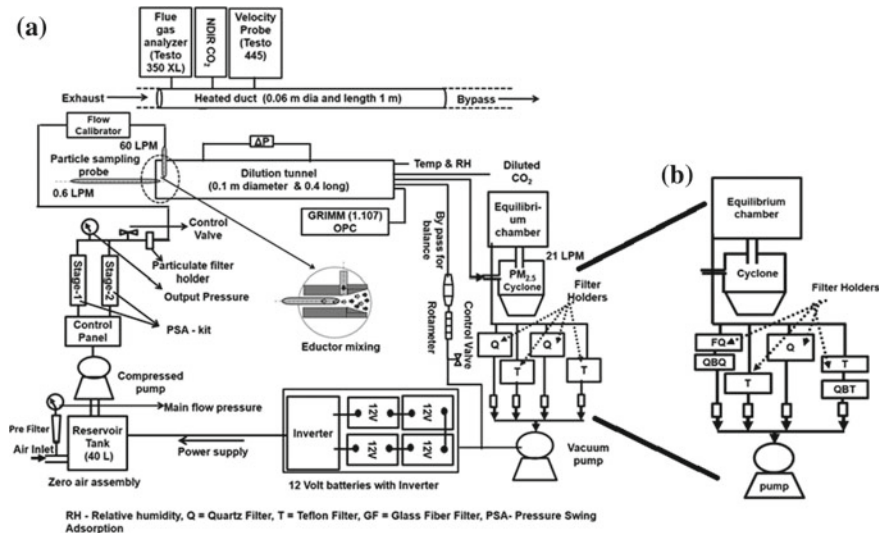
Fig. 9.1 Set-up of portable dilution sampling (PDS) system containing duct, dilution tunnel, particle sampling probe, zero air assembly, multi-stream particle sampler, and power supply unit

around the tip of the sampling probe and creates a negative pressure zone which draws the sample exhaust inside the probe without applying any control device (Harsha et al. 2019). The exhaust sample flow (~0.2–1 LPM) was induced in the sampling probe by maintaining zero air. In order to achieve the maximum dilution ratio of 100:1 (i.e. volume of zero air ÷ volume of sample exhaust) and complete aerosol formation and growth to stabilize in 3 s, the dilution tunnel of 3 L capacity was designed. The total six sampling ports were used to measuring a particle, number particle, diluted CO_2, moisture, temperature, at the downstream of dilution tunnel. One port was fixed to measure the $PM_{2.5}$ particles using a multi-stream $PM_{2.5}$ sampler.

9.2.2 Multi-stream Aerosol Sampler

A multi-stream $PM_{2.5}$ sampler, which consists of an AIHL aluminium cyclone and two dual stage and two single stage filter holders (Habib et al. 2008; Venkataraman et al. 2005). The configuration details of multi-stream $PM_{2.5}$ sampler is shown in Fig. 9.1b. This sampler provides the collection of particles with cut off aerodynamic diameter smaller than 2.5 μm at 20.2 LPM. The two filter holders were used to collect $PM_{2.5}$ mass on a quartz filter (Pall flex 2500 QAT-UP; 47 mm, Tissue quartz) and another 2 filter holders were used to collect $PM_{2.5}$ on Teflon membrane filters (47 mm, 2-mm pore size, Whatmann Corp., PA, USA). The flow rates of these filter holders are maintained by critical orifices (6.3, 4.5, 5.0, and 4.4 LPM) (Fig. 9.1b). In dual-stage of filter, the backup quartz filter was used to collect the artifacts, which

were determined by OC-EC analysis using Thermal optical transmittance (TOT) analyzer.

9.2.3 Evaluation of Dilution Tunnel

9.2.3.1 Gas-to-Particle Conversion

The new particle formation from gas to particle partitioning during the dilution favors the absorption of volatile organic compounds and adsorption on pre-existing inert components such as elemental carbon and minerals (sorptive material). The residence time is the time the aerosol remains in the dilution tunnel before collection, it is calculated as the ratio of the volume of dilution tunnel to total flow rate (Eq. 9.1). For dilution tunnel experiments the residence time of 2–3 s (Lipsky and Robinson 2005) and the ratio of residence time to phase equilibrium time greater than 4 are recommended to accomplish complete gas-to-particle partitioning for particles of size few 0.03–1.0 µm. The phase equilibrium time is defined as the time required by supersaturated cool vapour phase species to form new particles or to condense on existing organic particles. The residence time and phase equilibrium time scale (τ) were estimated using the following equations (Eqs. 9.1–9.4):

$$t = \frac{V_{dt}}{Q_{ex} + Q_{air}} \tag{9.1}$$

$$\tau = \frac{1}{2\pi D \sum d_p N(d_p) f_n(K_n)} \tag{9.2}$$

$$f_n(K_n) = \frac{1 + \mathrm{Kn}}{1 + 1.71\mathrm{Kn} + 1.33\mathrm{Kn2}} \tag{9.3}$$

$$\mathrm{Kn} = \frac{2\lambda}{d_p} \tag{9.4}$$

where, V_{dt} is the volume of dilution tunnel in (m^3), Q_{ex} and Q_{air} are the flow rate (m^3 s^{-1}) of exhaust sample and zero air. d_p is the count median diameter of particle, N is the total number of concentration, D is the diffusion coefficient for the organic vapor in air (assumed 5×10^{-6} m^2 s^{-1}), $f_n(K_n)$ is the correction factor accounting for non-continuous effects, K_n is the Knudsen number, and λ is mean free path (assumed 0.065×10^{-6} m).

The phase equilibrium time for 99% condensation of volatiles was estimated by assuming heterogeneous condensation of vapor phase species in a typical particle number distribution in the dilution tunnel reported for diesel vehicles (Venkataraman et al. 2005; Matti Maricq and Maricq 2007). The size distribution was used in Eqs. (9.1)–(9.4) to determine the phase equilibrium time (τ) at different dilution ratios 40–70. The residence and phase equilibrium time at different dilution ratios

were estimated in the range of 4.3–7.5 and 0.32–0.56 s, respectively. Thus, the ratio of t/τ was calculated in the range of 8–23, which indicates that complete gas to particle partitioning can be achieved at dilution ratios between 40 and 70.

9.2.3.2 Particle Losses and Homogenous Mixing

The determination of the particle loss of PDS was evaluated using sodium chloride NaCl (NaCl; 5 mg L^{-1}), which has polydisperse particle size range (20–600 nm). The schematic experimental set-up is shown in Fig. 9.2. The aerosol is generated from a 20 mL solution of NaCl using an aerosol generator (Model 3076, TSI Particle Instrumentation Inc., St. Paul, MN, USA) to generate 20–600 nm particle at 0.3 mL min^{-1} flow rate. NaCl generated particles withdraws in the dilution tunnel using sampling probe with 0.6 LPM by maintaining zero air flow at 18, 36, and 54 LPM, to achieve dilution ratios 30:1, 60:1, and 90:1, respectively. Afterward, a scanning mobility particle sizer (SMPS, Model 3936, TSI Inc., USA) containing differential mobility analyser (DMA, Model 3081, TSI Inc., USA), and a condensation particle counter (CPC, Model 3775, TSI Inc., USA) is used to measure the particle size distribution at upstream and downstream of dilution tunnel. The DMA gives a particle size in the range of 14–600 nm and it is scanned over the 135 s. Before the experiment, the system was operated with zero air and observed particle concentration in SMPS. Initially, the experiments were conducted with NaCl solution which is deliberated as without dilution tunnel (WODT), and then with dilution tunnel (WDT) (Fig. 9.2).

The number size distributions were recorded for WODT and WDT with three sets of experiments at the dilution ratios 30:1, 60:1, and 90:1, respectively. These particle
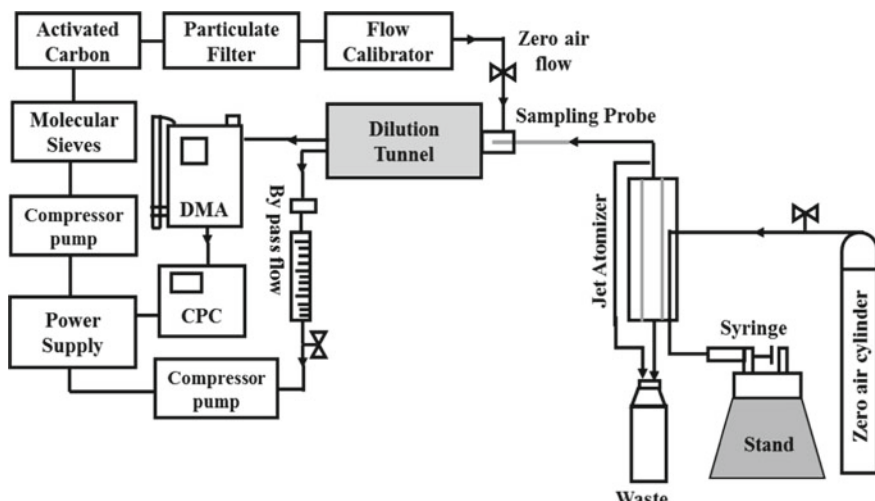

Fig. 9.2 Schematic diagram of the experimental setup used for measuring number-based particle loss in portable dilution system

size experiments are subjected to determine particle losses in the dilution tunnel. The percentage in difference between number concentration in WDT at dilution ratios and WODT were observed 6, 14, and 19%, respectively. The geometric mean diameters (GMD) were consistent 107 ± 4, 106 ± 4, and 104 ± 4 nm irrespective to dilution ratios implied that dilution did not affect the nucleation process. Similarly, the percentage difference between volume concentration in WDT at different dilution ratios with respect to WODT was found to be 17, 16, and 20% which shown few particle losses inside the dilution tunnel. Theoretically, thermophoresis losses were also calculated using the following equations [Eqs. (9.5)–(9.7)] (Hinds 1982):

$$Thermophoretic\ velocity\ (V_{th}) = \frac{-3\eta C_c H \nabla T}{2\rho_g T} \quad \text{for } d_p > \lambda \quad (9.5)$$

where

$$H = \left(\frac{1}{(1 + 6\lambda/d_p)} \right) \left(\frac{K_{a/K_p} + 4.4\left(\frac{\lambda}{d_p}\right)}{1 + 2(K_{a/K_p}) + 8.8\left(\frac{\lambda}{d_p}\right)} \right) \quad (9.6)$$

$$Thermophoresis\ losses\ (\%) = 100 * \left[1 - exp * \left(-\pi \frac{D_t L V_{th}}{Q} \right) \right] \quad (9.7)$$

where η = viscosity (PaS); C_c = slip correction factor, H = Thermophoretic coefficient; ∇T = Temperature gradient (K/m); ρ_g = gas density (kg/m^3); T = Exhaust temperature; λ = mean free path (m); d_p = particle diameter (μm); K_a = air thermal conductivity (W/m*K), assumed 0.026 (W/m*K); K_p = particle thermal conductivity (W/m*K), assumed 0.26 (W/m*K); D_t = dilution tunnel diameter (m; given 0.1 m); L = tube length (m, given = 0.4 m); Q = gas flow rate (m^3/s).

For particle mean diameter of 20, 50, and 130 nm, thermophoresis losses were estimated as <0.5% for diesel and gasoline engine. The particle and number size distribution was reported in previous studies (Gupta et al. 2010; Agarwal et al. 2015a), and adopted for calculating the thermophoresis losses.

The homogenous mixing reduces the possibility of wall losses in the dilution tunnel. To confirm homogenous mixing in dilution tunnel, PDS was performed controlled laboratory experiments using a medium duty diesel vehicle (INNOVA, BS-III, 2400 cc) on chassis dynamometer facility at Manesar Gurgaon. Only 4 experiments were planned due to high utilization rent and limited availability of chassis dynamometer. A small portion of the exhaust sample was carried from the tail-pipe using heated stainless steel (SS) sampling probe. The zero air (dilution air) flows at high pressure around the tip of sampling probe, which mixed rapidly and co-axially with exhaust sample in the dilution tunnel to attain adequate aerosol formation which occurs in the atmosphere.

For mixing, CO$_2$ concentrations were monitored at four ports such as 100, 200, 300 and 400 cm from the upstream of the dilution tunnel and also monitored at radial distances across the dilution tunnel. The CO$_2$ concentration showed insignificantly at

four ports along the distance of the dilution tunnel. The low coefficient of variances (4–10%) were observed around mean CO_2 concentration (1100 ± 60, 800 ± 40, 700 ± 30, and 400 ± 40 ppm at dilution ratios 30:1, 60:1, 90:1, and 120:1, respectively) indicate rapid and homogeneous mixing inside the dilution tunnel.

To confirm particle loss, $PM_{2.5}$ particle mass were collected on quartz filters using a multi-stream aerosol sampler and examined for elemental carbon (EC) using thermal optical transmittance (TOT model DRI 2001) analyzer. The EC mass emission factors ($g \ kg^{-1}$) were consistent at different dilution ratios (30, 60, 90, and 120), which indicated insignificant particle losses in the dilution with the increase in dilution ratio. These results are discussed earlier and detailed in Jaiprakash et al. (2016). However, a declining trend in $PM_{2.5}$ emission factor was observed with increasing dilution ratio, possibly due to decreasing particulate phase OC emission and increasing gas phase OC concentration, this implied that at high dilution ratios (>70:1) the reduction in residence time (less than 2 s) limit the gas-to-particle partitioning. Therefore, the dilution ratios between 30 and 70 were found appropriate for complete gas-to-particle partitioning, and further, these dilution ratios were used for on-road experiments.

9.2.4 Aerosol Emission Measurement System

For on-road experiments, a heated duct, a portable dilution system (PDS), multi-stream $PM_{2.5}$ sampler, a gas analyzer, an exhaust velocity probe, a temperature, and relative humidity probe is mounted on Aerosol Emissions Measurement System (AEMS) behind passenger cars (Fig. 9.3). The duct was tightly fixed to the vehicle tailpipe using a stainless steel coupler with silicon gasket to avoid intrusion of
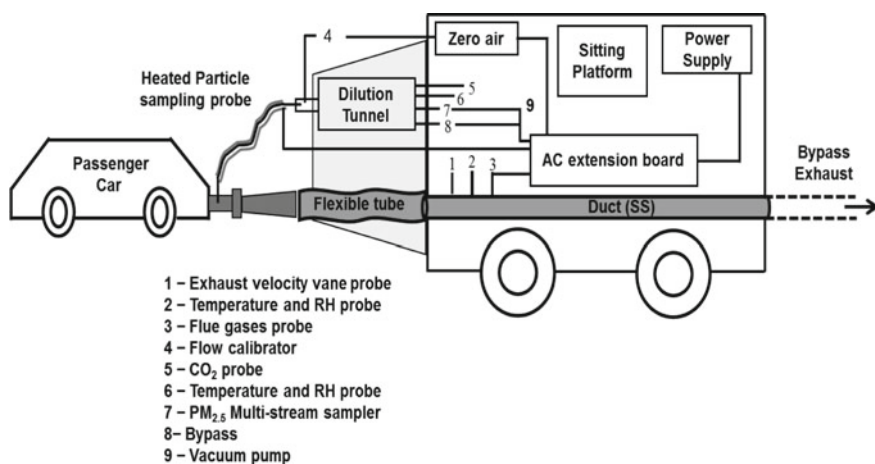

Fig. 9.3 Schematic experimental set up of aerosol emission measurement system

background air inside the duct. It should be noted that AEMS was dragged by 4-wheelers, therefore the on-road experiments were considered as under full engine load condition. In order to assess the effect of drag, three separate experiments were conducted with 4W-diesel vehicle [Bharat stage (BS)-IV 1.3 L, vehicle model post-2010] by removing the AEMS and PDS and other parts mounted in the backside of the vehicle and operate with same traffic route. The differences in PM$_{2.5}$ emissions between without AEMS and with AEMS were 20% for the same vehicle on the same route during the same traffic hours. This difference can be attributed to the drag on emissions due to towing the AEMS behind the vehicle.

For on-road experiment, 4W-passenger (4Ws) were chosen of the different fuel type such as diesel, gasoline, and CNG and various vintage age groups (post-2000, post-2005, and post-2010) considering to Bharat Stage (BS-II, III, and IV) norms and different fuel category such as compressed natural gas (CNG) for aerosol emission measurements. All vehicles specification of tested vehicles is tabulated in Table 9.1 and discussed in the next section.

In BS-II and BS-III of diesel vehicles, the after-treatment devices were equipped with exhaust gas recirculation (EGR) which does not have any special system for conversion of NO$_X$ and particulate matter (PM). In BS-IV, diesel vehicles engine was improved with turbocharger and after treatment device as diesel oxidation catalyst (DOC). A turbocharger is used for better air to fuel mixing for complete internal combustion and benefits to the oxidation process of DOC which oxidize CO, HC, and some of the soluble organic fraction (SOF) of diesel particulate matter but it is vain for soot particles (Dutkiewicz et al. 2009). In present study, tested Innova (post-2000, 2.4 L, BS-II), Swift Dzire (post-2012, 1.2 L, BS-IV) and Ertiga (post-2010, 1.3 L, BS-IV) diesel vehicles were equipped with common rail direct ignition (CRDI) engine, whereas Indica (post-2005, 1.4 L, BS-III) diesel vehicle equipped with direct ignition or compressed ignition (CI) (Table 9.1). For gasoline, old engines of Zen vehicle (post-2000, 1.0 L, BS-II) was equipped with spark ignition (SI) and new vehicles Swift Dzire (post-2005, 1.2 L, BS-III) and i10 (post-2005, 1.2 L, BS-IV) were found with multi-point fuel ignition (MPFI) (Table 9.1). In SI engines, the spark plug is used to adapt the combustion whereas CRDI engines are the direct injection of the fuel into the cylinders of a diesel engine from a single, common line. In gasoline-powered vehicles, the after-treatment device comprises three-way catalytic (TWC) and EGR. The function of TWC to reduce the Nitrogen Oxides (NO$_X$) to N$_2$ and O$_2$, and to react CO and HC, and converted into CO$_2$ and water (H$_2$O). In 3Ws-CNG, an old and new vehicle was found with SI and MPFI engines, which were equipped with carburetor and TWC as after-treatment devices. This catalyst converts all three harmful pollutants to harmless species (Haywood and Ramaswamy 1998).

Overall, nine 4W-passenger cars [4 diesel + 3 gasoline + 2 CNG, every 3 sets of the experiment] were performed for on-road experiments. Before each experiment, the vehicle engine is at rest for half an hour prior to being started [i.e. no vehicle soak time], therefore, in the present work, the emissions were considered as hot start condition only. The qualified drivers and a fixed traffic route of 10 km for ~45 min were used for on-road experiments in Delhi city. The traffic route was containing low and mixed traffic regions including 6 traffic signals. The vehicle speed was monitored

Table 9.1 Specification of tested vehicles for on-road experiments using AEMS

Vehicle model	Bharat stage norms	Year	Engine technology	After-treatment devices	Engine capacity (L)	Odometer reading (km)
Innova (N = 3)	BS-II	2004	CRDI	EGR[a]	2.4	185,032
Indica (N = 4)	BS-III	2007	CI	EGR	1.4	86,384
Swift Dzire (N = 3)	BS-IV	2012	CRDI	EGR + DOC	1.2	128,454
Ertiga (N = 6)	BS-IV	2014	CRDI	EGR + DOC	1.3	33,127
4W-gasoline						
Zen (N = 3)	BS-II	2001	SI	TWC + EGR	1.0	127,294
Swift Dzire (N = 3)	BS-III	2008	MPFI	TWC + EGR[b]	1.2	85,454
i10 (N = 3)	BS-IV	2010	MPFI	TWC + EGR[c]	1.2	46,550
4W-CNG						
Optra (N = 3)	BS-III	2006	SI	TWC + EGR	1.2	114,944
i10 (N = 3)	BS-IV	2010	MPFI	TWC + EGR[c]	1.2	46,956
3W-CNG						
Bajaj (N = 3)	BS-II	2008	SI	Carburetor + TWC	0.8	48,543
Bajaj (N = 3)	BS-III	2015	MPFI	Carburetor + TWC	0.8	14,817
2W-gasoline						
Caliber (N = 3)	BS-I	2001	SI	Carburetor	0.12	47,709
Activa (N = 3)	BS-II	2009	SI	Carburetor + TWC	0.12	28,543
Activa (N = 3)	BS-III	2014	SI	Carburetor + TWC	0.12	2973

Note N no. of the experiment; *CNG* compressed natural gas; *BS* Bharat stage; *EGR* exhaust gas recirculation; *TC* turbocharger; *DOC* diesel oxidation catalyst; *TWC* three-way catalytic converter
[a]EGR with cooler for diesel vehicle
[b]TWC + EGR with oxygen sensor heating capabilities for cold-start operation
[c]TWC + EGR with coupler catalyst

with pocket global positioning monitor (GPS, GarminModel 60 CSx). The vehicle speed ranged between 09 and 55 km h^{-1} with a mean speed of 25 km h^{-1} in Delhi city.

For 2Ws-gasoline and 3Ws-CNG, experiments were carried out on a stationary position by suspending the wheels with the help of jack. With the limitations of road friction and drag, 2Ws-gasoline and 3Ws-CNG vehicles were considered to be performed under no-load condition. In the present work, the driving cycle (108 s = one cycle) was followed Modified Indian Driving Cycle (MIDC) reported in ARAI (2008) it was repeated 20 times (total 10 cycles; 1080 s = 36 min) for the collection of adequate PM$_{2.5}$ mon the filter for chemical speciation analysis. Hence, the concentrations of 2Ws-gasoline and 3Ws-CNG were compared with earlier work and performed on engine dynamometer or stationary condition (Agarwal et al. 2015b; Aslam et al. 2006; Machacon et al. 2000).

Appropriate dilution of exhaust should be maintained during the measurement to accomplish complete gas-to-particle partitioning. In this work, the dilution ratio was calculated as the ratio of CO$_2$ concentration in the undiluted exhaust inside the duct and the diluted exhaust inside the dilution tunnel. The dilution ratio around 39–69 was found appropriate for complete gas-to-particle partitioning in separate experiments conducted with diesel vehicle operated on a chassis dynamometer under controlled laboratory conditions as discussed in Sect. 9.2.3.2. Significant particle losses were observed at the DRs lower than 39 and higher than 69. Therefore, during on-road experiments, the dilution ratio was maintained around DR 55 ± 11 by regulating the zero air. Out of 49 experiments 46 were finally selected based on appropriate dilution ratio, and rest three experiments were rejected due to high dilution ratio.

9.2.5 Gravimetric and Trace Metal Analysis

For gravimetric analysis, the Teflon filters were conditioned under controlled temperature (25 °C) and relative humidity (RH; 50%) for 24 h before and after the sampling. The before and after sampling, the filters were weighed using a microbalance (Sartorious, CPA2P-F). Gravimetrically PM$_{2.5}$ concentrations were calculated by the difference between post and pre-weight of the filters and dividing by sampled exhaust volume. Six Teflon filters (3 field + 3 dynamic) were considered as blank and subjected to same pre-and post-conditioning protocol.

For trace metal analysis, half of the Teflon filter was cut into several pieces and kept in a beaker. Twenty millilitre (ml) nitric acid (70% Supra Pure, Merck GR Grade) was added into a beaker and was heated for ~2 h at 180 °C until the nitric acid gets evaporate. The remaining amount was filtered with 0.22 µm MilliPore PTFE filter and mixed Milli-Q water to make up to 100 ml and then it is subjected to further metals analysis (Gupta et al. 2011; Herlekar et al. 2012). Seventeen trace metals (Al, Ag, As, Ba, Co, Cd, Cr, Cu, Fe, Mn, Ni, Pb, Se, Sr, Ti, V, and Zn) were analyzed using Inductively Coupled Plasma–Mass Spectrometer (ICP-MS, Agilent, 7900). The trace metals mass on dynamic and field blank filters were found in the

range of 0.2–22% of the mass is determined on samples. The blank filter mass was used to correct the trace element concentration.

9.2.6   Human Health Risk Estimation

The human health risk was assessed based on average mass concentrations of trace metals from on-road experiments, which is especially useful in understanding the health hazard associated with inhalation exposure to $PM_{2.5}$ emitted from diesel, gasoline, and CNG vehicles. During on-road emissions, the exhaust gets rapid dilution and dispersion after exiting the tail pipe. Therefore, human exposure should be calculated for ambient concentration after dilution. Similarly, in the present work, on an average 55 ± 11 times diluted particle collected on filter papers and detected metals concentrations and used for health risk estimates. Since inhalation is typically the main path to direct exposure to $PM_{2.5}$-bound metals. Therefore, this work examined the health risks associated with particle-bound trace metals over inhalation only.

9.2.6.1   Average Daily Dose

In the present work, the average daily dose (ADD) was estimated for particle-bound metals for inhalation route only, and following Singh and Gupta (2016). The $PM_{2.5}$ exposure was estimated in terms of lifetime average daily dose (ADD_{inh} in mg kg^{-1} day^{-1}). This can be expressed as follows:

$$ADD_{inh} = \frac{C \times IR \times CF \times EF \times ED}{BW \times AT_n} \tag{9.8}$$

where C is the concentration of the particle-bound metals (reported in μg m^{-3}), IR is the inhalation rate, CF is a correction factor as 0.001, EF is the exposure frequency (days year^{-1}), ED is the exposure duration during lifetime (in years), BW is the body weight and AT_n is the average time (in days). All values were assumed according to the Human Health Evaluation Manual (Part A and F) (USEPA 2004, 2009), and given in Table 9.2.

9.2.6.2   Non-carcinogenic Risk

Hazard quotient (HQ) and Hazard index (HI) are used to quantitatively represent the non-carcinogenic risk from species or pollutants. The hazard quotient (HQ) can be determined by Eq. (9.9) using average daily dose (ADD_{inh} in mg kg^{-1} day^{-1}) and reference exposure level (RfD_{inh}) for the inhabitants taken from USEPA (2016a).

Table 9.2 Parameters and reference value used for determining non-carcinogenic and carcinogenic risk due to inhalation

Parameter	Definition	Units	Value	
			Children	Adult
IR[a]	Inhalation rate	m^3 day^{-1}	10	20
EF[b]	Exposure frequency	days year^{-1}	350	350
ED[a]	Exposure duration	years	6	24
BW[b]	Body weight	kg	15	70
AT$_n$[a]	Average time	days	365*ED	365*ED
ET[*]	Exposure time	h day^{-1}	10	10
Trace metals	RfD$_{inh}^c$ (mg kg^{-1} day^{-1})	[d]IUR (μg m^{-3})$^{-1}$		
Cr(VI)[$]	2.86E−05	0.012		
Cu	4.02E−02	–		
Mn	1.43E−05	–		
Ni	3.52E−03	0.00024		
Pb	3.52E−03	0.000012		
Zn	3.01E−01	–		
As	3.0E−04	0.0043		
Cd	1.0E−03	0.0018		
V	7.0E−03	–		

[a]USEPA (2011)
[b]USEPA (2013)
[c]USEPA (2016b)
[d]USEPA (2016b)
[*]Exposure time is used in the present study 2 h day^{-1}
[$]Cr(VI) concentration is 1/7 of total Cr

$$HQ = \frac{ADD_{inh}}{RfD_{inh}} \tag{9.9}$$

The HQ $\leq$ 1 indicates no adverse health effects and HQ > 1 which describes likely to non-carcinogenic effects (USEPA 2016a). Hazard Index (HI) is the summation of all (HQ) estimated for different species calculated using Eq. (9.10) following Zheng et al. (2010). If the value of HI $\leq$ 1, it is ideally believed that there is no non-carcinogenic risk, while HI > 1, it means there is a significant chance of non-carcinogenic risk.

$$HI = \sum_{i=1}^{i=n} HQ_1 + HQ_2 + HQ_3 \cdots HQ_i; \quad i = 1^{st} \text{ to } n^{th} \text{ element} \tag{9.10}$$

9.2.6.3 Carcinogenic Risk

The carcinogenic risk (in terms of Excess cancer risk; ECR) can be assessed and it is defined as the incremental probability of emerging cancer cell due to exposure of carcinogen over a lifetime. The ECR can be articulated as the following equation:

$$ECR = \frac{C \times EF \times ET \times ED \times IUR}{AT} \tag{11}$$

where C is the average concentration of particle-bound metals (in $\mu g\ m^{-3}$), EF is the exposure frequency (days $year^{-1}$), ET is the exposure time (2 h day^{-1}), ED is the exposure duration (assumed to be 24 and 6 years for adults and children), AT_n is average time [(AT_n = years $\times$ 365 days $\times$ 24 h day^{-1}); assumed 70 and 15 years for adults and children]. Inhalation Unit Risk [IUR in $(\mu g/m^3)^{-1}$] of particle-bound metals (Table 9.2) were obtained from USEPA with the Integrated Information Risk System (https://www.epa.gov/iris) of USEPA.

The range of ECR has been reported by the USEPA (2009) for public health, and suggested The ECR value < 10^{-6}; it is ideally recommended as safe and ECR ~ 10^{-4} is considered as a tolerable risk, while ECR value > 10^{-4}, it means there is significant high risk. In present work, the ECR was calculated only for Pb, Cr, and Ni which are well known inhaling carcinogens.

9.3 Results and Discussion

9.3.1 Trace Metals Concentration

Total 17 trace metals (Al, Ag, As, Ba, Co, Cd, Cr, Cu, Fe, Mn, Ni, Pb, Se, Sr, Ti, V, and Zn) were detected, whereas selenium (Se) was found in NAs or below detection limit (BDL) in on-road vehicles experiments, while 28 samples out of 46, Aluminium (Al) was detected as BDL. Interestingly, trace metal concentrations were highest from 4W-CNG ($76 \pm 4\ \mu g\ m^{-3}$) followed by 3W-CNG ($62.5 \pm 15.4\ \mu g\ m^{-3}$), 2W-gasoline ($60 \pm 21\ \mu g\ m^{-3}$), 4W gasoline ($57 \pm 16\ \mu g\ m^{-3}$), and were lowest from 4W-diesel ($56 \pm 8\ \mu g\ m^{-3}$) (Fig. 9.4). It is noteworthy that the concentrations of all trace metals except Fe, Zn, Al, and Pb in present work were close to previous values ($3–10\ \mu g\ m^{-3}$) reported in the previous work (Geller et al. 2006; Alves et al. 2015a; ARAI 2008; Schauer et al. 2002).

The major trace metals (Fe, Zn, Al, and Pb) were higher compared to previously reported values ($40–200\ \mu g\ m^{-3}$) from diesel and biodiesel (Betha and Balasubramanian 2011, 2013). The diesel fuel and lubricant oil composition are examined by Agarwal et al. (2011) which shows diesel and lubricant oil contain high Ca, Zn, Mg, Ni and Fe in Indian fuel and it could be the possible reason which possibly due to in high concentration of these particle-bound metals in the 4Ws-diesel vehicle.
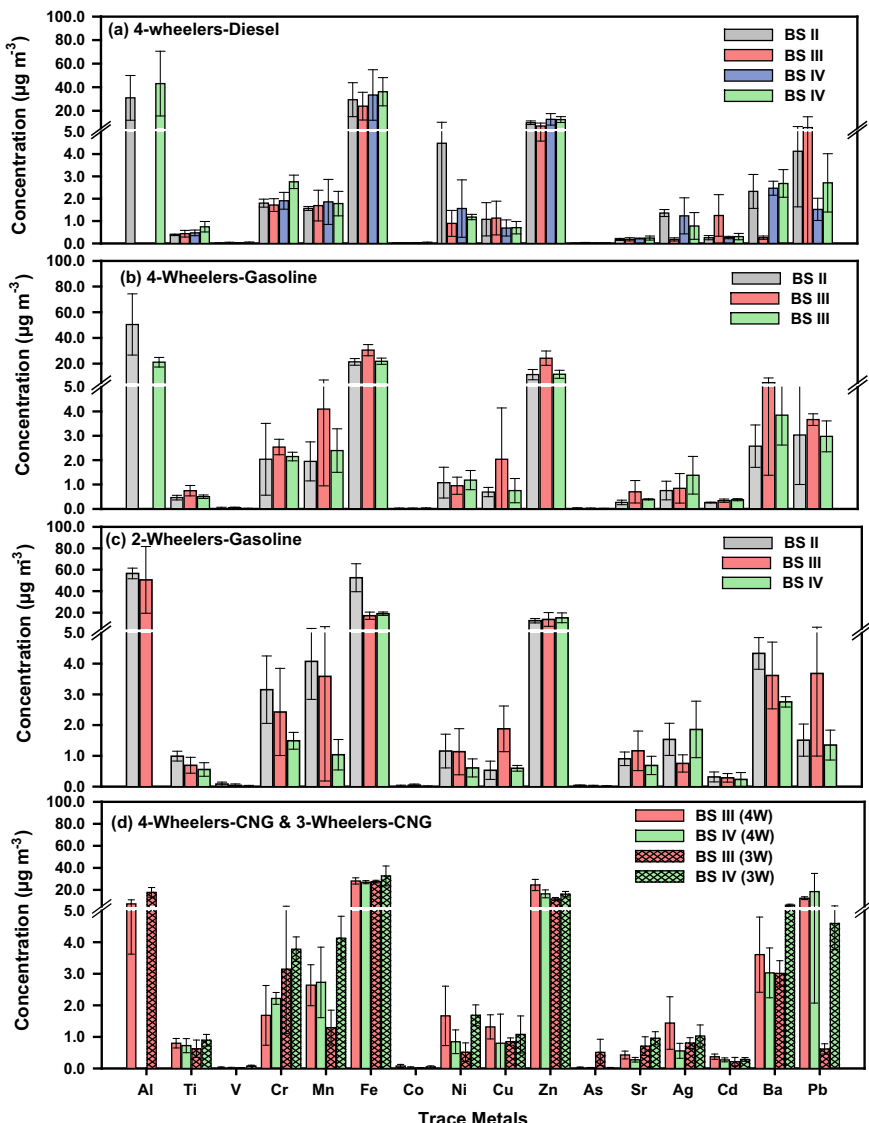
Fig. 9.4 Trace metals concentration of **a** 4-wheelers diesel; **b** 4-wheelers gasoline; **c** 2-wheelers; and **d** 4-wheelers-CNG and 3-wheelers-CNG in tail pipe exhaust

The high amount of Fe and Al can also be originated from abrasion of vehicle parts such as piston rings, valve, and cylinder liner (Agarwal et al. 2015b; Ulrich et al. 2012) and the aging of catalytic converter (Shukla et al. 2017b; Dallmann et al. 2014; Kam et al. 2012; Liati et al. 2013). The high load of zinc is mixed in lubricant oil, and antioxidant and anti-wear additive agent like Zinc-di-alkyl-di-thio phosphate (ZDDP) is used in lube oil (Alves et al. 2015a; Spikes 2004; Spencer et al. 2006). Lead (Pb) is originated in the wear of metal alloys and previous studies have been shown as contamination in diesel fuel (Dallmann et al. 2014; Chakraborty and Gupta 2010; Fabretti et al. 2009; Shukla et al. 2016). In 4Ws-diesel vehicles, the percentage of the relative contribution of trace metals were ranged 1.7–9.1%, which was higher than the range (2–5%) reported in the previous studies (Geller et al. 2006; ARAI 2009; Kam et al. 2012; Chiang et al. 2012; Kim Oanh et al. 2009; Schauer et al. 1999). Among 4Ws-gasoline vehicles, the trace metals concentrations were consistent with the age group of the vehicle (Fig. 9.4b). For 4Ws-gasoline, the concentration of trace metals was 2–4 times higher than previous studies (Geller et al. 2006; ARAI 2008; Chiang et al. 2012; Kim Oanh et al. 2009; Schauer et al. 1999) and they were contributed in the range 2.6–8.3% of $PM_{2.5}$, whereas the remaining trace metal contributions ranged between 0.5 and 2.0% of $PM_{2.5}$ and these ranges was close to percentage contribution of $PM_{2.5}$ reported in the literature. The 2Ws-gasoline showed a decrease in trend with age group of vehicles (see Fig. 9.4c). For 2Ws-gasoline, the percentage contribution of trace metals to $PM_{2.5}$ emissions was ranged between 10 and 12% and it was close to values (8–15%) examined by ARAI (2008, 2009). The percentage contribution of trace metals to $PM_{2.5}$ emissions from 3W-CNG and 4W-CNG vehicles was observed in the range of 11–13%. Again 4Ws-CNG the trace metals concentrations were consistent with age, while for 3Ws-CNG, major metals Fe, Zn, and Ba (Fig. 9.4d) varied with age.

Among trace elements, Fe and Zn have observed the highest percentage contribution to $PM_{2.5}$ in the range between 0.3 and 0.4%. Fe is mainly originated from motorised scrape of the engine and its parts (Agarwal et al. 2015a; Liati et al. 2013). The abundance of Zn is found in fuel as well as lubricant oil (Geller et al. 2006; Alves et al. 2015a; Agarwal et al. 2015a; Spencer et al. 2006). Other metals such as Cr, Cu, Fe, and Ni is also released from fuel combustion. Barium [Ba], and their oxides (barium carbonate) were also used as additives in nozzle and valves of the vehicles (Vouitsis et al. 2005). Further, Cr and Cd are also produced from engine parts (Alves et al. 2015a; Shukla et al. 2016; Gangwar et al. 2011; Gangwar et al. 2012) due to a lack of automated maintenance.

9.3.2 Human Health Risk Assessment

In the present work, 9 trace metals were considered as non-carcinogenic (As, Cd, Cr, Cu, Mn, Ni, Pb, V, and Zn) and 5 metals (As, Cd, Cr, Ni, and Pb) were considered as carcinogenic.

9.3.2.1 Average Daily Dose (ADD$_{inh}$)

The ADD$_{inh}$ of trace metals for adults and children is illustrated in Fig. 9.5a–e. The mean value of ADD$_{inh}$ for adults and children showed a decreasing trend in the following order: Zn > Pb > Mn > Cr > Ni > Cu > Cd > As > V for gasoline and CNG
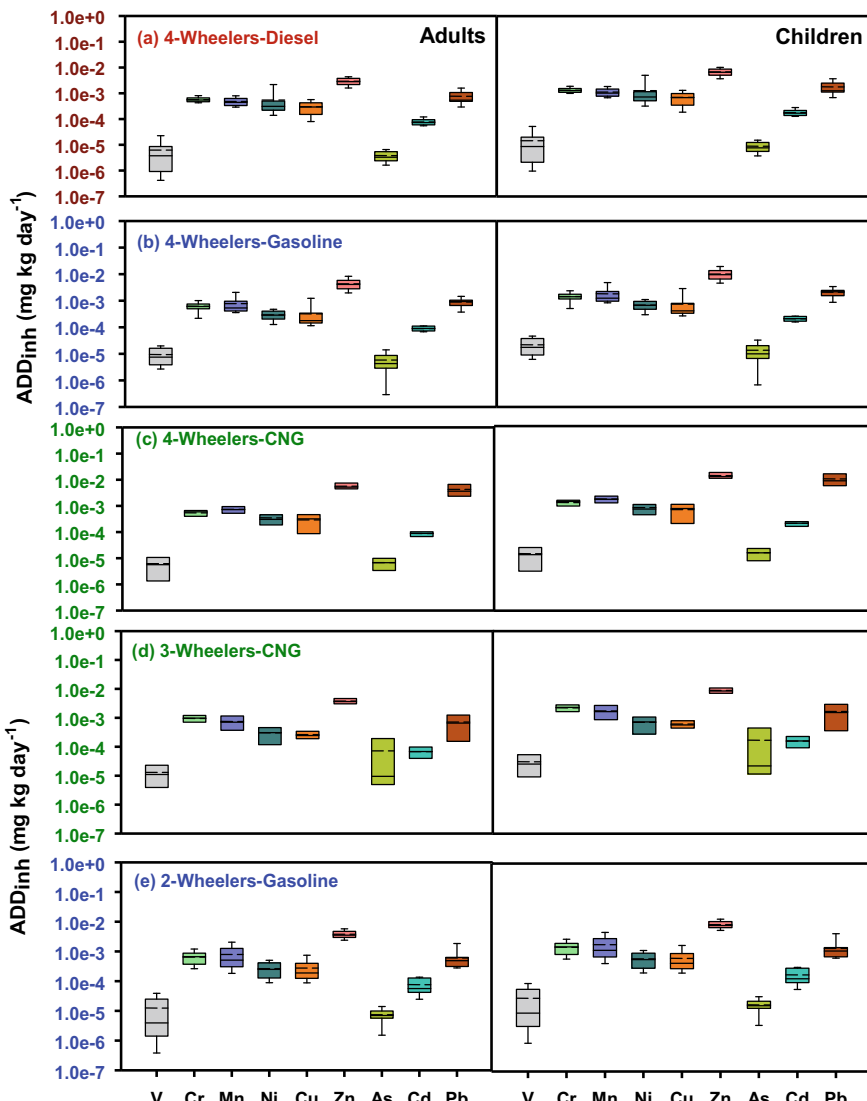

Fig. 9.5 Average daily dose (ADD$_{inh}$) of metals (mg kg^{-1} day^{-1}) on PM$_{2.5}$ for adults (left panel) and children (right panel) from **a** 4-wheelers diesel; **b** 4-wheelers gasoline; **c** 4-wheelers-CNG 2-wheelers; **d** 3-wheelers-CNG; **e** 2-wheelers gasoline

vehicles, while the order was found as Zn > Pb > Cr > Ni > Mn > Cu > Cd > V>As for diesel vehicle. The (ADD_{inh}) of Ni from 4W diesel vehicle was found to be high (~1.8 folds) as compared to (ADD_{inh}) of Ni of gasoline and CNG powered vehicles. The ADD_{inh} of Cr from gasoline and CNG vehicles were observed high (~1.6 times) as compared to diesel-powered vehicles. ADD_{inh} of Pb from 4W-CNG was observed to be 3.4 and 2.0 times higher than 3W-CNG and 2W-Gasoline vehicles. It is important to note that mean ADD_{inh} for children of metals including Cr, Mn, Ni, Cu, Zn and Pb in $PM_{2.5}$ were observed 2 times greater than mean ADD_{inh} for Adults. There was no significant difference ($p > 0.05$) observed between ADD_{inh} value of 4W Diesel and 4W-Gasoline for V, Cr, Mn, Cu, while significant difference ($p < 0.05$) in ADD_{inh} was observed for Zn and Pb emitted from 4W Diesel and 4W-CNG.

9.3.2.2 Non-carcinogenic Risk

Non-carcinogenic risk (in terms of HQs and HIs) for children and adults from on-road diesel, gasoline, and CNG vehicles were shown in Fig. 9.6a–e. The cumulative HIs from all vehicle were two times higher for children than for adults. Amongst non-carcinogenic metals, the mean level of HQ for both inhabitants (adults and children) showed in declining trend: Mn > Cr > Ni > Pb > Cd > Zn > As > Cu > V. For 4W-diesel vehicles, the HQ of Ni was 2 times higher than 4W-gasoline, 4W-CNG, 3W-CNG, and 2W-gasoline ($p < 0.05$) vehicles, however, other particle-bound metals such as Mn, Cr were found to be 1.6 times lower than 4W-gasoline, 4W-CNG, 3W-CNG, and 2W-gasoline vehicles. Interestingly, for adults and children, non-carcinogenic risk (HQ) was close to 1 for As, Cd, Cu, Ni, Pb, and Zn, while the HQs for Cr and Mn surpassed HQ > 1 (Fig. 9.6a–e) for all type of vehicles. For children, the average HI values were found in the following order: 3W-CNG > 2W-gasoline > 4W-gasoline > 4W-CNG > 4W-diesel. This indicates that possible non-carcinogenic risk due to exposure from vehicle tail pipe, abrasion of vehicle parts, which is a potential threat to inhabitants working near roads (Fig. 9.6).

This study also compared well with recent studies (Betha and Balasubramanian 2011, 2013) reported the non-carcinogenic risk of particle-bound trace metals of $PM_{2.5}$ for stationary diesel engine, biodiesel and ultra-low sulfur diesel (ULSD). Previous studies estimated HQs, and HIs using chronic daily intake (CDI), therefore present work also calculated CDI, HQs, and HIs for better comparison with previous studies. In this study, we also estimated chronic daily intake (CDI), HQs and HIs and compared with previous studies (Fig. 9.7). The present mean $\sum HQ$ was close to previously reported for ULSD engine and 36% (69 and 161 for adults and children) lower than Bio-diesel (114 and 270 for adults and children) engine for both adults and children. This shows the severity of risk from toxic metals from tail-pipe emissions in diesel, gasoline, and CNG vehicles. The composition of fuel and engine type are resulting in different level of metals emissions and their risk. It should also be noted that on-road emission and their particle bound metals could be diverse from stationary and idle tail pipe emission possibly due to the road, traffic, and driver characteristic.
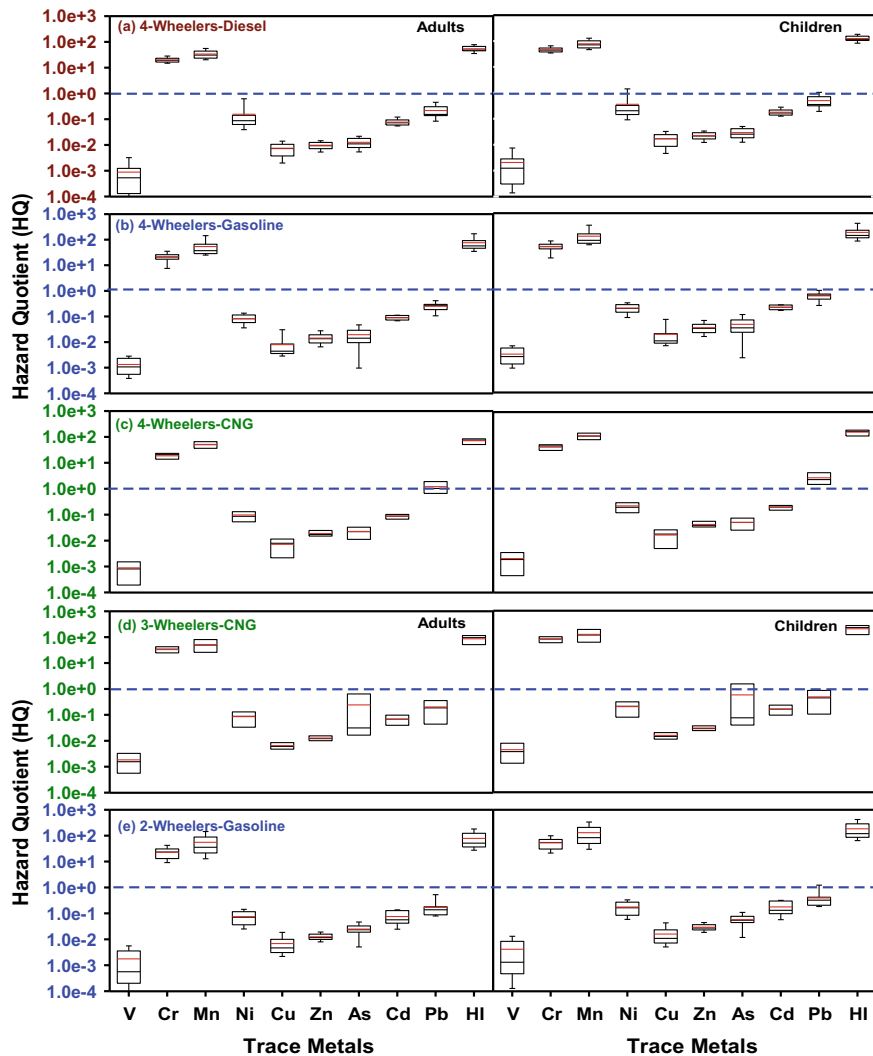
Fig. 9.6 Non-carcinogenic risks of particle-bound metals in PM$_{2.5}$ for adults (left panel) and children (right panel) from **a** 4-wheelers diesel; **b** 4-wheelers gasoline; **c** 4-wheelers-CNG; **d** 3-wheelers-CNG; **e** 2-wheelers gasoline
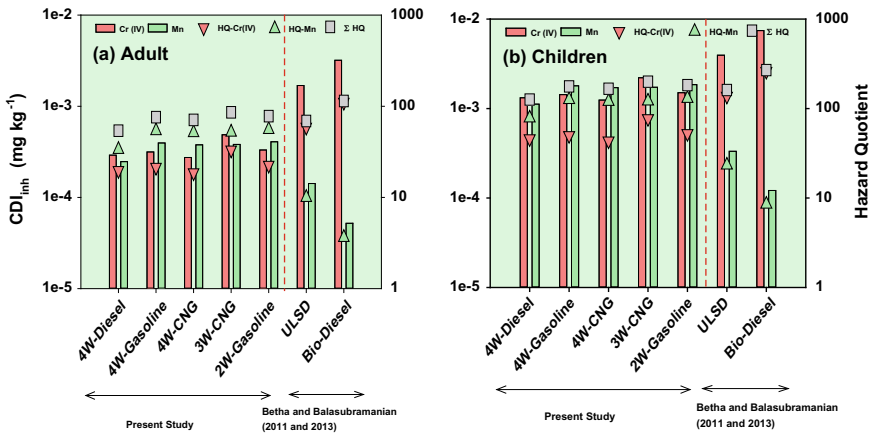
Fig. 9.7 The non-carcinogenic risk for adults (**a**) and children (**b**) in the present study and compared with previous studies (Betha and Balasubramanian 2011, 2013). Primary y-axis: bar line designates as chronic daily intake (CDI). Secondary y-axis: triangle and square represent HQs and $\sum$HQs for of present study and previous studies. The red dotted line and arrow split the present study and previous studies

9.3.2.3   Carcinogenic Risk

In the present work, carcinogenic risk (in terms of ECR) of trace metals were estimated for the diesel, gasoline, and CNG vehicles and presented in Fig. 9.8a–e. The sum of ECR for adults was estimated as 738×10^{-6}, 794×10^{-6}, 832×10^{-6}, 696×10^{-6}, and 1239×10^{-6} for 4W-diesel, 4W-gasoline, 2W-gasoline, 4W-CNG, and 3W-CNG powered vehicles, respectively. The value of ECR for adults was showed four times higher than the value of ECR for children. The average value of ECR for Cr was showed 7–12 times higher than the acceptable limit for adults, and also 2–3 times larger than the acceptable limit for children. Significantly, the ECR value of Cr in 3Ws-CNG vehicles was estimated at 1186×10^{-6}, which was 1.5–1.8 times higher than the 4Ws-diesel and 4Ws-gasoline vehicle for both inhabitants. In 4Ws-CNG, the ECR value of Pb was marginally higher than the other vehicles. However, the mean value of ECR from Ni, As, Cd, and Pb were showed in the range of 10^{-6}–10^{-4} for all type of vehicles (Fig. 9.8).

In the present work, the ECR from Cr for adults for diesel, gasoline, CNG vehicles are 12–24 times lower than previous work reported by Betha and Balasubramanian (2011, 2013) for ULSD and Bio-diesel engine exhaust at stationary conditions (Fig. 9.9a, b). Overall, the observed ECR values of vehicles exceed the acceptable level and suggesting that it is an alarming condition to the inhabitants of India, which works near the road. It is anticipated that the increased lung cancer mortality can arise amongst inhabitant close to road or traffic tail pipe emissions in urban cities due to inhalation of particulate-bound trace metals.
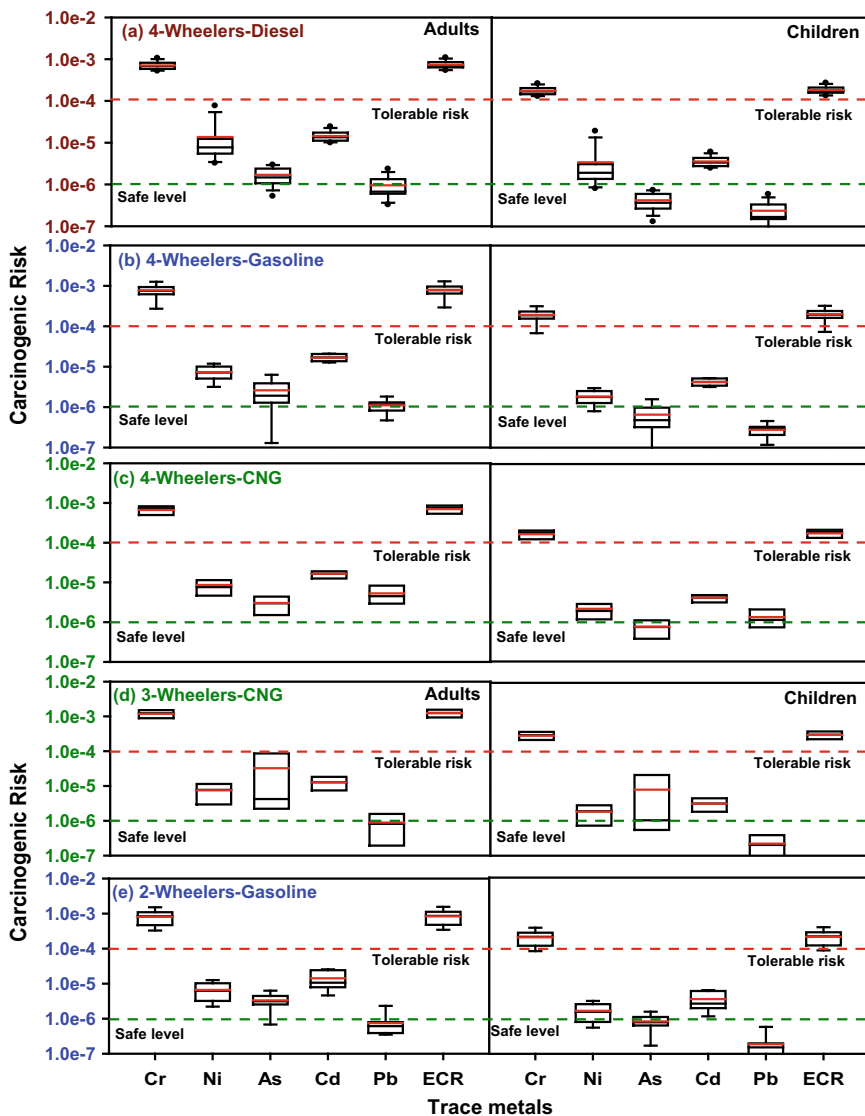
Fig. 9.8 Carcinogenic risk (as in ECR) of particle-bound metals in PM$_{2.5}$ for adults (left panel) and children (right panel) from **a** 4-wheelers diesel; **b** 4-wheelers gasoline; **c** 4-wheelers-CNG 2-wheelers; **d** 3-wheelers-CNG; **e** 2-wheelers gasoline
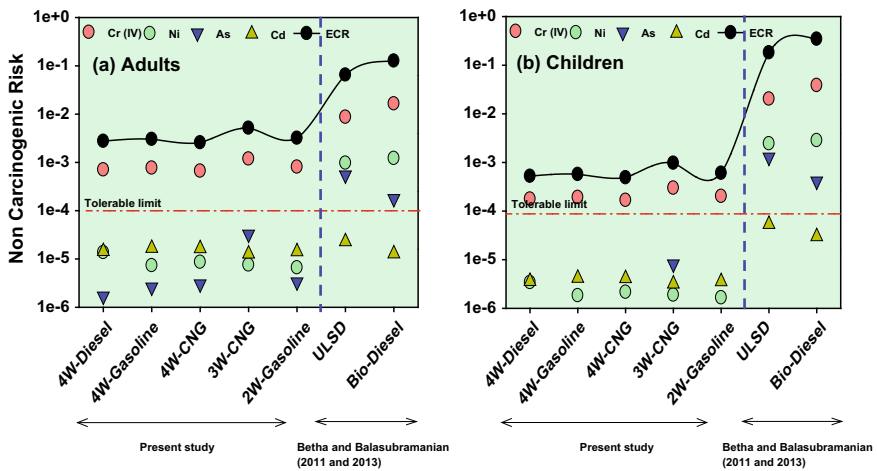
Fig. 9.9 The carcinogenic risk for adults (**a**) and children (**b**) in the present study and compared with previous studies (Betha and Balasubramanian 2011, 2013). The blue dotted line and arrow split the present study and previous studies

9.4 Conclusion

This study presents the concentration of $PM_{2.5}$ bound trace metals emitted from the diesel, gasoline, and CNG vehicles during on-road experiments. The total trace metal emission was highest from 4W-diesel. The emissions of toxic metals such as Zn, Cr, Pb were higher from 4W-CNG and 3W-CNG vehicles compared to 4W-diesel, and 4Ws/2Ws-gasoline. The concentration of Al, Fe, Mn, Ni, As, and Cd were highest from 4W-diesel and gasoline vehicles. Health risk assessment of the $PM_{2.5}$ bound trace metals showed that non-carcinogenic risks by Cr, and Mn, which exceeded the safe limit. The ECR of Cr was higher than the tolerance limit (10^{-4}), while ECRs from Ni, As, Cd, and Pb was higher than the safe limits (10^{-6}) for all types of vehicles. Additionally, it was found that the risk associated with PM emitted from 4Ws/3Ws-CNG vehicles were significantly higher compared to the risk associated with 4Ws-diesel/gasoline vehicles emissions. The present work suggests rationally robust benchmarking on emissions of $PM_{2.5}$ bound trace metals their health risk from on-road vehicles in the Indian context. Nevertheless, the present study assessed the carcinogenic risk of particle-bound metals, but other carcinogenic compounds such as poly-aromatic hydrocarbons (PAHs) and Per-fluorinated compounds (PFCs) were not included in the risk assessment.

References

Agarwal AK, Gupta T, Kothari A (2011) Particulate emissions from biodiesel vs diesel fuelled compression ignition engine. Renew Sustain Energy Rev 15:3278–3300. https://doi.org/10.1016/j.rser.2011.04.002

Agarwal AK, Gupta T, Bothra P, Shukla PC (2015a) Emission profiling of diesel and gasoline cars at a city traffic junction. Particuology 18:186–193. https://doi.org/10.1016/j.partic.2014.06.008

Agarwal AK, Bothra P, Shukla PC (2015b) Particulate characterization of CNG fuelled public transport vehicles at traffic junctions. Aerosol Air Qual Res 15:2168–2174. https://doi.org/10.4209/aaqr.2015.02.0084

Alves CA, Barbosa C, Rocha S, Calvo A, Nunes T, Cerqueira M, Pio C, Karanasiou A, Querol X (2015a) Elements and polycyclic aromatic hydrocarbons in exhaust particles emitted by light-duty vehicles. Environ Sci Pollut Res 22:11526–11542. https://doi.org/10.1007/s11356-015-4394-x

Alves CA, Gomes J, Nunes T, Duarte M, Calvo A, Custódio D, Pio C, Karanasiou A, Querol X (2015b) Size-segregated particulate matter and gaseous emissions from motor vehicles in a road tunnel. Atmos Res 153:134–144. https://doi.org/10.1016/j.atmosres.2014.08.002

ARAI (2008) Emission factor development for Indian vehicles. In: Air quality monitoring project-Indian clean air programme. The Automotive Research Association of India, Pune

ARAI (2009) Source profiling for vehicular emissions. In: Air quality monitoring project-Indian clean air programme. The Automotive Research Association of India, Pune. http://www.cpcb.nic.in/Source_Profile_Vehicles.pdf

Aslam MU, Masjuki HH, Kalam MA, Abdesselam H, Mahlia TMI, Amalina MA (2006) An experimental investigation of CNG as an alternative fuel for a retrofitted gasoline vehicle. Fuel 85:717–724. https://doi.org/10.1016/j.fuel.2005.09.004

Baron PA, Willeke K (1993) Aerosol measurement: principles, techniques, and applications. Van Nostrand Reinhold, New York

Betha R, Balasubramanian R (2011) Emissions of particulate-bound elements from stationary diesel engine: characterization and risk assessment. Atmos Environ 45:5273–5281. https://doi.org/10.1016/j.atmosenv.2011.06.060

Betha R, Balasubramanian R (2013) Emissions of particulate-bound elements from biodiesel and ultra low sulfur diesel: size distribution and risk assessment. Chemosphere 90:1005–1015. https://doi.org/10.1016/j.chemosphere.2012.07.052

Betha R, Balasubramanian R, Engling G (2012) Physico-chemical characteristics of particulate emissions from diesel engines fuelled with waste cooking oil derived biodiesel and ultra low sulphur diesel. Biodiesel Feed Prod Appl. https://doi.org/10.5772/53476

Chakraborty A, Gupta T (2010) Chemical characterization and source apportionment of submicron (PM$_1$) aerosol in Kanpur Region, India. Aerosol Air Qual Res 10:433–445. https://doi.org/10.4209/aaqr.2009.11.0071

Chiang HL, Lai YM, Chang SY (2012) Pollutant constituents of exhaust emitted from light-duty diesel vehicles. Atmos Environ 47:399–406. https://doi.org/10.1016/j.atmosenv.2011.10.045

Dallmann TR, Onasch TB, Kirchstetter TW, Worton DR, Fortner EC, Herndon SC, Wood EC, Franklin JP, Worsnop DR, Goldstein AH, Harley RA (2014) Characterization of particulate matter emissions from on-road gasoline and diesel vehicles using a soot particle aerosol mass spectrometer. Atmos Chem Phys 14:7585–7599. https://doi.org/10.5194/acp-14-7585-2014

Dutkiewicz VA, Alvi S, Ghauri BM, Choudhary MI, Husain L (2009) Black carbon aerosols in urban air in South Asia. Atmos Environ 43:1737–1744. https://doi.org/10.1016/j.atmosenv.2008.12.043

Fabretti J-F, Sauret N, Gal J-F, Maria P-C, Schärer U (2009) Elemental characterization and source identification of PM$_{2.5}$ using positive matrix factorization: the Malraux road tunnel, Nice, France. Atmos Res 94:320–329. https://doi.org/10.1016/j.atmosres.2009.06.010

Gangwar J, Gupta T, Gupta S, Agarwal AK (2011) Emissions from diesel versus biodiesel fuel used in a CRDI SUV engine: PM mass and chemical composition. Inhal Toxicol 23:449–458. https://doi.org/10.3109/08958378.2011.582189

Gangwar JN, Gupta T, Agarwal AK (2012) Composition and comparative toxicity of particulate matter emitted from a diesel and biodiesel fuelled CRDI engine. Atmos Environ 46:472–481. https://doi.org/10.1016/j.atmosenv.2011.09.007

Geller MD, Ntziachristos L, Mamakos A, Samaras Z, Schmitz DA, Froines JR, Sioutas C (2006) Physicochemical and redox characteristics of particulate matter (PM) emitted from gasoline and diesel passenger cars. Atmos Environ 40:6988–7004. https://doi.org/10.1016/j.atmosenv.2006.06.018

Grahame TJ, Schlesinger RB, Möhner M, Wendt A, Grahame TJ, Schlesinger RB (2010) Cardiovascular health and particulate vehicular emissions: a critical evaluation of the evidence. Air Qual Atmos Health 3:3–27. https://doi.org/10.1007/s11869-009-0047-x

Grieshop AP, Boland D, Reynolds CCO, Gouge B, Apte JS, Rogak SN, Kandlikar M (2012) Modeling air pollutant emissions from Indian auto-rickshaws: model development and implications for fleet emission rate estimates. Atmos Environ 50:148–156. https://doi.org/10.1016/j.atmosenv.2011.12.046

Gupta T, Jaiprakash, Dubey S (2011) Field performance evaluation of a newly developed PM$_{2.5}$ sampler at IIT Kanpur. Sci Total Environ 409:3500–3507. https://doi.org/10.1016/j.scitotenv.2011.05.020

Gupta T, Chakraborty A, Ujinwal K (2010) Development and performance evaluation of an indigenously developed air sampler designed to collect submicron aerosol. Ann Indian Natl Acad Eng 7:189–193

Habib G, Venkataraman C, Bond TC, Schauer JJ (2008) Chemical, microphysical and optical properties of primary particles from the combustion of biomass fuels. Environ Sci Technol 42. https://doi.org/10.1021/es800943f

Hao X, Zhang X, Cao X, Shen X, Shi J, Yao Z (2018) Characterization and carcinogenic risk assessment of polycyclic aromatic and nitro-polycyclic aromatic hydrocarbons in exhaust emission from gasoline passenger cars using on-road measurements in Beijing, China. Sci Total Environ 645:347–355. https://doi.org/10.1016/j.scitotenv.2018.07.113

Harsha S, Khakharia P, Huizinga A, Monteiro J, Vlugt JH (2019) In-situ experimental investigation on the growth of aerosols along the absorption column in post combustion carbon capture. Int J Greenh Gas Control 85:86–99. https://doi.org/10.1016/j.ijggc.2019.02.012

Haywood JM, Ramaswamy V (1998) Global sensitivity studies of the direct radiative forcing due to anthropogenic sulfate and black carbon aerosols. J Geophys Res Atmos 103:6043–6058. https://doi.org/10.1029/97JD03426

Herlekar M, Joseph AE, Kumar R, Gupta I (2012) Chemical speciation and source assignment of particulate (PM$_{10}$) phase molecular markers in Mumbai. Aerosol Air Qual Res 12:1247–1260. https://doi.org/10.4209/aaqr.2011.07.0091

Hinds WC (1982) Aerosol technology: properties, behavior, and measurement of airborne particles. Wiley, New York

Jaiprakash, Habib G (2017) Chemical and optical properties of PM$_{2.5}$ from on-road operation of light duty vehicles in Delhi city. Sci Total Environ 586:900–916

Jaiprakash, Habib G (2018) A technology-based mass emission factors of gases and aerosol precursor and spatial distribution of emissions from on-road transport sector in India. Atmos Environ 180:192–205. https://doi.org/10.1016/j.atmosenv.2018.02.053

Jaiprakash, Habib G, Kumar S, Habib G, Kumar S, Kumar S (2016) Evaluation of portable dilution system for aerosol measurement from stationary and mobile combustion sources. Aerosol Sci Technol 50:717–731. https://doi.org/10.1080/02786826.2016.1178502

Kam W, Liacos JW, Schauer JJ, Delfino RJ, Sioutas C (2012) On-road emission factors of PM pollutants for light-duty vehicles (LDVs) based on urban street driving conditions. Atmos Environ 61:378–386. https://doi.org/10.1016/j.atmosenv.2012.07.072

Kelly FJ (2003) Oxidative stress: its role in air pollution and adverse health effects

Kim Oanh NT, Thiansathit W, Bond TC, Subramanian R, Winijkul E, Paw-Armart I (2009) Compositional characterization of PM$_{2.5}$ emitted from in-use diesel vehicles. Atmos Environ 44:15–22. https://doi.org/10.1016/j.atmosenv.2009.10.005

Liati A, Schreiber D, Dimopoulos Eggenschwiler P, Arroyo Rojas Dasilva Y (2013) Metal particle emissions in the exhaust stream of diesel engines: an electron microscope study. Environ Sci Technol 47:14495–14501. https://doi.org/10.1021/es403121y

Lipsky EM, Robinson AL (2005) Design and evaluation of a portable dilution sampling system for measuring fine particle emissions. Aerosol Sci Technol 39:542–553. https://doi.org/10.1080/027868291004850

Lipsky EM, Robinson AL (2006) Effects of dilution on fine particle mass and partitioning of semivolatile organics in diesel exhaust and wood smoke. Environ Sci Technol 40:155–162. https://doi.org/10.1021/es050319p

Lovett CD (2018) Toxicity of urban particulate matter: long-term health risks, influences of surrounding geography, and diurnal variation in chemical composition and the cellular oxidative stress response. Faculty of the Graduate School

Machacon HTCC, Yamagata T, Sekita H, Uchiyama K, Shiga S, Karasawa T, Nakamura H (2000) CNG operation of a two-stroke, two-cylinder marine S.I. engine and its characteristics of self-ignition combustion. JSAE Rev 21:567–572. https://doi.org/10.1016/s0389-4304(00)00078-3

Matti Maricq M, Maricq MM (2007) Chemical characterization of particulate emissions from diesel engines: a review. J Aerosol Sci 38:1079–1118. https://doi.org/10.1016/j.jaerosci.2007.08.001

Reynolds CCO, Grieshop AP, Kandlikar M (2011) Climate and health-relevant emissions from in-use Indian three-wheelers fueled by natural gas and gasoline. Environ Sci Technol 45:2406–2412. https://doi.org/10.1021/es102430p

Rezaei F, Webley P (2009) Optimum structured adsorbents for gas separation processes. Chem Eng Sci 64:5182–5191. https://doi.org/10.1016/j.ces.2009.08.029

Ruthven DM, Farooq S, Knaebe KS (1994) Pressure swing adsorption. VCH Publishers, New York

Schauer JJ, Kleeman MJ, Cass GR, Simoneit BRT (1999) Measurement of emissions from air pollution sources. 2. C$_1$ through C$_{30}$ organic compounds from medium duty diesel trucks. Environ Sci Technol 33:1578–1587. https://doi.org/10.1021/es980081n

Schauer JJ, Kleeman MJ, Cass GR, Simoneit BRT (2002) Measurement of emissions from air pollution sources. 5. C$_1$–C$_{32}$ organic compounds from gasoline-powered motor vehicles. Environ Sci Technol 36:1169–1180. https://doi.org/10.1021/es0108077

Schwarze PE, Totlandsdal AI, Låg M, Refsnes M, Holme JA, Øvrevik J (2013) Inflammation-related effects of diesel engine exhaust particles: studies on lung cells in vitro. Biomed Res Int 2013:1–13. https://doi.org/10.1155/2013/685142

Shukla PC, Gupta T, Labhsetwar NK, Agarwal AK (2016) Development of low cost mixed metal oxide based diesel oxidation catalysts and their comparative performance evaluation. RSC Adv 6:55884–55893. https://doi.org/10.1039/C6RA06021H

Shukla PC, Gupta T, Labhasetwar NK, Khobaragade R, Gupta NK, Agarwal AK (2017a) Effectiveness of non-noble metal based diesel oxidation catalysts on particle number emissions from diesel and biodiesel exhaust. Sci Total Environ 574:1512–1520. https://doi.org/10.1016/j.scitotenv.2016.08.155

Shukla PC, Gupta T, Labhsetwar NK, Agarwal AK (2017b) Trace metals and ions in particulates emitted by biodiesel fuelled engine. Fuel 188:603–609. https://doi.org/10.1016/j.fuel.2016.10.059

Singh DK, Gupta T (2016) Source apportionment and risk assessment of PM_1 bound trace metals collected during foggy and non-foggy episodes at a representative site in the indo-gangetic plain. Sci Total Environ 550:80–94. https://doi.org/10.1016/j.scitotenv.2016.01.037

Spencer MT, Shields LG, Sodeman DA, Toner SM, Prather KA (2006) Comparison of oil and fuel particle chemical signatures with particle emissions from heavy and light duty vehicles. Atmos Environ 40:5224–5235. https://doi.org/10.1016/j.atmosenv.2006.04.011

Spikes H (2004) The history and mechanisms of ZDDP. Tribol Lett 17:469–489. https://doi.org/10.1023/B:TRIL.0000044495.26882.b5

Ulrich A, Wichser A, Hess A, Heeb N, Emmenegger L, Czerwinski J, Kasper M, Mooney J, Mayer A (2012) Particle and metal emissions of diesel and gasoline engines—are particle filters appropriate measures. In: 16th conference on combustion generated nanoparticles, Zürich, Switzerland, p 13

USEPA (2004) Risk assessment: guidance for superfund volume I: human health evaluation manual (part E, supplemental guidance for dermal risk assessment) final

USEPA (2009) Risk assessment guidance for superfund (RAGS): part F

USEPA (2011) Human health risk assessment

USEPA (2013) Regional screening levels (RSLs)—user's guide

USEPA (2016a) Regional screening levels (RSLs)—user's guide

USEPA (2016b) Regional screening levels (RSLs)—equations

Venkataraman C, Habib G, Eiguren-Fernandez A, Miguel AH, Friedlander SK (2005) Residential biofuels in South Asia: carbonaceous aerosol emissions and climate impacts. Science 307:1454–1456. https://doi.org/10.1126/science.1104359

Verma V, Fang T, Xu L, Peltier RE, Russell AG, Ng NL, Weber RJ (2015) Organic aerosols associated with the generation of reactive oxygen species (ROS) by water-soluble $PM_{2.5}$. Environ Sci Technol 49:4646–4656. https://doi.org/10.1021/es505577w

Vouitsis E, Ntziachristos L, Samaras Z (2005) Modelling of diesel exhaust aerosol during laboratory sampling. Atmos Environ 39:1335–1345. https://doi.org/10.1016/j.atmosenv.2004.11.011

Vreeland H, Schauer JJ, Russell AG, Marshall JD, Fushimi A, Jain G, Sethuraman K, Verma V, Tripathi SN, Bergin MH (2016) Chemical characterization and toxicity of particulate matter emissions from roadside trash combustion in urban India. Atmos Environ 147:22–30. https://doi.org/10.1016/j.atmosenv.2016.09.041

Wang Z, Wu Y, Zhou Y, Li Z, Wang Y, Zhang S, Hao J (2014) Real-world emissions of gasoline passenger cars in Macao and their correlation with driving conditions. Int J Environ Sci Technol 11:1135–1146. https://doi.org/10.1007/s13762-013-0276-2

Wu B, Shen X, Cao X, Zhang W, Wu H, Yao Z (2015) Carbonaceous composition of $PM_{2.5}$ emitted from on-road China III diesel trucks in Beijing, China. Atmos Environ 116:216–224. https://doi.org/10.1016/j.atmosenv.2015.06.039

Wu B, Shen X, Cao X, Yao Z, Wu Y (2016) Characterization of the chemical composition of $PM_{2.5}$ emitted from on-road China III and China IV diesel trucks in Beijing, China. Sci Total Environ 551–552:579–589. https://doi.org/10.1016/j.scitotenv.2016.02.048

Xu Y, Barregard L, Nielsen J, Gudmundsson A, Wierzbicka A, Axmon A, Jönsson BAG, Kåredal M, Albin M (2013) Effects of diesel exposure on lung function and inflammation biomarkers from airway and peripheral blood of healthy volunteers in a chamber study. Part Fibre Toxicol 10:1–9. https://doi.org/10.1186/1743-8977-10-60

Zhang X, McMurry PH (1992) Evaporative losses of fine particulate nitrates during sampling. Atmos Environ Part A Gen Top 26:3305–3312. https://doi.org/10.1016/0960-1686(92)90347-n

Zheng N, Liu J, Wang Q, Liang Z (2010) Health risk assessment of heavy metal exposure to street dust in the zinc smelting district, Northeast of China. Sci Total Environ 408:726–733. https://doi.org/10.1016/j.scitotenv.2009.10.075

Zhou J, Zotter P, Bruns EA, Stefenelli G, Bhattu D, Brown S, Bertrand A, Marchand N, Lamkaddam H, Slowik JG, Prévôt ASH, Baltensperger U, Nussbaumer T, El-Haddad I, Dommen J (2018) Particle-bound reactive oxygen species (PB-ROS) emissions and formation pathways in residential wood smoke under different combustion and aging conditions. Atmos Chem Phys 18:6985–7000. https://doi.org/10.5194/acp-18-6985-2018

Chapter 10
Role of Diesel Particulate Filter to Meet Bharat Stage-VI Emission Norms in India

Rabinder Singh Bharj, Gurkamal Nain Singh and Hardikk Valera

Abstract Majority of passenger vehicles run on diesel and sold in India, new millennium have become the preferred choice of the customers along with commercial vehicles due to lower fuel cost, more mileage and comparable performance as compared to petrol driven vehicle apart from having better thermal efficiency due to its high compression ratio. However, the diesel-powered vehicle produces relatively high particulate emissions along with other pollutants when compared to petrol vehicles. Bharat Stage (BS) VI requires a 90% reduction of Diesel Particulate Matter (DPM) from BS IV. This high level of reduction in the DPM can be achieved with the help of diesel particulate filter (DPF). Incorporating DPF in the tail-pipe of a diesel engine is challenging as it requires its appropriate size, accurate position in the tailpipe and minimum pressure drop. Adding a DPF not only reduces the amount of DPM released into the atmosphere, but also help to reduce the fuel consumption, better transient response, and minimize operating costs. This chapter discusses the comprehensive details of material and regeneration processes used in DPF, including action plan for developing it BS-VI compatible.

Keywords BS-VI emission norms · DPF · Diesel particulate matter

Abbreviation

BS   Bharat stage
CDPF   Coated diesel particulate filter
CO   Carbon monoxide
CPCB   Central pollution control board
DOC   Diesel oxidation catalyst
DPF   Diesel particulate filter
DPM   Diesel particulate matter

R. S. Bharj (✉) · G. N. Singh · H. Valera
Department of Mechanical Engineering, Dr. B. R. Ambedkar National Institute of Technology, Jalandhar 144011, India
e-mail: bharjrs@nitj.ac.in

EGR   Exhaust gas recirculation
HC   Hydrocarbon
HCCI   Homogeneous charge compression ignition
NO_X Nitrogen oxide
PAH   Polycyclic aromatic hydrocarbon
PFF   Partial flow filters
PN   Particle number
SCR   Selective catalytic reduction

Nomenclature

ULP   Unleaded petrol

10.1 Introduction

Air pollution is the most severe environmental degradation problem, which affects the entire civilization by human activities such as mining, transportation, industrial work, construction, agriculture, and smelting, etc. Some other natural sources of air pollution are volcanic eruptions and wildfires, but they cause negligible damage to the environment. Inhalation of polluted air causes problems in human health such as coughing and irritation in the entire respiratory system, which leads to asthma and chronic lung diseases. Due to air pollution, approximately 3 million premature deaths were globally encountered every year thereby, air pollution is becoming a big issue for every country especially, developing countries like India. Among various sources, the transportation sector is a significant contributor to harmful pollutants, i.e., carbon monoxide (CO), Hydrocarbon (HC), and nitrogen oxide (NO_X) which are polluting the air quality. Indian automotive sector has four segments such as passenger vehicles, commercial vehicles, 3-wheelers and 2-wheelers, where diesel is used as a motive fuel to high duty vehicles. Its combustion produces additional DPM. However, diesel engine powers vehicles also play a vital role in global transportation as its global production is going to increase up to 21.2 million units by 2021 as compared to 17.7 million units in 2015 (Diesel Progress International 2016). Diesel-fuelled engines are also used in construction, farming, power generation, and industrial activities. DPM is more brutal pollutants which have an adverse effect on human health. However, diesel exhaust DPM is smaller than 1 μm in diameter (Seaton et al. 1995) and enters into the human body (Prasad and Bella 2010). Some particles are in the range of 0.1–1.0 μm "accumulation" size and some particles are in the <0.1 μm called nano-particles (Seinfeld 1975; Kittelson 1998). These nanoparticles easily penetrate the lungs (Wichmann et al. 2000) and enter the bloodstream of the human

body (Zhu et al. 2007). Some particles are deposit from the air into the throat, nose, and lungs. Deposited particles are generally injected via sneezing, coughing, and nose.

DPM is composed of carbon, distinct accumulated compounds, a sulphur-containing compound, inorganic oxides, and polycyclic aromatic hydrocarbon (Corro 2002). Hydrocarbon compound which results due to incomplete combustion of diesel fuel. Its particle size varies from 5 to 20 nm, which generally depends on fuel composition, the intake air quality for combustion, specific engine design, engine wear, and operating point. This kind of nanoparticles are rapidly agglomerate to make a cluster of 50 mm −150 mm size. It is necessary to understand the in-cylinder combustion behaviour for understanding the cluster formation. Entire engine cylinder can be divided into three regions: (i) Central region of the cylinder (ii) Region closer to the injector (iii) Most far away region in the cylinder. Generally, the second region does not possess turbulence thereby, there is not enough oxygen in proximity of the fuel drop, which facilitates the complete combustion. This incomplete combustion forms the DPM, which generally happen during sudden acceleration and cold starting conditions. In the first region, no harmful pollutants are formed including DPM because generally, this region has a stoichiometric air-fuel ratio which leads to complete combustion. The third region generally has an excess of oxygen, which increases the temperature thereby, NO_X formation. Therefore, DPM forms into the second region, which follows the first four steps as shown in Table 10.1. This complex mechanism of DPM formation not only affects the human health, but also adversely affects the plants physiology (Saracco and Fino 2001), environment (Ramanathan 2007), building materials (Baedecker et al. 1992; Simão et al. 2006) and atmosphere (Subramanian et al. 2009).

However, to harness such kind of harmful pollutants, stringent emission standards were imposed by the Government of India on the motor vehicles. In India, standards are set by the Central Pollution Control Board (CPCB) which comes under the Ministry of Environment, Forests, and climate change. These standards are generally in compliance with European regulations, firstly proposed in 2000. Historical evolution of emission standards in India is shown in Table 10.2.

Table 10.1   Diesel particulate matter (DPM) formation method

S. no.	Step	Explanation
1	Pyrolysis	Thermochemical decomposition process takes place at high temperatures and in the absence of oxygen. C_2H_2, benzene, and polycyclic aromatic hydrocarbon (PAH) are DPM precursors
2	Nucleation	Formation of germs and nuclei DPM
3	Surface growing	Mass addition process to the surface of a nucleated soot particle
4	Coalescence and agglomeration	Fusion of primary particle leads to the agglomeration

Table 10.2 Timeline of implementation of emission regulations

S. no.	Year	Explanation
1	1991–1992	First times mass emission norms were implemented
2	1995	First time catalytic converters were fitted in vehicles of four metro cities: Delhi, Kolkata Mumbai and Chennai
3	2000–01	BS-II norms were imposed in four metro cities: Delhi, Mumbai, Chennai, and Kolkata
5	2010	Nationwide implementation of BS-III norms
6	2017	Nationwide implementation of BS-IV

To reduce vehicular pollution, India signed the Paris Climate agreement in October 2016. As per the agreement, India is obligated to decrease the carbon footprint by 33–55% compared to the levels recorded in 2005 within the next 12 years.[1] Therefore, the Indian government has decided to enforce the most robust BS-VI emission norms by April 2020 via leapfrogging BS-V emission standards and to join the league of US, Japan, and European Union, which follow EU-VI norms. BS-VI emission norms are going to tightening the DPM emission limit by 50% and 67% compared to BS IV levels as measured on steady-state and transient dynamometer test cycle, respectively. Further, the introduction of particle number (PN) emission standards of 6×10^{11}/kW h and 8×10^{11}/kW h for transient cycle testing and steady-state test cycle testing is going to affect the entire automotive sector.[2] Detailed BS-VI norms for diesel-powered vehicles are shown in Table 10.3. Therefore, these steps will be likely to force the automotive manufactures of diesel vehicle to utilize the DPF for harnessing the DPM.

Several methods have been developed by engineers to reduce the production of soot and NO_x emissions in diesel engines. Among the most successful is the introduction of conventional catalytic oxidizer, DPF, Homogeneous Charge Compression Ignition (HCCI), Exhaust Gas Recirculation (EGR). Currently, DPF is the most successful device to remove soot particles coming out from the tail-pipe, and it has more than 90% filtration efficiency (Suresh et al. 2009). Growth in sales of heavy commercial vehicles in the transport and construction industry leads to a significant increase in demand for DPF's. Environmental concern is top on the DPF market, which is why the demand for more durable DPF is sparking the market. The global market for DPF is expected to see significant growth during the forecast period due to the above-mentioned factors. Another factor driving the growth of the market for DPF is the increasing demand for used vehicles, which requires relatively higher maintenance. The most widely used approach to comply with emission legislation is to trap DPM in a porous wall flow DPF. DPF traps the soot particles coming in the exhaust emissions of a diesel engine. Placement of DPF is shown in Fig. 10.1. CDPF (Coated Diesel Particulate Filter), which uses a catalyst to break down the

---

[1]Environment Updates 2014–2016. www.scribd.com.

[2]India Bharat Stage VI Emission Standards. https://www.theicct.org/sites/default/files/publications/India%20BS%20VI%20Policy%20Update%20vF.pdf.

Table 10.3 BS-VI norms with technology options

BS-VI emission norms for vehicles having gross vehicle weight exceeding 3500 kg[a]

Pollutants/cycle	CO (mg/kW h)	THC (mg/kW h)	NO$_X$ (mg/kW h)	NH$_3$ (DPM)	DPM mass (mg/kW h)	DPM numbers (numbers/kW h)
WHSC	1500	130	400	10	10	8.0×10^{11}
WHTC	4000	160	460	10	10	6.0×10^{11}
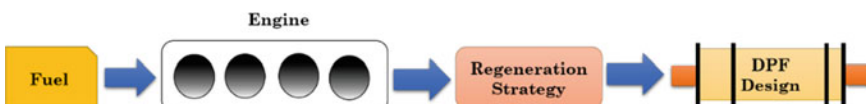
where
WHSC: world heavy duty steady-state cycle, WHTC: world heavy duty transient cycle

Technology options for past and post emission norms[b]

BS-IV	1. Combustion improvement
	2. EGR + DOC
	3. EGR + DOC + PFF
	4. SCR (or DOC + SCR)
BS-V (skipped)	1. Combustion improvement
	2. EGR + DOC + PFF
	3. SCR (or DOC + SCR)
BS-VI	1. Combustion improvements
	2. DOC + DPF + SCR

[a]Indian Emission Booklet 01 Nov 2018.cdr—Arai. https://www.araiindia.com/pdf/Indian_Emission_Regulation_Booklet.pdf
[b]Strategies for compliance of BS V/BS VI legislations on heavy duty commercial vehicles. http://www.ecmaindia.in/Uploads/image/2imguf_Mr.KVRBabu(ContinentalEmitec)Panel-2.pdf

Fig. 10.1 Schematic flow for DPF system

soot particles at low temperatures, has also improved the existing DPF technology. With the above general discussion on stringent emission norms, the objective of this chapter is to discuss the role of DPF in BS-VI emission norms.

10.2 DPF Material and Its Properties

In the last twenty-five years, several DPF system concepts are developed along with exploration of different geometric configurations and different filter media. Inside a DPF different ceramic materials are used such as cordierite, silicon carbide, mullite

aluminium titanate. Different metallic materials are also used such as sintered metal powder, non-woven fiber felt and metal foam. However, substrate medium plays a vital role in diesel filter system since it affects both its performance and durability. Also, affects material properties such as pore size, filtration area, cell density, melting point, thermal heat capacity, thermal expansion coefficient and resistant to a chemical in the exhaust. High filtration efficiency, high soot holding capacity, thermal shock resistance, strength and mechanical integrity, low-pressure drop, chemical stability, small size and low weight, long life, and high durability and low cost are the critical construction objectives for DPF.

The various type of design and materials used for building a DPF are

Honeycomb Design The design of the monolithic wall-flow honeycomb originally came into being in 1981. It is still versatile configuration as it shows a large ratio between the surface of the filter and the volume. This helps to reduce pressure and, more importantly, to increase the efficiency of soot filtration. The wall flow monoliths of the honeycomb are formed in an extruded square cell structure in which the channel is plugged at alternate ends to form a checkboard pattern on each face of the DPF (Hawker et al. 1997).

Cordierite and Silicon Carbide These are used for the filtration of Diesel Particulate Matter. Cordierite is MgAl silicate, which is extracted form of natural raw material such as caolin and talc. This ceramic material has been accounted as a strong contender for a DPF material, and already it was used in a substrate of catalytic converter before the introduction of DPF. In 1978, the first time an institution was developed an extruded cordierite wall flow filter to harness the DPM (Manson 2010). Moreover, SiC filter was popularized since 1990 however, first time it was commercialized, and it was used in Peugeot cars, which was launched in 2000. After that, SiC material was widely used in European car, and then cordierite has claimed a significant market share in the league of material used.

Aluminum Titanate This material was introduced with the commercial name Dura trap AT in Volkswagen made diesel car during 2005–2006. At that time, it was seen as an alternative of silicon carbide in the material market. However, the entire system was incorporated with advanced ceramic material. Generally, cordierite used with special design (Allansson et al. 2000).

Ceramic Base Fiber Filter Various type of high-temperature ceramic fiber filters was studied for different designs of DPF. In 1990 synthetic fibre was used for diesel exhaust soot particle where filter cartridges building block of the filter and working area of the cartridge was filled with fibres (Hawker et al. 1997). A different type of cartridge is used in fiber filters such as electric cartridge and concentric tube pack. The electric cartridge is incorporated with the electric heater where fiber supports the tube as a heating element. However, concentric tube cartridge has expanded filtration range because it is impractical to coordinate an electric heater into it. However, fiber filters are not popularized in wall flow monolith filters.

Ceramic Foam-Based Filters These filters are made from polymer foams using the so-called replication technique and prepared a rigid uniform cell network with more than 90% cell density. Because of some forming process pore/cell size of such filters is limited. Large filter volume and low soot handling capacity, however, put pressure to select another type filter because their commercial introduction to the diesel vehicle will never be accomplished. Foam based DPF was investigated under the STYFF-DEXA European FP6 project. The project's vision focused on better understanding and improving the filter's open-cell ceramic foam material for low-pressure drop and high regeneration efficiency.

Sintered Metal-Based Filters These are made of high-temperature porous metal resistance, which is why they are called sintered metal fiber. Wire mesh support with a coating of sintered Fe–Cr–Ni metal particles was first proposed in the 1990s. This type of filter has good filtration efficiency, low back pressure exhaust gas, and high capacity for ash storage, providing excellent flexibility in the design of the filter. Sintered metal filter technology was introduced by Bosch in 2002 and is now used in diesel passenger cars and light commercial vehicles after its worldwide acceptance. After a year, a reshaped form of sintered sheet material was produced for heavy-duty vehicles in which transparent material was produced in the form of dimpled sheets to maintain a tight spacing between the filter pleats. This provides proper compactness so that within the European COMET project light duty DPF of acceptable volume could be built and tested. For ash and soot accumulation, three different types of metal filters were evaluated. The overall results of the COMET project were the acquisition of good coating ability on the sintered metal plate material and the provision of a sound computational basis for understanding the distribution of flow behaviour and soot deposits in the plated structure. Due to the high sensitivity of soot oxidation concerning metal, there is no need for catalytic coating with this type of filter (Allansson et al. 2004). The sintered metal fiber has been equipped with several Daimler-made production vehicles.

These all materials have to deal with high exhaust temperature as it generally increases during regeneration process. Comprehensive details are discussed in upcoming section.

10.3 Regeneration Process in DPF Fitment

Regeneration is a burning process of deposited soot particle, generally deposits on DPF substrate channel wall. It is an essential process which requires for the expeditious filtration due to important reasons: (i) DPM thermally oxidize at approximately high 600 °C temperature or above. However, such a temperature cannot be achieved in tail-pipe during normal operating conditions. Even at high engine load, i.e., during high-speed driving or moving up an inclination, diesel exhaust temperature remains below 500 °C. (ii) Generally, accumulation of DPM leads to an exhaust back pressure problem, and it further leads to adverse impact on filtration efficiency. Generally, it
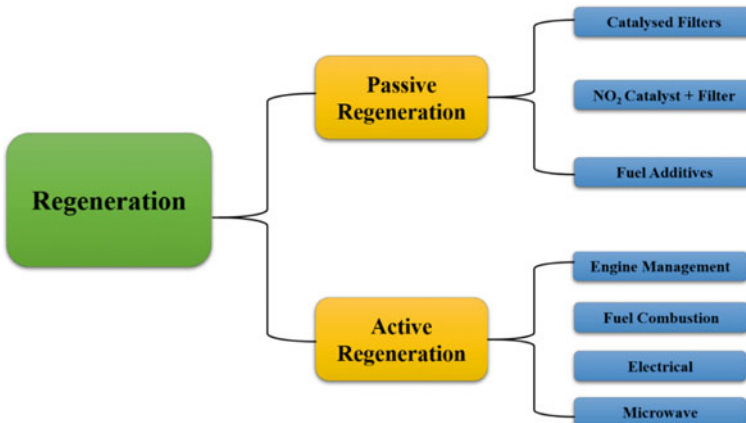
Fig. 10.2 DPF regeneration system

decreases with increment in the exhaust back pressure are observed. Therefore, it is essential to utilize the special intends to empower the regeneration; hence invariably primary mechanism is employed for decreasing the soot particle. The regeneration process can be divided into two types, as shown in Fig. 10.2.

10.3.1 Passive Regeneration

Passive regeneration process burns the coming out soot from the filter by continuous catalytic reaction mechanism without using any additional fuel. Passive regeneration occurs automatically during motorway-type runs where; exhaust temperature is already high. Therefore, any additional system is not required for burning the accumulated soot particle. The whole process is straightforward, inaudible and effective.

10.3.2 Active Regeneration

In the active regeneration process, DPM or soot is burned out periodically via heat. Generally, during soot loading filter reaches a 45% pressure drop across the DPF as monitored by the back-pressure sensor. In this type of heat generation an additional source of heat such as electric heater or fuel injection in the tail pipe is used to raise the temperature above 600 °C. Thus, accumulated soot particles burn easily (Dang et al. 2008). However, efficient regeneration can be achieved by just doing a temporary change in engine operation or oxidation catalyst for increasing the exhaust temperature (Huang et al. 2004). These temporary changes can be achieved by:

Table 10.4 Design parameters

Design parameters	Parameters to be affected
Thermal stress	• Soot loading • O_2 concentration • Flow rates
Thermal strength	• Substrate shape • Substrate diameter • Substrate cell density • Wall thickness
Material	• DPF thermal stability • Thermal shock resistance • Mechanical strength

Air Intake throttling: The suction of more air by facilitating the intake air system to each cylinder leads to increase the exhaust temperature by improving the in-cylinder combustion.

Post-injection of Diesel Fuel: Injection of a small amount of diesel fuel inside the cylinder when the piston reaches the top dead centre (TDC). The introduction of unburned fuel increases the exhaust temperature as it requires to oxidize the soot particle (Vincent et al. 2003).

If sufficient temperature does not reach in exhaust manifold using the above-discussed techniques, some other means such as an electric heater or fuel burner are used to raise the temperature required for oxidizing the soot particle. Regeneration can be done during vehicle operating condition or by especially turning off the vehicle for regeneration. However, later technique to achieve high temperatures may lead to a penalty in fuel economy.

Both regeneration processes are temperature sensitive thus, important design parameters have to be considered on base of exhaust temperature range as it affects the performance of the DPF as mentioned in Table 10.4.

Several researchers have explored the DPF using different materials and different design, including its filtration efficiency and effects on the exhaust back pressure.

Neeft et al. (1996) worked on the oxidizer system. They have studied the effect of desired characteristics such as trapping efficiency, lower backpressure, lower cost durability, resistance to high temperature during regeneration, minimal effect on diesel engine performance and fuel economy to find out the effect on the filter substrate.

Moreover, the author picked a cordierite wall flow monolith filter medium because it provides the best compromise in all desirable characteristics and positive experience. In their research work, the regeneration of the diesel particulate filter was done by supplying heat from fuel burner i.e. thermal regeneration. They also suggest that thermal regeneration is the simplest method of regeneration of DPM as less fuel quantity is required to burn the soot. Their work appears like a substantial achievement in trap technology development for a light vehicle.

Cooper and Thoss (1989) analysed necessity of catalyst to start the regeneration of a DPF substrate, which is used to activate the oxygen in the exhaust is causing increment in the temperature, which leads to initiation of particulate combustion. They addressed that variation of regeneration temperature remain in the range of 350 °C or above. He also added that regeneration took place as low as 265 °C temperature by using the catalyst, actually author checked regeneration capability for hundreds of hours.

Horiuchi et al. (1990) stated that DPM and sulphur content could be reduced using the flow-through oxidation catalysts under steady and dynamic engine condition. He founds a reduction of 40–90% in sulphur content, when exhaust gas temperature was observed 100–500 °C. This sulphur reduction is accomplished by its absorption on the catalyst surface at the low temperature and its decomposition at a high temperature. Different type catalyst was used such as Pt/Al_2O_3, Novel/Base/Al_2O_3, and Novel/Base Al_2O_3 with cordierite substrate.

Niura et al. (1986) practically tested ceramic foam based DPF to oxidize the diesel particulates. They attempted to see the possibility of "Trapless" trap (self-cleaning trap). A trapless trap which makes enable the collection of particulates in diesel exhaust. The conclusion of the study is DPF can be self-cleaned; it means it eliminates the complex procedure of cleaning the DPF.

Wade et al. (1983) developed the thermal and catalytic techniques for burning the deposited soot on the trap wall. In thermal technique, a burner is used which release the heat and increase the temperature which oxidizes the soot. HC, CO, and DPM pollutants were observed at 25–50% of allowable vehicle emission for one complete cycle. The author stated that problem with burner nozzle, clogging, ignition reliability, trap durability, and control systems were identified. Moreover, the authors also added that Lead and Copper fuel additives lead to a deposition in the cordierite trap of about 100% collection efficiency.

Pinturaud et al. (2007) studied DPF loading with the regeneration effects. The authors designed two specific experiments: (i) To observe the radial distribution of soot after loading and remaining soot or carbon black after controlled partial regeneration (ii) To observe the localization of soot in the longitudinal direction. The controlled regeneration is taking place when the filter is loaded at 6 g/L. The authors conduct this controlled regeneration experiments in the following conditions: 15 min post-injection period; engine speed of 1700 rpm and the engine torque is 94 N m.

Moreover, the amount of soot oxidation utterly depends upon the DPF inlet temperature which is controlled by the volume of injected fuel. The authors conclude that the soot layer has a uniform distribution on the four sides of the channel wall which is equally divided into the four walls of the channel. The author founds that more DPM is collected at the end of the channel than at the entrance of the channel.

Rao et al. (1985) developed advanced techniques for the regeneration of diesel particulate traps. The regeneration systems were: (i) By passable trap burner regeneration system (ii) By passable trap electric regeneration system and (iii) Catalytic regeneration. They measured the heat required for regeneration,

including its fuel consumption penalties. They concluded that catalytic fuel additives such as octate base compounds of copper, nickel, cerium lead to a reduction up to 210 °C in trap regeneration temperature.

Chatterjee et al. (2008) made the study to control the emissions to achieve Euro IV and Euro V norms on heavy-duty diesel engines. Diesel engine emitted low CO_2, high DPM, and NO_x emissions. Advanced after-treatment technologies such DPF, DOC, and SCR are introduced to comply the stringent emission standards which are capable for converting four harmful pollutants, i.e., NO_x, DPM, HC, and CO in other nonharmful gases. They concluded that DPF could significantly reduce DPM, HC, and CO emissions from the diesel engine.

Mizutani et al. (2007) described the characteristics of DPF and how the design of the DPF affects particulate filtration efficiency, emission levels, and the pressure drop of DPF. They reported that pore size smaller than 15-μm results in 100% filtration efficiency and filtration efficiency decreases with increasing mean pore size up to 20% and after they did not observe any change in filtration efficiency. He also stated that pore size has some effect on pressure drop with soot loading.

Tsuneyoshi and Yamamoto (2012) studied hexagonal and square type DPF under controlled and uncontrolled catalysed regeneration. They reported that a honeycomb monolith with a hexagonal cell structure offers a lower pressure drop compared to the square type cell structure.

The discussed investigations demonstrate that DPF is the best solution to meet BS-VI emission norms for diesel-powered vehicles. It can be understood from the above-discussed literature, that the DPF's design and operation for collecting and trapping particles has a prior effect on how easily the particles can be removed later. Proper maintenance of the DPF will benefit in aggregating the fuel economy, increasing horsepower, optimizing DPF performance, lower down the overall maintenance costs and will increase the life of a DPF. However, a particular plan is required to develop the DPF which can meet the BS-VI norms.

10.4 Action Plan for Developing BS-VI Compatible DPF

For diesel-powered light-duty and heavy-duty vehicles, DPF is considered as the best after treatment technology device, economically and technically. However, modifications are prerequisite for the existing DPF. Government of India (GOI) is first time introducing a stringent limit on PN. As exhaustive research has to be done to design the new DPF such that it can meet the BS-VI norms. Essential points that should be considered and investigated meticulously are as follows:

- Development of new material base DPF
- The chemical property of newly selected material should be studied well
- Development of new design based DPF, it must be other than honey comb structure
- Development of dedicated catalytic converter for the DPF
- Exhaustive study in the flow field and stress field of the DPF

- Reduction in exhaust back pressure and cost reduction
- Trials of newly designed DPF on the existing vehicle
- Durability studies of the DPF
- Ensure developed DPF is not increasing the exhaust back pressure
- Developed DPF must have a high filtration efficiency.

10.5   Conclusions

An exhaustive review of the DPF and its materials and properties has been done in this chapter. The requirement of regeneration in the DPF is also discussed. In India, DPF is narrated as the possible after treatment technology for the reduction of the DPM to meet the BS-VI norms, because of: (i) High filtration efficiency, (ii) technical difficulties such as material compatibility and high latent heat of vaporization, (iii) less exhaust back pressure, (iv) researchers acceptance because it is already proven technology in foreign countries where Euro-VI norms are already implemented. Firstly, DPF would play a significant role to cut out the exhaust DPM. Secondly, DPF utilization promotes the development of indigenous technology as it is possible to manufacture in India. DPF utilization in high duty vehicle may cause a fuel economy penalty. However, it can be resolved quickly if further research will be done in this field. The table below summarises various aspects of DPF to meet the BS-VI norms, meticulously discussed in this chapter.

Pollutants effects	• Tailpipe harmful pollutants such as DPM and NO_X are worsening the air quality
	• Diesel emitted DPM is more harmful pollutant than CO and HC
	• Inhalation of polluted air leading to a dangerous disease such as asthma and chronic lung diseases
	• DPM is made of inorganic oxides, sulphur-containing compound, and polycyclic aromatic hydrocarbon
BS-VI norm	• BS-VI emission norms have 50 and 67% lesser DPM emissions based on steady-state and transient dynamometer test cycle respectively compared to BS-IV norms
	• Restricted Particle number (PN) emission standards are 6×10^{11}/kW h and 8×10^{11}/kW h for transient cycle testing and steady-state test cycle for diesel-powered vehicles
DPF	• Diesel particulate filter (DPF) is a device which physically captures the particulates such that it cannot release into the atmosphere
	• DPF is the most effective technology to control the particle mass and numbers at high efficiencies

<div align="right">(continued)</div>

(continued)

Regeneration	• Regeneration is a burning process of deposited soot particle, and it required because DPM thermally oxidizes at high temperatures • Two types of regenerations: (i) Active regeneration where soot particles burn periodically using an additional heat source such as an electric heater or fuel injection. (ii) Passive regeneration where soot particle burns without any heat source, it burns by a complex reaction mechanism performs into a catalytic converter

Finally, DPF fitted vehicles are capable of meeting stringent BS-VI norms, including particle numbers. Diesel-fuelled vehicles can quickly meet the particulates limits in upcoming norms using DPF, which is considered as quite challenging as per the vehicle manufacturers. DPF makes sense as a best after-treatment technology as far as particle numbers are concerned.

References

Allansson R, Cooper BJ, Thoss JE, Uusimäki A, Walker AP, Warren JP (2000) European experience of high mileage durability of continuously regenerating diesel particulate filter technology (no. 2000-01-0480). SAE technical paper

Allansson R, Goersmann C, Lavenius M, Phillips PR, Uusimaki AJ, Walker AP (2004) The development and in-field performance of highly durable particulate control systems (no. 2004-01-0072). SAE technical paper

Baedecker PA, Reddy MM, Reimann KJ, Sciammarella CA (1992) Effects of acidic deposition on the erosion of carbonate stone—experimental results from the US national acid precipitation assessment program (NAPAP). Atmos Environ Part B Urban Atmos 26(2):147–158

Chatterjee S, Walker AP, Blakeman PG (2008) Emission control options to achieve Euro IV and Euro V on heavy duty diesel engines (no. 2008-28-0021). SAE technical paper

Cooper BJ, Thoss JE (1989) Role of NO in diesel particulate emission control. SAE Trans:612–624

Corro G (2002) Sulfur impact on diesel emission control—a review. React Kinet Catal Lett 75(1):89–106

Dang Z, Huang Y, Bar-Ilan A, Sud-Chemie Inc (2008) Oxidation catalyst on a substrate utilized for the purification of exhaust gases. US patent 7,332,454

Diesel Progress International, Jan–Feb 2016

Hawker P, Myers N, Hüthwohl G, Vogel HT, Bates B, Magnusson L, Bronnenberg P (1997) Experience with a new particulate trap technology in Europe (no. 970182). SAE technical paper

Horiuchi M, Saito K, Ichihara S (1990) The effects of flow-through type oxidation catalysts on the particulate reduction of 1990's diesel engines. SAE Trans:268–1278

Huang Y, Zhongyuan D, Amiram B (2004) Catalyzed diesel particulate matter with improved thermal stability. US patent 2004/0116285 A1, Süd-Chemie

Kittelson DB (1998) Engines and nanoparticles: a review. J Aerosol Sci 29(5–6):575–588

Manson I (2010) Self-regenerating diesel exhaust particulate filter and material. US patent 6013599

Mizutani T, Kaneda A, Ichikawa S, Miyairi Y, Ohara E, Takahashi A, Yuuki K, Matsuda H, Kurachi H, Toyoshima T, Ito T (2007) Filtration behavior of diesel particulate filters (2) (no. 2007-01-0923). SAE technical paper

Neeft JP, Makkee M, Moulijn JA (1996) Metal oxides as catalysts for the oxidation of soot. Chem Eng J Biochem Eng J 64(2):295–302

Niura Y, Ohkubo K, Yagi K (1986) Study on catalytic regeneration of ceramic diesel particulate filter (no. 860290). SAE technical paper

Pinturaud D, Charlet A, Caillol C, Higelin P, Girot P, Briot A (2007) Experimental study of DPF loading and incomplete regeneration (no. 2007-24-0094). SAE technical paper

Prasad R, Bella VR (2010) A review on diesel soot emission, its effect, and control. Bull Chem React Eng Catal 5(2):69

Ramanathan V (2007) Global dimming by air pollution and global warming by greenhouse gases: global and regional perspectives. In: Nucleation and atmospheric aerosols. Springer, Dordrecht, pp 473–483

Rao VD, White JE, Wade WR, Aimone MG, Cikanek HA (1985) Advanced techniques for thermal and catalytic diesel particulate trap regeneration (no. 850014). SAE technical paper

Saracco G, Fino D (2001) Advances in environmental and pollution control materials, vol 1. MRS Singapore Publisher, pp 273–285

Seaton A, Godden D, MacNee W, Donaldson K (1995) Particulate air pollution and acute health effects. Lancet 345(8943):176–178

Seinfeld JH (1975) Air pollution: physical and chemical fundamentals. McGraw-Hill Inc, New York

Simão J, Ruiz-Agudo E, Rodriguez-Navarro C (2006) Effects of diesel particulate matter from gasoline and diesel vehicle exhaust emissions on silicate stones sulfation. Atmos Environ 40(36):6905–6917

Subramanian R, Winijkul E, Bond TC, Thiansathit W, Oanh NTK, Paw-Armart I, Duleep KG (2009) Climate-relevant properties of diesel particulate emissions: results from a piggyback study in Bangkok, Thailand. Environ Sci Technol 43(11):4213–4218

Suresh A, Yezerets A, Currier N, Clerc J (2009) Diesel particulate filter system–effect of critical variables on the regeneration strategy development and optimization. SAE Int J Fuels Lubr 1(1):173–183

Tsuneyoshi K, Yamamoto K (2012) A study on the cell structure and the performances of wall-flow diesel particulate filter. Energy 48(1):492–499

Vincent MW, Richards PJ, Catterson DJ (2003) A novel fuel borne catalyst dosing system for use with a diesel particulate filter. SAE Trans:212–224

Wade WR, White JE, Florek JJ, Cikanek HA (1983) Thermal and catalytic regeneration of diesel particulate traps. SAE Trans:253–277

Wichmann HE, Spix C, Tuch T, Wölke G, Peters A, Heinrich J, Kreyling WG, Heyder J (2000) Daily mortality and fine and ultrafine particles in Erfurt, Germany—part I, role of particle number and particle mass. HEI Research Health Effects Institute, Cambridge, MA

Zhu L, Yu J, Wang X (2007) Oxidation treatment of diesel soot particulate on $Ce_xZr_{1-x}O_2$. J Hazard Mater 140(1–2):205–210

Part V
Miscellaneous

Chapter 11
Design and Development of Small Engines for UAV Applications

Utkarsha Sonawane and Nirendra Nath Mustafi

Abstract   Unmanned Aerial Vehicles (UAVs) have been extensively used for a wide range of applications since World War-II. UAVs are used for several defence purposes such as surveillance, communication, terrain mapping, reconnaissance, and attack. In this chapter, we discuss reciprocating internal combustion engine as a propulsion system for UAVs and the challenges in development of such an engine for aviation. The reciprocating piston engine is one of the most effective powerplants to energise the UAVs. The purpose of these propulsion systems in UAVs is to provide durable, reliable, and extended flight. Currently, no such engine for UAV applications are manufactured in India, and defence sector relies on imported engines only, which severely restricts their application for various other defence applications. This chapter addresses technical issues present in these systems, thus contributing to their development. Aspects related to structural and thermal analysis of engine components have also been discussed, which are essential for designing such engines. This chapter gives broad idea about future of UAV propulsion systems and associated challenges.

Keywords UAVs · Structural analysis · Thermal analysis · Defence · Small engines

Present Address:
U. Sonawane (✉)
Department of Mechanical Engineering, Indian Institute of Technology Kanpur, Kanpur,
Uttar Pradesh 208016, India
e-mail: utkarsha@iitk.ac.in

N. N. Mustafi
Department of Mechanical Engineering, Rajshahi University of Engineering and Technology,
Rajshahi 6204, Bangladesh

11.1 Introduction

11.1.1 Background of UAVs

UAV has been known by a remotely piloted vehicle, a drone, a robot plane, or a pilotless aircraft. Public and media often use the term "drone" for this application. A UAV is defined as a powered, pilot-less aerial vehicle, which can transfer a lethal or non-lethal pay load. They can fly for long period at controlled speed and height and have many applications in defense, industrial and civilian sectors. They were initially developed for 3-D missions: "Dull, Dirty or Dangerous" for humans. A sophisticated UAV may cost up to tens of millions of US dollars, and their weight may range from ½ to 20,000 kg (Friedrich 2014).

UAVs have been used across the globe since last couple of centuries. The earliest reported use of a UAV was by Austrians, who destroyed the Italian city of Venice with unmanned explosive balloons in 1849. In 1930s, use of a drone as moving target shooting by aircrafts was an important application, in which a two-stroke gasoline engine was used to power these drones. Remote-controlled aircrafts gained popularity during this phase. These aircraft featured in model Aircraft Nationals Competition held in Detroit in 1937. Later, in 1980s, USA developed aircraft to meet growing demand of the market with the aim of cost optimization. In 1986, USA and Israel worked together to develop a new aircraft named as RQ2 Pioneer (Tsach et al. 2004; Kumar et al. 2015). In 2000, USA introduced drones for the search of Osama Bin Laden in Afghanistan. In 2014, Amazon planned to use drones for doorstep delivery to enhance customer service experience. There is a vast potential for research and development of UAVs and their expansion to numerous fields of life.

11.1.2 Potential Applications of UAVs

There are many sectors, where UAVs can be used, such as military, agriculture, civilian, healthcare, and many more. Below are some sectors for applications of UAVs:

11.1.2.1 Geomorphic Mapping

UAVs provide a low-cost and high-pixel aerial photography in different areas. Such photography is vital for mapping studies in earth sciences. Techniques like laser scanning and low-altitude aerial photography by light aircrafts may provide excellent spatial resolution, however they are expensive and time-consuming. There are strict restrictions for UAVs usage in many areas, however due to their application in a broad range of resolutions, popularity of UAVs in geomorphic studies has increased. Recent technological developments have seen UAVs act as a means, by which we can collect

high-resolution aerial photos over large spatial areas. The flexibility and shorter response time of UAVs are the reason for increasing interest of geomorphological community (Hackney and Clayton 2015).

11.1.2.2   Pedestrian Traffic Monitoring

UAVs are used for collecting data, and controlling pedestrian traffic flows, in order to monitor the pedestrian demand. Present methods such as manual observers, video recording on site, questionnaire survey are less efficient and less accurate. Such practices have several limitations, when surveying a large area. UAV technology has been used in many foreign countries such as Thailand (Tsach et al. 2004), where UAVs collect data comprehensively to overcome space constraints. It is a safe and less costly technology to use. However, UAV have few limitations in terms of technical, working, and legal issues, therefore use of UAVs need legal permissions from aviation authorities, which makes its deployment challenging for various applications, including pedestrian traffic monitoring (Sutheerakul et al. 2017).

11.1.2.3   Agriculture

UAVs have been used in agriculture due to their ability to cover large areas quickly without damaging the growing field. They are quickly becoming popular in developing countries like India. They are widely used to achieve precision farming and smart agriculture in crop research and development. For monitoring small and medium sized areas in lesser time, UAVs can provide detailed information about the soil condition, crop, and soil moisture. Precision farming includes sensor data and real-time data analysis in order to improve farm productivity. Data collected from drones are used for soil health scans, in order to monitor crop health, and planning irrigation schedules. Upcoming agricultural revolution is predicted to be driven by data, which will help increase agricultural productivity with minimum damage to the environment and provide benefits to farming communities.

11.1.2.4   Aerospace and Military

The aerospace industry has been exploring the use of UAVs to provide increased accuracy and ease of documentation. These UAVs are capable of offering onboard image processing, and locking onto a target, apart from tracking it. UAVs are extensively used in military operations since last one decade for collecting information, surveillance, monitoring enemy activities, and to attack military targets and terrorist hideouts. Generally, they are preferred for a mission that is too dangerous for manned aircraft. Drones are a real-time tool for commanders to make better decision in resource allocation and to search for lost or injured soldiers. Military UAVs are

classified based on the kind of operations they perform. Advantages such as light-weight, quieter operation, smaller size and high efficiency render them useful for defence applications.[1]

11.1.2.5 Civil Engineering

Most civil engineering inspections pose a risk to inspection staff, inconvenience to the public, and potential damages to the structures. Traditional inspection methodology requires significant human resources and equipment, resulting in increased costs. UAV's vertical and oblique photography can collect real-time data for site data analysis. UAVs add great value by safely navigating into hazardous and harsh terrains. Innovative and rapidly evolving drone technology would benefit civil engineers and surveyors enormously.[2]

11.1.2.6 Healthcare

Drones are used for surveillance of sites affected by biological and chemical disasters. One of the best application of drones for healthcare is to deliver emergency medication or equipment to remotely located patients. Flood, earthquakes, fire, and severe drought can prevent on-site interaction with medical persons. Drones could be helpful in an emergency, where no one might be available. They can deliver medical aids to refugees and victims of war or military conflict. In future, smaller drones would provide medicine to patients at home, leading to rapid care and reduction in cost of assisting people.

On the other hand, there are technical challenges such as improving the ability of drones to detect and avoid objects during flight, reducing their size and weight, and preventing hackers from misusing this technology. It is therefore required to accelerate research efforts related to safety, response time, and privacy-related issues. Other challenges for UAV systems include flexibility of refueling and overall efficiency compared to manned aircraft.

11.2 Prospects and Limitations of Various Propulsion Systems for UAVs

A propulsion system provides effort to the aircraft for traveling from one point to another. Hence propulsion system should be durable, controllable, and energy

---

[1] https://www.isro.gov.in/applications-of-unmanned-aerial-vehicle-uav-based-remote-sensing-ne-region.

[2] http://www.asctec.de/en/uav-uas-drone-applications/uav-civil-engineering-buliding-stock-condition-survey/.

efficient. Failure of propulsion may lead to loss of aircraft control. Therefore an in-depth research study on pros and cons of different propulsion systems available in the market should be done before their implementation for UAV applications. In the following sections, few propulsion systems are listed, along with their advantages, disadvantages, and associated technical challenges.

Extended range and reliability of UAVs are two major constraints for the Wankel rotary engines, gas turbine engines and electric motor-based systems. Internal combustion (IC) engines are a potential solution to overcome some of these challenges. In the next section, reciprocating piston engines as a propulsion system for UAVs is discussed (Table 11.1).

11.3   IC Engine as UAV Propulsion System

Engines used in civil aviation and general aviation sectors are either gas turbines fuelled by aviation kerosene or IC engines fuelled by gasoline. These engines operate on the same principle as spark ignition (SI) engines used for automotive sector (Masiol and Harrison 2014). Reciprocating piston engines are classified based on the number of cylinders used (single-cylinder, two-cylinders and so on), the arrangement of cylinders (in-line, radial, opposed, V-configuration etc.) and working cycle (two-strokes and four-strokes). High power-to-weight ratio, compactness, low-cost, high efficiency, and reliability are the essential requirements for designing a piston engine for aviation sector and UAVs. Two stroke engines offer advantages such as high mechanical efficiency and high-power density. Supercharging of these engines may further improve power density and fuel efficiency at higher altitudes. The main issue with two-stroke engine is its poor scavenging process. Many researchers have given attention to scavenging models in order to optimize the design of port arrangement. Qiao et al. (2018) performed optimization of geometric parameters of the scavenging ports of a two-stroke small aero engine. This work provides necessary information about the design of crankcase scavenging system of aero engines. Visualization tool such as AVL FIRE software was used to study the gas composition and its distribution inside the combustion chamber during scavenging process. Borghi et al. (2017) investigated the design and modifications of a two-stroke single-cylinder engine. The primary step of this study involved fabrication of scavenging and combustion systems. The air metering system was modified for the constructed prototype during the second step. This modified engine was compared with the four-stroke engine developed for the same application. The only problem with the two-stroke engine was poor emission compliance of low NO_x limits, which can be possibly solved by using an efficient exhaust gas after-treatment device. Carlucci et al. (2016) simulated two-stroke engine by varying the design parameters such as modification of exhaust valves, scavenging ports (area of each port and number of ports), compression ratio, pressure ratio of both compressors (high and low) and air-fuel ratio (AFR). The objective was to increase the brake power output and to reduce the specific fuel consumption of the engine for having an economical flight.

Table 11.1 Types of propulsion system used in UAVs

S. No.	Propulsion system	Advantages	Disadvantages	Technical challenges
1.	Reciprocating piston engines (Griffis et al. 2009)	Light in weight, small in size, forced induction for high altitude application	Noisy, produce vibrations as it has many moving parts, lubrication and cooling required	Noise and vibrations affect reliability and life of the engine; seal failure may cause power loss, high temperature may lead to engine seizure or failure
2.	Wankel rotary engines	High power-to-weight ratio, compact, less noisy, less vibrations, lighter in weight, not prone to knock	Fuel consumption is more, not capable to meet emission norms, limited information available, complex	High exhaust gas temperature, engine cooling is difficult due to the intricate and complex design
3.	Gas turbine engines (Griffis et al. 2009)	High power density, tremendous thrust capability, insensitive to fuel quality	Expensive, loud, complex, less efficient than reciprocating engines at idle, high internal temperatures	Blade imbalance leads to vibrations, wear in bearing due to improper lubrication, high operating temperature, high energy rotation of the engine may damage the system
4.	Electric motor-based systems (Chan 2019)	Reliable and robust, high torque, less noisy, less maintenance required	Interference caused due to electromagnetic field, requires an enormous amount of current (Wu and Bucknall 2016). May be sensitive to water and other conductive liquids	Electromagnetic interference, corrosion, transients and noise produced by electromagnetic activity may obstruct the UAV electronics and communication devices, high current densities can corrode terminals

11.4   Design and Development of Engine for UAV Application

The constraints of time and range of UAV flight are the two main challenges, which need to be resolved for strengthening UAV applications. This study can be viewed as an attempt to resolve these problems to some extent. Engines are a viable alternative due to the advantages they offer such as high power output, greater refinement, and smoothness during the engine operation. Also, compact and small sized engine designs can enhance their usage in defence applications.

The methodology for design of UAV engines is summarised as follows: (Fig. 11.1).

- CAD model development of engine components,
- Structural and thermal analysis of the engine prototype,
- Manufacturing and testing of engine components for prototype development,
- Development of experimental setup for the prototype engine testing and experimental investigation for engine performance and durability characteristics,
- Powering the UAV using a compact engine and its functional flight testing.

IC engines have played a great role in human life, and researchers continuously seek to develop an engine with higher efficiency, low brake fuel consumption, and lower emissions from exhaust tailpipe. The transport industry uses IC engines to transfer people and goods from one place to another. If we look closely, an IC engine operates best when there is perfect synchronization between its components. Therefore, different IC engine component such as piston, piston rings, cylinder liners, valve assembly, connecting rod, crankshaft, camshaft, cylinder block, bearing cap, cylinder head, gear trains, etc. have to go through essential structural and thermal failure analysis to prevent any accident. These design aspects are discussed in the following sections.
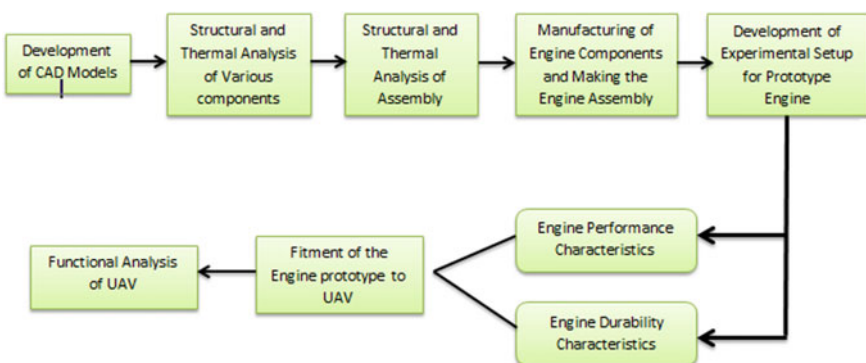

Fig. 11.1 Methodology for design and prototyping of UAV engine

11.4.1   Structural Analysis of Engine Components

Yu and Xu (2005) studied the crankshaft failure due to propagation of a fatigue crack in a stress concentration region. The crankshaft failed in a lesser than average life cycle. It was observed that surface hardening by nitriding could increase the fatigue strength of the material. Çevik and Gürbüz (2013) reported the effect of fillet rolling on the fatigue behavior of the crankshaft. The result showed that induced compressive residual stresses provide remarkable advancement in the fatigue strength of the component. Ktari et al. (2011) investigated the failure of three crankshafts made of forged carbon steel. Reasons for all failures was crack propagation and fatigue caused due to high stresses at fillet radius. Witek et al. (2017) performed numerical modeling of the crankshaft of a compression ignition (CI) engine using Finite Element Method (FEM). They reported that the main reason for early fatigue failure was the alternating bending stresses due to notch effect. Oil filters got clogged due to collection of metal debris in the lubrication channels, causing catastrophic engine failure, which further led to damage of other components such as piston, connecting rod, bearing, crankcase.

11.4.1.1   Piston

Piston is one of the most important components in the engine. Its function is to convert force from high pressure, high-temperature expanding gases to reciprocating motion, which is eventually converted to crankshaft rotation by crank-slider mechanism. Reciprocating motion of the piston leads to balancing issues in the engine, which cause vibrations. Friction between the cylinder wall and piston rings leads to components wear and degradation, hence reduces useful life of the engine. Noise generated by the engine can be unbearable sometimes. To diminish the loudness of engines, many reciprocating engines use heavy noise suppression devices. Figure 11.2 shows the induced stresses in the piston.

Generally, Aluminum alloys are used for manufacturing piston since it has excellent thermal conductivity and they are light in weight. Aluminum expands when the temperature increases, hence appropriate clearance should be given to provide free piston motion inside the cylinder bore under high temperature conditions. Insufficient clearance may lead to piston seizure in the cylinder, however excessive clearance may result in loss of compression and generate piston noise.

The piston includes the piston head, piston pin bore, piston pin, skirt, ring grooves, and piston rings. Piston head is the top surface of the piston, which bears immense pressure and heat during the engine operation. Piston pin bore is created to hold the piston pin, which connects the small end of the connecting rod to the piston. A portion of the piston closest to the crankshaft is called skirt, which aligns the piston during reciprocating motion in the cylinder bore. The secondary aim of the skirt profile is to reduce piston weight and to provide space for rotating crankshaft counter-weights (Siva Prasad et al. 2016).

Fig. 11.2 Induced stresses in typical piston (Hemasundaram and Suresh 2015)

11.4.1.2   Piston Rings

A ring grooves are provided on the outer diameter of the piston and are used to hold different piston rings (Fig. 11.3). A piston ring is a dynamic seal, which prevents leakage of high-temperature gases from the pressurized combustion chamber. Piston rings are subjected to wear since they move in the cylinder bore. They get worn out in preference to cylinder walls, in order to prevent frequent replacement cylinder liner. Piston rings are generally made of cast iron, which provides good wear resistance. Piston rings also transfer heat from the piston to the cylinder walls and also scrap the excess lubricating oil back to the engine crankcase. Piston ring configuration and number of rings used in an engine depends on the engine capacity and material of the cylinder liner (Satyanarayana and Renuka 2016).

Piston rings used commonly include compression rings, wiper ring, and oil ring. A compression ring is located in the ring groove closest to the piston head, in order to prevent any gas leakage during combustion. Wiper ring is inserted in between

Fig. 11.3 Typical piston rings (Hemasundaram and Suresh 2015)

the compression and the oil ring. Its function is to seal the combustion gases further and wipe excess oil from the cylinder wall. Oil ring is generally located near the crankcase, and it mainly transfers excess lubricating oil to the oil reservoir during piston motion.

11.4.1.3 Camshaft

Camshaft (Fig. 11.4) function is to open and close inlet and exhaust valves in sync with the motion of piston. Main part of camshaft is lobes. Camshaft is forged from a single piece of steel. There are twice as many lobes as the number of cylinders plus one additional lobe for the fuel pump actuation (Swamulu et al. 2015; Naga Manendhar Rao et al. 2017). Crankshaft powers the camshaft. Rotational speed of the camshaft is always half that of crankshaft. For a four-stroke engine cycle, camshaft rotates by 180° for every 360° rotation of the crankshaft.

The most common configurations of the overhead camshafts are:

I.   Single Over Head Cam (SOHC): In this configuration, a single camshaft is used to actuate all valves of the engine—Inlet valves and exhaust valves.
II. Dual/Double Over Head Cam (DOHC): In this configuration, two separate camshafts are used to operate the intake and exhaust valves, respectively.
III. Over Head Valve (OHV): This particular configuration is suited for V engine configuration. In this arrangement, a single camshaft is mounted between the two banks of cylinders. The cam lobes actuate the intake and exhaust valves through pushrods.

11.4.1.4 Crankshaft

The function of crankshaft is to convert the reciprocating motion of the piston into rotary motion and vice versa. Crankshaft is connected to a flywheel in order to damp pulsations in the cycle. Flywheel acts as an energy reservoir, which stores excess energy from the piston generated during the power stroke and uses the same energy for piston movement during remaining three strokes due to its high inertia. The
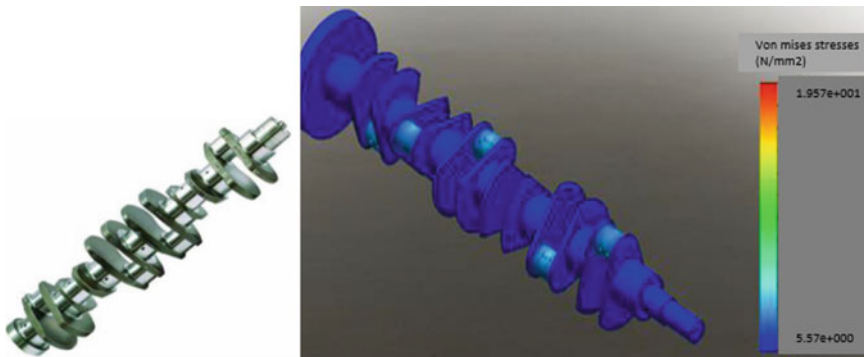
Fig. 11.5 Induced stresses in a typical crankshaft (Hemasundaram and Suresh 2015)

crankshaft is connected to camshaft via a belt-drive, which controls the opening and closing of inlet and exhaust valves. Crankshaft should be carefully designed for its weights and balances in order to reduce engine vibrations. Both ends of crankshaft are fixed on the engine block by using crank bearings. Balancing of crankshaft is vital for perfect functioning of the engine. Material selection and weight distribution on the sides of the journal should be done carefully. Failure analysis of crankshaft using ANSYS software helps predict critical design points in the model for UAV application. Figure 11.5 shows the crankshaft and its variation of induced stresses. Generally, heavy cast iron is used for manufacturing crankshaft for automotive applications and stainless steel for high-performance UAV engines (Reddy et al. 2017).

11.4.1.5   Connecting Rod

Connecting rod links the piston to the crankshaft, and its function is to transfer forces from the piston to the crankshaft, which further passes it on to the transmission (Kushwaha and Parkhe 2018).

Connecting rod is often a major source of catastrophic engine failure; therefore it requires care to ensure that it does not fail. Figure 11.6 shows the variations of induced stresses in a typical connecting rod. The traditional connecting rod used in the automotive industry is forged, and is suitable for lower horsepower engines (Singh et al. 2017). The materials used for manufacturing the connecting rods are steel alloy, aluminium, and titanium, depending on application requirements. A lightweight connecting rod is preferred for improved efficiency of the engines for UAV applications. However this goal should not be achieved by removal of material or changing design parameters but by using lightweight stronger materials.
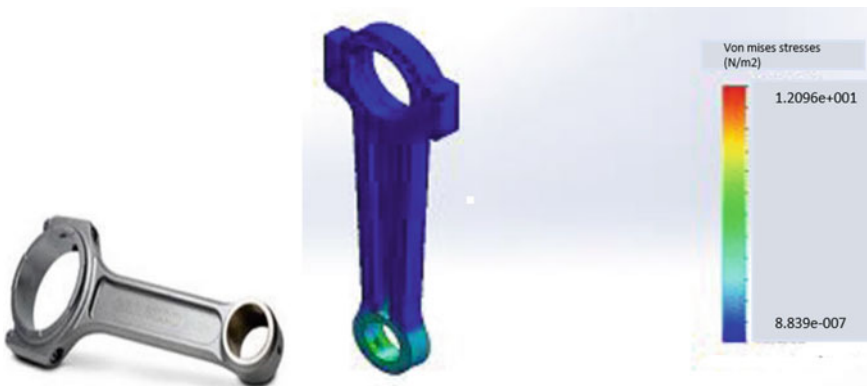
Fig. 11.6 Induced stresses in typical connecting rod (Hemasundaram and Suresh 2015)

11.4.2 Thermal Analysis of Engine Components

Thermal failure is a bottleneck for engine development, which affected engine performance and efficiency. Engine heat transfer phenomenon is still not well understood by designers due to complex geometry and lack of understanding of combustion phenomenon. Therefore, it is necessary to study temperature distributions in the engine components for controlling thermal stresses and strains within acceptable limits and avoid component deformation. Thermal analysis allows researcher to design components and understand their temperature distribution even before the construction of the first prototype (Li 1982). It saves time and is a cost-effective way to optimize component design. Many researchers have reported critical design considerations for thermal expansion, which ultimately lead to catastrophic failure of engine components.

Abbes et al. (2004) studied the behavior of a direct injection compression ignition (DICI) engine piston, which was subjected to both thermal and mechanical stresses. Results obtained from the simulation were used to analyze the working temperatures. In another study, Esfahanian et al. (2006) studied three combustion boundary conditions and investigated heat transfer through the piston using KIVA and NASTRAN codes. Lu et al. (2013) used an inverse heat transfer method to study thermal analysis of a marine CI engine piston. New design showed improved performance from piston thermal loading analysis perspective.

Yao and Qian (2018) carried out research involving improvement in engine performance when nano-ceramic coating was applied over aluminum piston. Steady-state thermal analyses were used to determine the effects of ceramic coating on piston temperature distributions. By using FEM analysis, comparison between coated and uncoated pistons were made, as shown in Fig. 11.7. They showed that the temperature of the coated piston crown was higher than the uncoated piston, which improved the thermal efficiency and reduced the emissions.
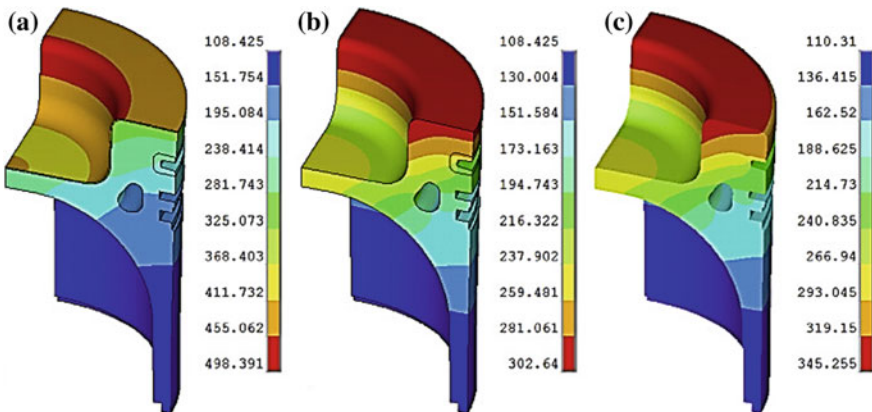
Fig. 11.7 Temperature distribution of the **a** thermal barrier coating (TBCs) piston, **b** aluminum alloy substrate of the TBC piston, and **c** conventional aluminum alloy piston (Yao and Qian 2018)

Satyanarayana et al. (2018) conducted quasi dynamic stress analysis for different compression ratios of a diesel engine. Figure 11.8 shows the variations in temperature, Von-mises stress, total heat flux, factor of safety (FOS), total deformation, and elastic
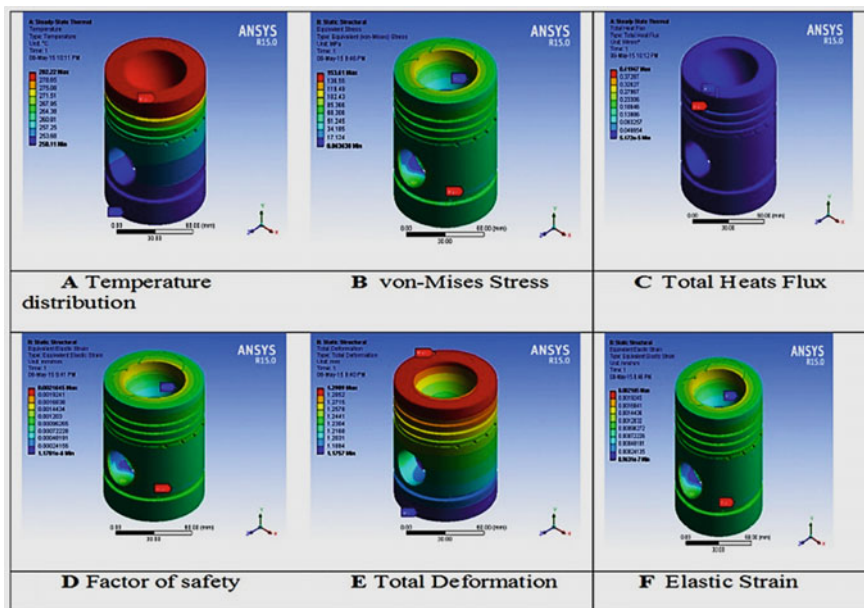

Fig. 11.8 Structural and thermal analysis of piston for a compression ratio of 16.5 (Satyanarayana et al. 2018)

strain on the piston. The maximum and minimum temperatures were observed at the piston crown and skirt respectively at all compression ratios. They reported that the compression ratio had a profound effect on the stresses developed.

11.5   Challenges of Research in UAV Propulsion Systems

Air pollution is a major concern for developing countries like India due to rapid expansion of transport and civil aviation sectors. Most studies highlighted that aviation emissions affect local as well as global air quality adversely. Emission standards for new aviation engines are enforced by the International Civil Aviation Organization (ICAO).

Design and optimization of small IC engines to achieve maximum efficiency includes modifications in various components of the engine. The intake port is one of the most vital part of the IC engine, which supplies air to the engine cylinder. It influences the quantity of air entering into the cylinder, velocity distribution, and in-cylinder air-flow characteristics. Therefore design of intake port becomes critical to reduce emissions and fuel consumption. For the optimization of in-cylinder air-flow characteristics, study of flow-field can be done by using advanced optical diagnostic techniques such as Laser Doppler Anemometry (LDA) and Particle Image Velocimetry (PIV). Computational Fluid Dynamics (CFD) analysis can help detect problems in the engine design.

Wang et al. (2019) proposed an AFR controlled fuel supply system to optimize the efficiency of UAV, when operating at required engine speed. The results showed 9–33% improvement in engine efficiency. Hassantabar et al. (2019) studied the electronic fuel injection system since carburetor was not suitable for two-stroke UAV engine. They investigated the airflow and fuel spray structure in the throttle body injection system using CFD tools. Simulation of two-stroke engine was performed using 'Lotus' engine. They also developed models to compute the performance of the system in different working conditions, which showed the effect of engine speed on the pressure drop, spray characteristics, and turbulence patterns.

Light weighing of the engine is an effective way to achieve small and compact UAVs. It involves use of lightweight material and advanced manufacturing processes to deliver enhanced technical performance. This concept is widely explored in automotive industry as well. Aluminium alloys have been used as major material used in aerospace industry. Nayak and Date (2018) redesigned the UAV engine piston using sheet metal manufacturing process consisting of deep drawing, redrawing, ironing, punching, and hole flanging. Die and punch of forming process were developed and implemented successfully. A 24% reduction in weight was achieved compared to the existing piston. Decisions like whether to use one or multiple propulsion for specific flight segment creates a new dimension of research for researchers. Opportunities do exist, however they also bring challenges such as engine design modifications

to optimize engine design parameters for UAV engines. we need to explore novel approaches to improve overall efficiency and flow simulation techniques to meet emission norms for these UAV engines.

References

Abbes MT, Maspeyrot P, Bouif A, Frene J (2004) A thermomechanical model of a direct injection diesel engine piston. Proc Inst Mech Eng D: J Automob Eng 218(4):395–409. https://doi.org/10.1243/095440704773599917

Borghi M, Mattarelli E, Muscoloni J, Rinaldini CA, Savioli T, Zardin B (2017) Design and experimental development of a compact and efficient range extender engine. Appl Energy 202:507–526. https://doi.org/10.1016/j.apenergy.2017.05.126

Carlucci AP, Ficarella A, Trullo G (2016) Performance optimization of a two-stroke supercharged diesel engine for aircraft propulsion. Energy Convers Manag 122:279–289. https://doi.org/10.1016/j.enconman.2016.05.077

Çevik G, Gürbüz R (2013) Evaluation of fatigue performance of a fillet rolled diesel engine crankshaft. Eng Fail Anal 27:250–261. https://doi.org/10.1016/j.engfailanal.2012.07.026

Chan CC (2019, March 1) Electric vehicles, electrical engineering—vol III—electric vehicles

Esfahanian V, Javaheri A, Ghaffarpour M (2006) Thermal analysis of an SI engine piston using different combustion boundary condition treatments. Appl Therm Eng 26(2–3):277–287. https://doi.org/10.1016/j.applthermaleng.2005.05.002

Friedrich G (2014) Application of military and non-military aircraft system (UAV). University of Applied Sciences Stralsund

Griffis C, Wilson T, Schneider J, Pierpont P (2009) Unmanned aircraft system propulsion systems technology survey

Hackney C, Clayton A (2015) Unmanned aerial vehicles (UAVs) and their application in geomorphic mapping

Hassantabar A, Najjaran A, Farzaneh-Gord M (2019) Investigating the effect of engine speed and flight altitude on the performance of throttle body injection (TBI) system of a two-stroke air-powered engine. Aerosp Sci Technol 86:375–386. https://doi.org/10.1016/j.ast.2019.01.006

Hemasundaram B, Suresh D (2015) Design and structural analysis of a V12 engine by using different materials. Int J Mag Eng Technol Manag Res

Ktari A, Haddar N, Ayedi HF (2011) Fatigue fracture expertise of train engine crankshafts. Eng Fail Anal 18(3):1085–1093. https://doi.org/10.1016/j.engfailanal.2011.02.007

Kumar G, Sepat S, Bansal S (2015) Review paper of the solar-powered UAV. Int J Sci Eng Res

Kushwaha S, Parkhe A (2018) Review on design and analysis of IC engine connecting rod. Int Res J Eng Technol (IRJET)

Li CH (1982) Piston thermal deformation and friction considerations (No. 820086) SAE Technical Paper. https://doi.org/10.4271/820086

Lu X, Li Q, Zhang W, Guo Y, He T, Zou D (2013) Thermal analysis on piston of marine diesel engine. Appl Therm Eng 50(1):168–176. https://doi.org/10.1016/j.applthermaleng.2012.06.021

Masiol M, Harrison RM (2014) Aircraft engine exhaust emissions and other airport-related contributions to ambient air pollution: a review. Atmos Environ 95:409–455. https://doi.org/10.1016/j.atmosenv.2014.05.070

Naga Manendhar Rao K, Reddy T, Mallela S (2017) Modelling and analysis of cam shaft. IJRAET

Nayak KC, Date PP (2018) Manufacturing of light automobile engine piston head using sheet metal. Procedia Manuf 15:940–948. https://doi.org/10.1016/j.promfg.2018.07.402

Qiao Y, Duan X, Huang K, Song Y, Qian J (2018) Scavenging ports' optimal design of a two-stroke small aeroengine based on the Benson/Bradham model. Energies 11(10):2739. https://doi.org/10.3390/en11102739

Reddy M, Chanduri RP, Reddy M, Kumar L (2017) Design & analysis of crankshaft by forged steel & composite material. Int J Eng Trends Technol (IJETT). https://doi.org/10.14445/22315381/IJETT-V46P207

Satyanarayana I, Renuka D (2016) Design and analysis of piston and piston rings with cast iron, aluminium alloy and cast steel materials. IJISET—Int J Innov Sci Eng Technol

Satyanarayana K, Rao SUM, Viswanath AK, Rao TH (2018) Quasi-dynamic and thermal analysis of a diesel engine piston under variable compression. Mater Today Proc 5(2):5103–5109. https://doi.org/10.1016/j.matpr.2017.12.090

Singh V, Verma S, Ray HC, Bharti V, Bhaskar A (2017) Design and analysis of connecting rod for different material using Ansys workbench 16.2. Int J Res Appl Sci Eng Technol (IJRASET)

Siva Prasad G, Dinesh Achari K, Dileep Kumar Goud E, Nagaraju M, Srikanth K (2016) Design and analysis of piston of internal combustion engine on different materials using CAE tool ANSYS. Int J Innov Res Sci Eng Technol

Sutheerakul C, Kronprasert N, Kaewmoracharoen M, Pichayapan P (2017) Application of unmanned aerial vehicles to pedestrian traffic monitoring and management for shopping streets. Transp Res Procedia 25:1717–1734. https://doi.org/10.1016/j.trpro.2017.05.131

Swamulu V, Nagaraju NS, Srinivas T (2015) Design and analysis of cam shaft for multi cylinder engine. Int Res J Eng Technol (IRJET)

Tsach S, Chemla J, Penn D, Budianu D (2004) History of UAV development in IAI and road ahead. In: 24th international congress of the aeronautical sciences

Wang Y, Shi Y, Cai M, Xu W, Yu Q (2019) Efficiency optimized fuel supply strategy of aircraft engine based on air-fuel ratio control. Chin J Aeronaut 32(2):489–498. https://doi.org/10.1016/j.cja.2018.10.002

Witek L, Sikora M, Stachowicz F, Trzepiecinski T (2017) Stress and failure analysis of the crankshaft of diesel engine. Eng Fail Anal 82:703–712. https://doi.org/10.1016/j.engfailanal.2017.06.001

Wu P, Bucknall RW (2016) Marine propulsion using battery power. Department of Mechanical Engineering, University College London, London

Yao Z, Qian Z (2018) Thermal analysis of nano ceramic coated piston used in natural gas engine. J Alloy Compd 768:441–450. https://doi.org/10.1016/j.jallcom.2018.07.278

Yu Z, Xu X (2005) Failure analysis of a diesel engine crankshaft. Eng Fail Anal 12(3):487–495. https://doi.org/10.1016/j.engfailanal.2004.10.001

Chapter 12
Automotive Lightweighting: A Brief Outline

Aneissha Chebolu

Abstract   Automotive emissions account for a substantial percentage of the planet's Greenhouse Gas (GHG) emissions and the numbers have been steadily soaring. Environmental bodies and governments are therefore constantly enforcing tighter legislations and as a result automotive OEMs are forced to ensure decreased emissions. While safety requirements and luxurious interiors have resulted in a gain of weight over the decades thus increasing emissions, OEMs are persistently being asked to cut down emissions from fossil fuel driven vehicles, especially given the rise of electric vehicles in recent years. OEMs have thus started replacing parts originally made with heavier materials with lighter materials in order to reduce the overall weight of the vehicle—also known as lightweighting. While the original cast iron engine blocks have long been replaced with steels followed by Aluminium, Magnesium alloys and the more recent carbon fibre for certain engine parts; studies have also started exploring the benefits of advanced composites such as cellulose based composites.

Keywords Lightweighting · GHG emissions · Aluminium

12.1   Introduction

Growing environmental awareness has constantly been highlighting the need for a reduction in GHG emissions across the globe. As such, there has been tremendous pressure on the transport industry in the form of various legislations continuously demanding lower vehicular emissions and setting ambitious targets for further reductions in new vehicles. Naturally, tighter regulations have had an impact on the design and development of new vehicles. Therefore, manufacturers have been steadily working on Vehicle Lightweighting—the process of reducing the weight of the vehicle.

Lightweighting is an established strategy known to improve fuel economy in vehicles, thereby reducing fuel consumption in the transport industry. A reduction in the mass of the vehicle results in lowering the inertial forces that the engine must

A. Chebolu (✉)
Department of Mechanical Engineering, IIT Madras, Chennai, India
e-mail: aneissha.mech@gmail.com

overcome when accelerating, thereby resulting in a reduction in the energy required to move the vehicle, thus saving fuel and resulting in reduced emissions. Literature reports that everytime a 10% reduction in vehicle weight occurs, a 5–7% reduction in the fuel consumption of vehicles follows (Cheah 2010).

However, increasing safety norms have in turn been adding to the overall weight of the vehicle forcing manufacturers to work twice as hard to cut down the weight further. The ever-increasing demands for comforts and entertainment by consumers have also led to a rise in the average vehicle weight over the years.

Car bodies have undergone a complete metamorphosis starting from heavy mild steel bodies in the 1950s to Aluminium to AHSS to carbon composites. Taking a cue from the aerospace industry which has been constantly investigating and investing in lighter materials, the automotive industry has been trying to catch up, replacing the traditional cast-iron and steels. Today we see an array of materials in a vehicle ranging from aluminum, carbon-fiber composites, high-strength steel, magnesium, titanium, to various types of foam, plastic and rubber as well as natural fibers such as bamboo and kenaf (Kulkarni et al. 2018). Mixed materials are now a norm with OEMs however joining different materials together impeccably is still an ongoing challenge, given the differences in material properties, textures, etc.

Car manufacturers have gone back and forth on the material used in the body depending on factors like weight reduction, cosmetic effects, costs amongst others. While car manufacturers are increasingly steering towards cleaner fuels like electricity, the additional weight contributed by heavy weight batteries, complex powertrains and other parts must not be overlooked.

This article aims to understand the choice of different materials in Automotive Lightweighting and also explores the impact of lightweighting on CO_2 emissions in Heavy Duty Vehicles.

12.2 Materials in Lightweighting

The first commercial car was designed in 1885 by Karl Benz as a combination of wood and steel, which was soon replaced by an all steel car in 1912 by Budd. Since then, the automotive industry has experimented with a variety of metals and alloys to achieve speed, crash resistance, creep resistance and of course taking into consideration the element of beauty. Various materials posed a plethora of challenges which has led to the constant development of newer manufacturing techniques, joining processes and opened up several opportunities for R&D in the automotive industry.

For example, the traditional ferrous castings had been cast aside and replaced by newer materials like Aluminium, HSS, AHSS and magnesium alloys.

12.2.1 Steel

Steel has long been known for its strength, stiffness and corrosion resistance amidst other critical properties. It has therefore been an integral part of the automotive body structure. Although steel had been the best solution for almost all body structures, manufacturers started to look for cheaper and lighter alternatives. This led to the evolution of steel grades such as advanced high-strength steel (AHSS) which have been a huge hit in the automotive sector.

Some recent examples of lightweighting with steel include the 2015 Nissan Murano which saved 146 lbs using AHSS; the 2015 Chrysler 200 body structure with 60% AHSS, the 2016 Hyundai Tucson with more than 50% of the new structure and chassis being AHSS (ICCT 2017).

12.2.2 Aluminium

Aluminium is well known for its light weight, can be recycled from one product to the next several times without losing its properties even after going through several rounds of recycling. The transport industry has been demanding aluminium at an increasing rate every year as illustrated in Fig. 12.1. However, its use in safety critical parts was questioned, before stronger Aluminium alloys were developed with strength multiplied three times (Bertram et al. 2007).
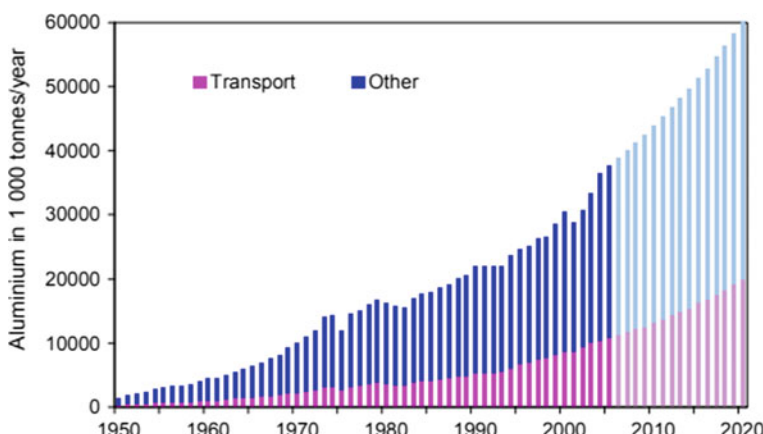

Fig. 12.1 Global total and transport related aluminium use (1990–2020) (Bertram et al. 2007)

12.2.3 Magnesium Alloys

Magnesium is the lightest of the structural automotive metals. Its alloys find applications in Magnesium alloys have a high strength to weight ratio and a very high specific strength but have issues such as corrosion resistance, creep resistance and high costs.

Magnesium is less stiff than aluminium, thus requiring the addition of stringers and stiffeners. It also has to be formed at a higher temperature if it is to be used for stamped parts. Welding the alloys is a huge challenge as there is a high potential for porosity in these alloys, along with a tendency for distortion and cracking.[1] Presently, magnesium is mostly used in die casting process in the automotive industry (Tang 2017). The resultant die castings are more robust than plastic moldings and have tighter dimensional tolerances. With die castings, the problem of joining various parts together does not arise and therefore, the question of weak joints does not arise.

12.2.4 Composites
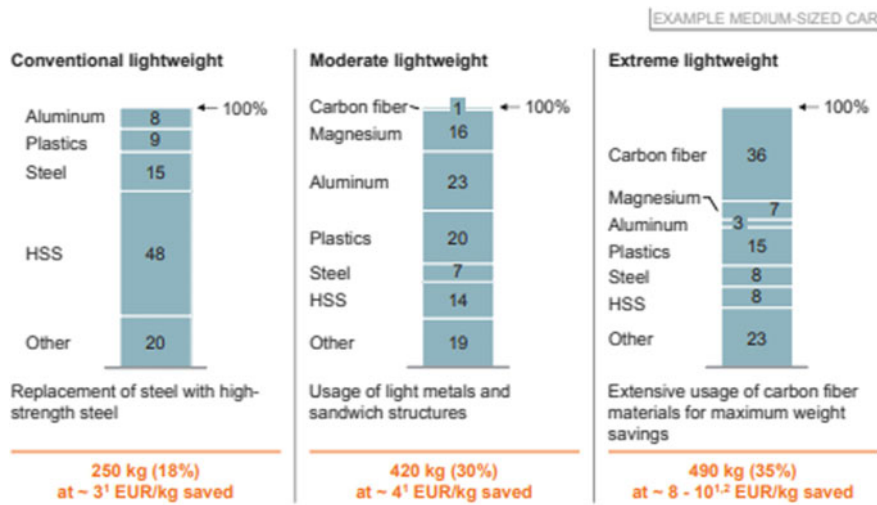
The introduction of novel materials replacing existing materials is very challenging. This is because of the need to set up new tooling, designing joining mechanisms, training the workforce, changing the shop floor arrangement and so on. Although initial studies might seem lucrative, practical deployment often pose problems and unsolved hurdles causing delays, wastage and escalating costs. A transition to a new material is always expensive initially and then the costs start yielding returns as the technology matures and competitors emerge. For instance—there is a high energy consumption for carbon fibre production, there is a risk for negative CO_2 impact; it is expensive to tool/hard to form and so on. However, manufacturers are increasingly steering towards carbon fibres as it is an extreme lightweight material with superior material properties.

Thermoset as well as thermoplastic composites are currently used in the automotive industry. These include sheet molding compounds or bulk molding compounds (SMCs/BMCs), glass fibre mat thermoplastics (GMTs) and long fibre reinforced thermoplastic composites (LFRT), with glass fibre being the fibre component. Using natural fibres in the place of glass fibres allows further lightweighting because natural fibres have a lower density (Pervaiz et al. 2016).

Studies also show the introduction of natural cellulose and kenaf in place of glass fibres for automobile components (Boland et al. 2016) (Fig. 12.2).

The resistance to the introduction of new materials right away is due a variety of reasons, principally the costs. To begin with, most automotive manufacturers have already invested heavily into in-house metal work to save the costs incurred by buying from suppliers. In order to use new materials, the entire investment into the metalworking becomes redundant. In 2013, several new applications helped create

---

[1] https://doi.org/10.1533/9780857095466.150. Last accessed on 01 June 2019.

Fig. 12.2 Lightweight packages apply different lightweight material mixes with different weight and cost impact (Heuss et al. 2013)

an interest in composites especially for automotive applications (promising to reduce weight thereby increasing the fuel economy), but eventually plateaued once the costs started added up.

This trend can be observed in the BMW's i-Series wherein the i3 boasted of a massive percentage of composites. Enthusiasts projected that 60% of vehicles would have 20% composites usage by 2020. However, one can see a much lower percentage of composites in BMW's i5 and i7 models.[2]

12.3 Lightweighting Versus Fuel Consumption and CO_2 Emissions

Sections 12.1 and 12.2 talk about the potential weight saving that can be achieved by replacing the existing materials by lighter alternatives, the advantages and disadvantages of the various substitute materials. However, this leads to the most important question—What levels of energy and CO_2 savings can be accomplished by lightweighting? This section talks about the targets set by the EU for emissions reduction in HDV (heavy duty vehicles) and predicts if these targets might be met by lightweighting. The following are the proposed targets for average CO_2 emissions from new lorries: The CO_2 emissions should be 15% lower in 2025 than in 2019;

---

[2]http://compositesmanufacturingmagazine.com/2017/09/feedback-composites-global-automotive-lightweighting-materials-conference/. Last accessed on 01 June 2019.

and in 2030, the emissions should be at least 30% lower than they are in 2019 (these are the proposed targets, and will be reviewed in 2022) (EU Directorate-General for Climate Action (DG CLIMA) 2016).

While cars like the Audi A8 have made headlines for their high Aluminium content exceeding 500 kg, the aluminium content in cars has been steadily growing and tripled between 1990 and 2012 and is expected to go higher (European Aluminium Association 2013).

There is no one way to quantify the relationship between lightweighting and the corresponding reduction CO_2. Several theories have been proposed and several simulation tools have been developed to arrive at an empirical relation between the two. For example, lightweighting without reducing the engine size versus lightweighting with an increase/decrease in engine size will yield different results. There are one too many variables involved and additionally certain studies include the emissions involved in the material lifecycle—i.e., from its production to end of life cycle stage.

On an average, various studies have reported a reduction in CO_2 emissions from a meagre 3 g/km to as high as 15 g/km for a weight reduction of 100 kg.

In order to appreciate the reason behind this variation, one needs to understand the fundamental difference between weight savings and fuel savings.

It can be seen from Fig. 12.3 that a combination of direct weight savings and primary fuel savings exclusively will result in the lowest CO_2 emissions reduction. Correspondingly, the highest CO_2 reductions can be targeted by combining indirect weight-saving with secondary fuel saving (European Aluminium Association 2013).

In order to design new vehicles with lower emissions, several tools and simulation models have been developed. Most models make use of Artificial Neural Networks for their emissions predictions (Uslu and Celik 2018). VECTO is one such simulation tool, developed by the European Commission and is used for determining CO_2 emissions and Fuel Consumption from Heavy Duty Vehicles (trucks, buses
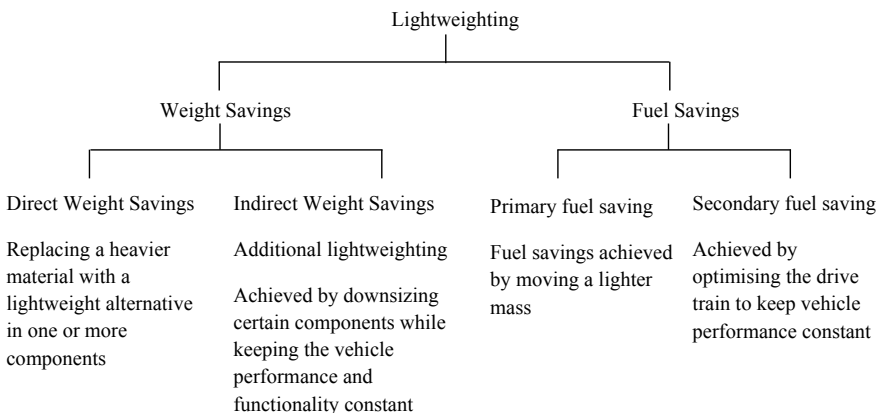

Fig. 12.3 Lightweighting classification [inspired from European Aluminium Association (2013)]
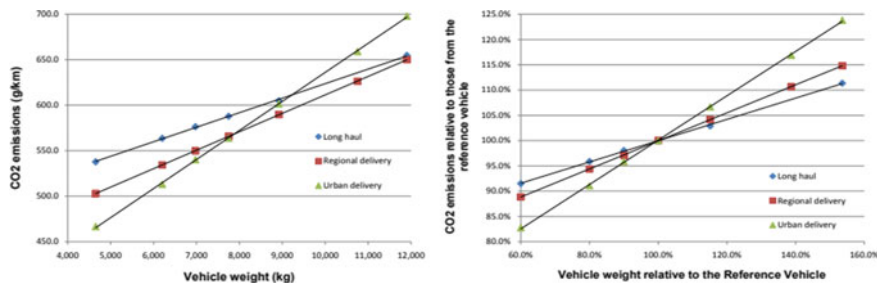
Fig. 12.4 Simulated CO_2 emissions from a 12 t GVW rigid truck having various weights (reference weight (100% point) for the vehicle in VECTO was 7750 kg) (Ricardo-AEA 2015)

and coaches) with a Gross Vehicle Weight above 3500 kg. Figure 12.4 shows the simulated emissions computed using the VECTO tool as reported in Ricardo-AEA (2015).

For the different vehicle categories, when driven over their commonly used drive cycles, the CO_2 emissions were calculated as:

Reference mass, Mref;
Reference CO_2 emissions (in g CO_2/km) CO_{2ref};
The gradient in the linear relationship between CO_2 emissions and vehicle light weighting, LWG;
The constant in the linear relationship between CO_2 emissions and vehicle light weighting, LWC;
The general formula for the emissions from a truck with Y% lightweighting is:
CO_2 emissions/km for lighter vehicle $= CO_{2ref} \times [(1 - Y) \times LWG + LWC]$ (Ricardo-AEA 2015).

12.3.1 The Global Impact of Light-Weighting

Apart from a per vehicle based analysis to understand the effect of lightweighting, estimates have also been made to determine the prospective contribution of lightweighting to a reduction of the global transport energy consumption and GHG emissions (Helms and Lambrecht 2004). Reports welcome a global initiative to implement lightweighting across various sectors.

Studies determined that as of 2000, a total of about 7600 million tonne (Mt) of greenhouse gas emissions (CO_2 eq) were released by a combination of all the modes of transport. About 660 Mt of GHGs could be saved by replacing all the transport units with lightweight vehicles with the same functional properties; with supplementary savings of about 220 Mt of GHGs if these units were built by utilising additional possibilities of light-weighting (Figs. 12.5 and 12.6).
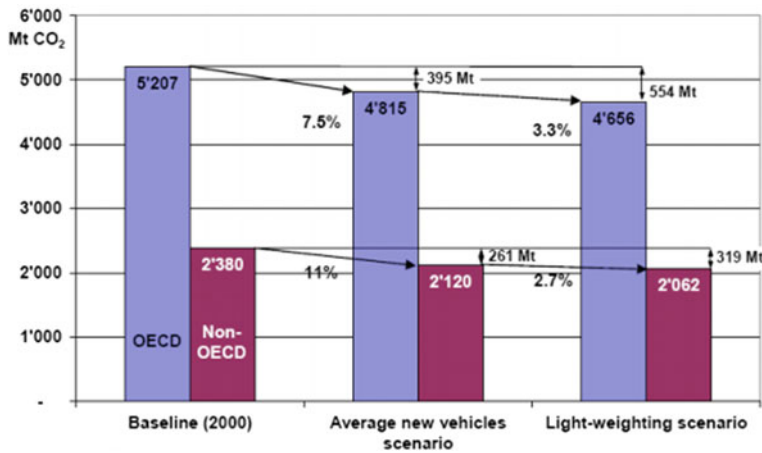
Fig. 12.5 Potential of global annual greenhouse gas savings by lightweighting of vehicles (Bertram et al. 2007)

Vehicle type	Weight (at full load for trucks)	Average diesel consumption (at full load for trucks)	Diesel consumption per 100 kg weight	Percentage air friction	Diesel savings per 100 kg weight savings	CO₂ savings per 100 kg weight savings*	Lifetime performance	Lifetime Diesel savings per 100 kg weight savings	Lifetime CO₂ savings per 100 kg weight savings*
	t	l/100 km	l/100 km	%	l/100 km	gCO₂/km	km	litres	Tonnes CO₂
City bus, few stops	15.0	40.5	0.27	45%	0.15	4.0	1 000 000	1 485	4.0
City bus, many stops	15.0	45.0	0.30	15%	0.26	6.9	1 000 000	2 550	6.8
Long distance bus, high speed	18.0	30.0	0.17	75%	0.04	1.1	1 200 000	500	1.3
Long distance bus, medium speed	18.0	35.0	0.19	50%	0.10	2.7	1 200 000	1 167	3.1
Truck/trailer, long distance, medium speed	40	59	0.15	50%	0.074	2.0	1 200 000	889	2.4
Truck/trailer, long distance, high speed	27	35	0.13	70%	0.039	1.0	1 200 000	467	1.2
Truck/trailer, long distance, medium speed	27	40	0.15	50%	0.074	2.0	1 200 000	889	2.4
Light-duty vehicle, average use	3.5	12	0.34	50%	0.171	4.5	375 000	643	1.7
Light-duty vehicle, urban commercial use	3.5	13.5	0.39	25%	0.289	7.7	450 000	1302	3.5
Light truck, average use	7.5	18	0.24	50%	0.120	3.2	300 000	360	1.0
Light truck, urban commercial use	7.5	20	0.27	25%	0.200	5.3	570 000	1140	3.0

Fig. 12.6 Savings per 100 kg weight reduction for different vehicle categories and their drive cycles (Bertram et al. 2007; Ricardo-AEA 2015)

12.4 Conclusions

The weight of a vehicle impacts the energy consumed in overcoming the total resistance (sum of rolling, gradient and acceleration resistance which is directly proportional to the weight of the vehicle being considered). As such, reducing the vehicle weight is of prime importance when aiming for a reduction in the emissions and energy consumed. While various material alternatives are being explored in the transport industry, each has its limitations ranging from costs, material properties, manufacturing techniques to sustainability and recyclability. When the lifecycle of the material itself is taken into account, the overall GHG emissions starting from material production raise questions about the utility of such a choice. Tougher regulations

aiming at increasingly ambitious reductions in emissions are pushing manufacturers towards alternatives to traditional IC engines which in turn increase the vehicle weight due to the heavy parts involved. Implementing lightweighting techniques is therefore the ideal solution for reducing emissions and must be investigated so as to be able to use novel materials in the automotive bodies.

Rather than treating lightweighting exclusively as an option, it must be coupled with other techniques aimed at increasing the fuel economy or decreasing emissions. For example, fuel additives help in better and complete combustion, modifying the engine or other principal components of the car like the powertrain or even developing smarter catalytic converters especially in the case of diesel fuelled vehicles. In systems as complicated as automotive vehicles—which are a combination of several mechanical, electrical and electronic subsystems there is no direct solution to the problem of reducing emissions, as seen in the course of this article. Furthermore, the demand from consumers for bigger cars with an increasing focus on comfort and entertainment coupled with stringent safety regulations adds to the overall weight of the vehicle. This once again increases the energy consumption and therefore the fuel emissions. Each time lightweighting takes some weight off the vehicle, it is added back on because of factors such as the above. This was indeed the reason why vehicles in the 2000s weighed more than those in the 1980s despite replacing all the heavier steel. Therefore, in conclusion the problem of reducing vehicular emissions needs to be solved modularly, yet needs to be looked at universally with all the subsystems considered together.

References

Bertram M et al (2007) Improving sustainability in the transport sector through weight reduction and the application of aluminium. International Aluminium Institute. http://transport.world-aluminium.org/fileadmin/_migrated/content_uploads/1274789871IAI_EAA_AA_TranspoSustainability_final.pdf. Last accessed on 1 June 2019

Boland CS, De Kleine R, Keoleian GA, Lee EC, Kim HC, Wallington TJ (2016) Life cycle impacts of natural fiber composites for automotive applications: effects of renewable energy content and lightweighting. J Ind Ecol 20(1):179–189. https://doi.org/10.1111/Jiec.12286

Cheah LW (2010) Cars on a diet: the material and energy impacts of passenger vehicle weight reduction in the US. Doctoral thesis at MIT

EU Directorate-General for Climate Action (DG CLIMA) (2016) Report indicating emissions targets for heavy duty vehicles. https://ec.europa.eu/clima/policies/transport/vehicles/heavy_en#tab-0-0. Last accessed on 01 June 2019

European Aluminium Association (2013) Aluminium in cars—unlocking the light-weighting potential; case study. https://european-aluminium.eu/media/1326/aluminium-in-cars-unlocking-the-lightweighting-potential.pdf. Last accessed on 01 June 2019

Helms H, Lambrecht U (2004) Energy savings by light-weighting, part II. IFEU Institute for Energy and Environmental Research

Heuss R, Müller N et al (2013) Lightweight, heavy impact. McKinsey https://www.mckinsey.com/~/media/mckinsey/dotcom/client_service/automotive%20and%20assembly/pdfs/lightweight_heavy_impact.ashx. Last accessed on 01 June 2019

ICCT (2017) Technical brief no. 6, Mar 2017. Last accessed on 01 June 2019. http://www.theicct. org/sites/default/files/publications/PV-Lightweighting_Tech-Briefing_ICCT_07032017.pdf

Kulkarni S, Edwards DJ, Parn EA, Chapman C, Aigbavboa CO, Cornish R (2018) Evaluation of vehicle lightweighting to reduce greenhouse gas emissions with focus on magnesium substitution. J Eng Des Technol. https://doi.org/10.1108/JEDT-03-2018-0042

Pervaiz M, Panthapulakkal S, Birat KC, Sain M, Tjong J (2016) Emerging trends in automotive lightweighting through novel composite materials. Mater Sci Appl 7:26–38. https://doi.org/10. 4236/msa.2016.71004

Ricardo-AEA (2015) Light weighting as a means of improving heavy duty vehicles' energy efficiency and overall CO_2 emissions. Heavy duty vehicles framework contract—service request 2: report for DG climate action. Ref: CLIMA.C.2/FRA/2013/0007

Tang HH (2017) Comprehensive considerations on material selection for lightweighting vehicle bodies based on material costs and assembly joining technologies. Int J Manufact Mater Mech Eng 7(4):1–14. https://doi.org/10.4018/IJMMME.2017100101

Uslu S, Celik MB (2018) Prediction of engine emissions and performance with artificial neural networks in a single cylinder diesel engine using diethyl ether. Eng Sci Technol 21(6):1194–1201